TOWARDS GREEN SYNTHESIS OF ORGANIC CARBONATES: UTILIZATION OF CO2 AS A CHEMICAL FEEDSTOCK

Laia Cuesta Aluja

Towards green synthesis of organic carbonates: Utilization of CO$_2$ as a chemical feedstock

Laia Cuesta Aluja

DOCTORAL THESIS

Supervised by Dra. Anna Maria Masdeu i Bultó

Departament de Química Física i Inorgànica

UNIVERSITAT ROVIRA I VIRGILI

Tarragona

2015

UNIVERSITAT ROVIRA I VIRGILI

Departament de Química Física i Inorgànica

FAIG CONSTAR que la present memòria, titulada "**TOWARDS GREEN SYNTHESIS OF ORGANIC CARBONATES: UTILIZATION OF CO$_2$ AS A CHEMICAL FEEDSTOCK**", que presenta Laia Cuesta Aluja per a l'obtenció de títol de Doctor en química, ha estat realitzada sota la meva direcció al Departament de Química Física i Inorgànica de la Universitat Rovira i Virgili d'aquesta universitat i que compleix els requeriments per a poder optar a Menció Internacional.

Tarragona, Setembre de 2015

El director de la tesi doctoral

Dra. Anna Maria Masdeu i Bultó

A la meva família per tot el vostre suport,

I en especial, al meu avi,

espero que et sentis orgullós

El mejor científico está
abierto a la experiencia, y
ésta empieza con un
romance, es decir, la idea de
que todo es posible.

Ray Bradbury

Agraïments

El temps passa volant i ja és hora de tancar una nova etapa, la meva tesi doctoral. Encara que aquest treball porti el meu nom, me n'adono que hi hauria d'aparèixer molta més gent, ja que sense la vostra col·laboració i incondicional suport no hagués sigut capaç de finalitzar-la amb èxit.

Per començar m'agradaria agrair a la meva directora de tesi la Dra. Anna Mª Masdeu i Bultó l'oportunitat que m'ha donat per realitzar aquesta Tesi. Anna, no acabaria mai d'agrair-te el que significa per mi aquesta gran oportunitat de no només créixer a nivell científic sinó a nivell personal alhora de treballar i conviure en diferents països i amb gent de tota mena. Gràcies per aquests fantàstics anys en aquest grup petit però amb molta personalitat. ☺

A Carmen, Cyril i Aurora per acollir-me aquests últims mesos en les reunions de grup i tenir l'oportunitat de formar part d'un gran i multitemàtic equip on he pogut aprendre, discutir i tenir una visió més àmplia de la química. Gràcies per fer-me sentir una més.

Als demés professors del departament, la Pilar, per les bones estones que hem passat en les pràctiques de laboratori i per sempre estar disposada a ajudar, xerrar o animar-me en tot moment. A l'Elena, pel seu somriure i la seva simpatia cada cop que ens veiem. Gràcies sobretot per ajudar-me en tot alhora de fer papers mentre estava fora, ets la millor! A la Mar, perquè sense tu bona part d'aquest treball no hagués estat possible. A l'Oscar, la Montse, la Núria, gràcies per tots els bons moments que hem compartit.

Ara toca fer memòria de tots els membres que han passat pel grup supercrític durant aquests 4 anys que han fet que la recerca sigui molt més amena. Primer voldria començar pel meu professor preferit; ja durant la carrera ens ho passàvem molt bé durant les pràctiques de laboratori i, sobretot, en "temes especials de la química inorgànica". Gracias Ali por enseñarme como trabajar en el laboratorio, por las risas, por siempre estar cuando más te necesitaba y por ser más que un mentor. Que pena no haber podido compartir más en el laboratorio pero quiero que sepas que este trabajo ha podido realizarse, en parte, gracias a ti. A l'Ariadna, vam compartir molt poquet temps

al laboratori però em vas ensenyar moltíssim i amb molta il·lusió i passió. Es notava que eres cul inquiet per la química i gràcies a això vas ajudar a transmetre'm aquest neguit per la investigació. A la Siham i la Najlaa, amb les quals vaig compartir molt bones experiències al laboratori i sobretot practicar una mica el meu francès. Najlaa tenemos un viaje pendiente por Tetuán. A Dolores, que también estuviste muy poquito por el labo pero que junto con Marlene, ese labo se transformó y cobró vida. Gracias chicas, espero que os vaya muy muy bien en vuestra carrera y alcanceis vuestras metas. En especial voldria agrair a en Xavi per tot el temps que vam compartir en el labo, durant el qual no només eres un gran company i un pou de saviesa sinó que ets un amic de veritat. Me n'alegro que tot t'hagi anat com desitjaves ja que et mereixes tota aquesta felicitat i més. Per cert, tenim una "quedada" pendent per barna. A la nova generació, la Clàudia, aquesta energia i ganes d'aprendre et portarà lluny, pensa en tot el que hem parlat ;). A en Mansoor, la Natàlia i en Diego molta sort amb tot.

Com no, voldria agrair a la Mª José i a en Josep per totes les estones de xerrameca que hem tingut fent-me oblidar que estava sola al labo. Gràcies per estar disposats a donar-me un cop de mà sempre i preocupar-vos quan hi havia algun que altre soroll estrany al labo. A en Ramón i la Irene per la seva perseverança i motivació alhora de resoldre els meus problemes químics, gràcies nois, sou els millors. A les dues Silvies, i la Yolanda per tota l'ajuda que m'heu donat alhora de fer papers, i a l'Elisenda per tenir la paciència d'ajudar-me amb els ordinadors.

A vosaltres amics i companys dels labos 216 i 217, què dir-vos que no sapigueu? Hem sigut com una gran família durant tots aquests anys. Amb molts moments bons, festes, excursions, congressos, amics invisibles increïbles, sopars, vídeos i molt i molt més. Què puc dir-vos, Xavi, Marc, Gerard, Margalinya... amb vosaltres va començar tot durant aquelles mortals classes del màster. Ens vam unir molt i espero que això mai ho perdem. Al món nanos de la Jessi, la nostra petita veterana que quan va marxar va deixar un gran buit al seminari. Encara se'm fa estrany no sentir-te xerrant amb la Eli o dient "Quina bona sort!!!", no canviïs mai; i en Fran, el gran numismàtic amb el qual he compartit molts riures en el seminari. I parlant de la "isla" i de coses "chics", em ve al cap a la Charly!! Una gran persona, que malgrat ser tan glamourosa sóc molt fan teva, i m'encanta la teva personalitat. Per cert, Fran i Charly, m'encanten les vostres converses de parella de casats ;). A la Mercè, per ser sempre la nostra mama, preocupar-te sempre

de que fem les coses bé i sempre enrecordant-te de tots. A l'Alberto i en Toni, els nois de la column, molt treballadors i grans companys amb els quals es pot comptar per a tot.

A las chicas con más arte del laboratorio, mi Ana y Itzi... como te echamos de menos. Sois geniales chicas, de lo mejorcito que he conocido. Ana me lo pasé muy bien viéndote sufrir con Josep mano a mano poniendo a punto la reacción que tanto te gustaba :p

A l'Eli, que en aquest últim any s'ha convertit en companya de fatigues i en el suport moral. M'ha encantat ensenyar-te tot el que sé i que t'interessés tant i tant. M'he sentit molt realitzada amb el que faig gràcies a tu. Ànims en aquesta última etapa, juntes ho superarem. Visca les pretèsiques!!

Com no, a la meva Raquel, la meva tècnica preferida. Ets la millor, ho saps? Quins bons moments, moments d'estrès, moments caòtics en el labo i en reactors hem passat juntes. De veritat que gràcies a la teva professionalitat, simpatia i espontaneïtat puc dir que ets una amiga de veritat dins i fora del labo. Moltes gràcies per tot.

A les noves generacions que sou uns cracks, la Núria (el bolso que ens vam comprar és ideal :p), en Marc petit, la Laura, l'Aaron, la Fàtima i com no a Enrico. Continueu amb aquesta força.

A tots els veterans que han passat per el seminari, l'Amadeu, l'Angélica, Javi, Sabina, les Cristines i la Cid, que m'has ajudat moltíssim amb els temes informàtics que tan malament se'm donen.

No m'oblido tampoc d'alguns companys de dalt com l'Adrià, el meu "pupilo" supercrític, amb moltes passió i ganes d'aprendre. Les teves idees arribaran lluny. Mi compañera zumbera Macarena, que bien nos lo pasabamos junto con Eli en esas clases. La Míriam, l'Emma, en Joan, i molts més. Sou molt macos.

A los del CTQC en especial a Jorge, eres una gran persona y gran amigo, espero que tengas un gran futuro y que de vez en cuando nos echemos unos bailecitos en la isla del Mojito :p

A Lorraine, por la oportunidad que me brindaste al poder realizar mi estancia en la belle Lyon. Pasamos muy buenos ratos juntas platicando de muuuchas cosas y enseñándome muchos trucos. De verdad que te estoy muy agradecida por todo y por decir que mi francés es bueno. Espero que nos volvamos a ver prontito. My friend Lisa, for all the talks and laughs we had in and out the lab. Y sobre todo a mis papis, Sonia y Johann. Sonia de verdad que coincidir contigo en mi estancia en Lyon se convirtió en la mejor aventura que haya tenido nunca. Lo que nos reímos, nos divertimos y celebramos no tiene precio. Me alegro que hayáis conseguido todo lo que os propusisteis pareja, lo que yo digo, no hay barreras para lo que de verdad se quiere lograr. Disfrutad de vuestra vida juntos y ya sabéis que Tarragona es vuestra casa ;) Emil, Fenia, Michalis, thank you for all the drinks and funny moments.

Vorrei anche ringraziare la Dott. Angela D'Amora e il Prof. Busico per avermi accettato nel vostro gruppo. Thank you Angela for all the good moments in the lab, with also Prof. Ruffo group. All you guys are amazing, I will miss you all: Macco Pammese, Roberto (it was very funny to be the princess Leila ☺), Marina, Augusta, Fiorella, Felicia, Claudia… Thanks also to my office mates: Anttonio, Enrica, Peppino (molto carino), Eric, Yue, Ilaria, Selene, Chiara and Alessia. And I would like to thank to Alessio, my favourite engineer. Grazie mille per preoccuparsi di me nei momenti brutti in core modul e prendere lo scooter per no passare ore in attesa del bus.

También me gustaría agradecer al grupo de la Prof. Mariette Pereira por la colaboración que hemos tenido en investigar la eficacia de varios de sus catalizadores porfirinas para la reacción de CO_2 y epóxidos.

I per últim però no menys important està agrair a la família i amics per ser capaços d'aguantar-me durant aquest 4 anys de nervis i fatigues. Patri guapa creo que tu más que nadie sabes por lo que he estado pasando, gracias por apoyarme y no regañarme mucho por no hacerte mucho caso en estos últimos meses. Creo que sabes que aunque he estado un poco ausente de todo eres mi gran amiga de alma. Ya casi está!!! Raquel y mi francesita Sarita, que deciros, que sois las mejores amigas que una pueda tener, que aunque estemos lejos y no nos veamos lo suficiente, sabed que os quiero mucho mucho. A la meva Sandreta, gràcies per animar-me tant en molts i molts temes, ets la millor!

A mi Yesid, no lo he comentado antes pero ya sabes que una de las causas de que la estancia en Lyon fuera una gran aventura fue por haberte conocido a ti. Gracias por elegirme a mi, en mostrarme mundo y en compartir tu vida conmigo, no quiero que esta aventura se acabe nunca. De verdad que lo que has tenido que aguantar estos últimos meses no tiene nombre, gracias también por tu paciencia y tu profesionalidad en tratar temas de mi "química perroflauta" como tu dices, aunque no sea cierto :p. De verdad que gracias a ti he podido salir adelante.

Al Luis per el seu gran interés en temes de la meva tesi. A la meva germana i artista Esther per tot el teu suport, ets la millor germana del món. Als meus pares per l'ajuda incondicional en tot i tot. A mis abuelos que aunque esten lejos sacan pecho por su nieta casi doctora en el pueblo. A mis tíos y primos por entender lo que hago mejor que nadie y apoyarme en todo. A la meva àvia, que sé que has patit molt durant les meves estàncies a l'estranger.

Gràcies de tot cor a tothom!! Muchas gracias a todos!!
Thank you very much everybody!! Merci beaucoup à tous!!
Graccie mille a tutti!!

Laia Cuesta Aluja

Table of Contents

Chapter 1

Chapter 2

Chapter 3

Chapter 4

Chapter 5

Chapter 6

Chapter 7

From alkenes to valuable organic carbonates using low-toxic and easy-to-handle Fe(III)-NN'O Schiff-based catalysts 179

Chapter 8

Conclusions 217

Chapter 9

Chapter 10

Chapter - 1

Carbon dioxide as a chemical feedstock for the synthesis of organic carbonates: A general introduction

Abstract

Green chemistry encourages the production of new valuable chemicals derived from natural and renewable resources instead of using fossil fuels as starting materials. An important renewable source of carbon for C-C bond formation could be carbon dioxide because of its low cost, its natural abundance and relatively low toxicity.

This introductory chapter reviews the literature background about the use of carbon dioxide as C_1 building block for the synthesis of highly value-added industrial chemicals and about its use as an alternative solvent at supercritical conditions. Particularly, this chapter highlights the most important developments in the field of catalytic synthesis of cyclic carbonates and polycarbonates focusing on homogeneous catalytic systems based on different metal complexes. Special attention is given to catalytic systems that reveal improved activity and selectivity using mild conditions and environmentally friendly, low cost and easy to handle metal catalysts.

1.1 Green chemistry

Sustainable chemistry can be defined as a scientific concept that *seeks to improve the efficiency with which natural resources are used to meet human needs for chemical products and services.*[1]

Inside the broad field of sustainable chemistry, green chemistry encourages *the design of chemical products and processes that minimize or eliminate the use and generation of hazardous substances* based upon the 12 principles of Green Chemistry developed by Anastas and Wagner.[2] The green chemistry approach not only seeks to reduce or eliminate waste, pollution and environmental damage but also seeks to redesign the materials that make up the basis of our society and our economy in ways that are benign for humans and possess intrinsic sustainability.

One of the major goals of green chemistry is to seek for sustainably chemical feedstock from renewable resources instead of petroleum, which is predicted to be exhausted. For instance, nature produces biomass on the scale of about 180 billion metric tons year,[2] of which only about 4 % is currently used by humans. About 75 % is in the form of carbohydrates, around 20 % is lignin, and the remainder includes fats, proteins and terpenes.[3] The industrial development of new methodologies to take advantage of natural biomass is, nowadays, a hot topic but still needs more investigation.

On the other hand, another important renewable source of carbon for C-C bond formation is the CO_2.[4] While the application of CO_2 as a raw material is not expected to significantly reduce levels of CO_2 in the atmosphere, this non-toxic and non-flammable gas is still considered to be an environmental friendly reagent and potential C_1 building block in catalysis.

Catalysis is clearly one of the fundamental pillars to achieve the goals in green chemistry with success. The design of catalysts that both activate inert starting materials as well as enhance reaction rates will reduce the current reliance on reactive and toxic reagents. Also the movement towards catalytic processes rather than the use of stoichiometric reagents will enhance the atom economy and reduce undesirable byproducts and waste treatments.

Another important issue in green chemistry is the use of alternative solvents such as supercritical carbon dioxide ($scCO_2$) or water in order to avoid the commonly

hazardous and toxic organic solvents and also to facilitate the catalyst recovery and recycling.

Over the last 20 years researchers have contributed with new ideas and techniques to move towards green chemistry and connecting diverse scientific disciplines with a common thread: reducing environmental impact through design at the molecular level.

1.2   *CO$_2$ as a C$_1$ building block*

Nowadays, it exists an ever-growing effort to implement a real change from a fossil fuel-based society to one that rely on the sustainable use of renewable resources. In our society much of the needed materials and chemicals will continue to be carbon-based and one of the most easily available renewable resources of carbon is carbon dioxide, which has the advantages of being abundant, inexpensive and non-toxic. Although we are far away about solving the growing concern over the greenhouse effect, which is mainly caused by anthropogenic CO_2 emission, carbon capture technologies are being improved[5] to capture a part of the CO_2 emissions, which was calculated in 2006 to be around 36,600 million metric tons of CO_2 annually.[6] A significant contribution to the annual production of carbon-based materials and chemicals could be supplied if only a fraction of the captured CO_2 stream could be made available for chemical production.[6]

Processes involving the use of CO_2 in organic synthesis have been extensively studied for academic and industrial scientists.[7,8,9,10,11,12,13,14,15,16] In fact, CO_2 is currently used as a phosgene substitute in the chemical industry for the production of bulk chemicals, such as urea, salicylic acid, cyclic carbonates and poly(propylene carbonate).[17] However, CO_2 is so thermodynamically and kinetically stable that is rarely used to its fullest potential as a raw material. The low free energy of CO_2 (ΔG_f^o = -394.39 kJ mol^{-1}) is the biggest obstacle to convert it into useful chemicals. It is worth to consider that shifting from phosgene to CO_2 means to use much safer but less reactive species (for $COCl_2$, ΔG^0_f = -204.9 kJ mol^{-1}). So, to establish more industrial processes is still a challenge.
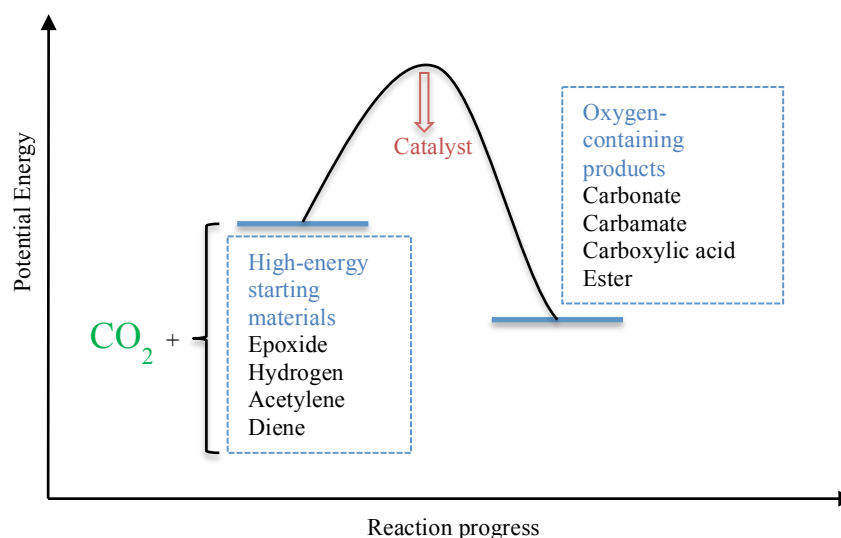
Figure 1.1. Organic synthesis using CO_2.[4]

Nevertheless, there are several strategies to overcome the thermodynamic stability of CO_2: (1) To use high free energy starting materials such as H_2, unsaturated compounds, small-membered ring compounds and organometallics. (2) To choose thermodynamically stable synthetic targets such as organic cyclic carbonates. (3) To displace the equilibrium reaction towards the product side by removing a particular compound. (4) To supply physical energy such as light or electricity. Selecting an appropriate substrate and catalyst the reaction with CO_2 can led to a negative Gibbs free energy (Figure 1.1).[4]

In order to expand the synthetic potential of converting CO_2 into useful compounds, the election of an adequate catalyst is crucial. A large number of inorganic, organic and metal catalysts have been developed for chemical CO_2 conversion. It is particularly noteworthy the development of new reactions and catalysts over the past several years. The syntheses of organic carbonates and carbamates, carboxylation reactions, reduction of CO_2 and other reactions with CO_2 have been studied extensively producing an increasing development of this research field. Figure 1.2 exemplifies the latest highlighted progress with CO_2, classifying it in different categories.
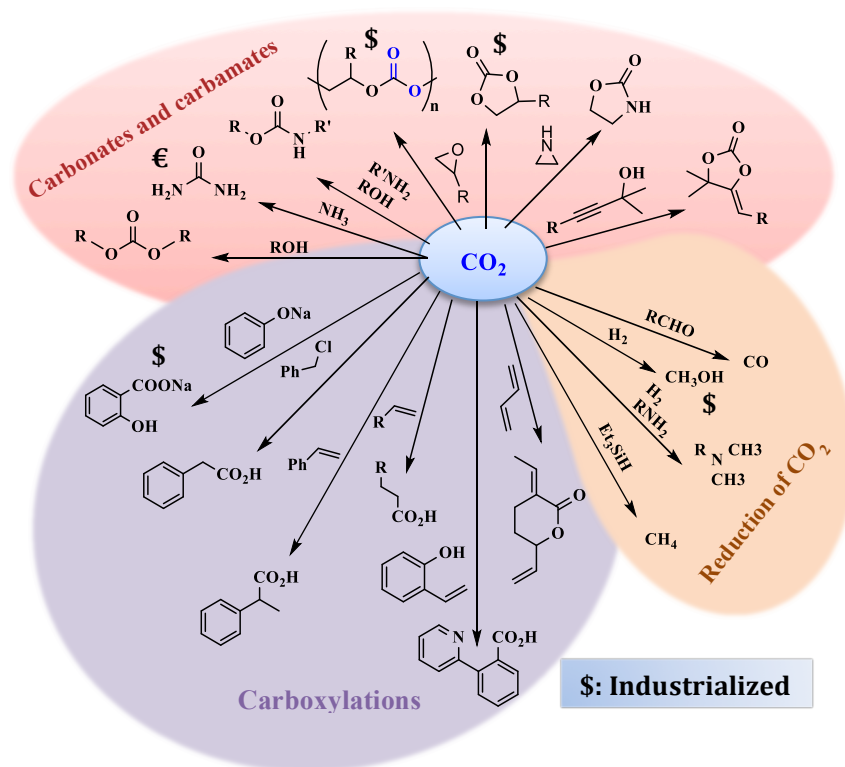
Figure 1.2. Examples of CO_2 transformation.[18]

Among the several reactions in this field, the addition of CO_2 to epoxides is a relevant topic of research since is a highly atom-efficient reaction that can generate useful compounds such as cyclic carbonates and polycarbonates producing no by-products (Scheme 1.1).[8,18,19,20,21] The reaction of CO_2 and epoxides can generate two types of products: cyclic carbonates (a in Scheme 1.1) and polycarbonates (b in Scheme 1.1).[18,22] Moreover, the consecutive insertion of two epoxides in the polymer chain can occur leading to the presence of ether linkages in the polycarbonate (c in Scheme 1.1).
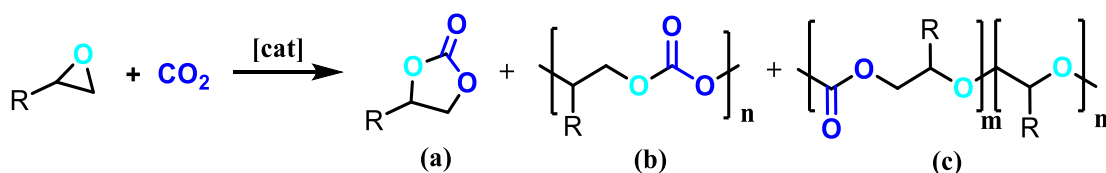
Scheme 1.1. General reaction of CO_2 and epoxides coupling and the possible products: (a) cyclic carbonate, (b) polycarbonate, (c) polycarbonate containing ether linkages.

In the next sections of this introductory chapter we will focus on this reaction and on the different catalytic systems used to promote it. Moreover, as in this Thesis we also use CO_2 both as reactive and solvent at supercritical state, a general introduction about supercritical fluids and, particularly, $scCO_2$ is given.

1.2.1 Synthesis of cyclic carbonates and polycarbonates from CO_2 and epoxides

The synthesis of cyclic carbonates and linear polycarbonates (Scheme 1.1) using carbon dioxide may represent an interesting alternative to conventional reactants used so far in chemical industry.

1.2.1.1 *Organic cyclic carbonates*

Cyclic carbonates are valuable synthetic targets that are widely used as raw materials for the synthesis of small molecules[23,24] and polymers.[25,26] They are also used as electrolytes in lithium-ion secondary batteries,[27] which are increasingly used in electric vehicle, paint strippers[28] and also have applications in the chemical industries as excellent polar aprotic solvents,[29,30,31] capable of replacing traditional solvents such as DMF, DMSO, NMP, HMPA and acetonitrile which generate NO_x or SO_x when incinerated. Moreover, they are also found in natural products[32,33] and potential pharmaceuticals.[34]

On an industrial scale, the synthesis of cyclic carbonates from CO_2 and epoxides is usually carried out using Lewis acid or base catalysts, which requires drastic conditions such as high temperatures and pressures.[17] The increasing demand of these compounds implies the development of new, commercially viable, catalysts and processes which operate at mild reaction conditions, close to room temperature and atmospheric pressure. These conditions will minimize the energy price and the overall cost of the production of cyclic carbonates.

There is a general mechanism for the catalytic synthesis of cyclic carbonates from epoxides and CO_2 (Scheme 1.2). Epoxides are typically activated by interaction with a Lewis acid catalyst through M-O coordination, followed by a nucleophilic attack and subsequent ring opening forming a metal-alkoxide. This reacts with CO_2 to form a metal-carbonate. The nucleophile should be a good leaving group as in the final step of

the mechanism it is displaced intramolecularly by the carbonate to form the five-membered ring. Although the nucleophile itself can act as a single catalyst for this reaction, usually, (sub)stoichiometric amounts and elevated temperatures and pressures are required.[35]
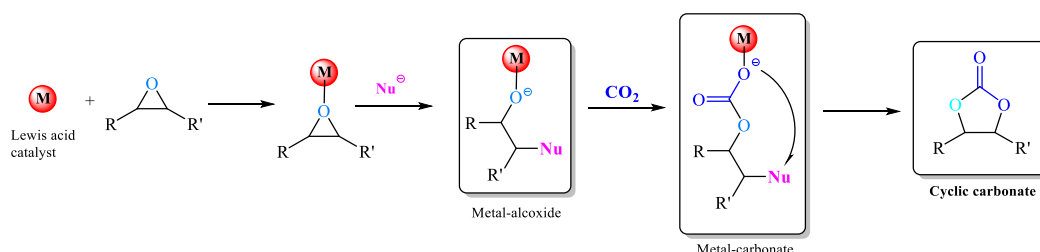
Scheme 1.2. General mechanism for cyclic carbonate synthesis.[35]

The most common nucleophiles and good leaving groups are halides (especially bromide and iodide). Usually many catalytic systems for the synthesis of cyclic carbonates contain a halide as part of their structure. Some commercial processes use tetraalkylammonium or phosphonium halides as catalysts.[36] Other catalytic systems are also known in which the nucleophile/leaving group is not a halide, for example 4-dimethylaminopyridine (DMAP), which can perform a role in some catalytic systems.[18,35,37]

1.2.1.1.1 *Alkali metal catalysts*

High yields of cyclic carbonates have been reported using main group metal halide salts as catalysts in the cycloaddtion of CO_2 to epoxides. In particular, at 50 bar and 120 ºC, simple metal salts such as K_2CO_3, KCl, KI, LiBr and NaOH catalyzed propylene carbonate formation in quantitative yields,[38] although turn over frequencies (TOFs) were only 30 h^{-1} even when were used in conjunction with crown ethers. In nearly all cases, potassium iodide was superior to other potassium and sodium based catalysts. Nevertheless, KI had limited activity when used alone in cyclic carbonate synthesis. Due to this the large majority of effort in this field has been focused on development and application of co-catalysts to enhance conversions. Song *et al.*[39] showed the enhancing effect when KI was combined with hydroxyl containing β-cyclodextrin as co-catalyst. The conversion of propylene oxide into propylene carbonate increased from 27 % using 2.5 mol % of KI to 98 % using 2.5 mol % KI and 8 wt % β-

cyclodextrin after 4 hours at 120 °C and 60 bar. Interestingly, potassium chloride and bromide salts gave only conversions of 4 % and 48 %, respectively, when were used in combination with the β-cyclodextrin co-catalyst. This was attributed to the increased ability of iodide to act as a leaving group.[40] The authors suggested that the enhanced activity observed when β-cyclodextrin was used as a co-catalyst was due to the hydrogen bond donating hydroxyls on the cyclic oligosaccharide being able to both activate the epoxide and stabilize the carbonate anion (Scheme 1.3).
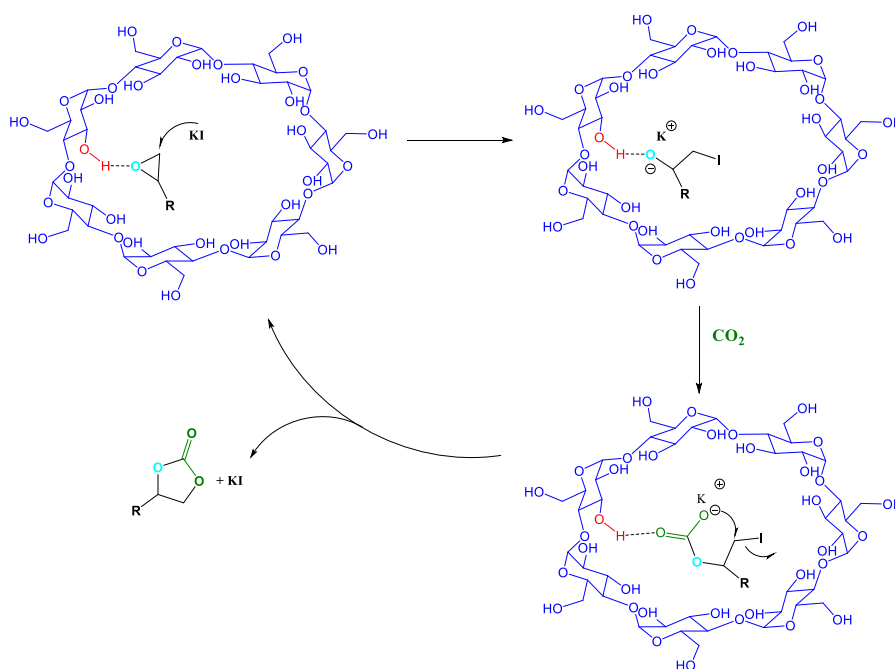
Scheme 1.3. Suggested reaction mechanism for KI/β-cyclodextrin catalyst system.[40]

Other co-catalysts such as triethanolamine, cellulose, formic acid, and lecithin offer the benefit to be inexpensive, simple or natural and readily available products. However, they often require higher loadings of catalyst and harsher reaction conditions to achieve good conversions.[41]

1.2.1.1.2 *Aluminum catalysts*

(a) Monomeric aluminum-based complexes

In 1978, Inoue and co-workers reported the synthesis of propylene carbonate catalyzed by an aluminum tetraphenylporphyrin (TPP) complex **1a** (Figure 1.3) in the

presence of *N*-methylimidazole (NMIM) as co-catalyst.[42] The catalytic reaction was carried out at room temperature and atmospheric pressures of CO_2, employing 5 mol % of catalyst **1a** (Figure 1.3) and 8 mol % of NMIM. After 45 h a 39 % conversion to propylene carbonate was achieved. Similar aluminum porphyrin catalyst **1b** (Figure 1.3) was used to study the reaction mechanism with spectroscopic methods.[43]

Later, Kasuga *et al.* developed aluminum phthalocyanine complexes **2a,b** (Figure 1.3) for the synthesis of propylene carbonate, using quaternary ammonium salt **3** or NMIM as co-catalysts.[44] Unfortunately, these systems did not exhibit high catalytic activity at mild conditions and the conversion to propylene carbonate was only 2 %. Subsequently, Ji *et al.* showed that at 140 °C, aluminum phthalocyanine complex **2b** (Figure 1.3) with NMIM afforded propylene carbonate in 96 % yield after a reaction time of 72 minutes.[45]

1a: X = OMe
1b: X = 1-chloro-3,3-dimethyl-2-butoxide

2a: X = OH
2b: X = Cl
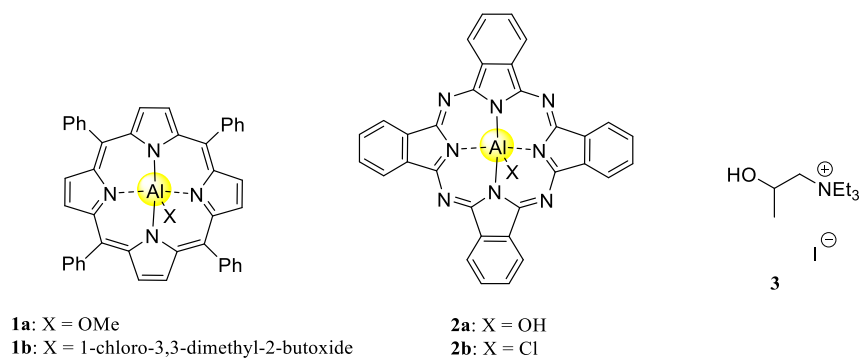
Figure 1.3. Examples of aluminum porphyrin and phtalocianine catalysts.

Aluminum triphenolate complexes have been also extensively studied as Lewis acid catalysts.[46] Kleij and co-workers discovered the high potential of hexachlorinated aluminum(III)-aminetriphenolate complex **4a** (Figure 1.4) for the synthesis of organic carbonates with CO_2 and epoxides.[47,48] Initial experiments were carried out using 1,2-epoxyhexane as substrate and tetrabutylammonium iodide (TBAI) as co-catalyst. At a catalyst loading of 0.05 mol % and co-catalyst loading of 0.25 mol %, good conversion to cyclic carbonate was achieved at 90 °C and 10 bar of CO_2 pressure within 2 hours (TOF = 960 h^{-1}). Moreover, lowering the catalyst/co-catalyst loading to 0.0005/0.05 mol %, higher initial TOF of 24000 h^{-1} was obtained. To further improve the catalytic activity, a number of Al(III)-aminetriphenolate analogues **4b-d** as well as a nonsymmetrical aluminum complex **5** (Figure 1.4) were synthesized and tested under the same conditions. Amongst these catalysts, **4a** was found to be the most active. The

wide applicability of Al(III)-aminetriphenolate **4a** (Figure 1.4) was demonstrated transforming a wide range of terminal epoxides bearing various functional groups, as well as internal epoxides into the corresponding cyclic carbonates, employing low amounts of catalyst (0.05 mol %-0.10 mol %) and co-catalyst (0.25 mol % - 0.50 mol %).

4a: R = Bu^t
4b: R = Me
4c: R = H
4d: R = Cl

5
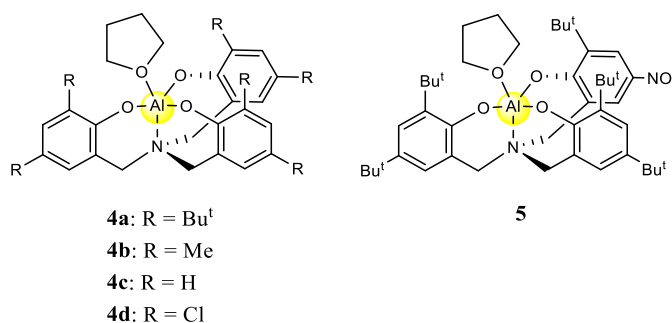
Figure 1.4. Aluminum triphenolate complexes developed by Kleij and co-workers.

Homogeneous salen complexes (salen = N,N'-ethylenebis(salicylimine), Figure 1.5) have received considerable attention in the synthesis of cyclic carbonates, mainly due to pioneering work of Darensbourg *et al.* on the formation of polymeric and cyclic carbonates catalyzed by chromium(salen) complexes.[49,50] Particularly, aluminum(salen) complexes have received more attention because of its low environmental impact, high earth abundance and its high catalytic activity.

He and co-workers have reported an Al(salen)Cl catalyst **6** (Figure 1.5) for the synthesis of ethylene carbonate. **6** together with TBAB as co-catalyst gave a rapidly formation of ethylene carbonate at supercritical carbon dioxide conditions of 150 bar pressure and 110 ºC, with a substrate to catalyst to co-catalyst ratio of 5000 : 1 : 1 (TOF up to 3070 h^{-1}).[51] However, the conversion of ethylene oxide was reduced significantly in the absence of the co-catalyst. Furthermore, the rate of conversion was reduced to a half when the reaction was carried out at less than 40 bar pressure of CO_2. Lu *et al.* also demonstrated that the binary catalyst system **6**/TBAI showed better catalytic activity at extremely mild conditions compared to other catalytic systems reported.[52,53] At 25 ºC and 6 bar of CO_2, with a propylene oxide to catalyst to co-catalyst ratio of 400 : 1 : 1 the reaction gave 61 % yield after 8 h (TOF = 61.5 h^{-1}).

Darensbourg and co-workers have developed a series of bifunctional aluminum(salen) complexes bearing appended pyridinium salt substituents.[54] At 120 ºC

and 30 bar of CO_2, complexes **7a,b** (Figure 1.5) both proved to be highly efficient catalysts for propylene carbonate formation (TOF up to 297 h^{-1}) even without any co-catalyst addition. Catalysts **7a,b** (Figure 1.5) also showed a good recyclability without significant loss in catalytic activity. Similarly, an aluminum(salen) complex bearing imidazolium-based ionic liquid moiety and containing polyether chain **8** (Figure 1.5), was introduced by Ji and co-workers.[55] This catalyst was capable to operate at 10 bar of CO_2, 100 ºC at 0.5 mol % catalyst loading. Complete conversion to propylene carbonate was achieved within 2 h.

Recently, a kind of non-symmetrical Al(salacen) complex (**9**, Figure 1.5) was introduced by Styring and co-workers for the conversion of styrene oxide to styrene carbonate using TBAB as co-catalyst.[56] The use of dichloromethane was found to be essential because of the low solubility of the catalyst in the substrate. The biphasic catalytic system at 1 mol % provides a 90 % of conversion of styrene oxide at 110 ºC and 1 bar of CO_2 within 48 h (TOF = 0.85 h^{-1}). Nevertheless, 73 % of conversion was reached with TBAB itself showing the not necessity of introducing the aluminum catalyst for this reaction.
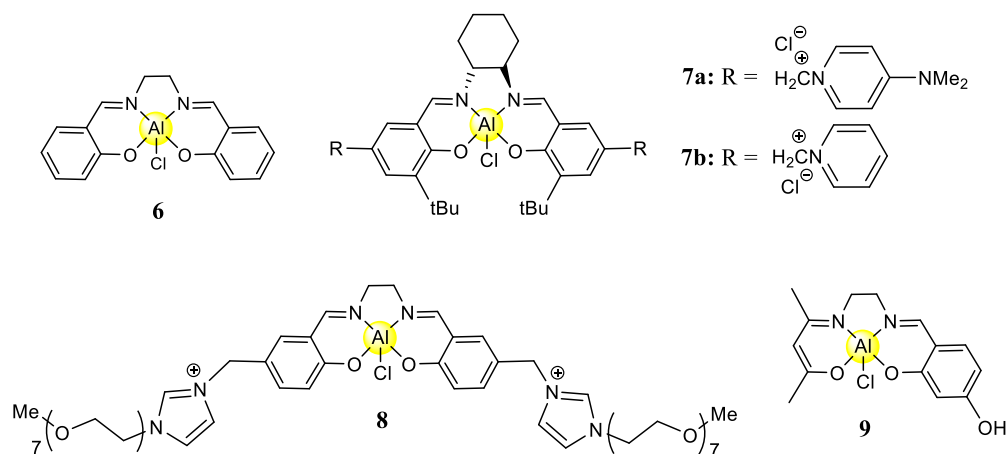
Figure 1.5. Monometallic aluminum(salen) and (salacen) complexes.

(b) Bimetallic aluminum-based complexes

In 2007, North and co-workers reported the use of dimeric aluminum(salen) complexes for the synthesis of cyclic carbonates from CO_2 and epoxides.[57] Under solvent-free conditions and using TBAB as co-catalyst, this system displayed a unique activity at atmospheric pressures of CO_2 and at 25 ºC. When styrene oxide was used as substrate, 2.5 mol % of catalyst **10** (Scheme 1.4) and 2.5 mol % of TBAB catalyzed the

formation of styrene carbonate with 62 % conversion after 3 h and 98 % conversion after 24 h. A number of other terminal epoxides were employed as substrates under the same conditions, thus 3-phenylpropylene oxide, 1,2-hexene oxide and 1,2-decene oxide were transformed into the corresponding cyclic carbonates with yields of 99 % (after 24 h), 88 % (after 3 h) and 64 % (after 3 h) respectively. Propylene oxide was used at 0 ºC and gave propylene carbonate in 77% yield after a reaction time of 3 h. Complex **10** (Scheme 1.4) could be reused over 60 times without loss of catalytic activity, though periodic re-addition of TBAB was necessary.[58]
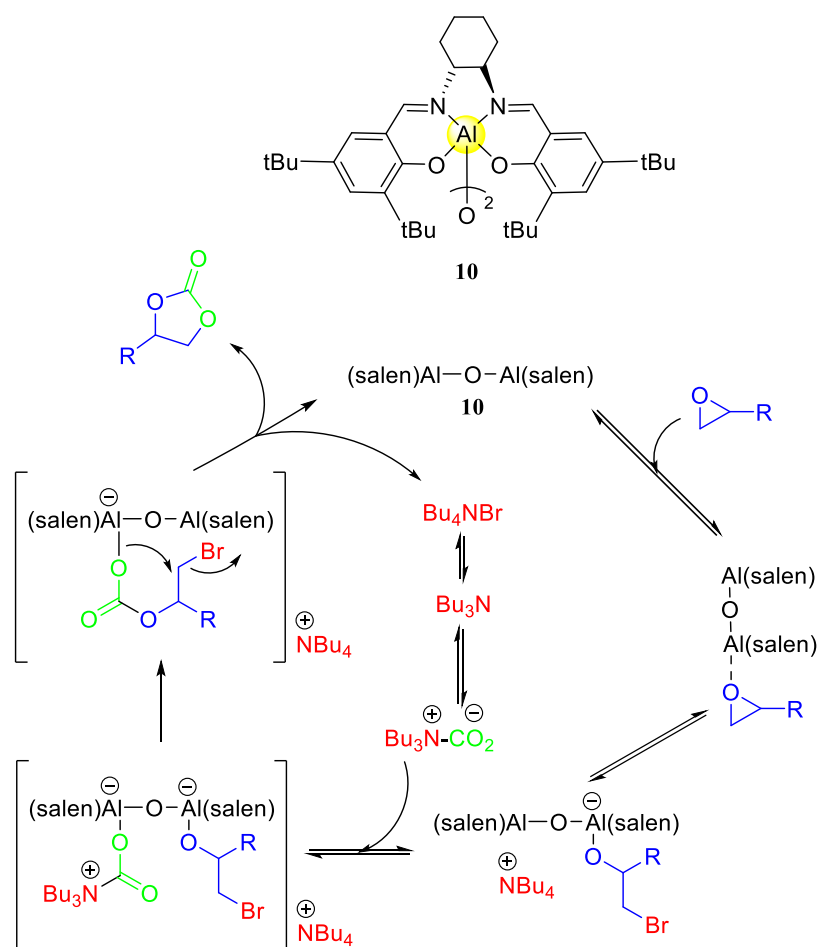
Scheme 1.4. Catalytic cycle for the addition of CO_2 to epoxides catalysed by complex **10**.[58]

Kinetic studies of **10**/TBAB catalytic system were carried out and showed that the reaction was second order in TBAB as well as being first order in catalyst **10**, in styrene oxide and in CO_2.[59] Moreover, it was observed that TBAB decomposed to tributylamine under the reaction conditions. With these results a catalytic cycle was proposed, (Scheme 1.4), in which the epoxide was first activated by one of the

aluminum atoms of the catalyst and, then, ring-opened by the bromide anion of the co-catalyst. At the same time, the CO_2 formed a carbamate salt with tributylamine and subsequently coordinate to the other aluminum atom of the complex. Thus, the molecule could be reorganized intramolecularly forming the carbonate species. Finally, the ring-closure and the elimination of bromide formed the cyclic carbonate and regenerated the catalyst. The support for this mechanism, which involved both aluminum atoms, come from the inactivity of monomeric aluminum(salen) complexes at atmospheric pressure and ambient temperature.[58]

To avoid the need for a co-catalyst, the same group developed a one-component analogue of their bimetallic aluminum(salen) complex, in which quaternary ammonium bromide groups were covalently attached to the salen ligand.[60] Thus, catalyst **11** (Figure 1.6) was found to convert a variety of ten epoxides into cyclic carbonates at ambient temperature and atmospheric pressure of CO_2 in the absence of TBAB. Conversions of 66-100 % were achieved after reaction times of 6-24 h. Even more, an analogue catalyst **12** (Figure 1.6) was designed by the same author for use in a flow system. They subsequently developed a flow reactor system for the addition of CO_2 to ethylene oxide.[61]

11: R = Ph
12: R = Merrifield resin
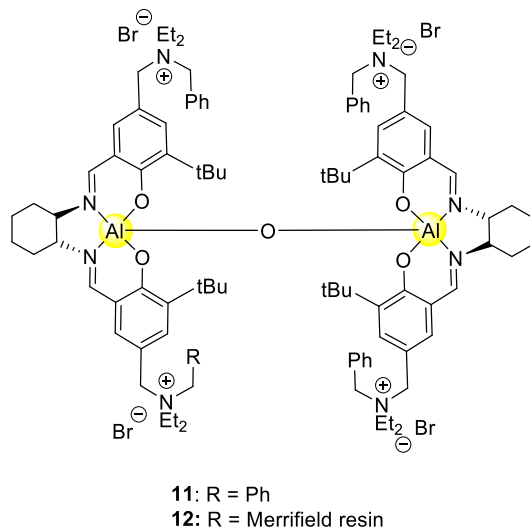
Figure 1.6. One-component bimetallic aluminum(salen) catalyst system.

1.2.1.1.3 *Iron catalysts*

There is an increasing interest to search sustainable catalytic systems for the coupling of CO_2 and epoxides that combine low toxicity and low cost. Specially, iron offers significant advantages compared with other metals since it is the second most

abundant metal in the earth crust (4.7 wt %), it is relatively low-toxic and not expensive. Furthermore, various iron salts and iron complexes are commercially accessible in a large scale or they are easy to synthetize. All of these advantages make this metal an extremely interesting candidate for develop new catalytic systems. Over recent years, only few reports of iron-based catalytic systems, which are able to catalyze the cycloaddition of CO_2 to epoxides yielding cyclic carbonates, have been published.

The most important classes of iron catalysts up to now are those developed by Kleij and co-workers based on the high powerful amine triphenolate ligands.[62,63] The complexes are formed as oxo-bridged dimers **13** but in the presence of epoxide or coordinating solvent the monometallic complex **13a** is formed (Figure 1.7). These complexes in the presence of TBAI co-catalyst displayed catalytic activity for a wide range of substrates, even with internal epoxides such as cyclohexene oxide and oxetanes.[63] If the selection of the co-catalyst and the catalyst to co-catalyst ratio is adequate a control over the stereochemistry of the cyclic carbonate is possible.

Most recently, the same group reported an analogous iron(III) catalyst bearing a pyridylamine-bis(phenolate) ligand (**14**, Figure 1.7), which was also highly versatile in the conversion of a broad scope of substrates. Particularly, with terminal epoxides the cyclic carbonate was the main product, whereas with cyclohexene oxide and vinylcyclohexene oxide as substrates, it was also possible to selectively obtain polycarbonates with high percentage incorporation of carbonate linkages.[64]
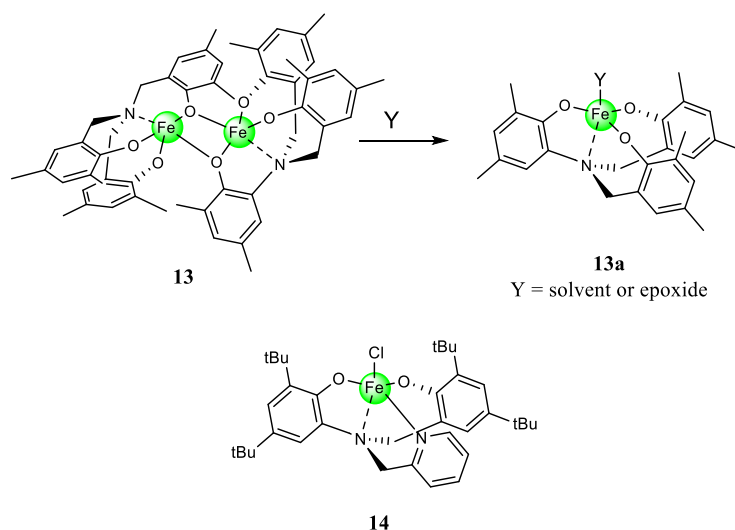
Figure 1.7. Iron complexes with amine triphenolate and pyridylamine-bisphenolate ligands.

Williams and co-workers reported a bimetallic macrocyclic iron(III) complex **15** (Figure 1.8) capable of both the formation of cyclic carbonate and polycarbonates from CO_2 and epoxides.[65] Williams showed that in the presence of bis(triphenylphosphinine) iminium chloride (PPNCl) as a co-catalyst, complex **15** (Figure 1.8) was able to convert cyclohexene oxide in a 90 % to cyclohexene carbonate under 1 bar of CO_2, 80 ºC, 24 h of reaction time using 1 mol % of catalyst and 2 mol % of PPNCl.

An iron(II) tetraamine complex **16** (Figure 1.8) has also been investigated as catalyst for propylene carbonate synthesis by Rieger and co-workers.[66] This complex was able to achieve complete conversion of propylene oxide within 2 hours at 100 ºC and 15 bar of CO_2 using 1.5 mol % of catalyst **16** (Figure 1.8) without the use of an additional co-catalyst.

Döring and co-workers reported some easy-to-handle ionic iron(III) complexes. Among all, the most active **17** (Figure 1.8) incorporate iodide as a counterion and two coordinated pyridines, which act as a nucleophilic co-catalyst.[67] This catalyst gave almost complete conversion of propylene oxide to propylene carbonate after 20 h using only 0.2 mol % of **17** at 50 bar and 80 ºC. The same group reported catalyst **18**, bearing a pyridine amide ligand, (Figure 1.8). This catalyst was shown to be effective for a range of monosubstituted terminal epoxides. Even more, catalyst **18** was effective for both the conversion of propylene oxide to propylene carbonate and for the production of polycarbonate when cyclohexene oxide was used.[68] Yields to propylene carbonate up to 91 % were obtained after 20 h at 80 ºC and 35 bar of CO_2 using low catalyst loading of 0.5 mol %. Again, no co-catalyst was needed since complex **18** (Figure 1.8) contains chloride anions that could ring-open the epoxide.
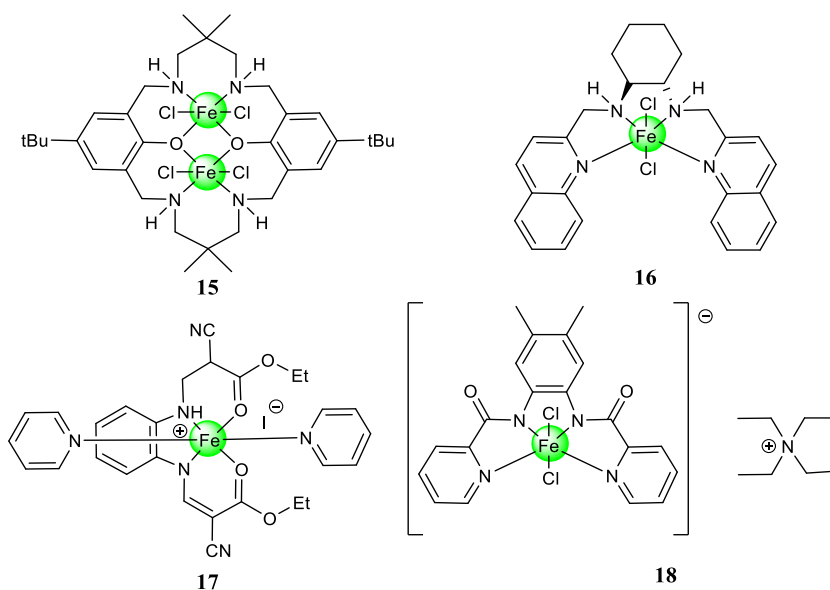
Figure 1.8. Different iron complexes for the cycloaddition of CO_2 and epoxides.

The recent work of Sunjuk and co-workers continues with similar iron(II) and iron(III) complexes based on salicylaldimine, tiophenaldimine and quinolinaldimine ligands, **19-22** (Figure 1.9) complexes.[69] They have been investigated in the coupling reaction of styrene oxide and CO_2 with TBAB as co-catalyst. Catalyst **19** (Figure 1.9) was the most active providing a TOF of 73 h^{-1} at 130 ºC and 5 bar of CO_2.

Moreover, iron(III) porphyrin complexes have also been used as catalyst for cyclic carbonate synthesis by Bai *et al.*[70] Complex **23** (Figure 1.9), not require a co-catalyst as it contains iodide anions in its structure. Not only can convert propylene oxide to propylene carbonate with high yields at low catalyst loading of 0.1 mol % but also can be recovered for five sequential reaction cycles with no significant reduction of activity.
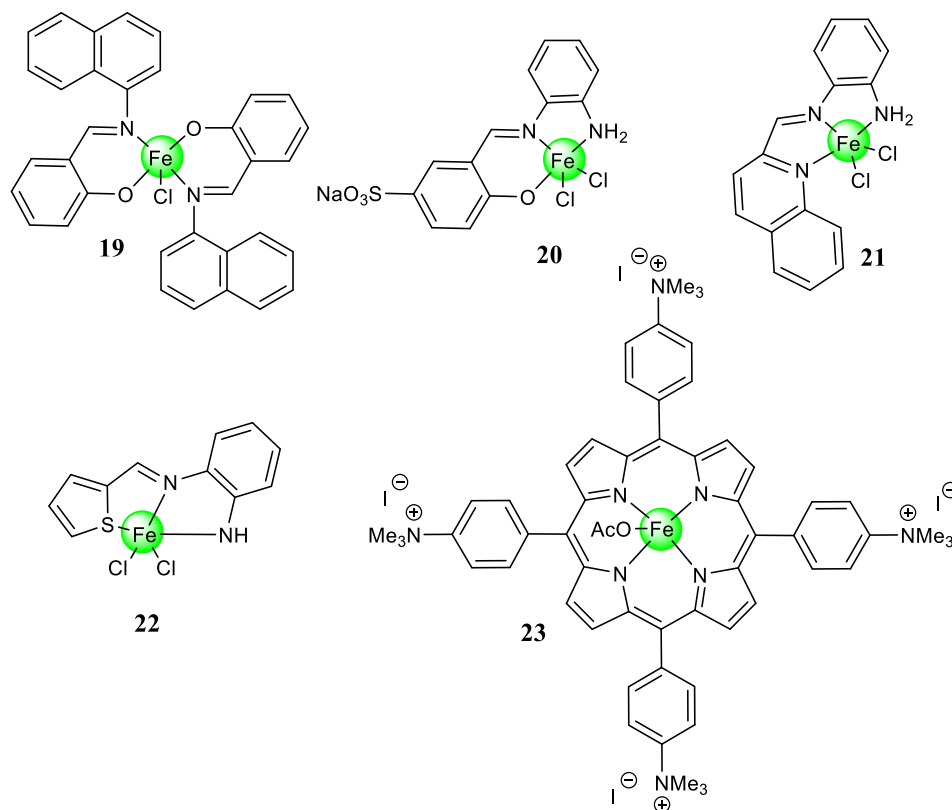
Figure 1.9. Iron complexes based on salicylaldimine, tiophenaldimine, quinolinaldimine and porphyrin ligands.

1.2.1.1.4 *Zinc catalysts*

Zinc complexes have extensively been studied in catalysis. The advantages of Zn(II) based complexes over other catalysts such as those based on chromium, cobalt and manganese include their lower toxicity[71] and their higher stability towards oxidation.[72] A lot of attention has been devoted to the formation of polycarbonates, especially with cyclohexene oxide or propylene oxide using zinc complexes. Interestingly, these complexes are relatively unexplored as catalysts for the formation of cyclic carbonates.

Besides being greener and/or cheaper alternative in comparison with other metal(salen) complexes, zinc(salen) have not been studied as catalysts for CO_2 and epoxides coupling until recently. Kleij and co-workers found that zinc(salphen) **24** (Figure 1.10) combined with a nucleophilic ammonium halide salt,[73,74] or an analogous bifunctional system (Figure 1.10) containing a Lewis acidic and nucleophilic center in a single molecule **25** (Figure 1.10)[75] were active for the synthesis of cyclic carbonates with terminal epoxides under mild conditions. The most remarkable feature of their

study was the kinetic studies to compare both systems. In particular, they found that both catalytic systems behave differently. A first-order dependence on the catalyst concentration for the **24**/TBAI binary system was found, while a second-rate dependence was observed for the bifunctional catalyst **25** (Figure 1.10). These observations thus support a monometallic mechanism for binary catalyst system and bimetallic mechanism in the case of bifunctional system (Figure 1.10).[76]
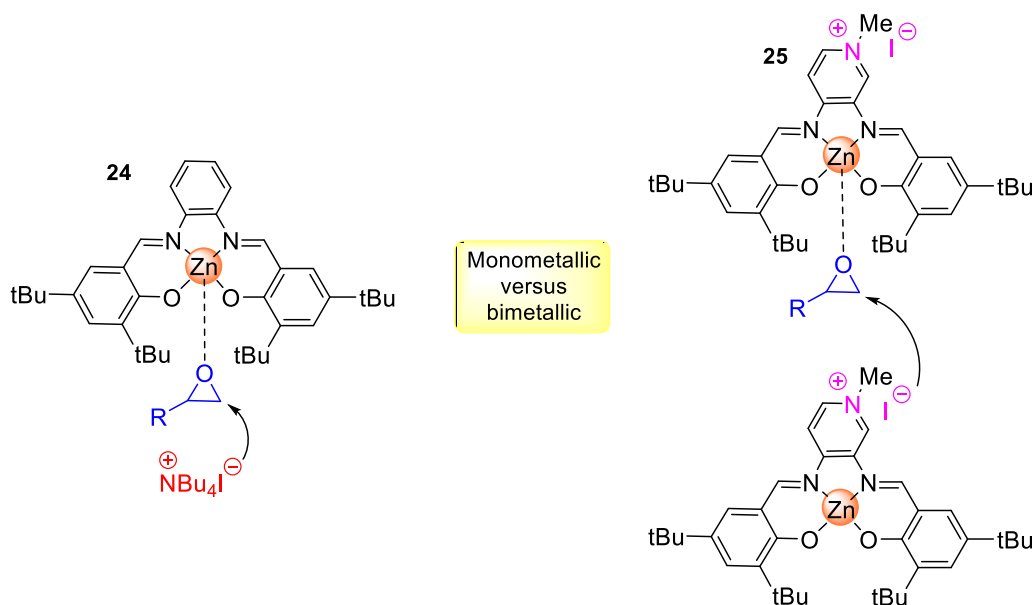
Figure 1.10. On the left a monometallic mechanism for binary catalyst **24**/TBAI and on the right a bimetallic mechanism for bifunctional catalyst **25**.[76]

Apart from Kleij and co-workers zinc(salphen) systems, they exist few reports about catalysts based on zinc, which produce selectively the cyclic carbonates but with lower activities. For example, similar zinc(salphen) catalysts based on tetradentate NNOO-donor ligands[77,78] and tridentate NNN-donor ligands[79,80] (**26-29** depicted on Figure 1.11), were selective to the formation of the cyclic carbonates but their activity was rather low.
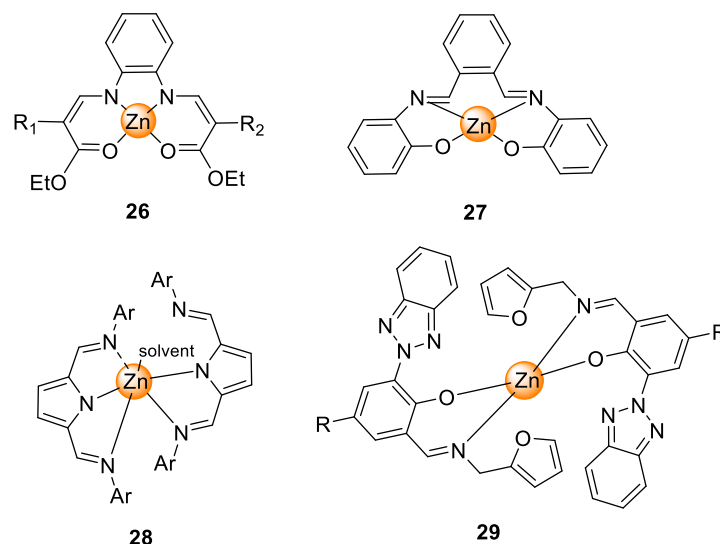
Figure 1.11 Selective zinc complexes for the production of cyclic carbonates.

1.2.1.1.5 *Cr, Mn, Co catalysts*

Although metal halides, Al, Fe and Zn metal complexes are the most challenging catalysts for cyclic carbonate synthesis, other catalytic systems based on metals such as Cr, Mn or Co have to be also considered. There is a wide range of suitable catalytic systems for cyclic carbonate systems but, particularly, porphyrin and salen-based complexes bearing chromium, cobalt and manganese are the most used, even though most of them are more active in polycarbonate synthesis.

(a) Porphyrin based complexes

Chromium(III) and chromium(IV) porphyrin derivatives (**30** and **31**) (Figure 1.12) produced quantitative yields of cyclic carbonates with moderate TOFs (36-89 h^{-1}), when used in conjunction with NMIM or DMAP, with both terminal and disubstituted epoxides. The methyl substituents onto the phenyl rings improved the solubility in dichloromethane enhancing the catalytic activity.[81]

Nguyen and co-workers reported the use of a cobalt porphyrin/DMAP systems (**32a-b**, Figure 1.12) to provide cyclic carbonates The best result in the formation of cyclic propylene carbonate was obtained using the more electrophilic complex **32b** with two equivalents of DMAP at 17 bar of CO_2 and 120 ºC with a TOF of 826 h^{-1}.[82] Other metal porphyrin complexes such as manganese [Mn(TPP)Cl] and ruthenium [Ru(TPP)(PPh$_3$)Cl] were also tested, but the TOF values using

phenyltrimethylammonium tribromide (PTAT) were inferior (33 and 46 h^{-1}, respectively).[83]
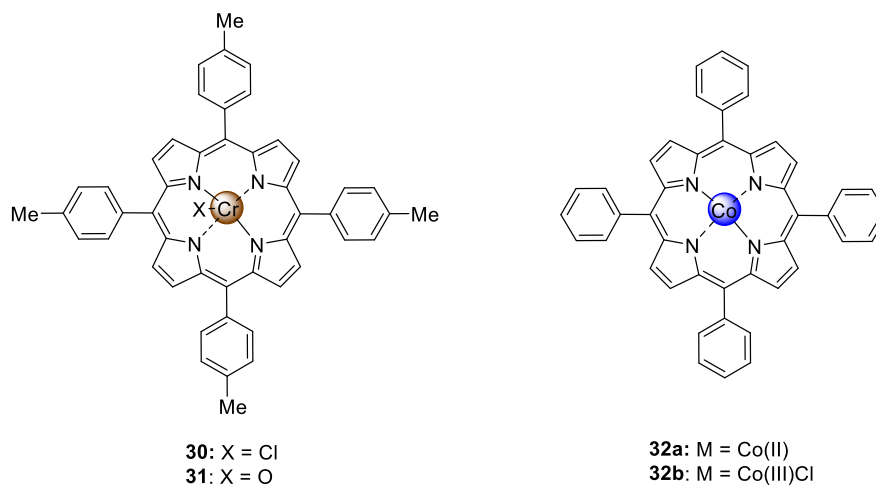
Figure 1.12. Chromium and cobalt porphyrin complexes.

(b) Salen based complexes

Inspired by Krupper's work on chromium(III) porphyrins (**30** and **31**) (Figure 1.12), Paddock and co-workers investigated the use of chromium(III)(salen) complexes for propylene carbonate synthesis obtaining a high TOF of 916 h^{-1} for catalyst **33** (Figure 1.13) with DMAP as co-catalyst at 100 ºC and 4 bar of CO_2.[84]

Following the work on the copolymerization reaction with CO_2 and epoxides (see Section 1.2.2), Darensbourg and co-workers studied also the synthesis of cyclic carbonates with chromium(III)(salen)Cl complex **34** (Figure 1.13), under 25 bar of pressure at 40 ºC with toluene as solvent.[85] Under identical reaction conditions the addition of CO_2 to CHO with catalyst **34** (Figure 1.13) gave alternating copolymer, whereas with propylene oxide resulted in the formation of cyclic carbonate.[86]

Cobalt(III)(salen) complexes are known to be active catalysts for the stereo-controlled synthesis of polycarbonates from propylene oxide and CO_2. However, these complexes were also found to produce cyclic carbonates at specific reaction conditions. Lu and co-workers used Co(III)(salen) derivatives to obtain enantioselective propylene carbonate.[87] A catalyst based on chiral [Co(III)(salen)(O$_2$CCCl$_3$)] **35** (Figure 1.13) in conjunction with TBAB exhibited a high TOF of 245 h^{-1} at room temperature and 15 bar pressure and gave the product with 50% enantiomeric excess.

Paddock and Nguyen reported that the combination of [Co(III)(salen)]Cl **36** (Figure 1.13) and DMAP was highly active for the synthesis of propylene carbonate.[88] The reaction exhibited a high TOF of 1200 h^{-1} at 100 °C and 10 bar pressure using dichloromethane as solvent. The system showed high activity for a wide range of epoxides, producing cyclic carbonates as the only product.

In 2008, Baiker and co-workers investigated various homogeneous and immobilized [Mn(III)(salen)X] complexes as catalysts for the addition of CO_2 to propylene and styrene oxide under supercritical conditions.[89] Complex **37** (Figure 1.13) catalyzed the synthesis of propylene carbonate in 91 % yield, obtaining a TOF of 203 h^{-1} at 140 °C and 200 bar of CO_2. Complex **37** showed comparable activity (TOF 213 h^{-1}) for the synthesis of styrene carbonate.

33: R = *meso*-Ph
34: R-R = *trans*-(CH$_2$)$_4$-

35: X = O$_2$CCCl$_3$
36: X = Cl

37: X = I, R = H
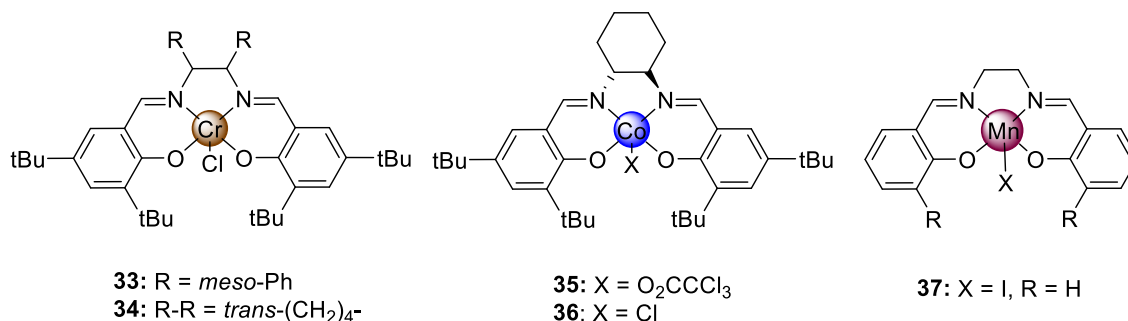
Figure 1.13. Metal-salen complexes for cyclic carbonate formation.

1.2.1.1.6 *Alternative cyclic carbonate synthesis via oxidative addition of CO₂ to olefins*

Oxidative addition of CO_2 to olefins is an alternative single-step route for the synthesis of cyclic carbonates (Scheme 1.5). Niobium(V) oxide and other metal oxides or Rh(I) complexes catalysts in the presence of molecular oxygen showed modest activity for styrene carbonate synthesis, though the process required DMF as the solvent, and the selectivity for the carbonate was quite low. In addition, high pressures and temperatures were necessary (50 bar, 125 °C, 5 h).[90]
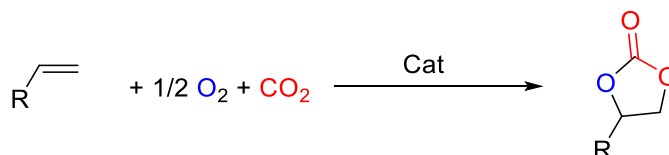
Scheme 1.5. Oxidative cycloaddition of CO_2 to olefins.

Arai and co-workers reported that the oxidative carboxylation of styrene using *tert*-butylhydroperoxide (TBHP) as oxidant and TBAB as catalyst.[91] A moderate yield of 38 % of styrene carbonate was obtained after 6 hours using 10 bar of CO_2 with 11.6 mol % TBAB at 80 ºC. Using either H_2O_2 or O_2 in place of TBHP significantly reduced the amount of styrene carbonate produced and increased the amount of benzaldehyde by-product formed. The same group also reported a second system for the direct synthesis of styrene carbonate from styrene without isolation of the intermediate epoxide.[92] By using a one-pot catalytic system consisting of gold on silica, with $ZnBr_2$, TBAB, and TBHP as oxidant, styrene carbonate could be successfully obtained in the presence of 80 bar of CO_2 at 80 ºC for 4 h. With 2.5 mol % of $ZnBr_2$ and 5 mol % of TBAB, 31-37 % of styrene carbonate could be obtained using 1-8 weight % loading of gold on silica.

38
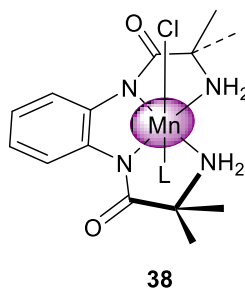
Figure 1.14. Manganese(III) complex developed by Ghosh and co-workers.

More recently, Ghosh and co-workers successfully employed a manganese(III) complex bearing an acyclic amide-amine ligand to convert a variety of olefins to cyclic carbonates in the presence of CO_2 (**38**, Figure 1.14). TBHP was used as oxidant, TBAB as a co-catalyst and acetonitrile as solvent in a single-pot reaction at 17.23 bar of CO_2 pressure and 100 ºC. High turn over frequencies (50-240 h^{-1}) and yields (up to 72 %) were obtained when various alkenes were employed.[93]

1.2.1.1.7 *Carbonates from bio-based epoxides*

As discussed during this chapter, sustainable atom-economical insertion of CO_2 into epoxides is attractive because these epoxides can be easily obtained by oxidation of the corresponding alkenes. Nevertheless, these alkenes come directly from crude oil cracking, which is not considered a sustainable starting material. Sustainable starting

materials are thus required to decrease the dependence from petrochemicals. Some alkene functions derive directly from natural resources. For example, oleo compounds are very attractive because they can be obtained from vegetables and they could be easily extracted and transformed into useful products. For this reason, the conversion of epoxy derivatives of oleo compounds opens up a new direction utilising renewable substrates from biogenic feedstock and CO_2 as the sole carbon source. Even more, these complex structures can be epoxidized from alkenes by employing hydrogen peroxide as a green and selective oxidant.[94]
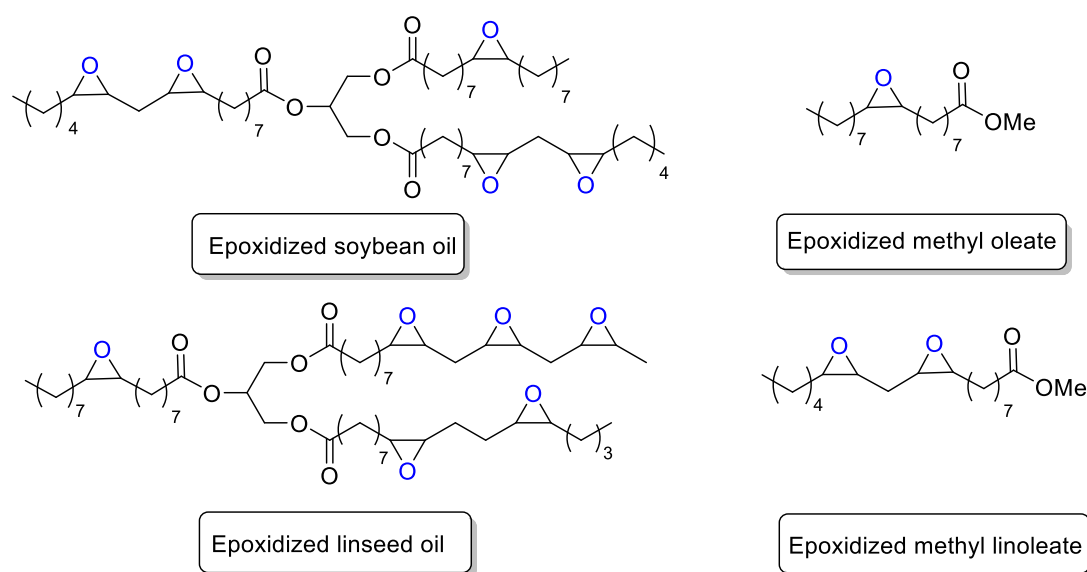
Figure 1.15. Epoxy derivatives of renewable oleo compounds.

The carbonates obtained from vegetable oils have been used as intermediates for the synthesis of non-isocyanate polyurethanes (NIPUs). Thus, epoxidized soybean oil, linseed oil, methyl oleate and linoleate (Figure 1.15) have been transformed to the corresponding carbonates by reaction with CO_2 using different catalytic systems. Quaternary ammonium salts, such as TBAB, catalyzed this transformation with catalysts loadings between 3 to 5 mol %.[95] The obtained carbonate from soybean oil was successfully transformed in polyurethane by reaction with amines.[96]

Another example was reported by Leitner and co-workers using the combination of TBAB and polyoxometalates (POMs).[94] Best results in the carboxylation of several oleo-based epoxides were obtained with a tetraheptylammoniumsilicontungstate containing chromium. An increase in the catalytic activity was also observed by using $scCO_2$. This has been attributed to an increase of the oil-CO_2 solubility due to the

increased pressure. Nevertheless, the solubility of the catalyst in the condensed CO_2 phase was also important, since as the density of the CO_2 phase increased, the ionic catalyst became insoluble and the conversion droped.[94]

An example of the overall reaction sequence with methyl oleate is shown in Scheme 1.6.
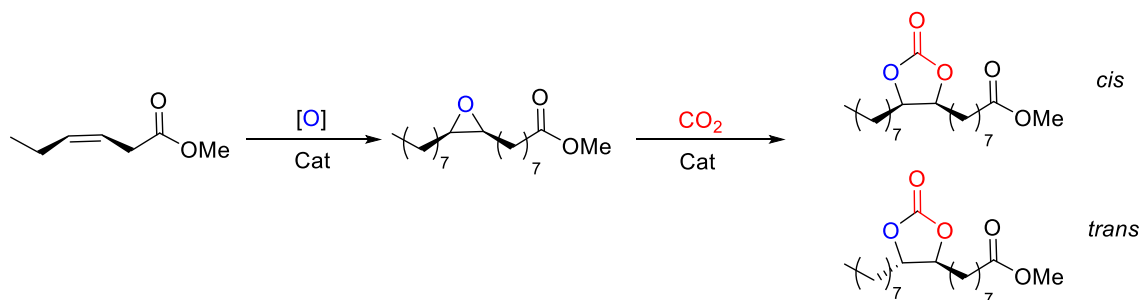
Scheme 1.6. Cyclic carbonate synthesis from methyl oleate as substrate.[94]

1.2.2 Production of polycarbonates from CO_2 and epoxides

Polycarbonates are high performance, sustainable and eco-efficient materials used in a large variety of essential applications. They have a unique combination of properties offering high transparency, durability, safety, versatility, heat and shatter resistance, good electrical insulation, strength, lightness and biodegradability.[97] Products made from polycarbonate include sheets for roofing and glazing, optical media, spectacle lenses, medical devices, leisure articles, automotive goods, and food contact materials. Indeed, polycarbonates enable the manufacture of technical high performance products in sophisticated forms and sizes, ranging from bicycle helmets to stadium roofs. Some important commercialized products are Makrolon® (Bayer) and Lexan® (General Electrics). The estimated annual production of organic carbonates in 2014 was 2.6 Mt.[98]

However, all these attractive properties belong to bisphenol-based polycarbonates, which the industrial production of these materials involves the polycondensation of high toxic phosgene and bisphenol A (Scheme 1.7). On the other hand, other polycarbonates such as for example poly(propylene carbonate) display lower rigidity than bisphenol-based polycarbonates and moderate thermal stability.[20,22] These features limit the application of these polymers, despite that they can be prepared in a green process from renewable carbon dioxide.
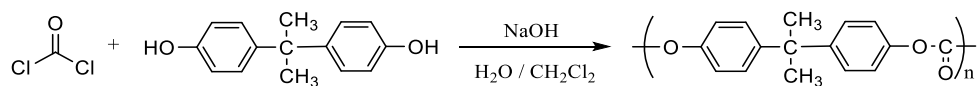
Scheme 1.7. Polycondensation reaction of phosgene and bisphenol A.

Thus, the main challenge is to improve the polycarbonate properties obtained by CO_2 and epoxides coupling reaction in order to obtain similar applications as bisphenol-based polycarbonates. The investigation of different substrates; the optimization of the catalyst, cross-linking of polymer chains and the copolymerization involving two different epoxides or monomers through blending with other polymers are different ways to enhance the polymer properties.[22,99]

The first remarkable copolymerization of CO_2 and epoxides was discovered by Inoue and co-workers in 1969 since they found that a mixture of $ZnEt_2$ and H_2O could catalyzed the alternating copolymerization of propylene oxide and CO_2 to yield a small quantity of polymeric materials.[100,101]

As a result, a significant amount of research studies have been focused on the development of new catalysts and ligands for this reaction. The main representative homogeneous catalytic systems are based on porphyrins (A, Figure 1.15),[102] phenoxides (B, Figure 1.15),[103] β-diiminates (C, Figure 1.15)[104] and salen (D, Figure 1.15)[105] chelating ligands combined with active metals such as Al, Cr, Co, Mg, Li, Zn, Cu, Cd, and Fe.
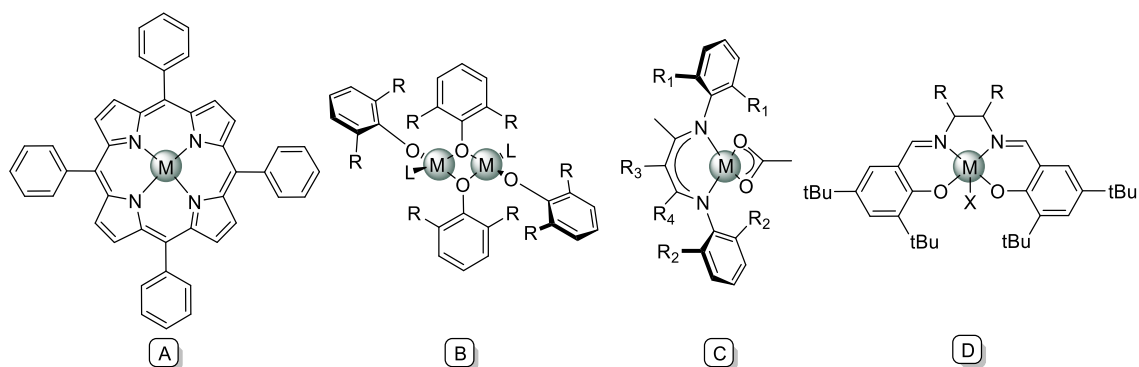
Figure 1.15. Representative homogeneous single-site catalysts for epoxide/CO_2.

1.2.2.1 Copolymerization mechanism

The mechanistic aspects of the copolymerization of CO_2 and epoxides with homogeneous catalysts are under continual investigation and review. Generally, homogeneous catalysts with the form L_nMX can be easy adapted by modifying either the ligand framework (L_n), the Lewis acid metal center (M) or the nucleophilic group (X). For instance, there are several different mechanism proposals for the initiation step of this reaction with L_nMX complexes forming the active metal alkoxide (Scheme 1.8).[106]

(A) Bimetallic initiation pathway: This mechanism involves two metal complexes with an intermolecular interactions of two active sites as observed by Jacobsen and co-workers.[107] The bimetallic pathway generally is thought to occur in the absence of a co-catalyst at low epoxide/catalyst loadings.

(B) Monometallic initiation pathway: This involves an intramolecular attack of the nucleophile of the coordinated epoxide. Such a mechanism is, however, rather unlikely as the corresponding transition state in commonly metal complexes is thermodynamically unfavorable.

(C) Binary initiation pathway: This involves the interaction of a binary catalyst/co-catalyst system, where the added co-catalyst adopts the role of a nucleophile, attacking the coordinated epoxide.
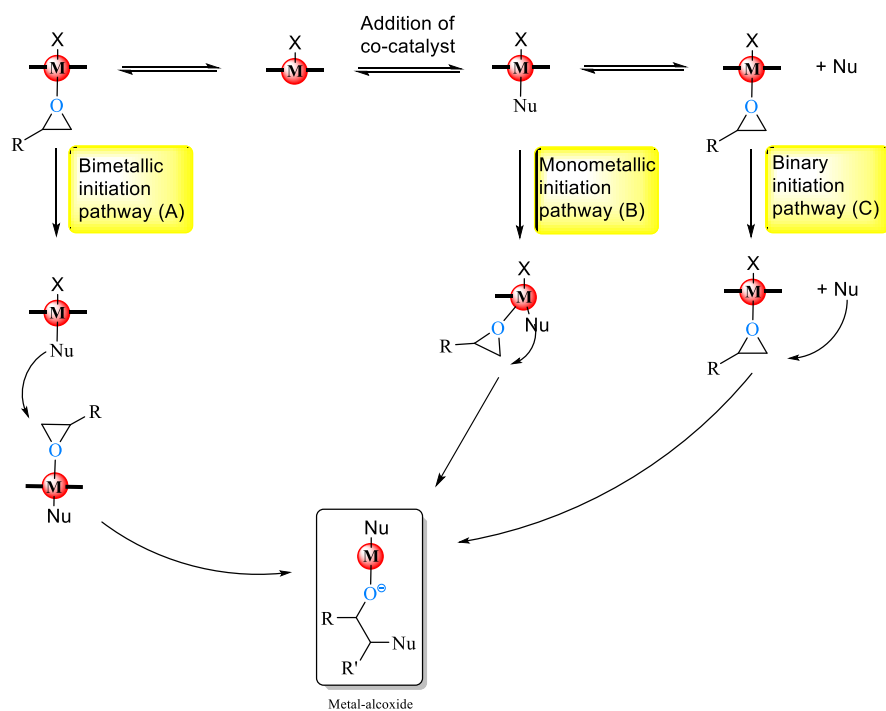
Scheme 1.8. Initiation mechanism for a generalized five-coordinated complex.[106]

Once the metal alkoxide is formed, the general mechanism of copolymerization of CO_2 and epoxides proceeds, then, by subsequent insertions of CO_2 and epoxide leading to the desirable polycarbonate (Scheme 1.9, a).
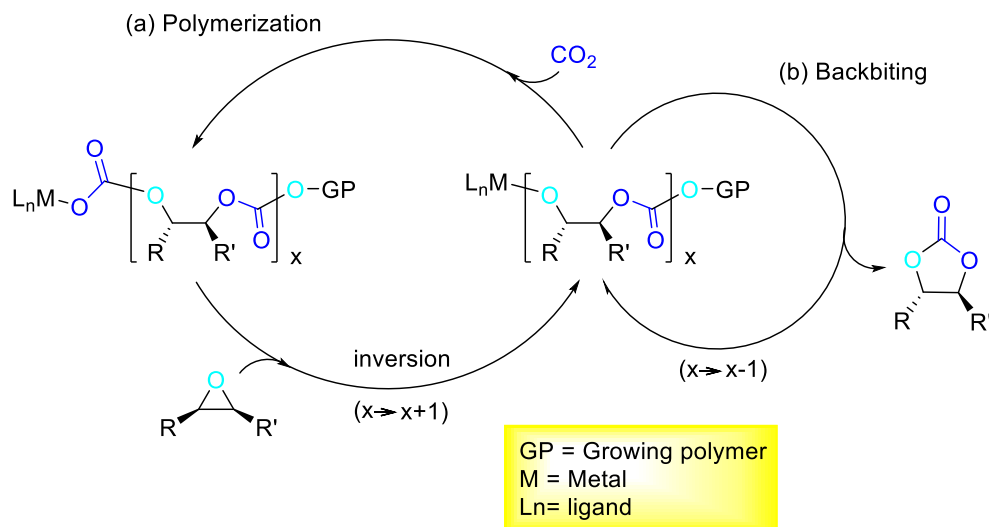
Scheme 1.9. The general mechanism of epoxide-CO_2 copolymerisation and the backbiting formation of cyclic carbonates.

It should be taken into account that there are several factors that affects the copolymerization of CO_2 and epoxides besides the evident effect of temperature, pressure and catalyst/co-catalyst concentration.[106]

-Viscosity an dilution problems: During the copolymerization process, the viscosity of the reaction media increases with polymer formation and the diffusion of the epoxide to the active site of the catalyst is, therefore, impeded and limits the polymer yields. The addition of a proper solvent could help the monomer diffusion but the spatial separation of the interacting species at high-diluted mixtures could also produce a decrease of activity.

-Side reactions: As explained in last section side reactions in copolymer formation typically occur when epoxides are consecutively inserted into the growing polymer chain leading to polyether fragments and also via backbiting pathway (Scheme 1.9, b). The consecutive insertion of two CO_2 molecules has never been observed as this is strongly disfavored from a thermodynamic perspective,[20] unless under specific conditions.[108] The factors that enhance the selectivity towards cyclic carbonate include high temperature and the nature or concentration of the co-catalyst, which can help the dissociation of the growing polymer-chain from the metal center.

-Chain transfer: Any traces of water, alcohol and acid in the polymerization medium could initiate a chain transfer, which results in lower molecular weights than theoretically expected.[109] Nevertheless, those polyols with low molecular weights and low incorporation of CO_2 are also useful for the industrial synthesis of polyurethanes.[110]

1.2.2.2 *Stereochemistry of the polycarbonates*

In the copolymerization of CO_2 with cyclohexene oxide, C-O bond cleavage typically occurs with inversion of configuration at the site of attack (bimolecular nucleophilic substitution, S_N2 type mechanism) generating *trans*-1,2-diol units (ring opened product). Thus, three different copolymers can be obtained: syndiotactic (*RSRSRS*), isotactic (*RRRR* o *SSSS*) and atactic (irregular distribution).[105] The tacticity of the copolymer chain is determined by ^{13}C NMR spectroscopy analyzing the

carbonate region (δ 150-160 ppm). The m-centered tetrads (syndiotactic) appeared at δ 153.7 ppm, whereas isotactic r-centered tetrads appeared at δ 153.1 ppm. The signals appearing at δ 153.2 ppm corresponds to an irregular atactic polymer distribution (Figure 1.16).
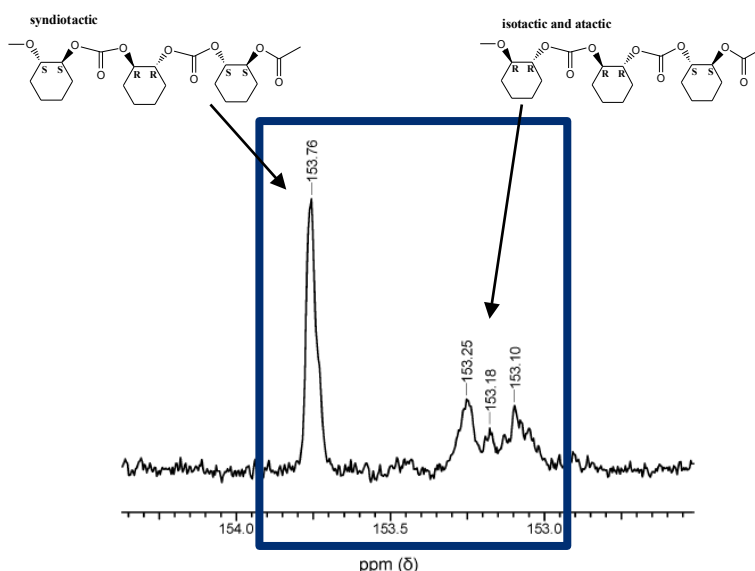
Figure 1.16. ^{13}C NMR spectrum of the carbonate region in a poly(cyclohexene carbonate) (PCHC).[105]

1.2.2.3 *Aluminum and manganese catalysts*

Inoue *et al.* developed the first monometallic catalyst for copolymerization of CO_2 and epoxides in 1978. This catalyst was based on a TPP ligand framework (**38a-d,** Figure 1.17).[111] **38a** and **38b** porphyrins were found to be active for the polymerization of CO_2 and propylene oxide to poly(propylene carbonate) (PPC).[43,102]

38a: X = Cl
38b: X = OMe
38c: X = Me
38d: X = OR
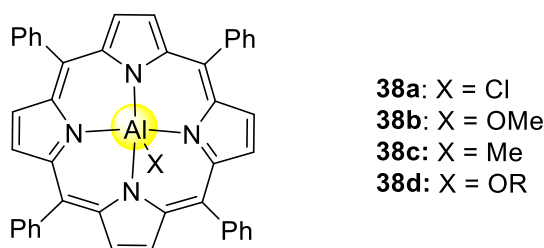
Figure 1.17. Aluminum porphyrin for the copolymerization of CO_2 and epoxides. (R = alkyl, oligomer of PPO).

38a and **38b** (Figure 1.17) reacted with PO to form poly(propylene oxide) (PPO) with narrow polydispersity (PDIs) between 1.07-1.15 (Scheme 1.10). The chloride

anion was proposed to act as an initiator ring-opening the less hindered C-O epoxide bond and generated regioregular PPO. **38b** (Figure 1.17) copolymerized PO and CO_2 at 20 ºC and 8 bar of CO_2, giving PPC (M_n = 3900 g mol^{-1}; M_w/M_n = 1.15) with only 40 % carbonate linkages over 19 days of reaction.[112] Although the low carbonate linkages and long reaction time, this reaction was the first example of polycarbonate having a narrow PDI.

In the case of catalyst **38d** (Figure 1.17), where R is an oligomer of PO, it did not react with CO_2. However, upon addition of a co-catalyst such as NMIM, reversible CO_2 insertion was observed. It was proposed, on the basis of ^{1}H NMR studies, that NMIM bond to aluminum metal activated the metal towards CO_2 insertion.[43] The addition of ammonium or phosphonium salts as co-catalysts, increased the percentage of carbonate linkages to > 99 % (Scheme 1.10). Additionally, **38a**/EtPh$_3$PBr catalytic system was also active for ethylene oxide (EO)-CO_2 and CHO-CO_2 alternating copolymerization producing poly(ethylene carbonate) (PEC) with 70 % carbonate linkages, a M_n of 5500 g·mol^{-1}, and a PDI of 1.14. Poly(cyclohexene carbonate) was produced with >99 % carbonate linkages, a M_n of 6200 g·mol^{-1}, and a PDI of 1.06. While this system yielded cyclic carbonates for propylene oxide, neither EC nor cyclohexene carbonate (CHC) were observed.
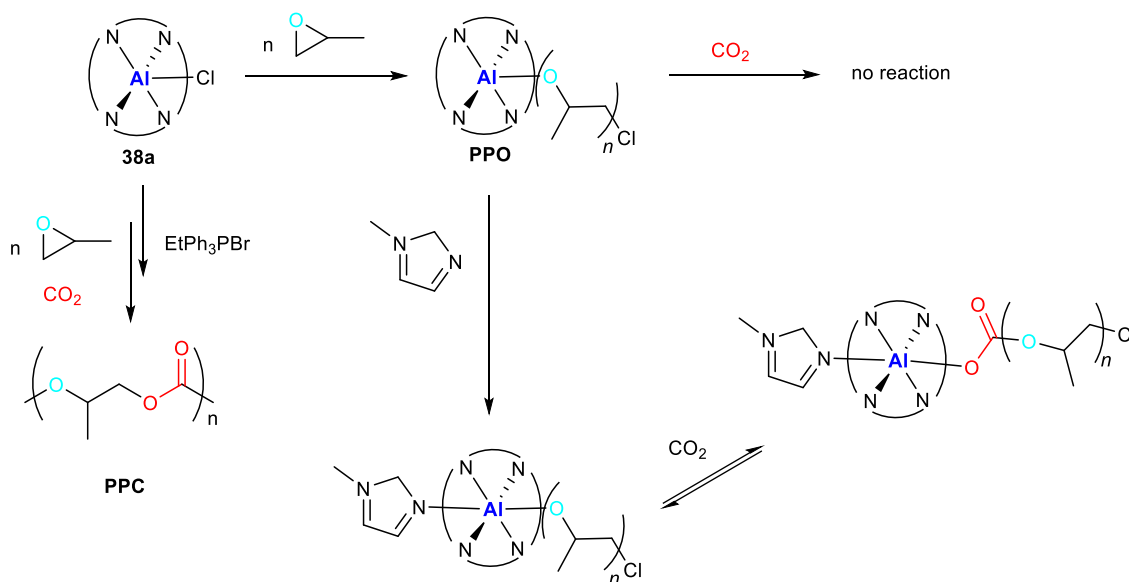
Scheme 1.10. Reactivity of aluminum porphyrins complexes.

The low-molecular-weight polymers produced by aluminum(TPP) catalysts suggest chain transfer, which supports Inoue's proposal of an "immortal" type

polymerization (Scheme 1.11).[111] An immortal polymerization allows that one metal center can propagate multiple chains, whereas a living polymerization grows only one chain per metal center. Protic sources facilitate chain swapping such that there are more polymer chains than active catalytic sites (Scheme 1.11). Free chains are inactive but continue to grow polymer when exchanged onto the active site. If the chain swapping is more rapid than propagation, polymer chains with narrow PDIs are produced. For example, addition of HCl does not quench the polymerization. Instead, it affords **38a** (Scheme 1.11), which allows for new polymer chains to be initiated. The catalyst reinitiates polymerization and grows a new polymer chain in the same "immortal" manner.
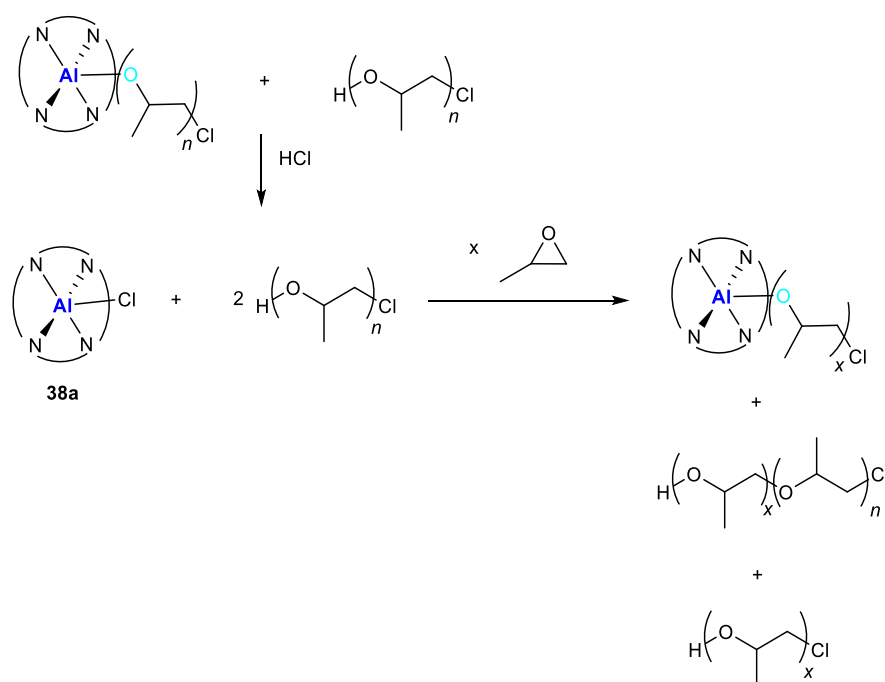
Scheme 1.11. "Inmortal" polymerization of PO using aluminum porphyrins complexes.

In 2003, the same group developed an analog porphyrin system utilizing manganese as the active metal center.[113] At 80 ºC and 50 bar of CO_2, **39** (Figure 1.18) reacted with CHO to produce PCHC (> 99 % carbonate linkages; $M_n = 6700$ g mol^{-1}; $M_w/M_n = 1.3$) with a moderate TOF of 16.3 h^{-1}. In this system, co-catalysts such as PPh$_3$, pyridine or NMIM decreased the percentage of carbonate linkages in the polycarbonate.

39
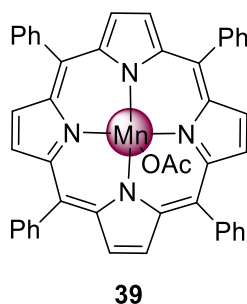
Figure 1.18. Manganese porphyrin for the copolymerization of CO_2 and epoxides.

Aluminum(salen) complexes **40a-m** (Figure 1.19) in conjunction with a series of anionic and neutral co-catalysts were found to be highly active for the copolymerization of CO_2 and CHO. Darensbourg and co-workers showed that a more electron-withdrawing salen framework was necessary to produce significant quantities of copolymer with a high CO_2 content in absence of cyclic carbonate by-product. Nevertheless, the TOF's obtained, ranged from 5.2 to 35.4 h^{-1}, while chromium(salen) systems under similar conditions provided TOF's as high as 1150 h^{-1}.[114]
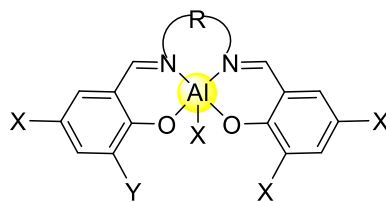
40a: X = NO_2; Y = tBu; Z = Et; R = -C_2H_4-
40b: X = NO_2; Y = tBu; Z = Cl R = -C_2H_4-
40c: X = NO_2; Y = tBu; Z = Et; R = -C_6H_4-
40d: X = NO_2; Y = tBu; Z = Cl; R = -C_2H_4-
40e: X = Cl; Y = Cl; Z = Et; R = -C_2H_4-
40f: X = H; Y = H; Z = Et; R = -C_6H_4-
40g: X = NO_2; Y = H; Z = Et; R = -C_2H_4-
40h: X = tBu; Y = tBu; Z = Et; R = -C_6H_4-
40i: X = tBu; Y = tBu; Z = Cl; R = -C_2H_4-
40j: X = Cl; Y = Cl; Z = Cl; R = -C_2H_4-
40k: X = H; Y = H; Z =Cl; R = -C_6H_4-
40l: X = Cl; Y = Cl; Z = Cl; R = -C_6H_4-
40m: X = tBu; Y = tBu; Z = Cl; R = -C_6H_4-

Figure 1.19. Aluminum(salen) complexes for copolymerization of CHO and CO_2.

Aluminum alkoxides have also been shown to convert epoxides and CO_2 to polycarbonates. Beckman and co-workers reported several aluminum complexes, including **41**, **42**, and **43** (Figure 1.20) that reacted with CHO and CO_2 to give PCHC with a maximum TOF of 2.7 h^{-1}.[115,116,117] At 80 bar CO_2 and 60 ºC, **41** produced PPC (M_n = 5000 g mol^{-1}; M_w/M_n = 2.89) with only 22 % carbonate linkages and a TOF of

2.0 h^{-1}. These low-carbonate content polymers have shown potential applications as solubilizers in supercritical CO_2 (scCO$_2$).[115]
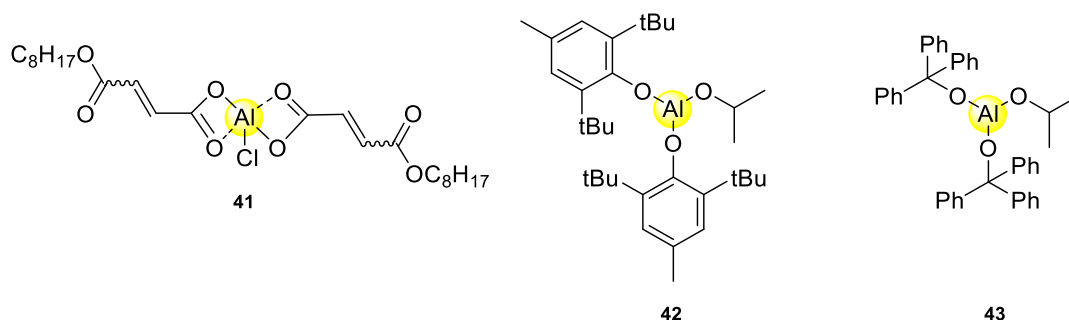
Figure 1.20. Several aluminum alkoxides for the copolymerization of CO_2 and epoxides.

To sum up, aluminum and manganese complexes are indeed active for the copolymerization of epoxides and CO_2; however, they provide low activities and selectivity towards the polycarbonates, which contain a high percentage of ether linkages compared with other metal catalysts.

1.2.2.4 *Chromium catalysts*

The first example, in the academic literature, of the use of a chromium complex as a catalyst in the fixation of CO_2 was developed by Holmes and co-workers who reported a fluorinated chromium(III) porphyrin complex **44** (Figure 1.21), which showed TOFs of up to 173 h^{-1} for the alternating copolymerization of CHO and CO_2 at 225 bar of CO_2 (scCO$_2$) and 110 ºC in the presence of DMAP as co-catalyst.[118] The fluorinated aromatic moieties improved catalyst solubility in scCO$_2$, and consequently increased the yields of PCHC. Similar to aluminum porphyrin catalysts for epoxide-CO_2 copolymerization, these chromium analogs yielded polycarbonates with narrow PDIs (M_w/M_n=1.08-1.50) and low molecular weights (M_n = 1500-9400 g mol^{-1}). Furthermore, the resultant PCHC contained high percentages of carbonate linkages (97 %). In the same year, Jacobsen and co-workers published the first patent revealing that chromium salen complexes were viable catalysts for production of poly(propylene carbonate) at 1 bar of CO_2 pressure.[119] That discovery inspired a lot of researchers to investigate more in this kind of catalytic reaction. For instance, Darensbourg's group developed the air-

stable chromium salen complexes, which showed high activity, stereoselectivity and stability, as catalysts for CO_2 epoxides copolymerization. These systems together with cobalt analogues have become a reliable reference for this catalysis.[21] Catalyst **45a** (Figure 1.21) was active for CHO copolymerization but always with a nucleophilic co-catalyst, NMIM. Similarly to aluminum porphyrins with NMIM, the co-catalyst function is generally proposed to bind at a site *trans* to the initiating group, weakening the axial bond and allowing for facile epoxide insertion.[21] A wide scope of co-catalysts and ligand substitutions have been investigated leading to increased activity, with complex **45b** (Figure 1.21) and bis(triphenylphosphine)iminium azide (PPNN$_3$) giving a maximum TOF of 1153 h^{-1} at 80 ºC and 35 bar. Indeed, these complexes have also shown activity for PO copolymerization.[120] Complex **46** (Figure 1.21) produce PPC with a TOF of 192 h^{-1} at 60 ºC and 34 bar, with 93 % of polymer selectivity, 99 % of carbonate linkages and high molecular weights in the range of 13000-26000, with PDIs around 1.10.[121]
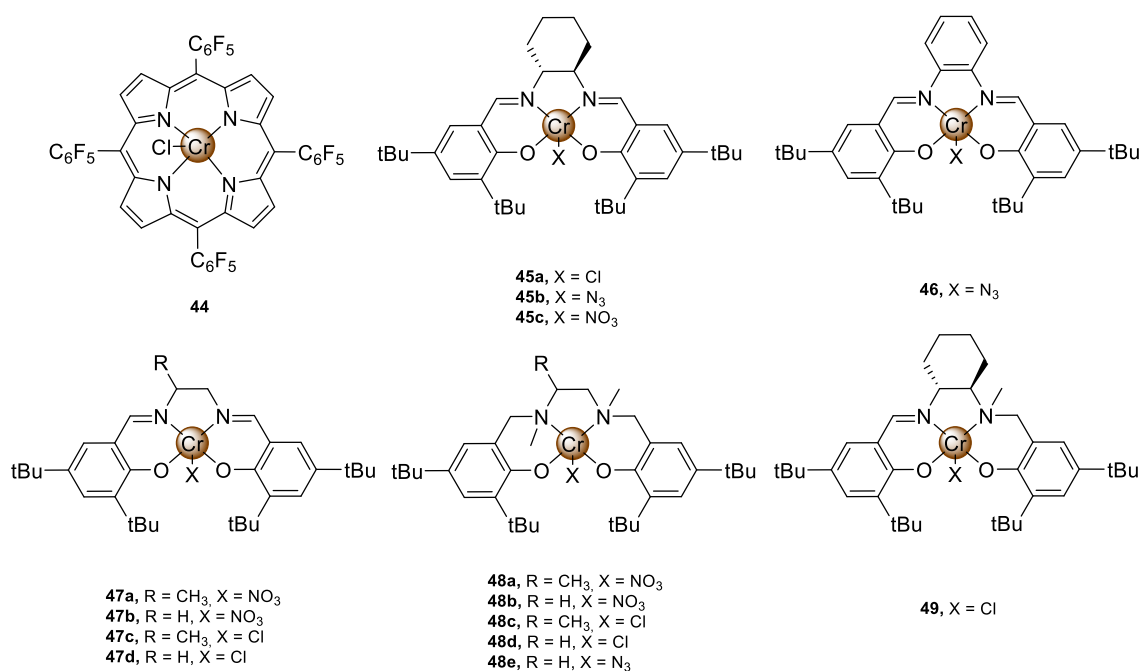
Figure 1.21. Chromium porphyrin, salen and salan complexes.

More recently, Rao and co-workers reported a variety of chromium salan complexes **48a-e** (Figure 1.21), with DMAP as co-catalyst. These complexes were found to be up to 30 times more active for the copolymerization of PO and CO_2 than salen analogs **47a-d** (Figure 1.21).[122] The differences in the activity was proposed to be

due to the sp^3 hybridized amino donors in the salan ligands reducing the electrophilicity of the metal center and facilitating reversible epoxide/DMAP binding. It was proposed that the dissociation and re-association of DMAP and growing chains was essential for high activity.[122] ESI mass spectrometry of copolymers, at low conversions, showed DMAP as a chain end-group and demonstrating that bases can initiate the copolymerization and suggesting reversible coordination to the metal center. The active species was proposed to be [(salan/salen)-CrX(DMAP)] (C in Scheme 1.12), observed using *in situ* ESI-MS upon the combination of salan complexes with DMAP and also with NMIM. It was observed in the mass spectra that salen complexes formed [salenCr(DMAP)$_2$]$^+$ (B in Scheme 1.12), corroborating the stronger binding of DMAP with more electrophilic salen complexes.

Half-reduced "salalen" complexes were also active with CHO; for instance, complex **49** (Figure 1.21) and 1 equivalent of PPNCl produced PCHC with a TOF of 230 h^{-1}, at 70 ºC and 34 bar.[123]
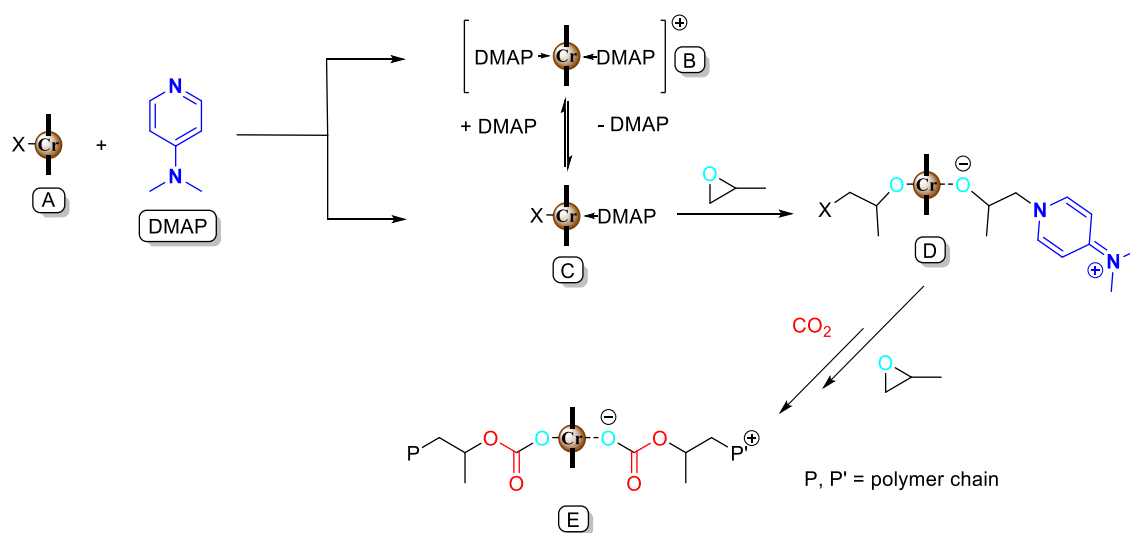
Scheme 1.12. Proposed mechanism of copolymerization with [(salen/salan)CrC] and DMAP.

1.2.2.5 *Other active catalysts*

Together with chromium salen complexes, cobalt analogues are the most powerful catalysts for polycarbonate formation. However, chromium catalysts are more active towards PCHC and cobalt ones towards the formation of PPC.

The most significant development involving the use of cobalt salen catalysts was discovered by Coates and co-workers in 2003 for the effective production of PPC from *rac*-propylene oxide and CO_2.[124] Complexes **50a-e** (Figure 1.22) were found to provide PPC in > 99 % selectivity with 90-99 % carbonate linkages at a CO_2 pressure of 55 bar, at room temperature and in the absence of co-catalyst, with TOFs over a range of 17-81 h^{-1}.

Another important discovery was found by Nozaki and co-workers with a novel cobalt salen catalyst with two "side arms" bearing piperidine and piperidinium groups (**51**) (Figure 1.22). The protonated piperidinium arm was proposed to prevent cyclic carbonate formation by protonating the copolymer chain upon the dissociation from the metal center, preventing the backbiting reaction that leads to the cyclic carbonate.[109] This discovery has led to the development of other two-component catalysts (or so called bifunctional systems) with specially designed arms, which act also as a co-catalyst, leading to both activity and selectivity improvements (**52-53**) (Figure 1.22).[125,126]

50a, X = OAc
50b, X = OBzF$_5$
50c, X = 2,4-dinitrophenolate (DNP)
50d, X = OOCCCl$_3$
50e, X = Br

51

52, X = DNP

53a, R = tBu
53b, R = ^{i}Pr
53c, R = Me
X = DNP
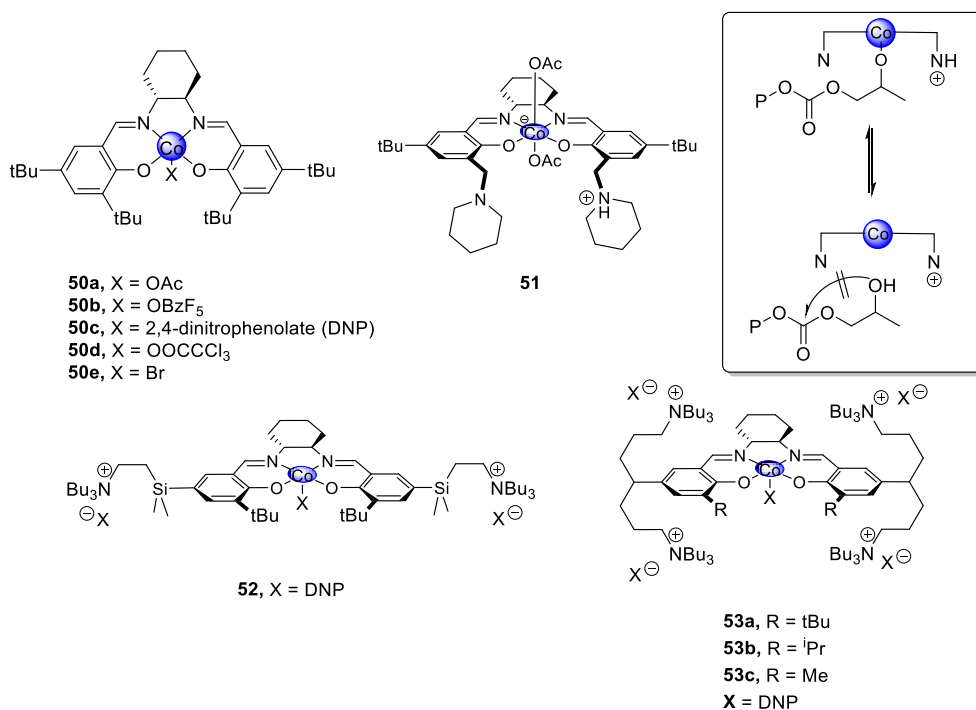
Figure 1.22. Different cobalt salen catalysts for copolymerization of PO and CO_2.

Various zinc catalysts were also found to be highly active for copolymerization reaction. In 1995, Darensbourg and Holtcamp reported the first discrete zinc complexes for the alternating copolymerization of epoxides and CO_2.[103] After this discovery some

different families of zinc catalytic systems were developed, such as: i) zinc dimmeric phenolates, studied by Darensbourg and co-workers, which promoted CO_2/CHO copolymerization efficiently (**54**, Figure 1.23); ii) β-diiminate (BDI) zinc catalysts, reported by Coates and co-workers (**55** and **56**, Figure 1.23), where complex **56** gave an high TOF of 2290 h^{-1};[104] iii) [L^{n}Zn$_2$(OX)$_n$] (where X = Et, Ac and n = 1, 2) and L was based on N,N,O-Schiff base ligands (**57, 58**, Figure 1.23);[127] iv) and anilide-aldimine zinc complexes (**59a-g**, Figure 1.23) with the highest TOF of 200 h^{-1} obtained with complex **59c**.[128]

57a, R = Me, Ar = Ph
57b, R = Me, Ar = 4-MePh
57c, R = Me, Ar = 3-MePh
57d, R = Me, Ar = 4-MeOPh
57e, R = Me, Ar = 4-PhPh
57f, R = Me, Ar = 4-CF$_3$Ph
57g, R = Me, Ar = 3,5-(CF$_3$)$_2$Ph
57h, R = Me, Ar = ClPh
57i, Ar = Ph, R = NO$_2$
57j, Ar = Ph, R = tBu

L$_n$Zn$_2$(OAc)$_2$

X = OAc
58a n = 1, R = tBu
58b n = 2, R = Me
58c n = 3, R = OMe

59a-g X = H

59a, R =^{i}Pr, R' = ^{i}Pr
59b, R = Me, R' = Me
59c, R = Me, R' = ^{i}Pr,
59d, R = Et, R' = Me
59e, R = Et, R' = ^{i}Pr
59f, R = ^{i}Pr,, R' = Et,
59g X = F; R = Me; R' = iPr
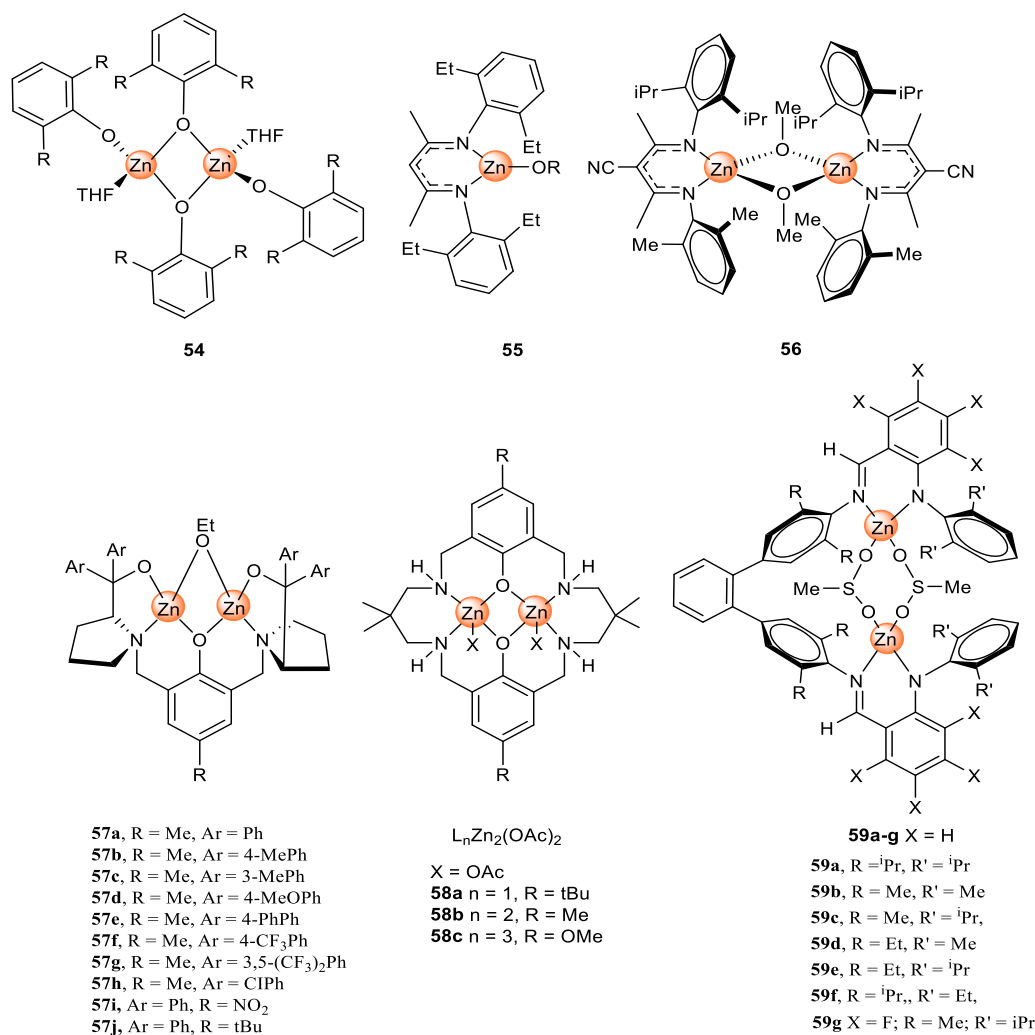
Figure 1.23. Example of copolymerization zinc catalysts.

There are few examples in the literature about iron catalysts for copolymerization reaction. The first example was catalyst **60** (Figure 1.24) reported by Williams and co-workers, which presents a good activity for the copolymerization of

CHO and CO_2 at 10 bar giving a TOF of 107 h^{-1} at 80 ºC. The polymer presented a M_n of up to 17200 and narrow polydispersity of 1.03.[129]

Furthermore, iron(III) amine triphenolate complexes were also found to be excellent catalysts for the copolymerization of CHO and CO_2 (**14** Figure 1.7**, 61a-b,** Figure 1.24). Kleij and co-workers found that the selectivity of the reaction towards the cyclic carbonate or the polycarbonate can be controlled carefully by selecting the co-catalyst used and by varying the ratio between the catalyst and the co-catalyst.[130]
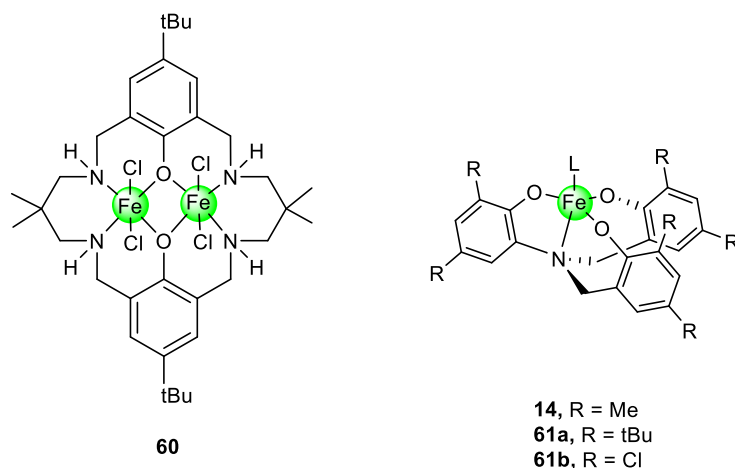
Figure 1.24. Example of iron catalysts for copolymerization reaction.

1.2.2.6 *Copolymerization of CO_2 and other epoxides*

Other alicyclic epoxides were examined as substrates for the copolymerization reaction with CO_2. Chromium salen systems, as well as second generation zinc phenoxide catalysts can convert 1,4-dihydronapthalene oxide **62**, *exo*-norbornene oxide **63**, (+)-limonene oxide **64**, and α-pinene oxide **65** (Figure 1.25) into polycarbonates with very limited success.[131] Importantly, these latter two monomers are of particular interest since these are derived from sustainable resources. Coates and co-workers have reported some encouraging results at copolymerizing *trans*- or *cis*-(*R*)-limonene oxide with CO_2 to produce poly(limonene carbonate).[132] These latter studies utilized *β*-diiminate zinc acetate catalysts, where a TOF of 33 h^{-1} was obtained under mild reaction conditions (35 °C and 6.9 bar CO_2 pressure). More recently, Kleij and coworkers investigated aluminum(III)amine triphenolate/PPNCl (**4b**, Figure 1.4) catalytic system for the same reaction. This catalyst was able to mediate the conversion of both stereoisomers of limonene oxide with a high conversion (up to 71 %) under neat substrate and mild conditions of 42-45 ºC and 5-10 bar of CO_2 pressure.[133]
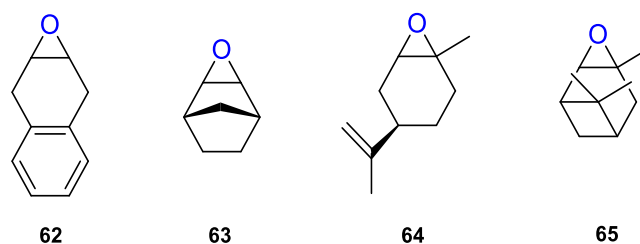
Figure 1.25. Different challenging epoxide substrates.

1.3 Alkene epoxidation

Epoxides or oxiranes are three-membered ring structures in which one of the vertices is oxygen and the other two are carbons. The carbons in an epoxide group are very reactive electrophiles, due in large part to the fact that substantial ring strain is relieved when the ring opens upon nucleophilic attack. This strained ring becomes a particularly interesting molecule for a wide range of intermediate reactions.[134] The epoxides not only are involved in fine chemistry as reactive intermediates, but also are present in molecules with biological activity such as fungicides[135,136] (**66**, Figure 1.26) and pheromones[137] (**67**, **68**, Figure 1.26).
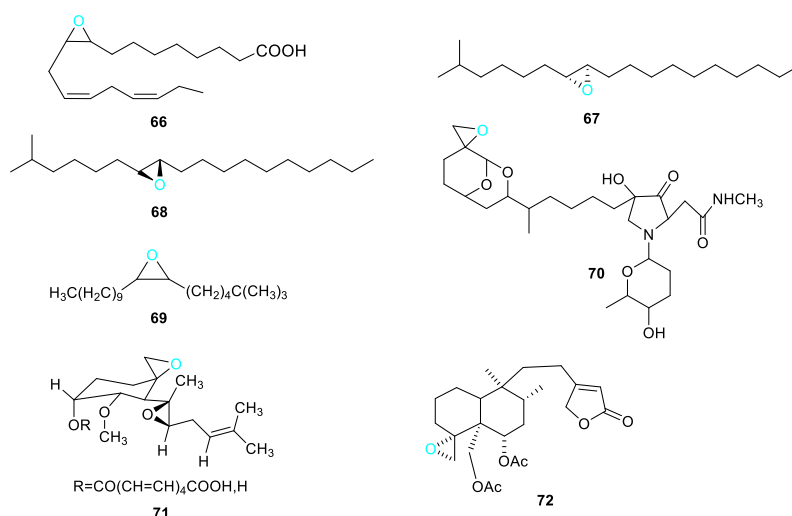
Figure 1.26. Biologically active and natural-derived epoxides.

Some natural epoxides were isolated from plants, insects or microorganisms. These are essentially pheromones[138] (**69**, Figure 1.26), ionophores,[139] (**70**, Figure 1.26), antibiotics[140] (**71**, Figure 1.26) and antibacterial[141] (**72**, Figure 1.26).

Epoxides are normally used as highly reactive intermediates that can be converted into a variety of useful products containing oxygen such as alcohols by

reduction or rearrangement (a and c, Scheme 1.13), ketones by rearrangement (b, Scheme 1.13) or leading to diols, amino alcohols, ketones, polyethers by ring-opening with various nucleophiles (d, Scheme 1.13).
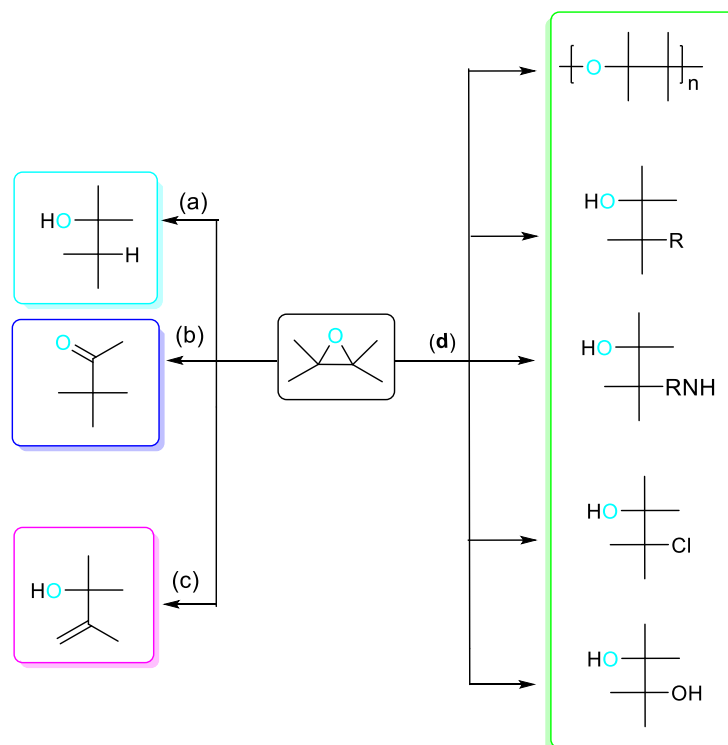
Scheme 1.13. Conversion of epoxides into a variety of useful products.

1.3.1 Synthesis of epoxides by catalytic epoxidation of alkenes

The selective and catalytic oxidation of organic substrates is an important area of research in both academia and industry.[142] Nature has successfully developed the molecular oxygen (O_2) activation and utilizes metalloenzymes to selective oxidize and functionalize hydrocarbons. Iron and copper are the metal of choice for many biological oxidations because of their abundance in the geosphere, inherent electronic properties and accessible redox potential.

1.3.1.1 *Iron-catalyzed olefin epoxidations*

A high number of iron-based enzymes catalyze the stereospecific oxidation of C=C bonds.[143] The most widely studied are the cytochromes P450 which have active sites consisting of a heme group that is attached to the protein backbone at one of the axial positions, leaving the *trans* position of the octahedral iron available for oxygen binding and activation (Figure 1.27). In the general accepted mechanism, molecular

oxygen (O_2) coordinates through the iron center, forming a ferric-hydroperoxo intermediate specie. Then, the heterolysis of the O-O hydroperoxo bond generates a Fe(IV)=O(porhyrin) as the active oxidative catalyst for olefin epoxidation (Figure 1.27).[144]

More recently, non-heme iron enzymes have also shown to promote similar oxidative transformations.[145] Particularly, Rieske dioxygenase family catalyzes the *cis*-dihydroxylation of arene double bonds.[146] These enzymes consist of an iron center facially ligated by two histidines and one aspartate, which is a common binding for oxygen activating non-heme iron enzymes (Figure 1.27).[147] In contrast to the heme-based systems, this complex results in the availability of two *cis* sites for O_2 binding and activation. Moreover, these enzymes carry out preferentially the *cis*-dihydroxylation of C=C bonds, instead of epoxidation.[148]
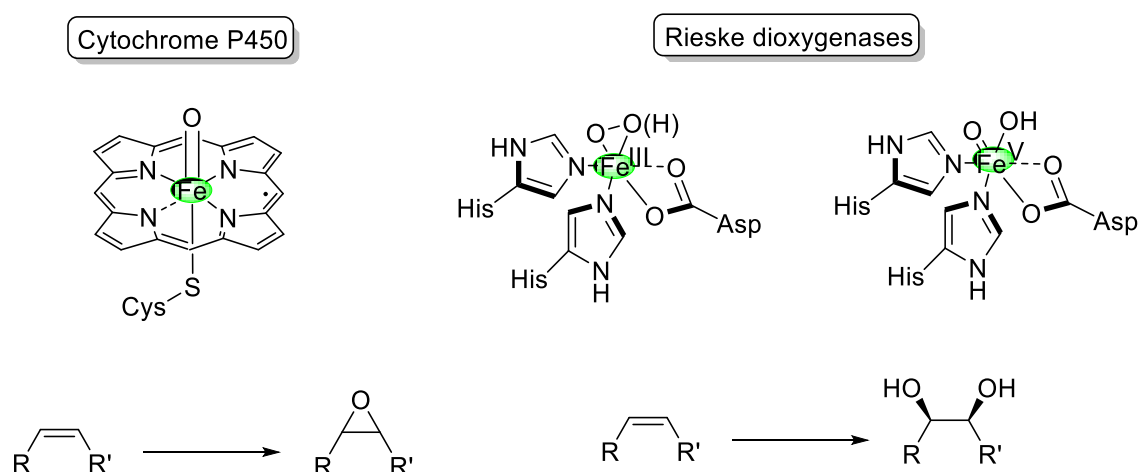
Figure 1.27. Structures of the proposed active oxidants from heme (left) and non-heme (right) iron oxygenases for C=C bond oxidations.

Different sources of oxygen (oxidants) have been used for olefin epoxidation with transition metal catalysts. The most used for iron catalysts are iodosylbenzene (PhIO),[149,150] alkyl peroxides (ROOH),[151] sodium hypochlorite (NaOCl),[152,153,154] peracids,[155] hydrogen peroxide (H_2O_2)[156,157,158,159] and molecular oxygen (O_2).[160]

The crucial task to develop greener industrial products and processes indicate that O_2 and H_2O_2 are the best reagents from economic and environmental considerations. H_2O_2 is the most preferred one considering its low safety risks.[160] Nevertheless, organic hydroperoxides (ROOH) are also relatively inexpensive and

convenient and safe to handle. In addition, organic hydroperoxides can readily be obtained and maintained in anhydrous form.

In fact, the reason of combination the metal complex with an oxidant system, such H_2O_2, is to inhibit the homolytic cleavage of the peroxo O-O bond that produces non-selective and unwanted hydroxyl radicals. Instead, the aim is to promote the cleavage towards the generation of a metal-based oxidant that carry out hydrocarbon oxidations with high chemo-, regio- and stereoselectivity.[161]

1.3.1.1.1 *Iron porphyrins*

Although iron porphyrins are highly active for epoxidation catalysis, the conversions and selectivities obtained tend to be inferior to their manganese analogs. Initially, those iron porphyrins worked only with oxidants such as PhIO and many scientists started to research to understand the epoxidation mechanism with these complexes.[162,163] Traylor and co-workers made some important discoveries in this research area.[164] For example, iron heme systems do not undergo homolytic cleavage to produce radicals and oxoiron intermediates ($Fe^V=O$), but instead, they give heterolytic cleavage to produce oxene species ($Fe^{IV}=O\cdot^+$). This Fe-oxene specie is the desired epoxidation catalyst; however, unconstructive side reactions, such as catalyst decomposition and unselective oxidation, happened when the oxidant and oxene react prior to the epoxidation (Scheme 1.14). Consequently, reactions of Fe-oxene species with the oxidant generate free alkoxy radicals that may partially explain why iron porphyrins have poor activities in catalytic epoxidations. Therefore, Traylor proposed that in order to minimize the radical production protic solvents should be used, as well as, keeping the concentration of the oxidant low, by slow addition.

A. Homolytic cleavage
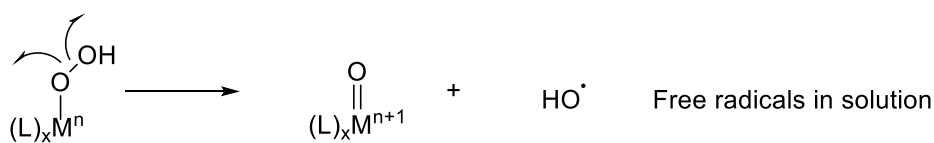
A. Heterolytic cleavage
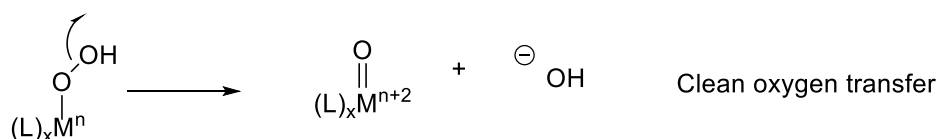
Scheme 1.14. Cleavage pathways for the O-O bond in H_2O_2.

Traylor also found that more electron-deficient porphyrins favored the epoxidation reaction. For instance, highly fluorinated porphyrins **73** (Scheme 1.15) and those with electron-withdrawing groups were shown to catalyze epoxidation of alkenes with H_2O_2.[165,166]

73 X = H or F
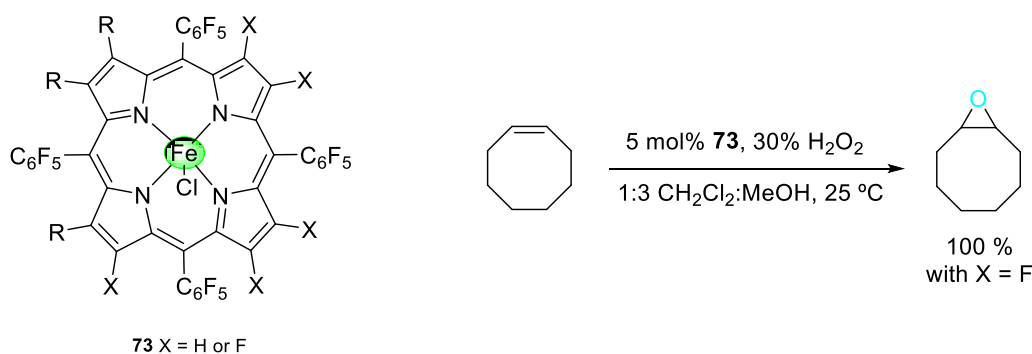
Scheme 1.15. Epoxidation with electron-poor iron porphyrin and protic solvent.

Sometimes imidazole was added into the epoxidation reaction as a co-catalyst. So, to deduce the role of imidazole in the iron porphyrin epoxidations, labeled water was used. If imidazole was added to the reaction, at 25 ºC, no incorporation of ^{18}O from water was observed. This suggests that imidazole coordinates to the axial position of the porphyrin that water originally occupied preventing a redox tautomerization of coordinated water with the oxo-ligand. Thus, imidazole additives can prevent axial coordination of water and attenuate the reactivity of the porphyrin complex. In fact,

even electron-rich porphyrins could be good catalysts if the reactions are performed in aprotic solvents and with imidazole additive (Table 1.1).[167]

The effect of using protic or aprotic solvents has been studied using competition experiments with different alkenes and oxidant sources.[168] In this study, reactions using *cis*- and *trans*-stilbene or cyclooctene were tested using H_2O_2, *m*-CPBA, or *t*-BuOOH in both protic and aprotic media. It was expected that if a common intermediate species was formed, similar ratios of products should be obtained. In protic solvents, all the oxidants gave the same ratio of products for a given catalyst. However, in aprotic solvents, the product ratios were dependent on the oxidant suggesting that the oxidizing species vary in aprotic solvent with the oxidant used.

Table 1.1. Effect of additive in the epoxidation of cyclohexene mediated by iron porphyrin complexes **73-76**.

73 R = H
74 R= 2,4,6-Me$_3$C$_6$H$_3$
75 R= 2,6-Cl$_2$C$_6$H$_3$
76 R= 2,6-F$_2$C$_6$H$_3$
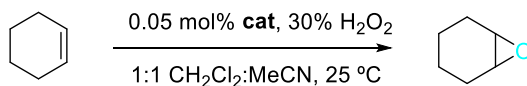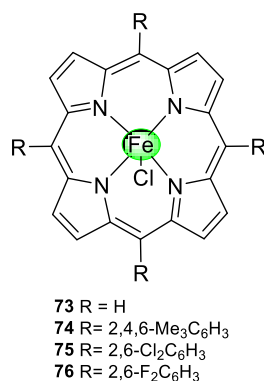
Catalyst	Yield (%)[a]	Yield with additive[b] (%)[a]
73	<2	51
74	0	63
75	0	79
76	<2	65

[a]Yield based on H_2O_2 used. [b]Additive = 5 mol% 5-chloro-1-methylimidazole.

For protic solvents, the reactive intermediate seems to be the highvalent Fe^{IV}-porphyrin radical cation complex formed by an iron hydroperoxide precursor (Scheme 1.16, pathway A). In aprotic solvents, the reactive intermediate is the iron hydroperoxide complex itself (Scheme 1.16, pathway B).
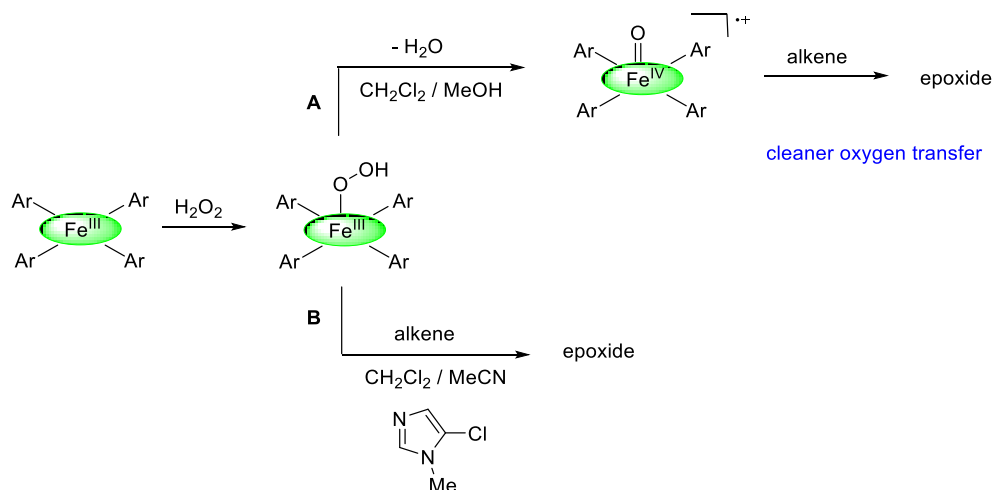
Scheme 1.16. Two distinct pathways for iron porphyrin epoxidation depending on the solvent used.

The data obtained with iron porphyrins epoxidation reflects the dependence on the electronic structure of the porphyrin ligand, the additives, and also the solvent used.

1.3.1.1.2 *Iron pyridyl-amine complexes*

Ligands bearing pyridine and amine groups from the perspective of biomimetic, nonheme catalysts, have been investigated by Que and co-workers among others.[169,170,171] The most representative ligands **77-85** (Figure 1.28) form octahedral mono- or dinuclear complexes with iron. Some of these complexes exhibit moderate epoxidation and/or dihydroxylation activity with H_2O_2.
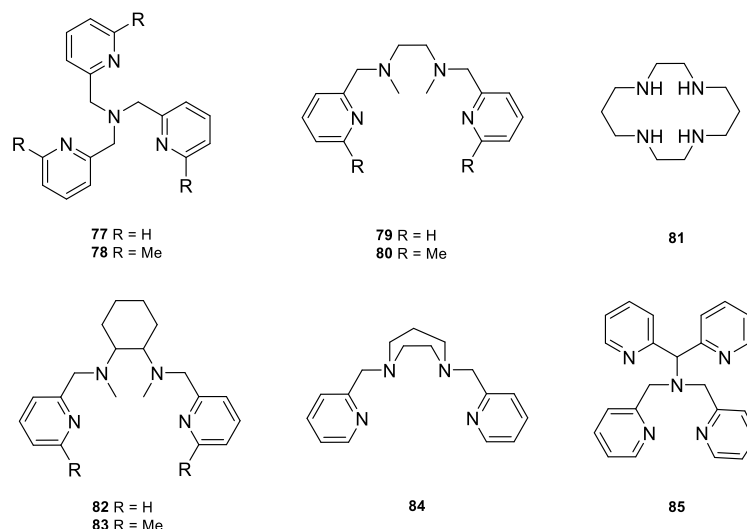
Figure 1.28. Some representative ligands used in nonheme biomimetic catalysts.

Some mechanistic studies explain why some of these catalysts yield epoxides while similar ones produce diols.[172] Figure 1.29 compares representative structures of non-heme iron for olefin oxidation catalysts and their relative oxidative preference.
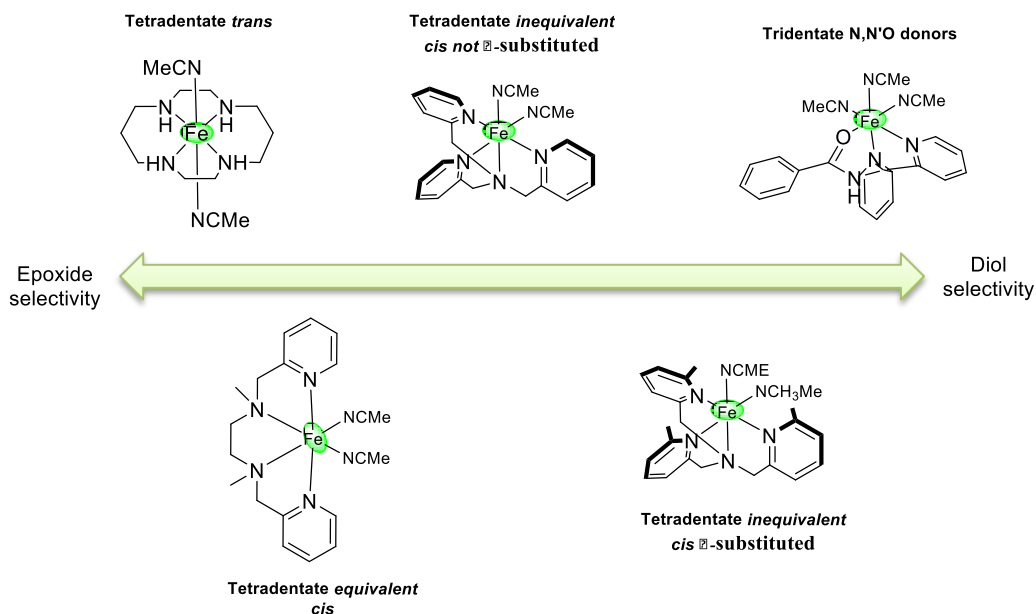
Figure 1.29. The epoxidation-dihydroxylation selectivity with representative nonheme iron catalysts with different ligand topology.

Pentadentated complexes, such as **85** (Figure 1.28)**,** favor epoxidation but with low stereoselectivity and catalyst activity.[173] Catalysts bearing tetradentate ligands that adopt a *trans* topology are highly epoxidation selective as they resemble to heme

systems.[174] Also, highly selective catalysts for epoxidation are tetradentate complexes that have equivalent *cis*-labile sites (Figure 1.29). However, the addition of water can increase the amount of diol product formed.[175]

Catalysts bearing inequivalent *cis*-labile sites (Figure 1.29), favor *cis*-dihydroxylation.[176] Also, those catalysts with α-methylated pyridil rings produce diol and those with no α-methylated groups are much more epoxide selective.[177] Thus, the ligand topology is an important factor that determines the selectivity of the oxidation reaction.

1.4 *Supercritical fluids*

In the reactions where carbon dioxide is employed as a reactant, it can be also considered the possibility of avoiding the use of co-solvents and running the reaction in compressed or supercritical CO_2 as the reaction media. In this section we present some considerations about the use of scCO$_2$ as a solvent.

A supercritical fluid (SCF) is any substance at pressure and temperature above its critical point. The critical point of a pure substance is defined as the end point of the gas-liquid separation line (evaporation or dew line) and characterized by the critical temperature T_c, the critical pressure P_c, and the corresponding critical density δ_c. Beyond this point, no distinct gas or liquid phase can exist and the supercritical fluid combines both gas-like, such as compression, and liquid-like, such as liquid density and therefore its characteristic dissolving power.[178,179]

Among the different supercritical fluids, carbon dioxide and water are considered the most environmentally benign alternative solvents for chemical synthesis.[180] Particularly, CO_2 has certainly attracted the largest interest because of several advantages such as inexpensive, non-flammable, readily available and totally miscible with gases.[180,181] Moreover, its non-toxicity makes CO_2 to be considered as a "green" solvent if compared with regular solvents such as cholofluorocarbons. An example where CO_2 represents a plausible alternative to avoid the use of chlorinated solvents is in the dry cleaning technology.[182]

In addition, unlike water, the supercritical regime of CO_2 is readily accessible, with a low critical temperature and pressure (T_c = 31.1 ºC, P_c = 73.8 bar) and critical density (δ_c = 0.468 g/ml) (Figure 1.30). Since these critical values are closed to ambient

conditions, CO_2 could be used in applications involving highly sensitive materials like enzymes and flavors.[183] Indeed, some food industries perform the extraction of caffeine from coffee beans using scCO_2 in replacement of toxic dichloromethane solvent.[184] Moreover, CO_2 can be easily depressurized at the end of a synthetic process without any traces of toxic residues. This clear advantage of no solvent contamination of the product is a benefit for many chemical processes, which eliminates the need of high expensive dying processes.
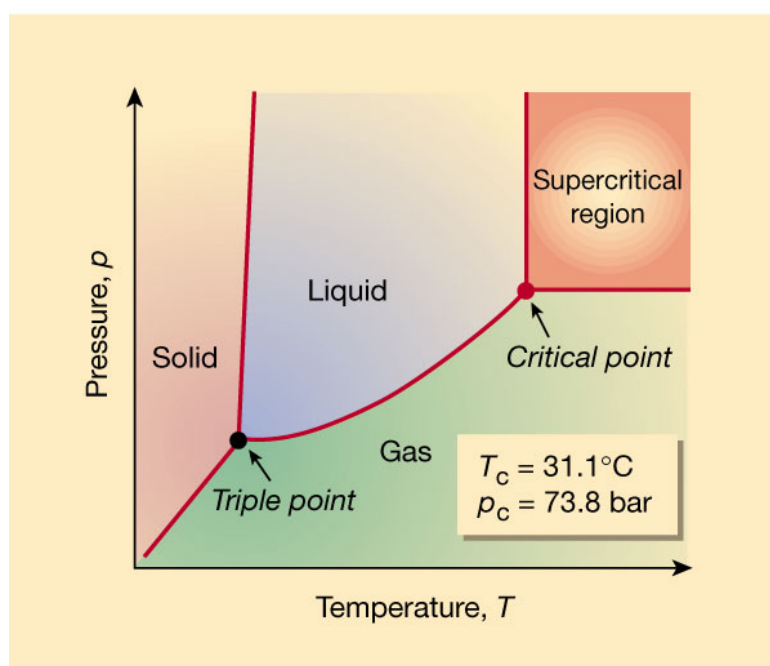
Figure 1.30. Qualitative representation of the CO_2 phase diagram.[185]

Using a reactor equipped with sapphire windows, the CO_2 phases can be easily observed. When the reactor is pressurized at vapor pressure, two separated phases can be observed, where the meniscus is clearly defined (Figure 1.31a). With an increase of temperature, the meniscus begins to diminish and further causes the gas and liquid densities become more similar (Figure 1.31b). Once the critical temperature and pressure have been reached the two distinct phases are no longer visible but only one homogeneous phase is observed (Figure 1.31c).

(a)   *(b)*   *(c)*
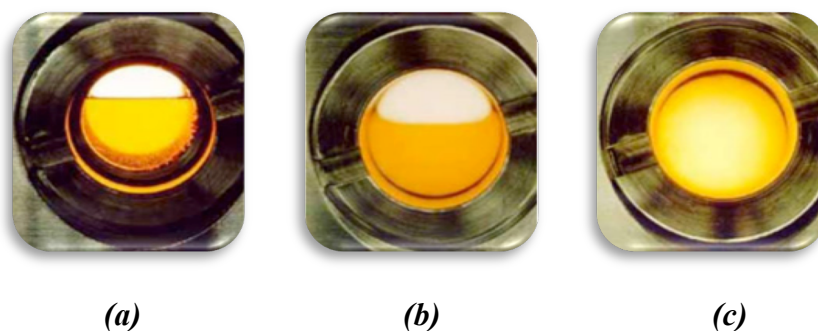
Figure 1.31. Phases adopted by carbon dioxide.[181]

However, carbon dioxide exhibits some inherent disadvantages such as low dielectric constant ($\varepsilon \approx 1.5$ in the liquid state, and supercritical CO_2 exhibit values between 1.1 and 1.5, depending upon density). This low dielectric constant implies that only non-polar catalysts will dissolve in $scCO_2$. The few exceptions that can dissolve more polar substances are either expensive (for example fluoroform, with a liquid dielectric constant of $\varepsilon \approx 10$) or toxic (CO, PF_3). In homogeneous catalysis, where the catalysts are often polar substances, the CO_2 does not seem to be the best solvent option, especially in the presence of highly polar functional groups such as charged complexes and non-polar complexes with many aryl-substituted ligands which strongly reduce the solubility.[186]

Nevertheless, the solubility of transition metal complexes could be adjusted by some ligand modification.[179] For example, replacing ligands containing aryl substituents with ligands containing alkyl groups,[187] and, even more, by CO_2-philic groups such as perfluoroalkyl, fluoro ether, or silicone groups, the solubility of metal complexes can be further improved.[188,189] Normally, perfluoroalkyl groups called "ponytails" ($-(CH_2)_x$-$(CF_2)_y$-CF_3) are introduced in *meta* or *para* position of the aryl groups. Generally, better solubilities are obtained when the fluorinated alkyl chain is longer.[190,182] Some examples of fluorinated ligands used in $scCO_2$ media are depicted in Figure 1.32.[179,191,192,193,194]

Moreover, another approach to increase the solubility of complexes could be the addition of co-solvents or surfactants.[195] Lin *et al.* found that 5 % of methanol quadrupled the solubility of bis(diethyldithiocarbamate)mercury(II) in $scCO_2$.[196] Also Cowey *et al.* found that a 10 % of methanol greatly enhance the solubility of a nickel complex with a cyclic tetraamine ligand. This Ni(II) complex was not soluble in $scCO_2$ in the absence of methanol.[197]
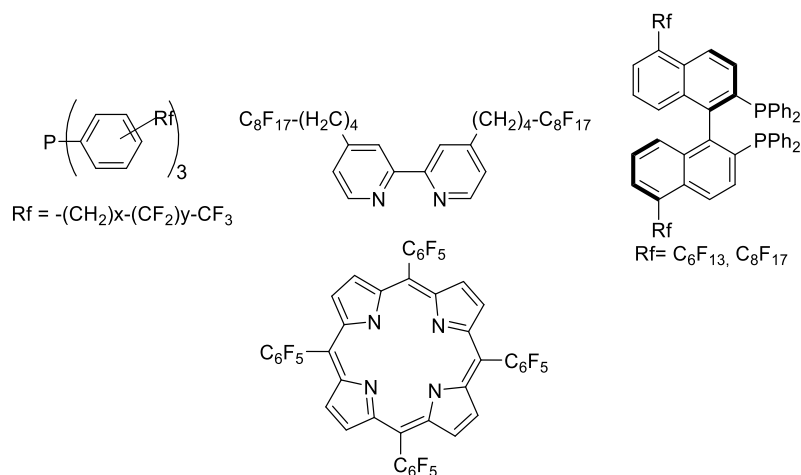
Figure 1.22. Some examples of perfluorinated ligands used in $scCO_2$.

Furthermore, cationic catalysts are proved to be useful in $scCO_2$ if the anion is soluble enough in this media. In the same way as previous ligands, the solubility of the complexes increases when the anion is large and highly fluorinated. Burk and co-workers [198] cited CO_2-philic anions such as $BArF^-$ (tetrakis(3,5-bis (trifluoromethyl)phenyl)borate) and CF_3SO_3 which enhances the solubility of their cationic rhodium complexes.

In conclusion, the use of compressed CO_2 (liquid or supercritical) can be considered to increase the CO_2 availability in the reaction phase although the solubility of the catalyst has to be also considered.

1.5   References

[1]   Organization for Economic Cooperation and Development (OECD); https://www.migreenchemistry.org/toolbox/definition-of-green-chemistry/ accessed online 11/08/2015.

[2]   Anastas, P. T.; Warner, J. C.; *Green Chemistry: Theory and practice*, Oxford University Press, **1998**, New York (USA).

[3]   Corma, A.; Iborra, S.; Velty, A., *Chem. Rev.* **2007**, *107*, 2411-2502.

[4]   Sakakura, T.; Choi, J.-C.; Yasuda, H., *Chem. Rev.* **2007**, *107*, 2365-2387.

[5]   Markewitz, P.; Kuckshinrichs, W.; Leitner, W.; Linssen, J.; Zapp, P.; Bongartz, R.; Schreiber, A.; Müller, T. E. *Energy Environ. Sci.* **2012**, *5*, 7281-7305.

[6]   Müller, T. E.; Leitner, W., *Beilstein J. Org. Chem.* **2015**, *11*, 675-677.

7   Aresta, M.; Dibenedetto, A.; Angelini, A. *Chem. Rev.* **2014**, *114*, 1709-1742.

8   Sakakura, T.; Choi, J.-C.; Yasuda, H. *Chem. Rev.* **2007**, *107*, 2365-2387.

9   Cokoja, M.; Bruckmeier, C.; Rieger, B.; Herrmann, W. A.; Kühn, F. E. *Angew. Chem., Int. Ed.* **2011**, *50*, 8510-8537.

10   Martin, R.; Kleij, A. W. *ChemSusChem* **2011**, *4*, 1259-1263.

11   Kielland, N.; Whiteoak, C. J.; Kleij, A. W. *Adv. Synth. Catal.* **2013**, *355*, 2115-2138.

12   Peters, M.; Köhler, B.; Kuckshinrichs, W.; Leitner, W.; Markewitz, P.; Müller, T. E. *ChemSusChem* **2011**, *4*, 1216-1240.

13   Tsuji, Y.; Fujihara, T. *Chem. Commun.* **2012**, *48*, 9956-9964.

14   Boogaerts, I. I. F.; Nolan, S. P. *Chem. Commun.* **2011**, *47*, 3021-3024.

15   Maeda, C.; Miyazaki, Y.; Ema, T. *Catal. Sci. Technol.* **2014**, *4*, 1482-1497.

16   Martín, C.; Fiorani, G.; Kleij, A. W., *ACS Catal.* **2015**, *5*, 1353-1370.

17   Aresta, M.; *Carbon Dioxide as Chemical Feedstock*, Wiley-VCH, **2010**, Weinheim.

18   North, M.; Pasquale, R.; Young, C., *Green Chem.* **2010**, *12*, 1514-1539.

19   Sakakura, T.; Kohno, K., *Chem. Commun.* **2009**, 1312-1330.

20   Coates, G. W.; Moore, D. R., *Angew. Chem, Int. Ed.*, **2004**, *43*, 6618-6639.

21   Darensbourg, D. J., *Chem. Rev.* **2007**, *107*, 2388-2410.

22   Kember, M. R.; Buchard, A.; Williams, C. K., *Chem. Commun.* **2011**, *47*, 141-163.

23   Li, Y.; Junge, K.; Beller, M., *ChemCatChem* **2013**, *5*, 1072-1074.

24   Cui, Z.-M.; Chen, Z.; Cao, C.-Y.; Song, W.-G.; Jiang, L., *Chem. Commun.* **2013**, *49*, 6093-6095.

25   Fleischer, M.; Blattmann, H.; Mülhaupt, R., *Green Chem.* **2013**, *15*, 934-942.

26   Nohra, B.; Candy, L.; Blanco, J.-F.; Guerin, C.; Raoul, Y.; Mouloungui, Z., *Macromolecules* **2013**, *46*, 3771-3792.

27   Etacheri, V.; Marom, R.; Elazari, R.; Salitra, G.; Aurbach, D. *Energy Environ. Sci.* **2011**, *4*, 3243-3262.

28   Marquis, T.; Baldwin, R.; Machac, J.; Darragas, K.; Woodrum, S. U.S. Patent 6169061, **2001**.

29 Beattie, C.; North, M.; Villuendas, P. *Molecules* **2011**, *16*, 3420-3432.

30 Schäffner, B.; Schäffner, F.; Verevkin, S. P.; Börner, A., *Chem. Rev,* **2010,** *110,* 4554-4581.

31 Shaikh, A.-A. G.; Sivaram, S., *Chem. Rev.* **1996,** *96*, 951-976

32 Liu, Z.; Jensen, V; Fenical, W., *Phytochemistry* **2003**, *64*, 571-574.

33 Davis, R. A.; Andjic, V.; Kotiw, M.; Shivas, R. G., *Phytochemistry* **2005**, *66*, 2771-2775.

34 Gauthier, J. Y.; Leblanc, Y.; Black, W. C.; Chan, C.-C.; Cromlish, W. A.; Gordon, R.; Kennedey, B. P.; Lau, C. K.; Léger, S.; Wang, Z.; Ethier, D.; Guay, J.; Mancini, J.; Riendeau, D.; Tagari, P.; Vickers, P.; Wong, E.; Xu, L.; Prasit, P., *Bioorg. Med. Chem. Lett.* **1996**, *6*, 87-92.

35 Decortes, A.; Castilla, A. M.; Kleij, A. W., *Angew. Chem., Int. Ed.* **2010**, *49*, 9822-9837.

36 Fukuoka, S.; Kawamura, M.; Komiya, K.; Tojo, M.; Hachiya, H.; Hasegawa, K.; Aminaka, M.; Okamoto, H.; Fukawa, I.; Konno, S., *Green Chem.* **2003**, *5*, 497-507.

37 Lu, X.-B.; Darensbourg, D. J., *Chem. Soc. Rev.* **2012**, *41*, 1462-1484.

38 Rokicki, G.; Kuran, W.; Pogorzelska-Marciniak, B., *Monatsh. Chem.* **1984**, *115*, 205-214.

39 Song, J.; Zhang, Z.; Han, B.; Hu, S.; Li, W.; Xie, Y., *Green Chem.* **2008**, *10*, 1337-1341.

40 Yu, T.; Weiss, R. G., *Green Chem.* **2012**, *14*, 209-216.

41 Comerford, J. W.; Ingram, I. D. V.; North, M., *Green Chem.* **2015,** *4*, 1966-1987.

42 Takeda, N.; Inoue, S., *Bull. Chem. Soc. Jpn.* **1978**, *51*, 3564-3567.

43 Aida, T.; Inoue, S., *J. Am. Chem. Soc.* **1983**, *105*, 1304-1309.

44 Kasuga, K.; Kato, T.; Kabata, N.; Handa, M., *Bull. Chem. Soc. Jpn.* **1996**, *69*, 2885-2888.

45 Ji, D.; Lu, X.; He, R., *Appl. Catal. A:General* **2000**, *203*, 329-333.

46 Licini, G.; Mba, M.; Zonta, C., *Dalton Trans.* **2009**, 5265-5277.

47 Whiteoak, C. J.; Kielland, N.; Laserna, V.; Escudero- Adán, E. C.; Martin, E.; Kleij, A. W., *J. Am. Chem. Soc.* **2013**, *135*, 1228-1231.

48   Whiteoak, C. J.; Kielland, N.; Laserna, V.; Castro-Gómez, V.; Martin, E.; Escudero-Adán, E. C.; Bo, C.; Kleij, A. W., *Chem. Eur. J.* **2014**, *20*, 2264-2275.

49   Darensbourg, D. J.; Yarbrough, *J. Am. Chem. Soc.* **2002**, *124*, 6335-6342.

50   Darensbourg, D. J.; Moncada, A. I., *Macromolecules* **2010**, *43*, 5996-6003.

51   Lu, X.-B.; Feng, X.-J.; He, R., *Appl. Catal. A: General* **2002**, *234*, 25-33.

52   Lu, X.-B.; Zhang, Y.-J. Jin, K.; Luo, L.-M.; Wang, H., *J. Catal.* **2004**, *227*, 537-541.

53   Lu, X.-B.; Zhang, Y.-J.; Liang, B.; Li, X.; Wang, H., *J. Mol. Catal. A: Chem.* **2004**, *210*, 31-34.

54   Tian, D.; Liu, B.; Gan, Q.; Li, H.; Darensbourg, D. J., *ACS Catal.* **2012**, *2*, 2029-2035.

55   Luo, R.; Zhou, X.; Chen, S.; Li, Y.; Zhou, L.; Ji, H., *Green Chem.* **2014**, *16*, 1496-1506.

56   Supasitmongkol, S.; Styring, P., *Catal. Sci. Technol.* **2014**, *4*, 1622-1630.

57   Meléndez, J.; North, M.; Pasquale, R., *Eur. J. Inorg. Chem.* **2007**, 3323-3326.

58   Clegg, W.; Harrington, R.; North, M.; Pasquale, R. *Chem.Eur. J.* **2010**, *16*, 6828-6843.

59   North, M.; Pasquale, R., *Angew. Chem., Int. Ed.* **2009**, *48*, 2946-2948.

60   Meléndez, J.; North, M.; Villuendas, P., *Chem. Commun.* **2009**, 2577-2579.

61   North, M.; Villuendas, P.; Young, C., *Chem.Eur. J.* **2009**, *15*, 11454-11457.

62   Taherimehr, M.; Al-Amsyar, S. M.; Whiteoak, C. J.; Kleij, A. W.; Pescarmona, P. P., *Green Chem.* **2013**, *15*, 3083-3090.

63   Whiteoak, C. J.; Martin, E.; Escudero-Adán, E.; Kleij, A. W., *Adv. Synth. Catal.* **2013**, *355*, 2233-2239.

64   Taherimehr, M.; Cardoso Costa Sertã, J. P.; Kleij, A. W.; Whiteoak, C. J.; Pescarmona, P. P., *ChemSusChem.* **2015**, *8*, 1034-1042.

65   Buchard, A.; Kember, M. R.; Sandeman, K. G.; Williams, C. K., *Chem. Commun.* **2011**, *47*, 212-214.

66   Dengler, J. E.; Lehenmeier, M. W.; Klaus, S.; Anderson, C. E.; Herdtweck, E.; Rieger, B., *Eur. J. Inorg. Chem.* **2011**, 336-343.

[67]   Fuchs, M. A.; Zevaco, T. A.; Ember, E.; Walter, O.: Held, I.; Dinjus, V; Döring, M., *Dalton Trans.* **2013**, *42*, 5322-5329.

[68]   Adolph, M.; Zevaco, T. A.; Altesleben, C.; Walter, O.; Dinjus, E., *Dalton Trans.* **2014**, *43*, 3285-3296.

[69]   Sunjuk, M.; Abu-Surrah, A. S.; Al-Ramahi, E.; Qaroush, A. K.; Saleh, A. *Transition Met. Chem.* **2013**, *38*, 253-257.

[70]   Bai, D.; Wang, X.; Song, Y.; Li, B.; Zhang, L.; Yan, P.; Jing, H., *Chin. J. Catal.*, **2010**, *31*, 176-180.

[71]   Salga, M. S.; Ali, H. M.; Abdulla, M. A.; AbdelwahabInt, S. I., *Int. J. Mol. Sci.* **2012**, *13*, 1393-1404.

[72]   Darensbourg, D. J.; Holtcamp, M. W., *Coord. Chem. Rev.* **1996**, *153*, 155-174.

[73]   Decortes, A.; Martinez-Belmonte, M.; Benet-Buchholz, J.; Kleij, A. W. *Chem. Commun.* **2010,** *46,* 4580-4582.

[74]   Decortes, A.; Kleij, A. W. *ChemCatChem* **2011,** *3,* 831–834.

[75]   Martin, C.; Whiteoak, C. J.; Martin, E.; Martinez-Belmonte, M.; Escudero-Adán, E. C.; Kleij, A. W. *Catal. Sci. Technol.* **2014,** *4,* 1615–1621.

[76]   Martín, C., Kleij, A. W.; *Beilstein J. Org. Chem.* **2014**, *10,* 1817-1825.

[77]   Fuchs, M. A.; Staudt, S.; Altesleben, C.; Walter, O.; Zevaco, T. A.; Dinjus, E., *Dalton Trans.* **2014**, *43*, 2344-2347.

[78]   Wang, Z.; Bu, Z.; Cao, T.; Ren, T.; Yang, L.; Li, W., *Polyhedron* **2012**, *32*, 86-89.

[79]   Babu, H. V.; Muralidharan, K., *Dalton Trans.* **2013**, *42*, 1238-1248.

[80]   Chen, T.-Y.; Li, C.-Y.; Tsai, C.-Y.; Li, C.-H.; Chang, C.-H.; Ko, B.-T.; Chang, C.-Y.; Lin, C.-H.; Huang, H.-Y., *J. Organomet. Chem.* **2014**, *754*, 16-25.

[81]   Kruper, W. J.; Dellar, D. V., *J. Org. Chem.* **1995**, *60*, 725-727.

[82]   Paddock, R. L.; Hiyama, Y.; McKay, J. M.; Nguyen, S. T., *Tetrahedron Lett.* **2004**, *45*, 2023-2026.

[83]   Jin, L.; Jing, H.; Chang, T.; Bu, X.; Wang, L.; Liu, Z., *J. Mol. Catal. A Chem.* **2007**, *261,* 262-266.

[84]   Paddock, R. L.; Nguyen, S. T., *J. Am. Chem. Soc.* **2001**, *123*, 11498-11499.

[85]   Darensbourg, D. J.; Yarbrough, J. C.; Ortiz, C.; Fang, C. C., *J. Am. Chem. Soc.* **2003**, *125,* 7586-7591.

86 Darensbourg, D. J.; Fang, V.; Rodgers, J. L., *Organometallics* **2004**, *23*, 924-927.

87 Lu, X.-B.; Liang, B.; Zhang, Y.-J.; Tian, Y.-Z.; Wang, Y.-M.; Bai, C.-X.; Wang, H.; Zhang, R., *J. Am. Chem. Soc.* **2004**, *126*, 3732-3733.

88 Paddock, R. L.; Nguyen, S. T., *Chem. Commun.* **2004**, 1622-1623.

89 Jutz, F.; Grunwaldt, J.-D.; Baiker, A., *J. Mol. Catal. A: Chem.* **2008**, *279*, 94-103.

90 (*a*) Aresta, M.; Quaranta, E. *J. Mol. Catal.* **1987**, *41*, 355-359; (*b*) Aresta, M.; Dibenedetto, A.; Tommasi, I. *Appl. Organomet. Chem.* **2000**, *14*, 799-802.(c) Aresta, M.; Dibenedetto, A., *J. Mol. Catal. A Chem.* **2002**, *182-183,* 399-409.

91 Sun, J.; Fujita, S.-I.; Bhanage, B. M.; Arai, M., *Catal. Today* **2004**, *93-95*, 383-388.

92 Sun, J.; Fujita, S.-I.; Zhao, F.; Hasegawa, M.; Arai, M., *J. Catal.* **2005**, *230*, 398-405.

93 Ramidi, P.; Felton, C. M.; Subedi, B. P.; Zhou, H.; Tian, Z. R.; Gartia, Y.; Pierce, B. S.; Ghosh, A., *J. CO$_2$ Util.* **2015**, *9,* 48-57.

94 Langanke, J.; Greiner, L.: Leitner, W., *Green Chem.* **2013**, *15*, 1173-1182.

95 a) Doll, K. M.; Erhan, S. Z.; *J. Agric. Food Chem.* **2005**, *53*, 9608-9614. b) Doll, K. M.; Erhan, S. Z., *Green Chem.* **2005**, *7*, 849-854. c) Meissner, A.; Scholz, P.; Ondruschka, B., *Collect. Czech. Chem. Commun.* **2008**, *73*, 88-96.

96 Tamami, B.; Sohn, S.; Wilkes, G. L., *J. Appl. Polym. Sci.* **2004**, *92*, 883-891.

97 Coates, W.G.; Jeske, R.C., Anastas, P. T. (Ed.) and Crabtree R.H. (Ed.) *Handbook of Green Chemistry-Green Catalysis Vol. 1: Homogeneous Catalysis*, Weinheim (Deutschland), WILEY-VCH, **2009**, 343-373.

98 English, N. J.; El-Hendawy, M. M.; Mooney, D. A.; MacElroy, J. M. D.; *Coord. Chem. Rev.* **2014**, *269,* 85-95.

99 Luinstra, G. A.; *Polym. Rev.* **2008**, *48*, 192-219.

100 Inoue, S.; Koinuma, H.;Tsuruta, T. *Makromol. Chem.* **1969**, *130*, 210-220.

101 Inoue, S.; Koinuma, H.; Tsuruta, T. *J. Polym. Sci., Part B: Polym. Lett.* **1969**, *7*, 287-292.

102 Aida, T.; Ishikawa, M.; Inoue, S.; *Macromolecules* **1986**, *19*, 8-13.

103 Darensbourg, D.J.; Holtcamp, M.W.; *Macromolecules*,**1995**, *28*, 7577-7579.

104 Cheng, M.; Lobkovsky, E.B.; Coates, G.W., *J. Am. Chem. Soc.* **1998**, *120*, 11018-11019.

105 Darensbourg, D.J., *Chem. Rev.* **2007**, *107*, 2388-2410.

106 Pescarmona, P. P.; Taherimehr, M., *Catal. Sci. Technol.* **2012**, *2*, 2169-2187.

107 Jacobsen, E. N. *Acc. Chem. Res.* **2000**, *33*, 421-431.

108 Hwang, C.-C.; Tour, J. J.; Kittrell, C.; Espinal, L.; Alemany, L. B.; Tour, J. M., *Nature Commun.* **2014**, *5*, 3961.

109 Nakano, K.; Kamada, T.; Nozaki, K., *Angew. Chem. Int. Ed.* **2006**, *45*, 7274-7277.

110 Müller, T. E.; Gürtler, C.; Wohak, M.; Hofmann, J.; Subhani, M. A.; Cosemans, M.; Leitner, W., Pat. US0155559, **2014**.

111 Inoue, S., *J. Polym. Sci. Part A,Polym. Chem.* **2000**, *38*, 2861-2871.

112 Aida, T.; Inoue, S., *Macromolecules* **1982**, *15*, 682-684.

113 Sugimoto, H.; Ohshima, H.; Inoue, S., *J. Polym. Sci. Part A, Polym. Chem.* **2003**, *41*, 3549-3555.

114 Darensbourg, D. J.; Billodeaux, D. R., *Inorg. Chem.* **2005**, *44*, 1433-1442.

115 Sarbu, T.; Styranec, T.; Beckman, E. J., *Nature* **2000**, *405*, 165-168.

116 Sarbu, T.; Beckman, E. J., *Macromolecules* **1999**, *32*, 6904-6912.

117 Sarbu, T.; Styranec, T. J.; Beckman, E. J., *Ind. Eng. Chem. Res.* **2000**, *39*, 4678-4683.

118 Mang, S.; Cooper, A. I.; Colclough, M. E.; Chauhan, N.; Holmes, A. B., *Macromolecules* **2000**, *33*, 303-308.

119 Jacobsen, E. N.; Tokunaga, M.; Larrow, J. F.; Pat. WO 00/09463, **2000**.

120 Eberhardt, R.; Allmendinger, M.; Rieger, B., *Macromol. Rapid Commun.* **2003**, *24*, 194-196.

121 Darensbourg, D. J.; Phelps, A. L., *Inorg. Chem.* **2005**, *44*, 4622-4629.

122 Rao, D.-Y.; Li, B.; Zhang, R.; Wang, H.; Lu, X.-B., *Inorg. Chem.* **2009**, *48*, 2830-2836.

123 Nakano, K.; Nakamura, M.; Nozaki, K., *Macromolecules* **2009**, *42*, 6972-6980.

124 Qin, Z.; Thomas, C. M.; Lee, S.; Coates, G. W. *Angew. Chem. Int. Ed.* **2003**, *42*, 5484-5487.

125   Noh, E. K.; Na, S. J.; Sujith, S.; Kim, S. W.; Lee, B. Y., *J. Am. Chem. Soc.* **2007**, *129*, 8082-8083.

126   Sujith, S.; Min, J. K.; Seong, J. E.; Na, S. J.; Lee, B. Y., *Angew. Chem. Int. Ed.* **2008**, *47*, 7306-7309.

127   *(a)* Xiao, Y.; Wang, Z.; Ding, K. *Chem. Eur. J.* **2005**, *11*, 3668-3678. *(b)* Kember, M.R.; White, A.J.P.; Williams, C.K. *Inorg. Chem.* **2009**, *48*, 9535-9542.

128   *(a)* Lee, B.Y.; Kwon, H.Y.; Lee, S.Y.; Na, S.J.; Han, S.; Yun, H., Lee, H.; Park, Y-W. *J. Am. Chem. Soc.* **2005**, *127*, 3031-3037. *(b)* Bok, T.; Yun, H.; Lee, B.Y. *Inorg. Chem.* **2006**, *45*, 4228-4237.

129   Buchard, A.; Kember, M. R.; Sandeman, K.; Williams, C. K., *Chem. Commun.* **2011**, *47*, 212-214.

130   Taherimehr, M.; Al-Amsyar, S. M.; Whiteoak, C. J.; Kleij, A. W.; Pescarmona, P. P., *Green Chem.* **2013**, *15*, 3083-3090.

131   Darensbourg, D. J.; Wildeson, J. R.; Lewis, S. J.; Yarbrough, J. C. *J. Am. Chem. Soc.* **2002**, *124*, 7075-7083.

132   Byrne, C. M.; Allen, S. D.; Lobkovsky, E. B.; Coates, G. W. *J. Am.Chem. Soc.* **2004**, *126*, 11404-11405.

133   Carrodeguas, L. P.; González-Fabra., J.; Castro-Gómez, F.; Bo, C.; Kleij, A. W., *Chem. Eur.J.* **2015**, *21*,6115-6122.

134   Sienel, G.; Rieth, R.; Rowbottom, K. T., Ullmann's Encyclopedia of Industrial Chemistry, **2005**, Weinheim: Wiley-VCH.

135   Kato, T.; Yamaguchi, Y.; Ueyahara, T.; Yokoyama, T. *Tetrahedron Lett*. **1983**, *24*, 4715-4718.

136   Kupchan, S. M.; Jarvis, B. J.; Daily, J. R. G.; Bright, R. F.; Bryan, R. F.; Shizuri, Y. *J. Am. Chem. Soc*. **1976**, *22*, 7092-7093.

137   Mori K.; Takigawa, T.; Matsui, M. *Tetrahedron*. **1979**, *35*, 833-837.

138   Botar, A. A.; Barabas, A.; Oprean, I.; Czonka-Hornai, J.; Hodosan, F., *Rev. Roum. Chim*. **1983**, *28*, 741-756.

139   Wierenga,W.; Evans, B. R.; Woltersom, J. A. *J. Am. Chem. Soc*. **1979**, *101*, 2828-2836.

140   Corey, E. J.; Snider, B. B. *J. Am. Chem. Soc.* **1972**, *94*, 2549-2550.

141   Kubo, I.; Lee, Y-W.; Balogh-Nair, V.; Nakamishi, K.; Chapya, A. *J. Chem. Soc. Chem. Comm.* **1976**, 949-950.

142   Tanase, S.; Bouwman, E., *Adv. Inorg. Chem.*, **2006**, *58*, 29-75.

143   Costas, M.; Mehn, M.P.; Jensen, M.P.; Que Jr. L., *Chem. Rev.* **2004**. *104*, 939-986.

144   Fujii, H., *Coord. Chem. Rev.* **2002**, *226*, 51-60.

145   Abu-Omar, M. M.; Loaiza, A.; Hontzeas, N., *Chem. Rev.* **2005**, *105*, 2227-2252.

146   Ferraro, D. J.; Gakhar, L.; Ramaswamy, S., *Biochem. Biophys. Res. Commun.* **2005**, *338*, 175-190.

147   Koehntop, K. D.; Emerson, J. P.; Que, Jr. L., *J. Biol. Inorg. Chem.* **2005**, *10*, 87-93.

148   Boyd, D. R.; Sheldrake, G. N., *Nat. Prod. Rep.* **1998**, *15*, 309-324.

149   Yang, L.; Wei, R.-N.; Li, R.; Zhou, X.-G.; Zuo, J.-L., *J. Mol. Catal. A: Chem.* **2007**, *266*, 284-289.

150   Suh, Y.; Seo, M. S.; Kim, K. M.; Kim, Y. S.; Jang, H. G.; Tosha, T.; Kitagawa, T.; Kim, J.; Nam, W., *J. Inorg. Biochem.* **2006**, *100*, 627-633.

151   Monfareda, H. H.; Sadighiana, S.; Kamyabia, M.-A.; Mayer, P., *J. Mol. Catal. A: Chem.* **2009**, *304*, 139-146.

152   Chattopadhyay, T.; Das, D., *J. Coord. Chem.* **2009**, *5*, 845-853.

153   Pietikäinen, P.; Haikarainen, A., *J. Mol. Catal. A: Chem,* **2002**, *180*, 59-65.

154   Zhang, W.; Jacobsen, E. N.; *J. Org. Chem.*, **1991** *56*, 2296-2298.

155   Lee, S. H.; Han, J. H.; Kwak, H.; Lee, S. J.; Lee, E. Y.; Kim, H. J.; Lee, J. H.; Bae, C.; Lee, S. N.; Kim, Y.; Kim, C., *Chem. Eur. J.* **2007**, *13*, 9393-9398.

156   Chisiro, T.; Kon, Y.; Nakashima, T.; Goto, M.; Sato, K., *Adv. Synth. Catal.* **2014**, *356*, 623-627.

157   Bruijnincx, P. C. A.; Buurmans, I. L. C.; Gosiewska, S.; Moelands, M. A. H.; Lutz, M.; Spek, A. L.; van Koten, G.; Gebbink, R. J. M. K., *Chem. Eur. J.* **2008**, *14*, 1228-1237.

158   Perandones, B. F.; del Río Nieto, E.; Godard, C.; Castillón, S.; De Frutos, P.; Claver, C., *ChemCatChem* **2013**, *5*, 1092-1095.

159   Mairata-Payeras, A.; Ho, R. Y. N.; Fugita, M.; Que, L. Jr., *Chem. Eur. J.* **2004**, *10*, 4944-4953.

160   Lane, B.S.; Burgess, K., *Chem. Rev.* **2003**, *103*, 2457-2473.

161   Denisov, I. G.; Makris, T. M.; Sligar, S. G.; Schlichting, I. *Chem. Rev.* **2005**, *105*, 2253-2278.

162   Traylor, T. G.; Fann, W.-P.; Bandyopadhyay, D., *J. Am. Chem. Soc.* **1989**, *111*, 8009-8010.

163   Traylor, T. G.; Xu, F. *J. Am. Chem. Soc.* **1987**, *109*, 6201-6202.

164   Traylor, T. G.; Tsuchiya, S.; Byun, Y.-S.; Kim, C. *J. Am. Chem Soc.* **1993**, 2775-2781.

165   Traylor, T. G.; Kim, C.; Richards, J. L.; Xu, F.; Perrin, C. L. *J. Am. Chem. Soc.* **1995**, *117*, 3468-3474.

166   Nam, W.; Jin, S. W.; Lim, M. H.; Ryu, J. Y.; Kim, C. *Inorg. Chem.* **2002**, *41*, 3647-3652.

167   Nam, W.; Lee, H. J.; Oh, S.-Y.; Kim, C.; Jang, H. G. *J. Inorg. Biochem.* **2000**, *80*, 219-223.

168   Nam, W.; Lim, M. H.; Lee, H. J.; Kim, C. *J. Am. Chem. Soc.* **2000**, *122*, 6641-6647.

169   Que, J., L.; Tolman, W. B. *Angew. Chem., Int. Ed. Engl.* **2002**, *41*, 1114-1137.

170   Rowland, J. M.; Olmstead, M.; Mascharak, P. K. *Inorg. Chem.* **2001**, *40*, 2810-2817.

171   Iyer, S. R.; Javadi, M. M.; Feng, Y.; Hyun, M. Y., Oloo, W. N.; Kimb C.; Que, Jr. L. *Chem. Commun.* **2014**, *50,* 13777-13780.

172   Bassan, A.; Blomberg, M. R. A.; Siegbahn, P. E. M.; Que, L. *J. Am. Chem. Soc.* **2002**, *124*, 11056-11063.

173   Bukowski, M. R.; Comba, P.; Lienke, A.; Limberg, C.; Lopez de Laorden, C.: Mas-Ballesté, R.; Merz, M.; Que, Jr. L., *Angew. Chem. Int. Ed.* **2006**, *45,* 3446-3449.

174   Mas-Ballesté, R.; Costas, M.; van den Berg, T.; Que, Jr. L., *Chem. Eur. J.* **2006**, *12*, 7489-7500.

175   Costas, M.; Que, Jr. L., *Angew. Chem. Int. Ed.* **2002**, *41*, 2179-2181.

176   Klopstra, M.; Roelfes, G.; Hage, R.; Kellogg, R. M.; Feringa, B. L.; *Eur. J. Inorg. Chem.* **2004**, *4*, 846-856.

177   Costas, M.; Tipton, A. K.; Chen, K.: Jo, D.-H.; Que, Jr. L., *J. Am. Chem. Soc.* **2001**, *123*, 6722-6723.

178   Jessop, P. G. and Leitner, W. *Chemical synthesis using supercritical fluids*, VCH, **1999**, Weinheim (Deutschland).

179   Jessop, G.P.; Ikariya, T. and Noyori, R. *Chem. Rev.* **1999**, *99,* 475-493.

180   *(a)* Kaupp, G. *Angew. Chem. Int. Ed. Engl.* **1994**, *33*, 1452-1455. *(b)* Jessop, P. G.; Ikariya, T.; Noyori, R. *Science* **1995**, *269*, 1065-1069.

181   Leitner, W. *Acc. Chem. Res.* **2002**, *35*, 746-756.

182   Beckman, E. J., *J. of Supercritical Fluids* **2004**, *28*, 121-191.

183   Aresta, M., *Carbon dioxide as chemical feedstock*, Wiley-VCH, **2010**, Weinheim (Deutschland).

184   K. Zosel, *Angew. Chem., Int. Ed.* **1978**, *17*, 702-709.

185   Leitner, W., *Nature* **2000**, *405*, 129-130.

186   DeSimone, J. M.; Tumes, W. (Eds.), *Green Chemistry using liquid and supercritical carbon dioxide,* Oxford University Press, **2003**, New York (USA).

187   Jessop, P. G.; Hsiao, Y.; Ikariya, T.; Noyori, R. *J. Am. Chem. Soc.* **1996**, *118*, 344-355.

188   Yazdi, A. V.; Beckman, E. J. *Ind. Eng. Chem. Res.* **1997**, *36*, 2368-2374.

189   Kainz, S.; Koch, D.; Baumann, W.; Leitner, W. *Angew. Chem., Int. Ed. Engl.* **1997**, *36*, 1628-1630.

190   Smart, N. G.; Carleson, T.; Kast, T.; Clifford, A. A.; Burford, M. D.; Wai, C. M. *Talanta* **1997**, *44*, 137-150.

191   Jessop, P.G. *J. Supercrit. Fluids* **2006**, *38*, 211-231.

192   Giménez-Pedrós, M.; Tortosa-Estorach, C.; Bastero, A.; Masdeu-Bultó, A. M.; Solinas, M.; Leitner, W. *Green Chem.* **2006**, *8*, 875-877.

193   Berthod, M.; Mignani, G.; Lemaire, M. *Tetrahedron: Asymmetry* **2004**, *15*, 1121-1126.

194   Wu, X.-W.; Oshima, Y.; Koda, S. *Chem. Lett.* **1997**, 1045-1046.

[195]   *(a)* Bhanage, B.M.; Ikushima, Y.; Shirai, M.; Arai, M. *Chem. Commun.* **1999**, 1277-1278. *(b)* Jacobson, G.B.; Lee, C.T.; Jr., Johnston, K.P.; Tumas, W. *J. Am. Chem. Soc.* **1999**, *121*, 11902-11903. *(c)* Bonilla, R.J.; James, B.R.; Jessop, P.G. *Chem. Commun.* **2000**, 941-942. *(d)* Tortosa-Estorach, C.; Ruíz, N.; Masdeu-Bultó, A.M. *Chem. Commun.* **2006**, 2789-2791. *(e)* Tortosa-Estorach, C.; Giménez-Pedrós, M.; Masdeu-Bultó, A.M.; Sayede, A.D.; Monflier, E. *Eur. J. Inorg.*

[196]   Lin, Y. H.; Smart, N. G.; Wai, C. M. *Trends Anal. Chem.* **1995**, *14*, 123-133.

[197]   Cowey, C. M.; Bartle, K. D.; Burford, M. D.; Clifford, A. A.; Zhu, S.; Smart, N. G.; Tinker, N. D. *J. Chem. Eng. Data* **1995**, *40*, 1217-1221.

[198]   Burk, M. J.; Feng, S.; Gross, M. F.; Tumas, W. *J. Am. Chem. Soc.* **1995**, *117*, 8277-8278.

Chapter - 2

Objectives

2.1   Objectives

As described in the introduction, a high number of catalytic systems and strategies have been developed in the recent years for the synthesis of organic carbonates from CO_2 and epoxides. Even though this reaction is known so far, this chemistry requires more efficient, economical and selective catalysts for the production of either cyclic carbonates or polycarbonates at mild operating conditions.

The main objective of these work focuses on the synthesis and development of efficient, non-toxic and low-cost metal complexes for selective cyclic carbonates or polycarbonates catalytic synthesis. The second objective is the utilization of one of those efficient catalysts for both consecutive olefin epoxidation and cyclic carbonate synthesis reactions. Based on the literature precedents of the most active catalytic systems exposed in the introduction, we resolved to prepare catalysts with tetradentate and tridentate-type ligands. Thus, the specific aims of this thesis for those two families of catalysts are:

1. Catalytic systems with tetradentate-type ligands (Figure 2.1).

(a)   To find effective and relative low toxic Al(III) and Fe(III) complexes as catalysts for epoxide/CO_2 coupling reaction with a tetradentate N_2O_2-donor ligand (a, Figure 2.1), reducing the presence of added co-catalysts and using milder reaction conditions as much as possible. Moreover, to elucidate the catalytic mechanism and the synergistic effect of catalyst/co-catalyst by kinetic experiments.

(b)   To increase the catalytic activity of Mn(III)-porphyrines (b, Figure 2.1) for the copolymerization of CO_2 and CHO for cyclic carbonate synthesis with aliphatic epoxides by introducing halogen atoms in the porphyrin skeleton. Furthermore, to investigate the recyclability of the Mn(III)-porphyrin catalyst by heterogenization in carbon nanotubes .

(c)   To find effective Cr(III) catalysts with N_4-donor Schiff base ligands that could act as porphyrins (N_4-ligands) having an open and flexible structure and similar easy-preparation as salen N_2O_2-donor ligands. Then, a family of neutral and cationic Cr(III) complexes with ligands **H₂L4** and **H₂L5** is proposed (c, Figure 2.1).

The aim is to optimize the reaction conditions using $scCO_2$ as reaction media and thus avoiding the use of highly toxic chlorinated solvents.
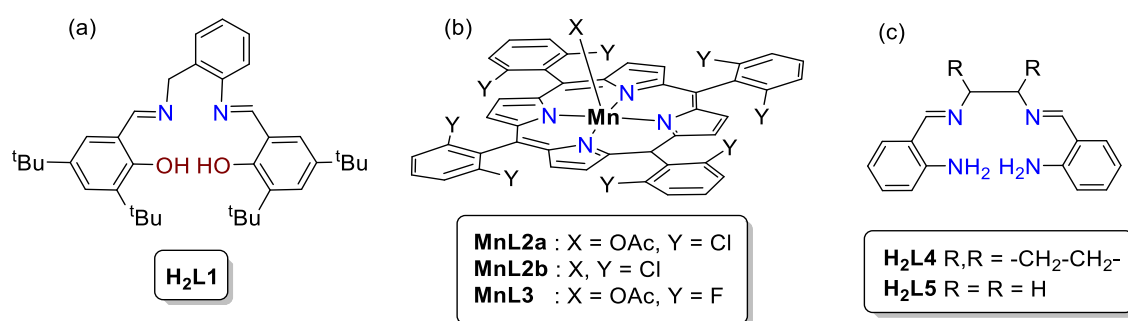
Figure 2.1. Tetradentate ligands and complexes for CO_2/epoxides coupling. (a) salabza **H₂L1** ligand; (b) manganese(III) porphyrin complexes and (c) N₄-Schiff base ligands.

2. Catalytic systems with tridentate-type ligands NN'O (Figure 2.2)

(a)   To enhance the cyclic carbonate yield obtained by our previously reported Cr-NN'O-donor catalytic system[1] and at the same time the replacement of Cr(III) by a less toxic metal such as Zn(II) and Fe(III). To optimize the reaction conditions for the CO_2 fixation. (a, Figure 2.2). To study those catalyst systems also for the insertion of CO_2 into epoxides originating from plant oils as biogenic feedstock. Specifically, we will focus on optimize the catalytically conditions for the formation of methyl oleate carbonate.

(b)   To find an effective catalytic system, able to obtain carbonates from alkenes by oxidation and carbonation consecutive sequence. For this, Fe(III) metal complexes with Schiff-base ligands NN'O (a and b, Figure 2.2) were chosen to be the best catalyst option for both epoxidation and carbonate formation because its relative low-toxicity and activity in epoxidation. Indeed, we want to find the best catalytic conditions trying to use greener oxidants as hydrogen peroxide and supercritical carbon dioxide as reaction media to avoid the use of highly toxic solvents.
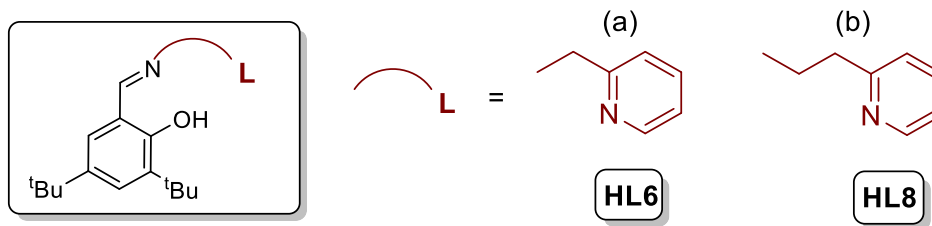
Figure 2.2. Tridentate NN'O ligands for Zn(II) and Fe(III) catalyzed CO_2/epoxides coupling and Fe(III) catalyzed epoxidation reactions.

2.2 References

[1]   Iksi, S.; Aghmiz, A.; Rivas, R.; Gonzalez, M. D.; Cuesta-Aluja, L.; Castilla, J.; Orejon, A.; El Guemmout, F.; Masdeu-Bultó, A. M., *J. Mol. Catal. A: Chem.* **2014**, *383-384*, 143-152.

Chapter - 3

Metal salabza complexes for the selective coupling reaction of CO$_2$ to epoxides: A mechanistic insight with low toxic aluminum complexes

Abstract

*Low toxic and earth-abundant Al(III) and Fe(III) as well as Cr(III) and Co(III) complexes bearing a tetradentate N$_2$O$_2$-donor **H$_2$L1** ligand are easily synthetized and characterized by only one-step reaction. Al(III), Fe(III) and Co(III) complexes, combined with a co-catalyst, are active for the cycloaddition of CO$_2$ and epoxides. Particularly, the binary **AlL1**/TBAB catalytic system provides cyclic carbonates selectively with excellent conversions at low pressures of CO$_2$. ^{27}Al NMR spectroscopy and kinetic experiments of styrene carbonate formation revealed the role of each catalytic component enabling a proposal of the corresponding reaction mechanism. Coupling of CHO and CO$_2$ with binary **AlL1**/PPNCl catalytic system produce poly(cyclohexene carbonate) with M$_w$ up to 2900 and a narrow polydispersity of 1.3 at room temperature.*
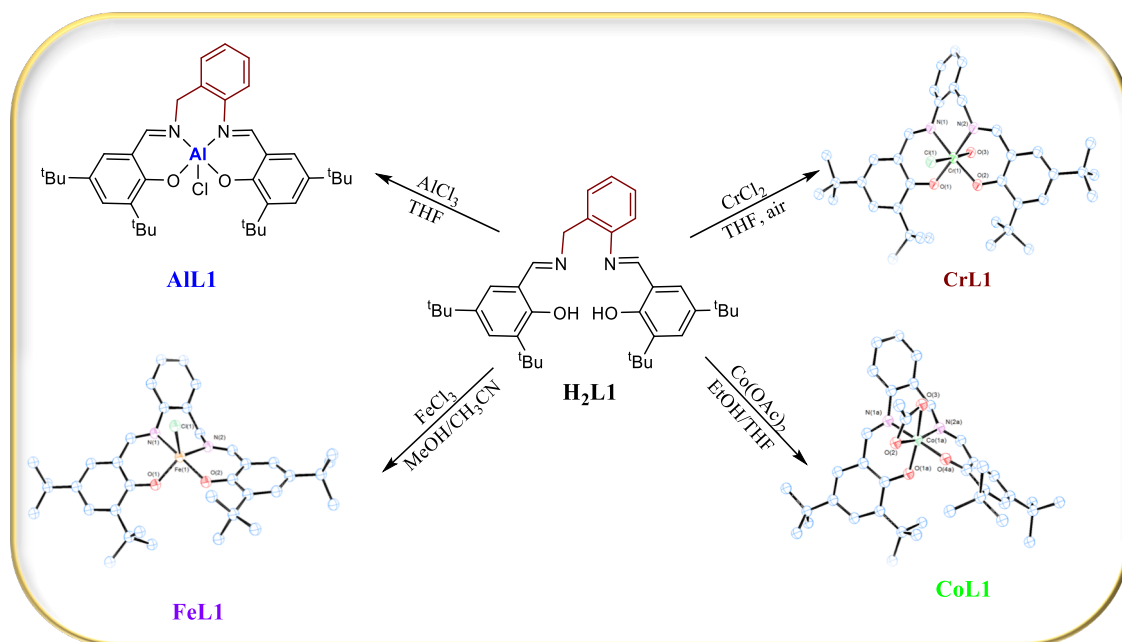
3.1 Introduction

As discussed in Chapter 1 the metal-catalyzed coupling of CO_2 and epoxides has become one of most interesting topics in CO_2 transformations, as it is an atom-efficient reaction to selectively obtain highly value-added cyclic carbonates or polycarbonates from inexpensive and ready available starting materials (Scheme 3.1).

Some of the most widely employed catalysts in the literature for this reaction are metal-salen type complexes. These catalysts are characterized by an easy preparation, with a possibility to perform a large-scale synthesis, high stability and robustness. Their properties can be easily fine-tuned from a reactivity point of view by changing the diimine skeleton or the substituents in the phenolate moiety.
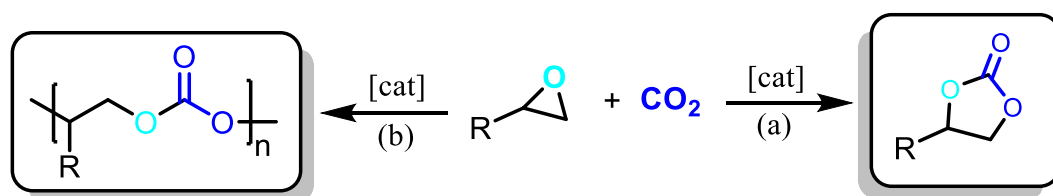
Scheme 3.1. a) Cycloaddition and b) copolymerization of CO_2 and epoxides

As it was shown that the catalytic activity often depends on the organic framework surrounding the metal center[1] most of the studies focus on the modification of the ligand scaffold to obtain better reactivity or selectivity. Taking this into account we are interested in a new type of N_2O_2-Schiff metal complexes similar to metal-salen complexes with a slight modification in the length of the diimine skeleton. These complexes will have a more flexible structure, and an open active site, which may provide higher reactivity maintaining the high stability of the tetradentate coordination (Figure 3.1).
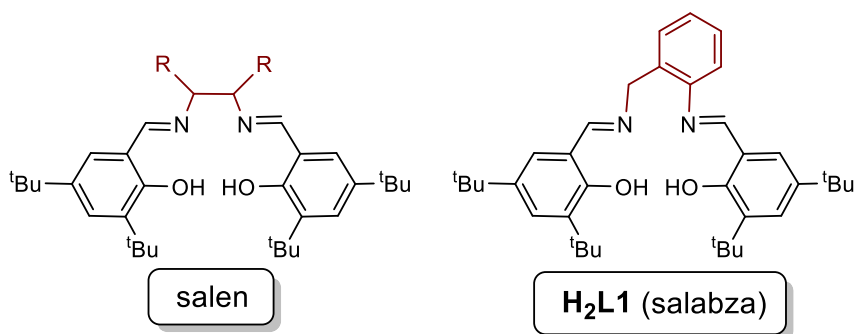
Figure 3.1. Salen and **H₂L1** (salabza) ligands.

It is remarkable that iron, sodium and aluminum are the most earth-abundant and widely distributed metals. Thus, they are the optimal compounds to consider for the development of metal complexes as catalysts for the large-scale production of carbonates. The toxicity of these metal catalysts has not been studied; nevertheless, it is preferable to use iron and aluminum instead of higher toxic metals. For this reason, we decided to prepare Al(III) and Fe(III) complexes bearing a tetradentate-N_2O_2 ligand (**H_2L1**, Figure 3.1). Chromium(III) and cobalt(III) complexes were also prepared. The aluminum(salabza) complex was chosen as a starting point to check its catalytic activity in the coupling of CO_2 and epoxides.

The synthesis of others Cu, Ti, Mn, Co, Zn and Al complexes with similar salabza-type ligands have already been reported, but there is no application of these complexes as catalysts for the reactions involving CO_2 and epoxides.[2,3,4,5,6]

3.2 Results and discussion

3.2.1 Synthesis of metal salabza complexes

H_2L1 was prepared following the general procedure described by Lin and co-workers by the reaction of 3,5-di-*tert*-butyl salicylaldehyde and 2-aminobenzylamine in ethanol (Scheme 3.3).[6] The same authors reported the synthesis of a series of aluminum complexes with a similar salen-type ligand containing sterically bulky cumyl groups. They proposed that the reaction of the ligand with AlMe$_3$ and further reaction of [Al(**L1-cum**)Me] with benzyl alcohol produced mononuclear alkoxo aluminum species [Al(**L1-cum**)(OBn)] (Scheme 3.2). These complexes were very active and highly stereoselectivite in the ring opening polymerization (ROP) of *rac*-lactide producing polylactide (PLA).[6]
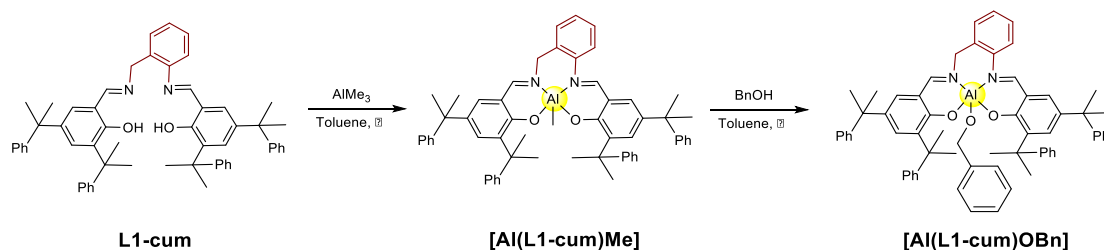
Scheme 3.2. Preparation of Al(III) complex bearing salabza-type ligand with bulky cumyl groups (**L1-cum**).[6]

Treatment of **H₂L1** with different metal halide precursors MCl₃ (M = Al(III), Fe(III)) afforded the corresponding metal(III) complexes in good (Al(III) and Fe(III)) yields (85 %) (Scheme 3.3). Cr(III) and Co(III) complexes were prepared in moderate yields (49 and 55 %, respectively) from M(II) salts (CrCl₂ and Co(OAc)₂·H₂O) by addition of **H₂L1** and subsequent oxidation with air.
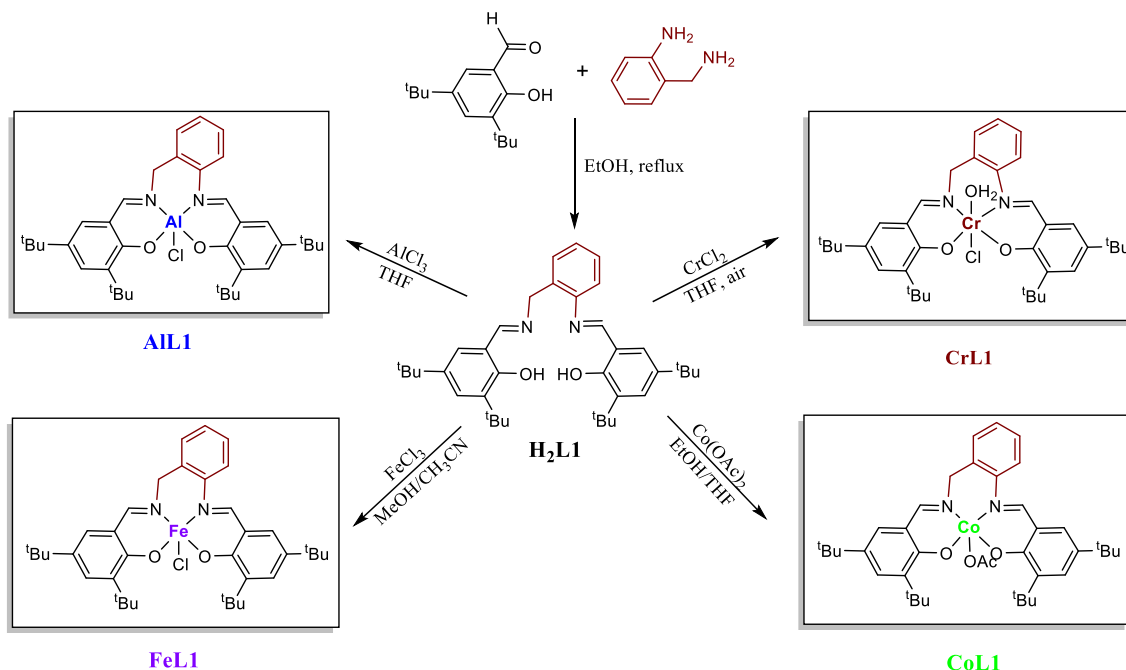
Scheme 3.3. Preparation of ligand **H₂L1** and the corresponding metal complexes.

In the mass spectra the peaks corresponding to the mononuclear fragment [M(**L1**)]⁺ were observed for Al(III), Cr(III) and Co(III) complexes. The microanalysis data of the solids agreed to non-solvated (Fe(III)) and solvated forms (Al(III), Cr(III) and Co(III)). The infrared spectral data of all metal(salabza) complexes showed two bands in the range of 1598-1615 cm⁻¹ attributed to the azomethine ν(C=N) stretching vibration, which has shifted to a lower frequencies (1620 cm⁻¹ for **H₂L1** free ligand) indicating the coordination through both imine groups. In addition, the absence of a strong absorption at the ν(O-H) region (*ca* 3600 cm⁻¹) pointed to the coordination by both phenolate fragments. The ring skeletal vibration of ν(C=C) appeared in the range 1554-1416 cm⁻¹ and the phenolate ν(C-O) stretching vibrations appeared in the range 1256-1230 cm⁻¹ all of them at lower vibration frequency than in the free ligand.[7] Moreover, information about the coordination mode of the acetate in **CoL1** could be

obtained from IR spectra[8,9]. The presence of one strong band at 1525 and another presumably in the overcrowded $\nu(C=C)$ range of 1478-1409 cm^{-1} ($\nu_a(COO)$ and ($\nu_s(COO)$ respectively) with a $\Delta\nu$ value between 116-46 cm^{-1} was in agreement with a chelating coordination of the acetate ion in [Co(**L1**)(O$_2$CMe)].[9]

The ^{1}H NMR spectra of **AlL1** and **CoL1** complexes in CDCl$_3$ showed the presence of two singlet signals characteristic of C*H*=N at δ 8.42 and 8.35 ppm (up field shifted from free **H$_2$L1**, Δδ = −0.11 and -0.24 ppm, respectively) for **AlL1** and δ 7.85, 7.75 ppm (down field shifted Δδ = +0.66 and +0.36 ppm, respectively) for **CoL1**. These signals confirm the expected non-equivalent structure of free **H$_2$L1** and the corresponding complexes. A broad singlet was seen in the case of **AlL1** at δ 4.80 ppm (Δδ = −0.15 ppm), and two doublet signals at δ 4.54 and 4.17 for **CoL1**, which were attributed to NC*H$_2$* protons. A singlet signal at δ 1.59 ppm in **CoL$_1$** spectrum accorded with the -C*H$_3$* from acetate fragment. The ^{13}C NMR spectrum of **AlL1** was assigned by 2D NMR experiments (^{1}H-^{13}C HSQC and ^{1}H-^{13}C HMBC, Supplementary Information).

X ray structures of CrL1, FeL1 and CoL1

Deep red crystals of **CrL1**, purple crystals of **FeL1** and brown crystals of **CoL1** suitable for X-ray diffraction analysis were obtained by slow diffusion of hexane into a diluted solution of the chromium complex in CH$_2$Cl$_2$ or slow evaporation of a diluted solution of the complex in diethyl ether/hexane for iron and cobalt complexes. **CrL1** and **FeL1** crystallized in the monoclinic space group *C2/c* and **CoL1** in the monoclinic space group *P2(1)/n*. The molecular structures are shown in (Figure 3.2, Figure 3.3 and Figure 3.5) with selected bond lengths and angles in Table 3.1.

CrL1 adopted an octahedral geometry around the chromium metal center where the anionic ligand **L1** was coordinated in the equatorial plane with a tetradentate fashion through the imine and phenolate O atoms (Figure 3.2). One chloride anion and a water molecule were located at the axial positions. The equatorial donor atoms presented a nearly planar geometry (bond angles for O(1)-Cr(1)-O(2), O(1)-Cr(1)-N(1), O(2)-Cr(1)-N(2) and N(1)-Cr(1)-N(2) of 91.8(2)°, 88.3(2)°, 90.2(2)° and 89.8(3)°, respectively). The chloride anion and the water molecule were located with an almost linear disposition (O(3)-Cr(1)-Cl(1) bond angle of 177.13(18)°). The Cr-N(imine) (2.012(6) and 2.059(6) Å), Cr-O(phenolate) (1.916(5) and 1.923(5) Å) as well as Cr-Cl (2.299(3)

Å) bond lengths observed were in concordance with the chromium(III) salen-type complexes reported in the literature.[10,11]
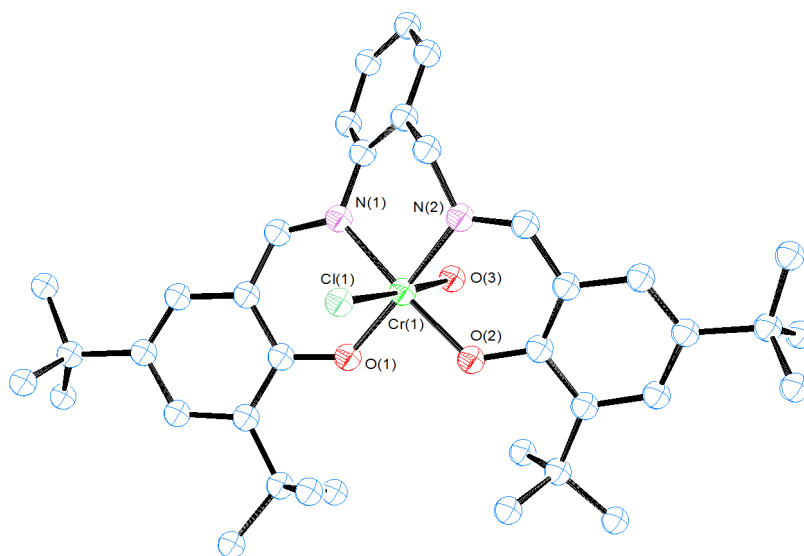
Figure 3.2. ORTEP drawing of complex of **CrL1**. All hydrogen atoms and solvent molecules are omitted for clarity. Thermal ellipsoids drawn at the 50 % probability level.

FeL1 presented a 5-coordinated environment (Figure 3.3) and the geometry around the iron center may be described as an intermediate between trigonal bipyramidal and square-pyramidal geometry with a τ-factor value of 0.7. The τ index describes the distortion of five-coordinate molecules and is given as $\tau = (\beta-\alpha)/60$, where α and β are the two largest basal angles in a five-coordinate complex (Figure 3.4). For a perfectly square-pyramidal geometry, τ is equal to zero, while it becomes unity for perfectly trigonal bipyramidal geometry.[12] This geometry differed from those reported for [Fe(salenR)Cl].C_6H_6[13], [Fe(salphen)Cl][14], and other iron salen-type complexes[15] which had perfectly square-pyramidal geometry (Figure 3.4). The length of the diimine ligand could be considered to influence the iron environment producing this change in the geometry. The Fe-N(imine) (2.139(2) and 2.0858(19) Å), Fe-O(phenolate) (1.8659(16) and (1.8995(16) Å) and Fe(Cl) (2.2466(7) Å) bond distances are in agreement with reported data from other salen-type iron complexes[13,14,16.]
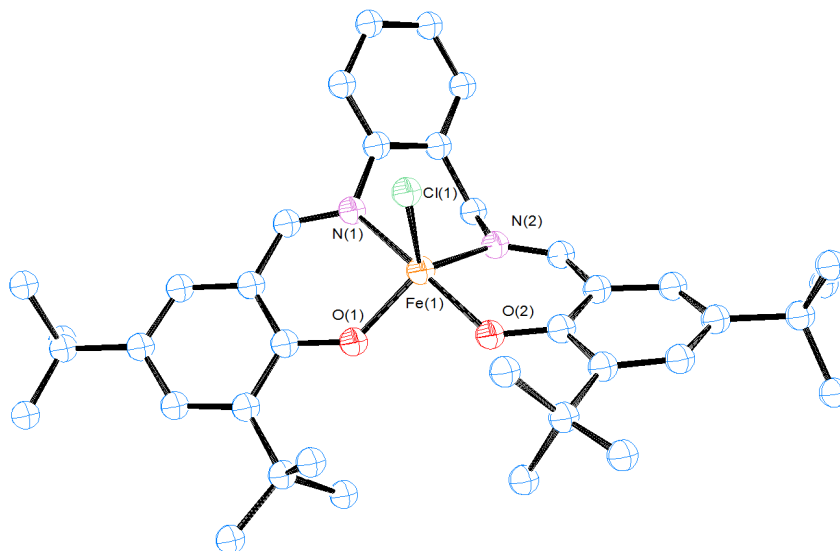
Figure 3.3. ORTEP drawing of complex of **FeL1**. All hydrogen atoms and solvent molecules are omitted for clarity. Thermal ellipsoids drawn at the 50 % probability level.

The Fe-N(imine) distance has been suggested as an indicator of the spin state for Fe(III) in salen iron complexes, with the distance of 2.00-2.10 Å for the high-spin state, and 1.93-1.96 Å for the low-spin state.[16]
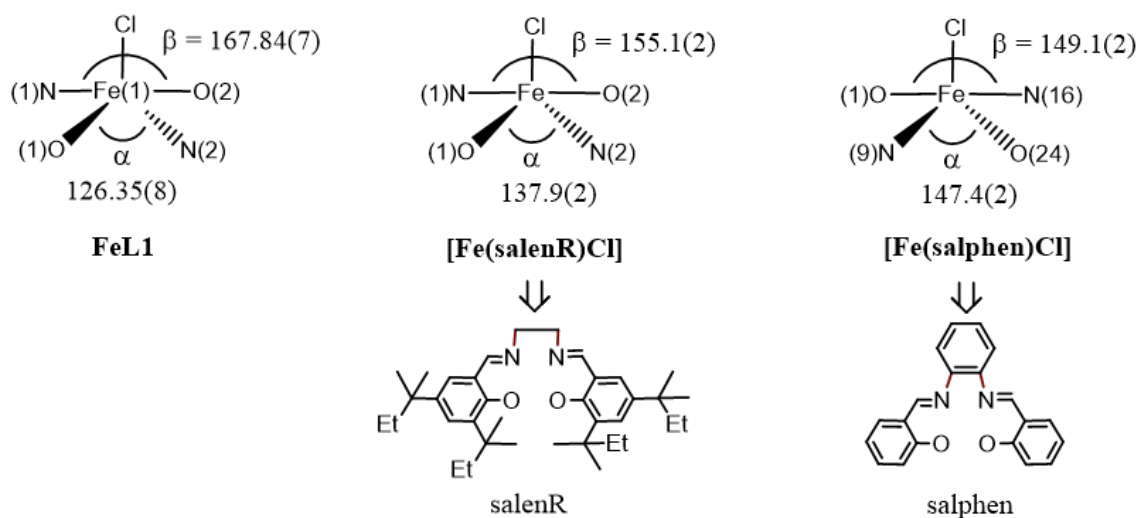
$$\tau\left(\mathbf{Fe(L1)}\right) = \frac{\beta - \alpha}{60} = 0.69 \qquad \tau([\mathbf{Fe(salenR)Cl}]) = 0.29 \qquad \tau\left([\mathbf{Fe(salphen)Cl}]\right) = 0.03$$

Figure 3.4. Angles α and β and τ factor for complex **FeL1** and reported [Fe(salenR)Cl][15] and [Fe(salphen)Cl][14]

The mean bond distance in the structure reported here suggests that the metal ion in **FeL1** is in the high-spin state, which is consistent with the results of room temperature magnetic susceptibility (μ_{eff} = 5.90 μ_B).[16]

As shown in Figure 3.5 the molecular structure of **CoL1** was monomeric with a six-coordinated central cobalt atom in which **L1** acted as a tetradentated and one acetate as bidentate chelate ligand. The geometry around the cobalt atom was a distorted octahedral as analogous Co(III) salen complexes in the literature.[17,18] It presented an axial O(1A)-Co(1A)-O(3) bond angle of 166.5(4)°, equatorial O(4A)-Co(1A)-N(2A), N(2A)-Co(1A)-N(1A), O(1A)-Co(1A)-O(2), and O(2)-Co(1A)-O(4A) bond angles of 94.2(3)°, 90.8(5)°, 101.7(3)°, and 85.9(3)°, respectively, and O(2)-Co(1A)-O(3) acetate bond angle of 64.8(18)°. Bond distances Co-N (imino) (1.894(7) and 1.898(6) Å), Co-O (phenolate) (1.866(8) and 1.867(6) Å) and Co-O (acetate) (2.053(5) and 1.975(5) Å) (Table 3.1) are in the average range as corresponding values in similar octahedral Co(III) systems.[18]
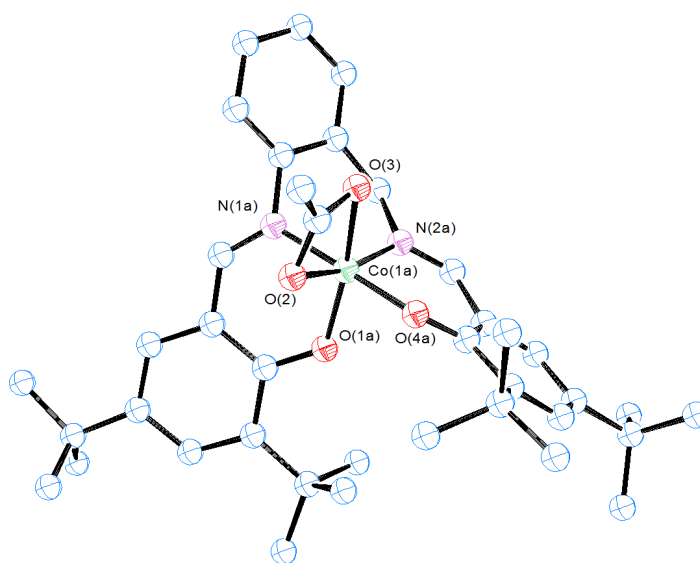
Figure 3.5. ORTEP drawing of complex of **CoL1**. All hydrogen atoms are omitted for clarity. Thermal ellipsoids drawn at the 50 % probability level.

Table 3.1. Selected bond lengths (Å) and angles (°) for **CrL1**, **FeL1** and **CoL1.**

CrL1		FeL1		CoL1[*]	
Cr1-O1	1.916(5)	Fe1-O1	1.8659(16)	Co1A-O1A	1.866(8)
Cr1-O2	1.923(5)	Fe1-O2	1.8995(16)	Co1A-O4A	1.867(6)
Cr1-N2	2.012(6)	Fe1-N1	2.139(2)	Co1A-N1A	1.894(7)
Cr1-N1	2.059(6)	Fe1-N2	2.0858(19)	Co1A-N2A	1.898(6)
Cr1-Cl1	2.299(3)	Fe1-Cl1	2.2466(7)	Co1A-O2	1.975(5)
Cr1-O3	2.052(5)			Co1A-O3	2.053(5)
O1-Cr1-O2	91.8(2)	O1-Fe1-O2	91.99(7)	O1A-Co1A-O4A	89.6(4)
O1-Cr1-N2	178.0(2)	O1-Fe1-N2	126.35(8)	O1A-Co1A-N1A	92.6(4)
O2-Cr1-N2	90.2(2)	O2-Fe1-N2	86.03(7)	O4A-Co1A-N1A	174.4(6)
O1-Cr1-O3	88.5(2)	O1-Fe1-N1	85.73(7)	O1A-Co1A-N2A	93.4(4)
O2-Cr1-O3	86.9(2)	O2-Fe1-N1	167.84(7)	O4A-Co1A-N2A	94.2(3)
N2-Cr1-O3	91.7(2)	N2-Fe1-N1	85.72(7)	N1A-Co1A-N2A	90.8(5)
O1-Cr1-N1	88.3(2)	O1-Fe1-Cl1	116.36(6)	O1A-Co1A-O2	101.7(3)
O2-Cr1-N1	172.0(3)	O2-Fe1-Cl1	100.42(6)	O4A-Co1A-O2	85.9(3)
N2-Cr1-N1	89.8(3)	N2-Fe1-Cl1	116.70(6)	N1A-Co1A-O2	88.6(6)
O3-Cr1-N1	85.1(2)	N1-Fe1-Cl1	91.27(6)	N2A-Co1A-O2	164.9(3)
O1-Cr1-Cl1	91.91(17)			O1A-Co1A-O3	166.5(4)
O2-Cr1-Cl1	95.95(17)			O4A-Co1A-O3	88.5(3)
N2-Cr1-Cl1	87.7(2)			N1A-Co1A-O3	88.2(5)
O3-Cr1-Cl1	177.13(18)			N2A-Co1A-O3	100.1(3)
N1-Cr1-Cl1	92.09(19)			O2-Co1A-O3	64.80(18)

[*] The complex is disordered into 2 positions with a 70:30. We selected only one position, A-atoms (70), in order to see the structure more clearly.

To sum up, new metal salabza complexes **AlL1**, **CrL1**, **FeL1** and **CoL1** were obtained in moderate to good yields and were characterized by NMR, IR spectroscopy, ESI-TOF spectrometry, X-ray diffraction, elemental analysis and magnetic susceptibility.

3.2.2 Catalytic results

3.2.2.1 *Cycloaddition of epoxides to CO_2*

Initially, **AlL1**, **FeL1** and **CoL1** were tested as catalysts, in conjunction with tetrabutylammonium bromide (TBAB), for the coupling reaction of CO_2 and 1,2-

epoxyhexane as a benchmark substrate with any addition of organic solvent (Scheme 3.4). With the best catalytic system, the effect of catalyst/co-catalyst ratio, pressure, temperature and reaction time were studied and then optimized. Then, the scope of the catalyst was studied with other epoxides. Unfortunately, **CrL1** could not be used as catalyst for this reaction because of its fast decomposition and its low catalysis reproducibility.
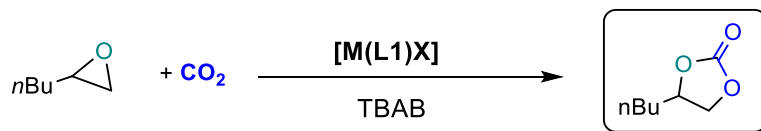
Scheme 3.4. General scheme of the cycloaddition reaction of CO_2 and 1,2-epoxyhexane using **ML1**/TBAB catalytic systems.

The initial conditions chosen for the reaction were 10 bar CO_2, 45 ºC using 0.2 mol % catalyst and TBAB in neat substrate during 18h. The results are given in Table 3.2.

Table 3.2. Effect of the nature of the catalyst and the catalyst/co-catalyst ratio in the cycloaddition of 1,2-epoxyhexane and CO_2 using **AlL1**, **FeL1**, **CoL1**.[a]

Entry	Cat	Co-cat	Temp. (ºC)	Cat/Co-cat (mol %)[b]	Conv (%)[c,d]	TOF (h^{-1})[e]	Y (%)[f]
1	**AlL1**	TBAB	45	0.2/0.2	49	14	n.d.
2	**FeL1**	TBAB	45	0.2/0.2	17	5	16
3	**CoL1**	TBAB	45	0.2/0.2	31	9	31
4	**AlL1**	TBAB	45	0.2/1.0	100	28	73
5	**AlL1**	-	80	0.2/-	1	0.2	1
6	-	TBAB	80	-/0.2	11	3	8

[a]Reaction conditions: time = 18 h, PCO_2 = 10 bar, 1,2-epoxyhexane: 33.15 mmol (4 ml); [b]mol % respect to the substrate; [c]measured by ^{1}H NMR; [d]Selectivity for the cyclic carbonate product > 99 % [e]averaged TOF (mol substrate converted·(mol catalyst)$^{-1}$·h^{-1}; [f]Yield of carbonate product determined by ^{1}H NMR using mesitylene as the internal standard.

This preliminary study showed that all complexes successfully catalyzed the coupling of CO_2 and 1,2-epoxyhexane in the presence of quaternary ammonium bromide. The best result was achieved with **AlL1**/TBAB catalytic system with almost 50 % of conversion and total selectivity towards cyclic carbonate (entry 1, Table 3.2).

In order to optimize the reaction conditions with the best **AlL1**/TBAB catalytic system the effect of the catalyst/co-catalyst ratio was studied. When this ratio was increased up to 1/5 (1.0 mol % co-catalyst loading) an enhancement in the catalytic activity was observed obtaining complete conversion towards cyclic carbonate (entry 4, Table 3.2). However, in the absence of a co-catalyst almost no cyclic carbonate was formed even running the reaction at 80 ºC (entry 5, Table 3.2). It is important to note that TBAB alone showed very low conversion under the employed catalytic conditions (entry 6, Table 3.2). This synergistic effect between **AlL1** and TBAB is in concordance with analogous behavior observed with other catalytic systems in the coupling of CO_2 and epoxides.[19,20]

The effect of pressure (10, 30 and 50 bar) and temperature (45, 60, 80 ºC) was evaluated at 18 h of reaction time with **AlL1**/TBAB catalytic system (Figure 3.5). As observed in the previous results, the temperature has a beneficial effect in the conversion even when the CO_2 pressure increases up to 50 bar. On the other hand, raising the pressure produced an increase of conversion when working at 45 and 60 ºC, whereas when the reaction was run at 80 ºC, no positive effect was observed increasing the pressure from 10 to 50 bar.
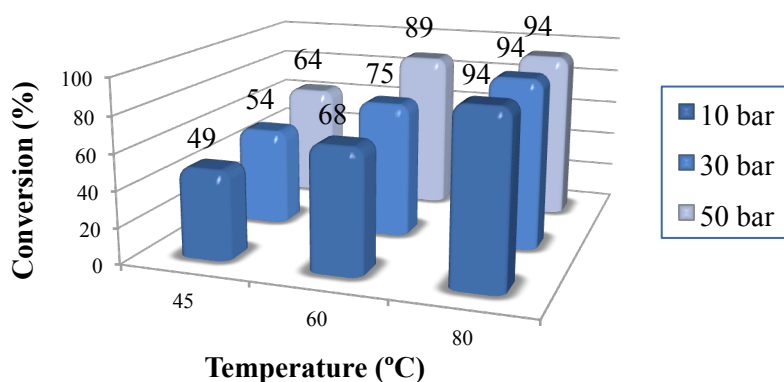
Figure 3.5. Effect of CO_2 pressure and temperature on the coupling of 1,2-epoxyhexane and CO_2 using **AlL1**/TBAB catalyst system. Reaction conditions: catalyst 0.2 mol%, TBAB 0.2 mol%, 18 h.

At the optimized temperature (80 ºC), pressure (10 bar) and catalyst/co-catalyst ratio of 5 we proceeded to optimize the catalyst loading and reaction time to obtain the initial maximum TOF at low conversion. With reduced amounts of catalyst and co-catalyst and also decreasing the reaction time to 1 h it was found that considerable conversion could still be achieved (up to 53 %) with a good initial TOF up to 531 h^{-1} (entry 1, Table 3.3) To assess if the catalytic activity was maintained under milder conditions the same reaction was done at 45 ºC (entry 2, Table 3.3) and at atmospheric pressure of CO_2 (entry 3, Table 3.3). In both cases a decrease in the catalytic activity was observed (TOF 90 and 267 h^{-1}), respectively, but the initial TOF at atmospheric pressure was still encouraging. A maximum TOF of 800 h^{-1} was obtained at a catalyst loading of 0.05 mol % in 0.5 h of reaction time (entry 4, Table 3.3).

Table 3.3. Optimization of TOF (h^{-1}) using catalytic system **AlL1**/TBAB.[a]

Entry	Cat/Co-cat (mol %)[b]	Temp. (ºC)	Pressure (bar)	Time (h)	Conv (%)[c,d]	TOF (h^{-1})[e]	Y (%)[f]
1	0.1/0.5	80	10	1	53	531	50
2	0.1/0.5	45	10	1	9	90	9
3	0.1/0.5	80	1	1	27	267	21
4	0.05/0.25	80	10	0.5	20	800	19

[a]Reaction conditions: 1,2-epoxyhexane: 24.86 mmol (3 ml); [b]mol % respect to the substrate; [c]measured by ^{1}H NMR; [d]Selectivity for the cyclic carbonate product > 99 % averaged TOF (mol substrate converted·(mol catalyst)$^{-1}$·h^{-1}; [f]Yield of carbonate product determined by ^{1}H NMR using mesitylene as the internal standard.

Although direct comparison with other catalytic systems from the literature is not possible due to different reactor set up, considering the conversion obtained with this newly developed **AlL1**/TBAB system compared with the most outstanding systems reported in the last years such as dimeric aluminum(salen) complex developed by North and co-workers[21] (A, Figure 3.6) and hexachlorinated-Al(III)(amine triphenolate) developed by Kleij and co-workers[19] (B, Figure 3.6), it was observed that at lower temperature the catalytic activity of **AlL1**/TBAB system was slightly higher than the dimeric aluminum(salen) (A, Figure 3.6) (TOF of 460 h^{-1} compared to 531 h^{-1} by **AlL1**/TBAB system). Nevertheless, the Al(III)(amine triphenolate), (B, Figure 3.6) still

remains as the highest active catalyst for organic carbonate formation with a high initial TOF of 24000 h^{-1} (entry 5, Table 3.4) .
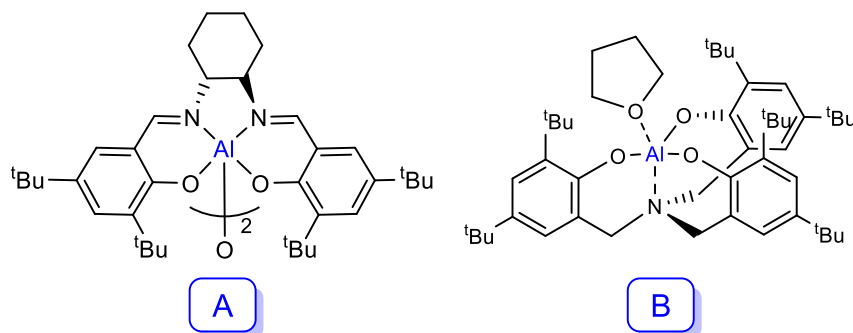
Figure 3.6 . Selected catalytic systems for the cycloaddition of CO_2 and 1,2-epoxyhexane.

Table 3.4. Al(III) based catalytic systems for the cycloaddition of CO_2 and 1,2-epoxyhexane.[a]

Entry	Cat/Co-cat (mol %)[b]	Temp. (ºC)	Pressure (bar)	Time (h)	Conv (%)[c]	TOF (h^{-1})[d]	Ref
1	**AlL1**/TBAB 0.1/0.5	80	10	1	53	531	This work
2	**A**/TBAI 0.05/0.25	90	10	2	47	460	[19]
3	**B**/TBAI 0.05/0.25	90	10	2	96	960	[19]
4	**AlL1**/TBAB 0.05/0.25	80	10	0.5	20	800	This work
5	**B**/TBAI 0.0005/0.05	90	10	0.5	6	24000	[19]

[a]Reaction conditions: 1,2-epoxyhexane: 24.86 mmol (3 ml); [b]mol % respect to the substrate; [c]measured by ^{1}H NMR; [d]averaged TOF (mol substrate converted·(mol catalyst)$^{-1}$·h^{-1}.

Discovered the great potential of **AlL1**/TBAB catalytic system towards cyclic carbonate using 1,2-epoxyhexane we then focused on investigation the scope of the cycloaddition of CO_2 with a variety of terminal and functionalized epoxides providing the corresponding cyclic carbonates (Figure 3.7). All of these selected substrates were converted into the corresponding carbonates with total selectivity in the cyclic product

and high turn over frequency between 120 and 3434 h^{-1} (Figure 3.7). This information indicated the high tolerance of the catalytic system especially with alkyl halide functionalities such epichlorohydrin, which presented the highest catalytic activity.

Catalyst system **AlL1**/TBAB was also active for internal hindered substrates, such as methyl epoxyoleate derived from a natural product, although higher concentration of catalyst was required (Figure 3.7). It is important to note that Leitner and co-workers found that TBAB alone (2 mol %) gave very low conversion of 11 % with a cis/trans ratio of 71/29 at 100 ºC, 125 bar during 6 h.[22]
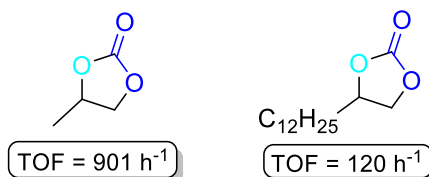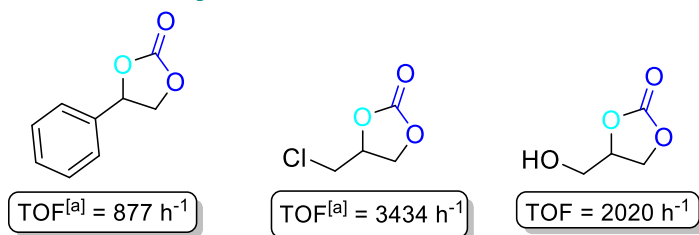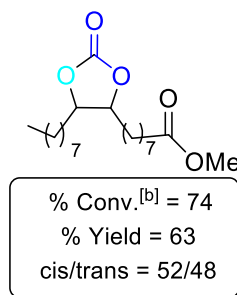
Figure 3.7 . Cycloaddition of different epoxides to CO_2 with catalytic system **AlL1**/TBAB. Reaction conditions: T = 80 ºC, time = 0.5 h, P_{CO2} = 10 bar, substrate: 3 ml; **AlL1**: 0.05 mol %, TBAB: 0.25 mol %; [a]**AlL1**: 0.03 mol %; TBAB: 0.15 mol; [b]**AlL1**: 2 mol %, TBAB: 2 mol %; T = 100 ºC; P_{CO2} = 100 bar.

3.2.2.2 *Copolymerization of CHO and CO₂*

Cyclohexene oxide is an internal epoxide with some steric hindrance around the epoxide ring, which makes it a less reactive substrate for reaction with CO_2 than other terminal or unsubstituted epoxides. This reaction normally led to moderate conversions and yielded a complex mixture of cyclic carbonates and polymeric species containing both carbonate and ether linkages.[23] Moreover, the structure of the cyclic cyclohexene carbonate consists of a six-membered ring interconnected to a five-membered ring and is, therefore, geometrically strained. As a consequence, polycarbonate is often observed as the major product.[24] For these reasons, cyclohexene oxide is generally considered a very challenging substrate for reaction with CO_2.

On the basis of previous studies which have shown that aluminum(porphyrin) and aluminum(salen) derivatives produced polycarbonates and cyclic carbonates[25,26,20] respectively, the reaction of CO_2 and cyclohexene oxide was then investigated using catalyst **AlL1** and changing the co-catalyst to the most effective Lewis base co-catalysts for this reaction, the PPNCl salt.[27]

The copolymerization reaction was carried out initially at 80 ºC and 50 bar during 18 h with **AlL₁** complex (0.2 mol %) in the presence of equimolar amount of co-catalyst PPNCl without the addition of solvent (entry 1, Table 3.5). The ^{1}H NMR of the crude of the reaction showed a peak at δ 4.6 ppm characteristic of poly(cyclohexene carbonate) (PCHC)[28] together with signals at δ 4.5 and 1.8 ppm attributed to the *cis*-cyclohexene carbonate[29] and at δ 4.0 ppm attributed to *trans*-cyclohexene carbonate (CHC) (ratio *cis/trans* 75/25).[30] The formation of mixtures of polycarbonate and cyclic carbonate in the reaction of CHO and CO_2 is consistent with the observation reported in the literature that the activation energy (E_a) for the formation of PCHC is lower compared for other substrates, nevertheless, the cyclic product is still the most stable thermodynamically.[31] Indeed, Darensbourg and co-workers observed almost total selectivity towards cyclic carbonate by-product using PPNCl with similar aluminum-salen complexes.[27] The polymer was isolated by extraction of the cyclic product with hexane obtaining a high degree of incorporation of carbonate (92%) measured by ^{1}H NMR spectroscopy. The number-average molecular weight (M_n) of the alternating copolymer and polydispersity (M_w/M_n), estimated by gel permeation chromatography (GPC), was 1700 and 1.3, respectively.

When temperature was diminished to 45 ºC and reaction time increased to 24 h

it was observed a similar conversion of the epoxide but with higher selectivity towards PCHC of 82 %, higher average molecular weight (M_n) of 2100 and narrower polydispersity, 1.2 (entry 2, Table 3.5). Similarly, when the CO_2 pressure decreased to 10 bar at the same temperature the reaction proceeds well although the % CO_2 incorporation decreased to 85 % (entry 3, Table 3.5). The polymers obtained by this catalytic system possessed lower molecular weights than the ones reported by Inoue and coworkers with similar aluminum Schiff base complex. [32] Nevertheless, the polydispersity obtained at lower pressures were higher (2.47, 20 bar, 80 ºC) compared with **AlL1**/PPNCl catalytic system (1.3, 10 bar, 45 ºC) and also we could remark the use of solvent-free conditions.

Table 3.5. Copolymerization of cyclohexene oxide (CHO) and CO_2 using catalytic system **AlL1**/PPNCl.[a]

Entry	**Cat/PPNCl** (mol %)[b]	T. (ºC)	P. (bar)	Time (h)	Conv (%)[c]	Y (%)[d], ($M_w \cdot 10^3$, M_w/M_n)[e]	% CO_2 content[c]	PCHC/ CHC (%)[f]	TOF (h^{-1})[g]
1	0.2/0.2	80	50	18	66	41 (1700,1.3)	92	71/29	11.4
2	0.2/0.2	45	50	24	63	50 (2100,1.2)	96	82/18	10.4
3	0.2/0.2	45	10	24	63	46 (2100,1.3)	85	79/21	9.6
4	0.2/0.2	25	50	90	58	45 (2900,1.3)	92	84/16	2.5

[a]Reaction conditions: Cyclohexene oxide: 29.70 mmol (3 ml); [b]mol % respect to the substrate; [c]measured by ^{1}H NMR; [d]Yield of PCHC determined by ^{1}H NMR using mesitylene as the internal standard; [d]determined by GPC using polystyrene as standard; [f]Selectivity determined by ^{1}H NMR; [g]averaged TOF (mol substrate converted into polycarbonate·(mol catalyst)$^{-1}$·h^{-1}).

Moreover, with **AlL1**/PPNCl catalytic system it was possible to achieve at room temperature the same epoxide conversion and polycarbonate yield than at 80 ºC but increasing the reaction time to 90 h (entry 4, Table 3.5). The polymer chains obtained possessed higher molecular weight of 2900, good polydispersity (1.2) and good carbonate linkage (92 %). These results are promising when were compared with the aluminum Schiff base catalytic system of Inoue that at the same conditions the

copolymerization reaction hardly occurred with 6 % of polymer yield containing chains with only 3 % of carbonate linkages.
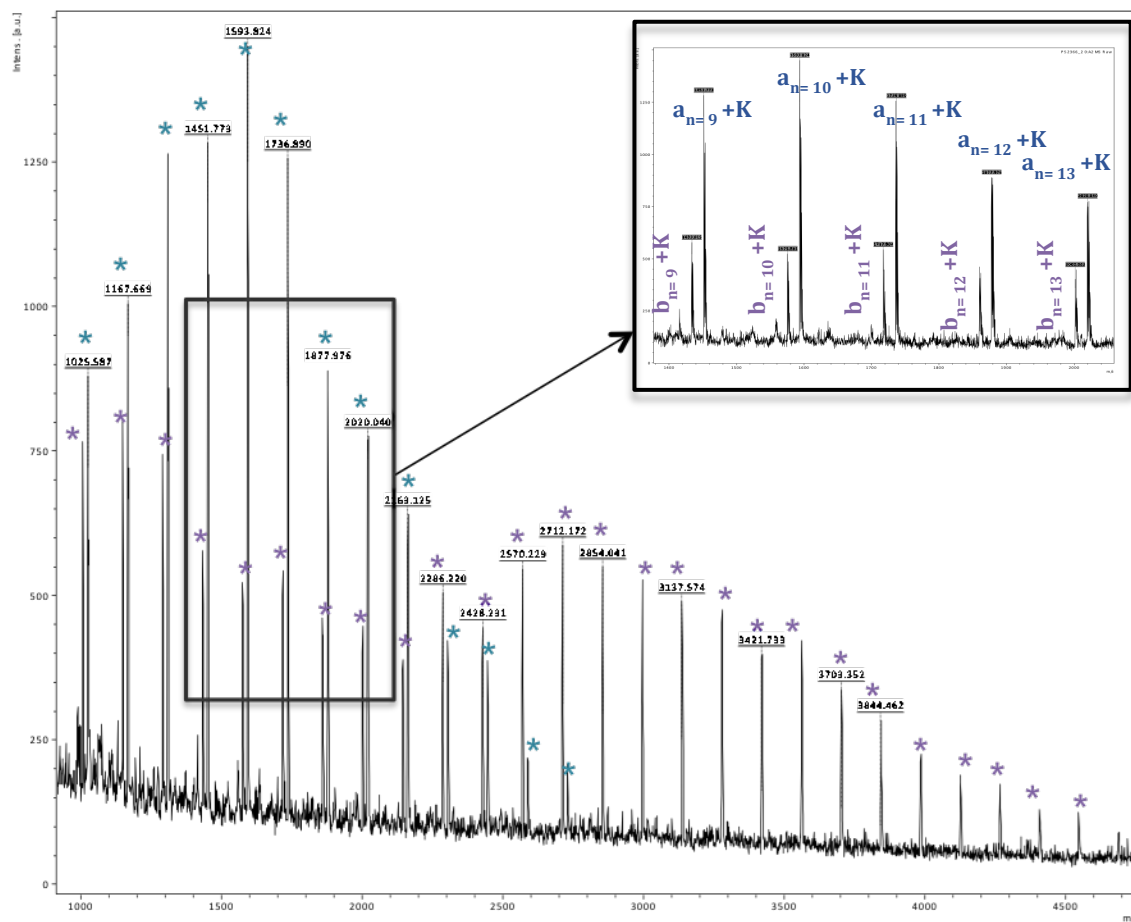
Figure 3.8. MALDI-TOF mass spectra of polycarbonate from entry 3, Table 3.5.

The chain end groups of the polycarbonates obtained in the four experiments from Table 3.5 were analyzed by MALDI-TOF mass spectra (Figure 3.8). They all present repeating units of 142 *m/z* corresponding to a cyclohexenecarbonate - $C_6H_{10}C(O)O$- repetitive unity. Two common distributions were observed in all catalytic experiments attributed to a chain with the presence of -Cl as well as -OH as end groups (**a** + K in Figure 3.9) and another distribution in the mass spectra, which fits with two -OH terminal groups (**b** + K in Figure 3.9).

Figure 3.9. Proposed chain ends on the basis of MALDI TOF analysis.

In summary, the MALDI-TOF analysis of the polymer synthetized with **AlL1**/PPNCl suggests that chain **a** (Figure 3.9) was formed by an initiation step involving the opening of the epoxide by a nucleophilic attack of chloride anion, which, presumably, comes from PPNCl co-catalyst, to the coordinated epoxide. On the other hand, chain **b** (Figure 3.9), which contains two terminal –OH, suggests that the initiation step involves the opening of the epoxide by a nucleophilic attack with –OH originated from traces of water present in the reactor. The termination step for both polymer chains was proposed to be produced by hydrolysis.
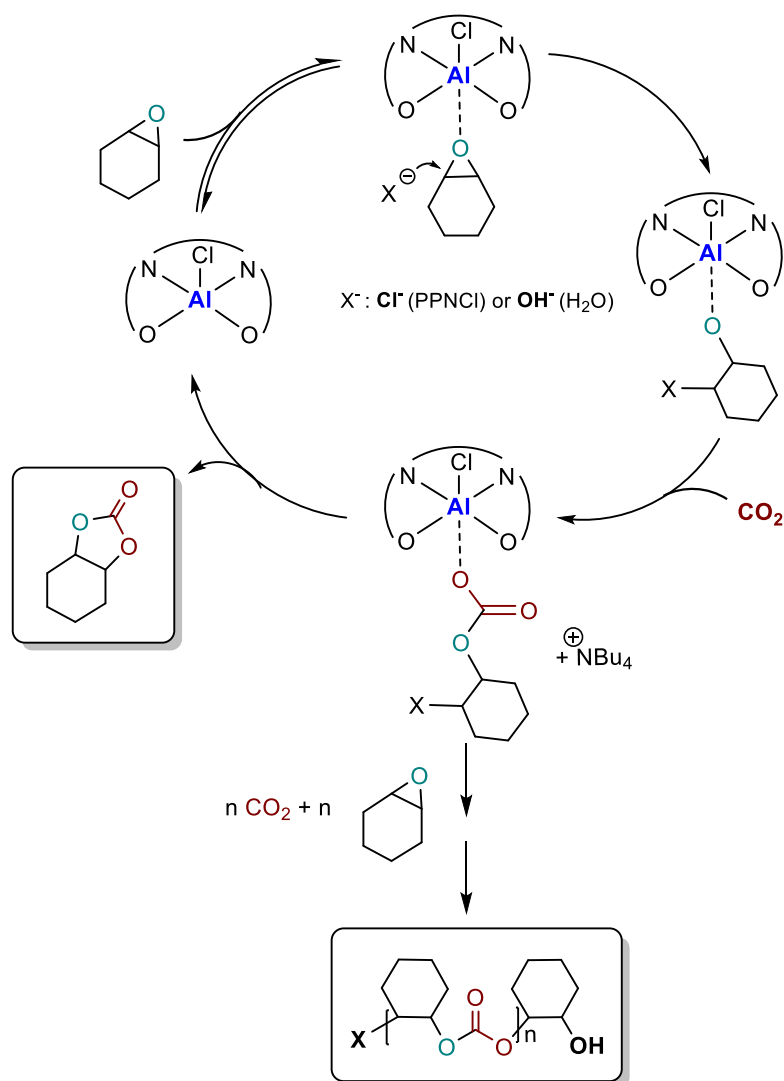
Scheme 3.5. Proposed reaction mechanism for the copolymerization of cyclohexene oxide with CO_2 using catalytic system **AlL1**/PPNCl.

With these evidences it is possible to propose a plausible catalytic cycle for the copolymerization of cyclohexene oxide and CO_2 (Scheme 3.5). When the coordination of the epoxide takes places (a, Scheme 3.5) subsequent nucleophilic attack with chloride anion (PPNCl) or hydroxo anion (H_2O) opens the epoxide forming the alkoxide fragment (b, Scheme 3.5). Then, CO_2 incorporates in the aluminum metal center and subsequent insertions of epoxide and CO_2 leads to the formation of the desirable polycarbonate (c and d, Scheme 3.5). The backbiting mechanism to form cyclic carbonate by-product was no negligible (e, Scheme 3.5).

3.2.2.3 *Mechanistic studies for the cycloaddition of CO_2 to styrene oxide*

(a) ^{27}Al NMR experiments

As, unfortunately, we could not obtain a suitable crystal for X-ray diffraction structure determination of **AlL1** complex, ^{27}Al NMR spectroscopy could be very useful to assess the complex structure in solution in the presence of the substrate as it is sensitive to the symmetry, chemical environment and coordination number around the metal center.[33,34,35] ^{27}Al NMR spectra are characterized by broad signals, depending on the coordination and the symmetry at the aluminum center. For example, Haraguchi and Fujiwara[36] showed that on the one hand, the line width becomes smaller when the complex symmetry at the aluminum center was higher and secondly, an upfield shift occurs with increasing the coordination number. In addition, Darensbourg and co-workers[37] showed that the ^{27}Al NMR spectra of [Al(salen)Cl] complexes consisted in two signals: a dominant, broad signal, at about 70 ppm and a weak, narrow signal, at about 7 ppm. The authors explained the observation of these two signals by the presence of an equilibrium between a pentacoordinate species (wide signal) and an octahedral complex (thinest signal).

Another feature to take into account in the ^{27}Al NMR spectra is that background from NMR probes is very broad; therefore, it is difficult sometimes to distinguish resonances of many aluminum species from the probe background.[38]
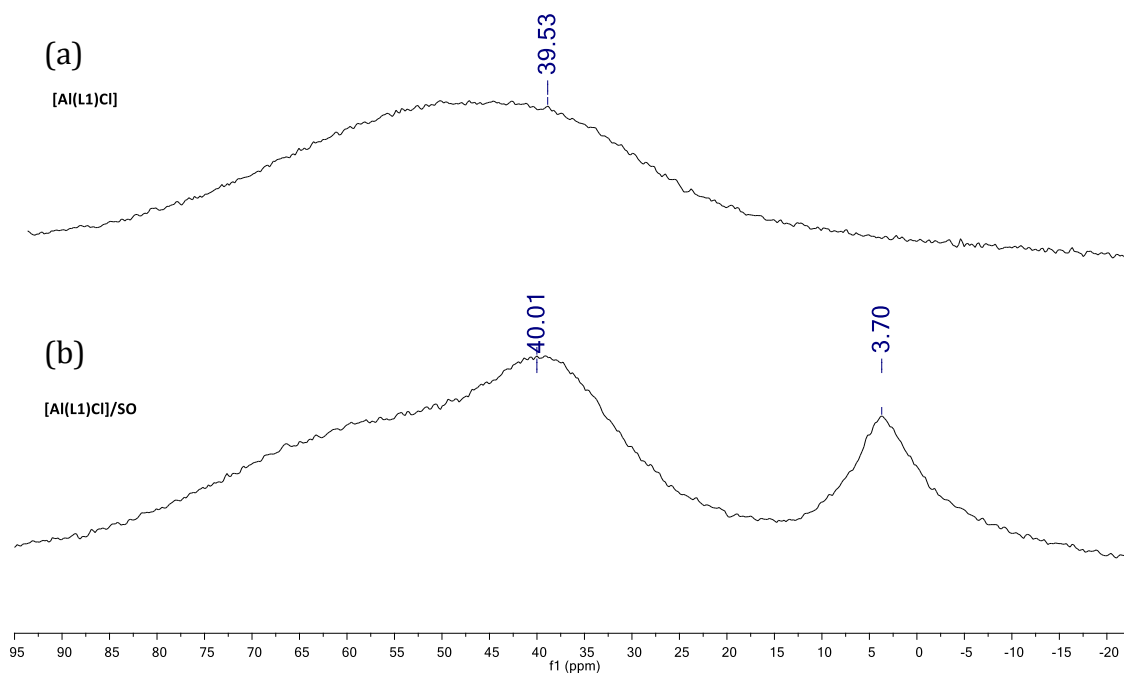
Figure 3.10 . ^{27}Al NMR spectra of complex **AlL1** alone (a) and mixture of **AlL1**/styrene oxide (1:1) (b) in CDCl$_3$.

^{27}Al NMR spectroscopy was employed to obtain an initial clue of the interaction of **AlL1** with a model substrate, styrene oxide, in CDCl$_3$. **AlL1** exhibits a single broad and strong resonance with a width of 65-35 ppm, which probably collapses with the probe background (aprox. 50 ppm) (a, Figure 3.10) and can be attributed to a pentacoordinated species. When equimolar amount of styrene oxide was added in the NMR tube containing **AlL1** two well defined signals appeared at 40.01 ppm and 3.70 ppm (b, Figure 3.10). The downfield broad signal corresponded to the pentacoordinate **AlL1** complex but here was better resolved from the probe background, whereas the upfield signal could be ascribed as an hexacoordinated complex formed by the coordination of styrene oxide to the aluminum metal center.[37,39] At this point it was proposed that in an initial step of the reaction mechanism, an equilibrium between the pentacoordinated **AlL1** complex and hexacoordinated, with styrene oxide coordinated through the aluminum center takes place (Scheme 3.8).
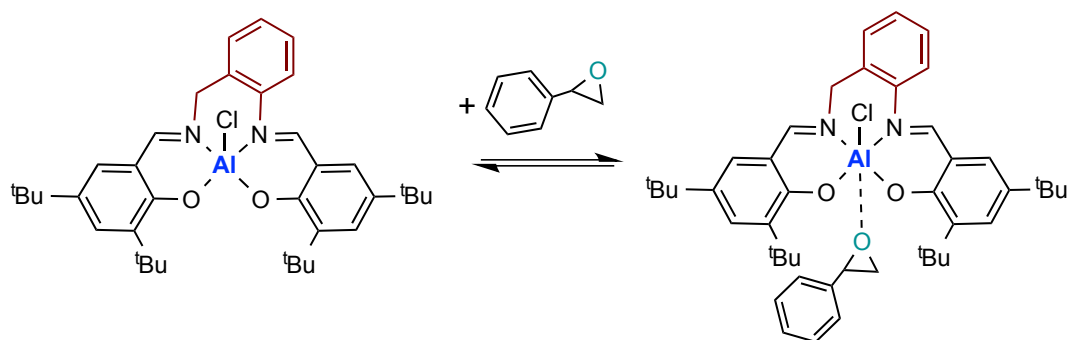
Scheme 3.8. Equilibrium between five and six-coordinated aluminum species.

(b) Kinetic studies

To continue with the investigation of the role of the aluminum complex, the co-catalyst and the CO_2 pressure in the reaction mechanism, a kinetic study of the formation of cyclic styrene carbonate catalyzed by **AlL1**/TBAB system was undertaken. Solvent-free conditions were chosen using neat substrate to work at a similar environment that in the catalytic studies. The reaction kinetics were monitored by sampling and subsequently analyzed by ^{1}H NMR spectroscopy to determine the conversion of epoxide to cyclic carbonate.

The general form of the reaction rate for the synthesis of styrene carbonate by using catalyst **AlL1** and TBAB is given by Equation (1). The approximations taken into consideration were those reported in the literature for similar studies[21,40,41,42,43]

$$\text{Rate} = k[\text{epoxide}]^a[CO_2]^b[\textbf{AlL1}]^c[\text{TBAB}]^d \tag{1}$$

Assuming that the concentration of **AlL1** and TBAB does not change during the reaction since they both act as catalysts, and CO_2 is present in large excess due to the semi-batch operation so that the Equation (1) can be rewritten as Equation (2)

$$\text{Rate} = k_{obs}[\text{epoxide}]^a \text{ where } k_{obs} = k[CO_2]^b[\textbf{AlL1}]^c[\text{TBAB}]^d \tag{2}$$

When the reaction is pseudo-zero order respect to the concentration of the epoxide (a = 0) there is a lineal dependence of the concentration of the epoxide respect to the time. When the reaction is first order respect to the substrate, the observed rate

constant can be determined from the slope of a linear plot of the natural logarithm of the changing sample concentration with time. (Eqs. (3) and (4)).

$$Rate = -d[epoxide]/dt \tag{3}$$

$$-\ln[epoxide] = k_{obs}t \tag{4}$$

As can be seen in (a), (Figure 3.11), the amount of styrene oxide decreased with reaction time, for a binary catalytic system **AlL1**/TBAB with CO_2. It is remarkable that no induction period can be observed in the reaction. North and co-workers reported that a shorter induction period and faster approach to steady state in the binary catalytic system indicate that TBAB is acting as a catalytic enhancer for styrene carbonate synthesis.[44] The same author showed that the reaction under solvent-free conditions is pseudo-zero order whereas in solvent it is first order with respect to the starting material.[44] Contrary with these observations, (b), (Figure 3.11) showed that the rate constant for styrene oxide conversion by **AlL1**/TBAB following Equation (4) is a pseudo-first order at these reaction conditions.
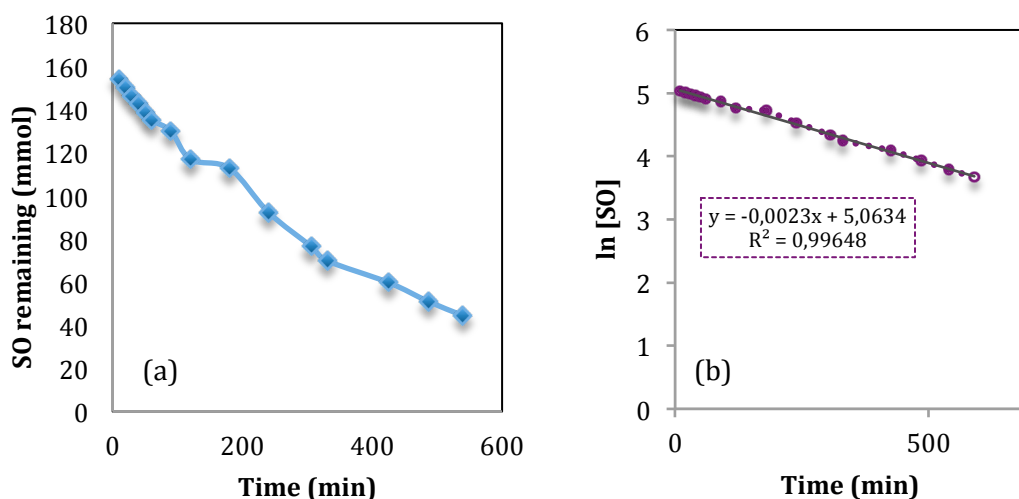
Figure 3.11. (a) Styrene oxide conversion for the **AlL1**/TBAB catalytic system as a function of time. (b) Pseudo-first order kinetic plot of styrene oxide against time for the **AlL1**/TBAB catalytic system. Reaction conditions: T = 80 °C, P_{CO2} = 10 bar, TBAB 0.2 mol %, catalyst 0.2 mol %.

To determine the order with respect to the catalyst **AlL1** and the co-catalyst, the reactions were performed maintaining constant the reaction temperature and working in the presence of an excess of CO_2. Since both CO_2 and epoxide concentration may be considered pseudo constant as we work at initial rates, the natural logarithm of the rate law (Equation (2)) results in Equation (5), from which is possible to afford the order c and d (Equation (5)) with respect to the catalyst and co-catalyst concentration by examination of a double logarithmic plot.

$$\ln\left(k_{obs'}\right) = \ln k + b\ln[CO_2] + c\ln[\mathbf{AlL1}] + d\ln[\mathrm{TBAB}] \tag{5}$$

Initially, the amount of TBAB was fixed at 0.2 mol % while the concentration of catalyst was varied between 0.1-0.4 mol %. Similarly, the concentration of **AlL1** was maintained at 0.2 mol % and TBAB concentration was changed from 0.2-1.0 mol %. Figure 3.12 and Figure 3.13 show the ^{1}H NMR data recorded at four different amounts of catalyst and co-catalyst, respectively. In both cases, the double logarithmic plot of the initial rates against catalyst or co-catalyst concentration showed a linear dependence providing a slope of 0.6618 and 1.1127, respectively, suggesting that the reaction was first order in the concentration of catalyst **AlL1** and TBAB (b, Figure 3.12; d, Figure 3.13).
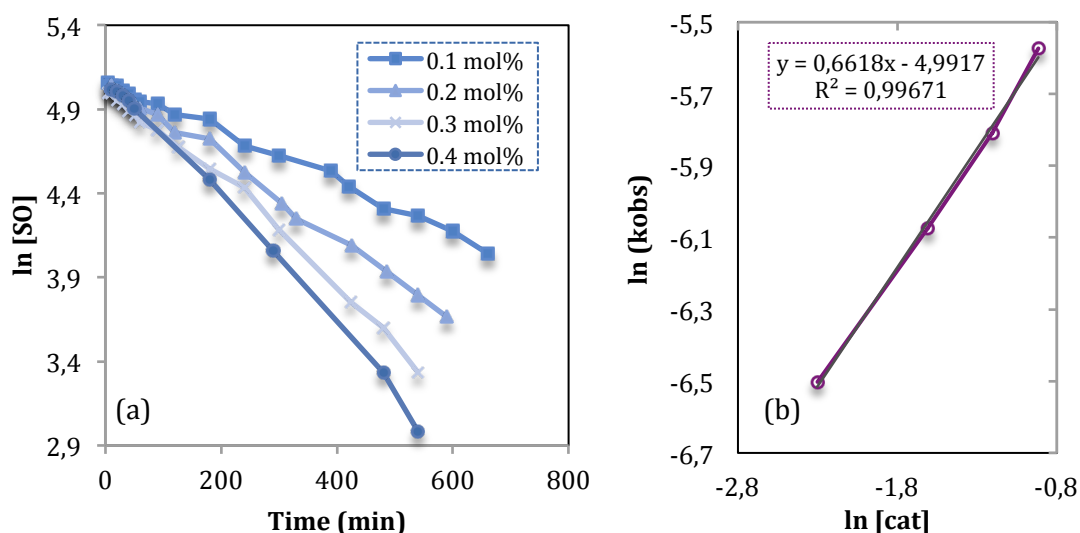
Figure 3.12. Styrene carbonate synthesis at four different concentrations of **AlL1**. Reaction conditions: T = 80 ºC, P_{CO2} = 10 bar, TBAB 0.2 mol %, catalyst 0.1-0.4 mol%.
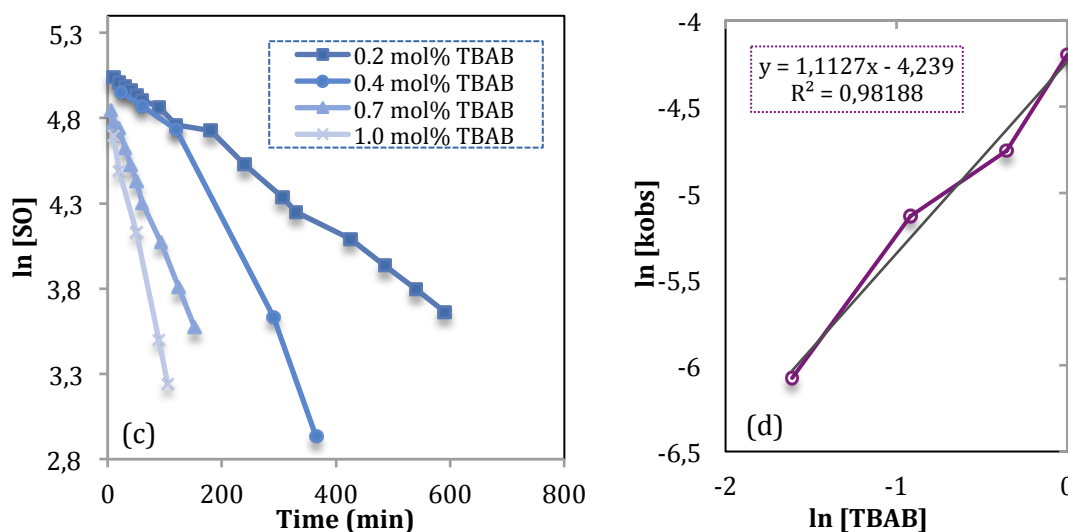
Figure 3.13. Styrene carbonate synthesis at four different concentrations of TBAB. Reaction conditions: T = 80 ºC, P_{CO2} = 10 bar, catalyst 0.2 mol %, TBAB 0.2-1.0 mol %.

The first order dependence on the binary catalyst system suggests that only one molecule of monometallic Al complex an also one molecule of TBAB is involved in the mechanism, before or during the rate-determining step of the catalytic cycle. Comparing with the previously reported kinetic analysis of cyclic carbonate synthesis, similar results were reported first by Otero and co-workers with bimetallic aluminum complex[45] and by Kleij and co-workers with binary Zinc(salen)-based complex.[43] It is well known that one role of the ammonium halide is to ring-open the coordinated epoxide to form a halo-alkoxide. Otherwise, North proposed a second-order dependence on TBAB with μ-oxo-Al(salen)/TBAB catalytic system cited above. In this case TBAB had a second role to generate tributylamine, which can activate the CO_2 (See Scheme 1.4 in Chapter 1).[44]

To investigate the role of the CO_2 pressure in the catalytic cycle, the conversion along the reaction time was analysed at four different CO_2 pressures between 10-40 bar, maintaining **AlL1**/TBAB concentration and temperature constant (80 ºC). Initially, it was observed a first-order dependence at low CO_2 pressures, between 10-30 bar, (slope of 0.6049, Figure 3.14) suggesting that one CO_2 molecule is involved in the catalytic cycle as reported by North.[44] However, further increase of the CO_2 pressure up to 40 bar

the reaction rate was maintained. This indicates that the solubility of the CO_2 in the reaction mixture is the limiting factor.
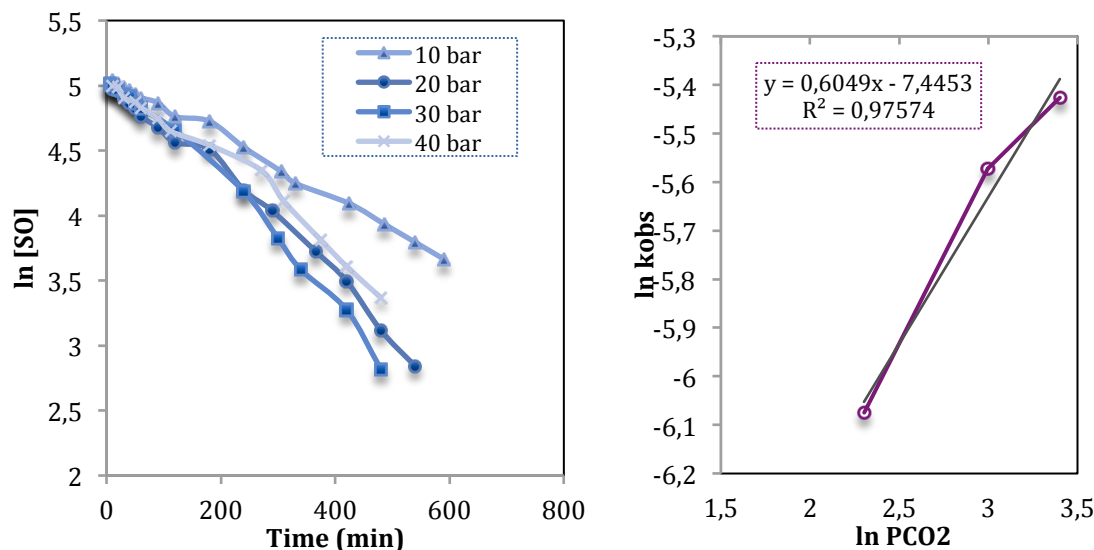
Figure 3.14. Styrene carbonate synthesis at four different CO_2 pressures. Reaction conditions: T = 80 ºC, catalyst 0.2 mol %, TBAB 0.2 mol %.

It is commonly observed a clear influence of temperature on the reaction rate for the formation of cyclic carbonates using homogeneous metal catalysts.[40] According to this we proceed to determine what is the temperature effect in **AlL1**/TBAB catalytic system. The activation energy (E_a) of the reaction can be calculated using the Arrhenius Equation (6), from the relationship between the observed rate constant (k_{obs}) and the reaction temperature, where A and E_a are the pre-exponential factor (min^{-1}) and the activation energy ($kJ·mol^{-1}$), respectively, R is the universal gas constant (8.314 $J·mol^{-1}·K^{-1}$), and T is the absolute temperature (K).

$$k_{obs} = A \cdot \exp\left(-\frac{E_a}{RT}\right) \qquad (6)$$

The activation energies for the formation of styrene carbonate catalyzed by **AlL1**/TBAB binary system were determined over the temperature range 40-100 ºC by fitting the data from a plot of the natural logarithm of the observed reaction rates against the reciprocal absolute temperature (1/T). Figure 3.15 showed the Arrhenius plot for this catalytic system and, therefore, the activation energy was calculated to be 38.0 $kJ·mol^{-1}$.
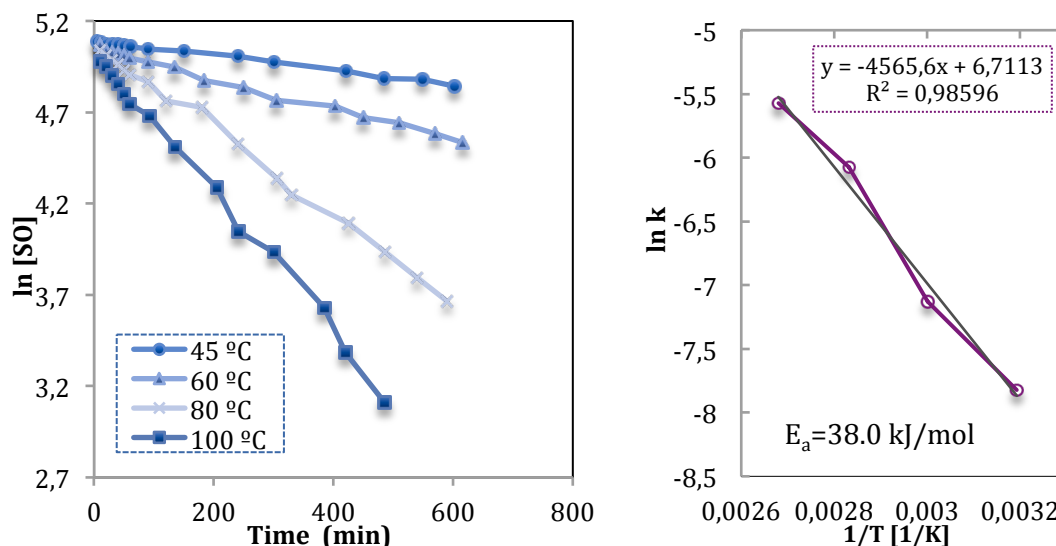
Figure 3.15. Styrene carbonate synthesis at four different temperatures and Arrhenius plot. Reaction conditions: P_{CO2}: 10 bar, catalyst 0.2 mol %, TBAB 0.2 mol %.

Comparing this value with the binary catalytic system studied by Styring and co-workers[41] for the synthesis of styrene carbonate with [Al(salacen)]/TBAB (Figure 3.16) they achieved a lower energetic activation barrier of 23 kJ·mol^{-1} and a similar value using [Al(salacen)] catalyst alone. Higher values (up to 78 kJ·mol^{-1}) were reported using Mg-Al mixed metal oxides.[46] An important feature observed by Styring was the potential catalytic activity of TBAB alone at 110 ºC, which was comparable with his aluminum catalyst meaning that aluminum catalyst could be eliminated from the process. In our case, as we worked at milder conditions the co-catalyst alone (1 mol %) only converted 20 % of styrene oxide at 80 ºC, 10 bar during 3 hours, whereas the combination of both **AlL1**/TBAB (0.2/1.0 mol %) at the same conditions gave 96 % of styrene oxide conversion. It is quite evident the high potential of our binary catalytic system.

9
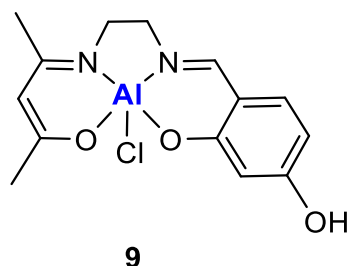
Figure 3.16. Structure od [Al(salacen)Cl] complex developed by Styring and co-workers.[41]

According with ^{27}Al NMR experiments and kinetics observations we could propose a plausible catalytic cycle (Scheme 3.9), which initiates with the activation of the epoxide by coordination to the metal center forming a hexacoordinated aluminum complex. The second step is the formation of a reactive aluminum-alkoxide species through a nucleophilic attack of the bromide anion from TBAB to the epoxide. This metal-alkoxide bond is known to react easily with CO_2 forming a carbonate Al(III) species. This intermediate can either form a polycarbonate through further alternating insertions of epoxide and CO_2 or a cyclic carbonate monomer via intramolecular rearrangement and leaving group liberation. Using this kind of substrates cyclic carbonates were selectively formed.
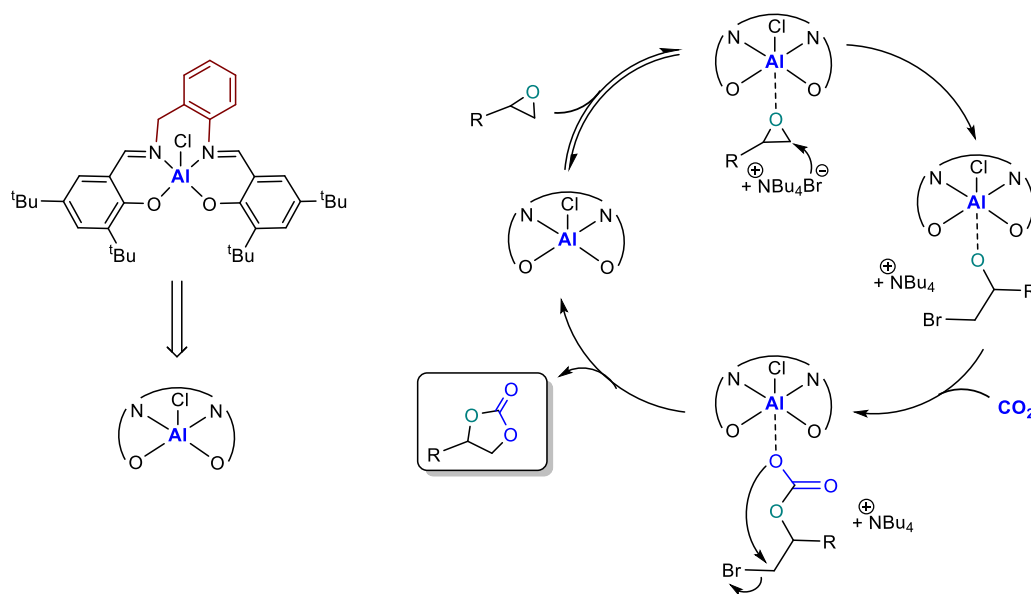
Scheme 3.9. Proposed reaction mechanism for the cycloaddition of epoxides into CO_2 with catalyst system **AlL1**/TBAB.

3.3 Conclusions

In this chapter, the high potential of tetradentate N_2O_2 salabza metal catalysts was reported. In particular, aluminium complex, **AlL1**, was found to be very stable and easy to synthesize from simple aluminium trichloride salt. It is also remarkable that this mononuclear aluminium complex, combined with TBAB, formed an active binary catalytic system for cycloaddition of CO_2 and epoxides. This catalytic system provides cyclic carbonates selectively with excellent conversions even at low pressures of CO_2 (up to 94 % at 10 bar). Higher catalytic activities were obtained with functionalized

terminal epoxides such epichlorohydrin with a maximum TOF of 3434 h^{-1}. Even though, more sterical hindered substrate such as methyl epoxyoleate was also transformed selectively in the cyclic carbonate product although at harsher reaction conditions. Also a detailed kinetic analysis of styrene carbonate synthesis catalysed by **AlL1**/TBAB system was carried out. As a result of the observed first order dependence of the reaction rate on catalyst, co-catalyst and CO_2 concentration, we proposed a catalytic cycle, which explains the role of each component. Furthermore, using the catalytic system **AlL1**/PPNCl in the reaction of cyclohexene oxide and CO_2 produces poly(cyclohexene carbonate) as a main product. The polymer formed contains good chain incorporation of CO_2, but suffers from low molecular weights. At room temperature and increasing the reaction time, higher molecular weight (2900 g/mol) and low polidispersity (1.3) was achieved. MALDI-TOF analysis of the polycarbonates obtained indicated that the initiating step involved the opening of the epoxide by Cl^- anion and OH^- (from water traces).

3.4   Experimental section

General Comments. H$_2$L1 was prepared following described procedures.[6] All complexes were prepared using Schlenk technique under inert conditions. Epoxides were dried over CaH_2, distilled and stored under inert atmosphere except 1,2-epoxyhexane, 1,2-epoxydodecane and epichlorohydrin, which were purchased at Sigma-Aldrich and used as received. Solvents were purified by the system Braun MB SPS-800 and stored under nitrogen atmosphere. Carbon dioxide (SCF Grade, 99.999 %, Air Products) was used introducing an oxygen/moisture trap in the line (Agilent). IR spectra were recorded on a Midac Grams/386 spectrometer in ATR (range 4000-600) cm^{-1} or KBr range (4000- 400 cm-1). UV-visible spectra were recorded on a UV-3100PC spectrophotometer. NMR spectra were recorded at 400 MHz Varian, with tetramethylsilane (^{1}H NMR, ^{13}C NMR) as internal standard and aluminum nitrate (^{27}Al NMR) as external reference. Electrospray ionization mass spectra (ESI-MS) were obtained with an Agilent Technologies mass spectrometer. Typically, a dilute solution of the compound in the indicated solvent (1:99) was delivered directly to the spectrometer source at 0.01 ml·min^{-1} with a Hamilton microsyringe controlled by a single-syringe infusion pump. The nebulizer tip operated at 3000–3500 V and 250 °C,

and nitrogen was both the drying and a nebulizing gas. The cone voltage was 30 V. Quasi-molecular ion peaks [M-H]⁻ (negative ion mode) or sodiated [M + Na]+ (positive ion mode) peaks were assigned on the basis of the m/z values. MALDI-TOF measurements of polymers were performed on a Voyager-DE-STR (Applied Biosystems) instrument equipped with a 337 nm nitrogen laser. All spectra were acquired in the positive ion reflector mode. Dithranol was used as matrix, which was dissolved in MeOH at a concentration of 10 mg·ml^{-1}. The polymer (5 mg) was dissolved in 1 mL of CHCl$_3$. 1 μl of sample, 1 μl of matrix and 1 μl of potassium trifluoroacetate (KTFA) solution (1 mg of KTFA in 1ml of THF) were deposited consecutively on the stainless steel sample holder and allowed to dry before introduction into the mass spectrometer. Three independent measurements were made for each sample. For each spectrum 100 laser shots were accumulated. The molecular weights (M_w) of copolymers and the molecular weight distributions (M_w/M_n) were determined by gel permeation chromatography versus polystyrene standards. Measurements were made in THF on a Millipore-Waters 510 HPLC Pump device using three-serial column system (MZ-Gel 100Å, MZ-Gel 1000 Å, MZ-Gel 10000 Å linear columns) with UV-Detector (ERC-7215) and IR- Detector (ERC-7515a). The software used to get the data was NTeqGPC 5.1. Samples were prepared as follow: 5 mg of the copolymer were dissolved with 2 ml of tetrahydrofuran (HPLC grade) and using toluene (HPLC grade) as internal standard. Magnetic susceptibilities were measured on a Sherwood MSBmk1 magnetic susceptibility balance with KK105 as a calibration standard. Elemental analyses were performed at the Serveis Tècnics de Recerca from the Universitat de Girona (Spain). All catalytic tests were done by duplicate.

3.4.1 Synthesis of [Al(L1)Cl] (AlL1)
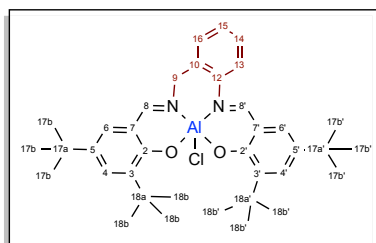
Anhydrous AlCl$_3$ (144.1 mg, 1.08 mmol) was added to a solution of (400 mg, 0.72 mmol) of **H₂L1** in 15 ml of dry THF. The yellow solution was stirred for 4 h at room temperature under inert atmosphere, filtered over celite and the filtrate was

evaporated under vacuum. The resulting solid was washed with acetonitrile, pentane and dried again. Bright yellow solid, 377.4 mg, (Yield 85 %).

Anal. Calcd. (found) for $C_{37}H_{48}AlClN_2O_2 \cdot 2H_2O$: C, 68.24 (68.11); H, 8.05 (8.21); N, 4.30 (4.03). HR ESI (THF) calculated for $C_{37}H_{48}AlN_2O_2$ m/z: 579.3531, found m/z: 579.3467 $[M-Cl]^+$; calculated for $C_{37}H_{45}AlClN_2O_2$ m/z: 611.3220, found m/z: 611.3726 $[M-3H]^+$. Selected IR bands (ATR, ν, cm^{-1}): 2952 m, 2904 m, 2868 m, 1615 ν(C=N) s, 1598 ν(C=N) m, 1554 m, 1540 s, 1387 m, 1360 m, 1257 ν(C-O) s, 1230 ν(C-O) m, 1202 m, 1174 s, 1037 m, 842 s, 787 m, 763 s. ^{1}H NMR (400 MHz, CDCl$_3$): δ 1.28 (s, 9H, *t*Bu), 1.33 (s, 9H, *t*Bu), 1.52 (s, 9H, *t*Bu), 1.57 (s, 9H, *t*Bu), 4.80 (br, 2H, ArC*H$_2$*N), 7.04 (d, 1H, C*H*-5-phenol, *J*= 2.4 Hz), 7.20 (d, 1H, C*H*-5-phenol, *J*= 2.4 Hz), 7.22-7.27 (m, 3H, Ar*H*), 7.38 (m, 1H, Ar*H*), 7.54 (d, 1H, C*H*-3-phenol, *J*= 2.4 Hz), 7.66 (d, 1H, C*H*-3 phenol, *J*= 2.4 Hz), 8.35 (s, 1H, C*H*=N), 8.42 (s, 1H, C*H*=N); ^{13}CNMR (75.43 MHz, CDCl$_3$): δ 29.78, 29.83 (C*H$_3$*, C$^{18b,b'}$*t*Bu), 31.37, 31.40 (C*H$_3$*, C$^{17b,b'}$*t*Bu), 34.09, 34.20 (C, C$^{17a,a'}$*t*Bu), 35.56, 35.67 (C, C$^{18a,a'}$*t*Bu), 62.63 (C^{9}H$_2$), 118.08 (C^2), 119.25 (C$^{2'}$), 123.15 (C^{15}), 126.78 (C^{16}), 127.41 (C^{13}), 127.57 (C^6), 128.51 (C$^{6'}$), 130.08 (C^{14}), 131.57 (C^4), 131.68 (C^{10}), 132.95 (C$^{4'}$), 138.96 (C^5), 139.55 (C$^{5'}$), 140.94 (C^3), 141.44 (C$^{3'}$), 148.28 (C^{12}), 162.84 (C^7), 164.02 (C$^{7'}$), 171.63 (C^8), 171.87 (C$^{8'}$). UV-vis (CH$_3$CN, $2.5 \cdot 10^{-5}$ M): λ(nm) (ε, L mol^{-1} cm^{-1}): 226.0 (116100), 282.0 (41884), 369.0 (18752).

3.4.2 Synthesis of [Cr(L1)Cl] (CrL1)
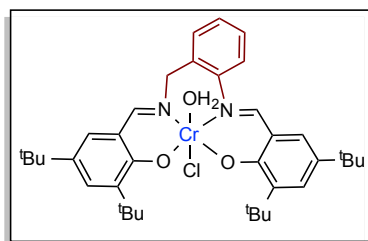
To a stirred solution of **H$_2$L1** (300.0 mg, 0.5407 mmol) in THF (15 ml) was added anhydrous CrCl$_2$ (66.5 mg, 0.5407 mmol). The resulting mixture was stirred under nitrogen at room temperature for 3 h. The mixture was further stirred under air for 3 h. The solution was filtered over celite and the filtrate was evaporated under vacuum. Cold hexane was added to the brown mixture. The suspension was filtered off and the solid was washed with hexane and dried under vacuum. Brown solid, 193.7 mg, (Yield

55 %). Deep red crystals suitable for X-ray diffraction analysis were obtained by slow diffusion of hexane into a diluted solution of the chromium complex in CH_2Cl_2

Anal. Calcd. (found) for $C_{37}H_{50}ClCrN_2O_3 \cdot H_2O \cdot OC_4H_8$: C, 65.80 (65.99); H, 8.08 (8.02); N 3.74 (3.86). HR ESI (THF) calculated for $C_{37}H_{48}CrN_2O_2$ m/z: 604.3121, found m/z: 604.3206 [M-Cl]$^+$. Selected IR bands (ATR, ν, cm^{-1}): 2952 m, 2904 m, 2868 m, 1611 ν(C=N) s, 1579, 1530 s, 1416 m, 1386 m, 1359 m, 1318 m, 1256 ν(C-O) s, 1225 ν(C-O) m, 1170 s, 1036 m, 837 s, 759 s.

3.4.3 Synthesis of [Fe(L1)Cl] (FeL1)
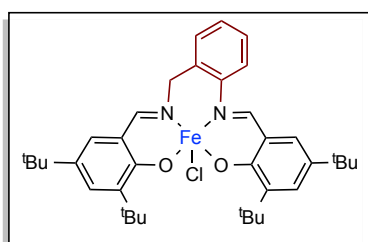
A 10 ml MeOH solution of FeCl$_3$ (90.5 mg, 0.56 mmol) was added dropwise to a 10 ml CH$_3$CN suspension containing (309.4 mg, 0.56 mmol) of **H$_2$L1** and Et$_3$N (0.15 ml, 1.12 mmol). The resulting solution changed color to dark purple and was gently refluxed for 2 h. When finished the solution was filtered while warm and concentred to one-third of the original volume. The filtrate was dissolved with CH$_2$Cl$_2$, filtered again over celite and removed the volatiles. The solid was further washed with hexane and dried under vacuum Black solid, 302 mg, (Yield 85 %). Purple crystals suitable for X-ray diffraction analysis were obtained by slow evaporation of a diluted solution of the complex in diethyl ether/hexane.

Anal. Calcd. (found) for $C_{37}H_{48}ClFeN_2O_2$: C, 69.00 (69.29); H, 7.51 (7.99); N 4.35 (4.40). HR ESI calculated for $C_{37}H_{48}FeN_2O_2$ m/z: 608.3065, found m/z: 608.3066 [M-Cl]$^+$;. Selected IR bands (ATR, ν, cm^{-1}): 2950 m, 2903 m, 2866 m, 1608 ν(C=N) s, 1592 ν(C=N) s, 1549 m, 1534 s, 1437 m, 1385 m, 1359 m, 1317 m, 1271 m, 1254 ν(C-O) s, 1226 ν(C-O) m, 1171 s, 855 m, 838 s, 785 m, 758 s. UV-vis (CH$_3$CN, $2.5 \cdot 10^{-5}$ M): λ(nm) (ε, L mol^{-1} cm^{-1}): 220.0 (86576), 240.0 (31304), 276.0 (23496), 332.0 (11528), 532.0 (3948). μ_{eff} (25 °C) = 5.90 μ_B.

3.4.4 Synthesis of [Co(L1)O₂CMe] (CoL1)
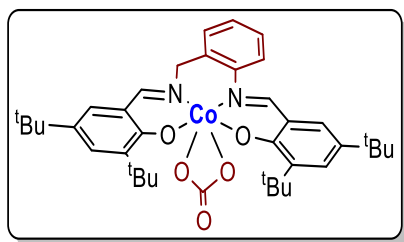
To a stirred solution of **H₂L1** (300 mg, 0.54 mmol) in THF (10 ml) at room temperature under inert atmosphere, an ethanol solution (10 ml) containing 1.0 equiv. of $Co(OAc)_2 \cdot 2H_2O$ (134.7 mg, 0.54 mmol) was added. The reaction mixture was refluxed for 1 h under inert atmosphere, cooled down to room temperature and was further stirred under air stream for 6 h. The resultant reaction solution was concentrated and hexane was added to precipitate the product, which was filtered off, washed with diethyl ether and hexane and dried under vacuum. Dark red solid, 180.3 mg, (Yield: 49 %). Brown crystals suitable for X-ray diffraction analysis were obtained by slow evaporation of a diluted solution of the complex in diethyl ether/hexane.

Anal. Calcd. (found) for $C_{37}H_{48}CoN_2O_2 \cdot H_2O \cdot CH_3CH_2OH$: C, 68.36 (68.42); H, 8.02 (7.83); N 3.99 (3.79). HR ESI (THF) calculated for $C_{37}H_{48}CoN_2O_2$ m/z: 611.3048, found m/z: 611.3060 [M-OAc]⁺. Selected IR bands (ATR, ν, cm⁻¹): 2953 m, 2899 m, 2861 m, 1613 ν(C=N) s, 1602 ν(C=N) m, 1547 m, 1525 s, 1447 s, 1460 m, 1428 m, 1409 m, 1257 ν(C-O) m, 1200 m, 1166 s, 1024 m, 949 m, 781 m, 761 m, 686 m. ¹HNMR (400 MHz, CDCl₃): δ 1.16 (br, 9H, *t*Bu), 1.25 (br, 9H, *t*Bu), 1.30 (br, 9H, *t*Bu), 1.45 (br, 9H, *t*Bu), 1.59 (br, 3H, C*H₃*-OAc), 4.17 (d, 1H, ArC*H₂*N, *J* = 13.6 Hz), 4.54 (d, 1H, ArC*H₂*N, *J* = 12.4 Hz), 6.99 (br, 1H, Ar*H*), 7.08 (br, 1H, Ar*H*), 7.16 (br, 1H, Ar*H*), 7.34-7.36 (br, 2H, Ar*H*), 7.44 (br, 1H, Ar*H*), 7.75 (br, 1H, C*H*=N), 7.85 (br, 1H, C*H*=N). UV-vis (CH₃CN, 2.5·10⁻⁵ M): λ(nm) (ε, L mol⁻¹ cm⁻¹): 217.0 (78980), 230.0 (35624), 258.0 (36144), 416.0 (6088). μ_{eff} (25 ºC) = 0.05 μ_B.

Standard procedure for the synthesis of cyclic carbonates. The catalytic tests were carried out in a 100 mL Berghof reactor, which was previously kept for 4 hours under vacuum at 100 ºC. After cooling, a solution under inert atmosphere containing the catalyst dissolved in neat distilled substrate and the co-catalyst, when indicated, was injected into the reactor. The autoclave was pressurized with CO_2, and then heated to the specific temperature to reach the desired pressure. After the reaction time, the

reactor was cooled with an ice bath and slowly depressurized (With PO a dichloromethane trap was used). The % conversion was determined by ^{1}H NMR of the crude mixture by integral ratio between alkene oxide and cyclic carbonate. The % yield was determined by ^{1}H NMR using mesitylene as internal standard.

Standard kinetic experiment procedure: A Parr 477 autoclave equipped with a proportional-integral-derivative (PID) temperature controller and gas reservoir was used for kinetic experiments in the reaction of styrene oxide with CO_2. In a typical experiment, the autoclave was charged with the catalyst and co-catalyst in neat distilled styrene oxide, heated and pressurized with CO_2. Samples were undertaken at determined time and the conversion of the product was determined by ^{1}H NMR spectroscopy. After the reaction time the autoclave was then depressurized.

Standard procedure for copolymerization with cyclohexene oxide: Using the same procedure for the synthesis of cyclic carbonates the % conversion was also determined by ^{1}H NMR of the crude mixture by integral ratio between alkene oxide with copolymer and cyclic carbonate. The % yield was determined by ^{1}H NMR using mesitylene as internal standard. The final mixture was dissolved in dichloromethane, the solvent was evaporated and the residue dried in vacuum at 100 ° C for 3 hours to remove excess of cyclohexene oxide. The final residue was washed several times with hexane to purify the poly(carbonate) and was analysed by ^{1}H NMR spectroscopy. % of CO_2 content was calculated from ^{1}H NMR data by the integral ratio between copolymer carbonate linkages ($\delta = 4.65$ ppm) respect to ether linkage signals ($\delta = 3.45$ ppm).

3.4.5 X-ray crystal structure determination

Diffraction data for the structures reported were carried out on a Smart CCD 1000 Bruker diffractometer system with Mo Kα radiation ($\lambda = 0.71073$ Å). Cell refinement, indexing and scaling of the data sets were carried out using programs Bruker Smart and Bruker Saint. All the structures were solved by *SIR97*[47] and refined by *Shelxl9*[48] and the molecular graphics with ORTEP-3 *for Windows*.[49] All the calculations were performed using the *WinGX* publication routines.[50] Crystallographic data is collected in Table 3.6

Table 3.6. Crystallographic data and details of structure refinement for compound **CrL1**, **FeL1** and **CoL1**.

	CrL1	FeL1	CoL1
Molecular formula	$C_{43}H_{62}ClCrN_2O_{4.50}$	$C_{78}H_{106}Cl_2Fe_2N_4O_5$	$C_{39}H_{51}CoN_2O_4$
Molecular weight	766.39	1362.26	670.74
Crystal system	Monoclinic	Monoclinic	Monoclinic
Space group	C2/c	C2/c	P2(1)/n
Temp. (K)	100(2)	100(2)	100(2)
Radiation (λ, Å)	Mo Kα (λ=0.7107 Å)	Mo Kα (λ=0.71073 Å)	Mo Kα (λ=0.7107 Å)
a (Å)	30.732(5)	19.0813(14	13.1775(8)
b (Å)	12.284(2)	19.8561(16)	23.4462(15)
c (Å)	26.514(4)	20.3191(13)	13.3026(8)
α (º)	90	90	90
β (º)	120.596(4)	101.408(3)	117.093(2)
γ (º)	90	90	90
Volume (Å3)	8616(2)	7546.4(10)	3659.0(4)
Z	8	4	4
Dx (Mg·m-3)	1.182	1.199	1.218
F (000)	3288	2912	1432
Crystal dimensions (mm)	0.10 x 0.10 x 0.02	0.03 x 0.02 x 0.01	0.40 x 0.30 x 0.30
μ (Mo Kα) (mm-1)	1.661	1.686	1.737
θmax (º)	25.042	27.930	25.421
Reflections collected	24685	28962	-
Unique reflections	7609	8355	6677
Rint.	0.1115	0.0479	0.0492
Parameters	562	524	756
R1 [I >2σ(I)]	0.0920	0.0477	0.0731
wR2	0.1730	0.1009	0.1982
Δρ (e/ Å3)	0.459, -0.509	0.517, -0.534	0.462, -0.510

3.5   Supporting information

NMR spectra, FTIR, ESI and MALDI-TOF mass spectra of the complexes, the NMR and GPC spectra of the catalytic products and the pdf file containing CIF files giving crystallographic data for **CrL1**, **FeL1** and **CoL1**, are available in the supporting information CD.

3.6   References

1   Coates, G. W.; Moore, D. R.; *Angew. Chem. Int. Ed*. **2004**, *43*, 6618-6639.

2   Sasaki, M.; Manseki, K.; Horiuchi, H.; Kumagai, M.; Sakamoto, M.; Sakiyama, H.; Nishida, Y.; Sakai, M.; Sadaoka, Y.; Ohbad, M.; Okawa, H., *J. Chem. Soc. Dalton Trans.* **2000**, 259-263.

3   Clarkson, G. J.; Gibson, V. C.; Goh, P. K. Y.; Hammond, M. L.; Knight, P. D.; Scott, P.; Smit, T. M.; White, A. J. P.; Williams, D. J., *Dalton Trans.* **2006**, 5484-5491.

4   Salmon, L.; Thuery, P.; Riviere, E.; Ephritikhine, M., *Inorg. Chem.* **2006**, *45*, 83-93.

5   Asadi, M.; Mohammadikish, M.; Mohammadi, K., *Cent. Eur. J. Chem.* **2010**, *8*, 291-299.

6   Chen, H.-L.; Dutta, S.; Huang, P.-Y.; Lin, C.-C.; *Organometallics* **2012**, *31*, 2016-2025.

7   Abou-Melha K.S., Faruk H., *J. Iran. Chem. Soc.* **2008**, *5* 122-134.

8   Szécsényi, K. M.; Leovac, V. M.; Jacimovic, Z. K.; Cesljevic, V. I.; Kovacs, A. M.; Pokol, G.; Gal, S., *J. Termal Analysis and Calorimetry* **2001**, *63*, 723-732.

9   a) Nakamoto, K., Infrared and Raman spectra of inorganic and coordination compounds, Wiley & Sons, New York, **1998**. b) Deacon, G. B.; Phillips. R. J., *Coord. Chem. Rev.* **1980**, *33*, 227-250.

10   Elmas, S.; Subhani, M.; Harrer, M.; Leitner, W.; Sundermeyer, J.; Müller, T.E.; *Catal. Sci. Technol.* **2014**, *4*, 1652-1657.

11   Darensbourg, D. J.; Moncada, A. I.; Wei, S-H.; *Macromol.* **2011**, *44*, 2568-2576.

12   Addison, A. W.; Rao, T. N.; Reedijk, J.; Rijn, J. V.; Verschoor, G. C., *J. Chem. Soc. Dalton Trans.* **1984**, 1349-1356.

13   Pascal Junior, R. A.; L'Esperance, R. P.; Van Engen, D., *private communication*, **2014**, CCDC990458.

14   Oyaizu, K.; Tsuchida E.; *Inorg. Chim. Acta* **2003**, *355*, 414-419.

15   Dyers, L. Jr.; Que, S. Y.; VanDerveer, D.; Bu, X. R.; *Inorg. Chim. Acta* **2006**, *359*, 197-203.

16   Shyu, H.L.; Wei, H.H.; Lee, G.H.; Wang, Y.; *J. Chem. Soc., Dalton Trans.* **2000**, 915-918.

17   Niu, Y.; Li, H., *Colloid Polym Sci.* **2013**, *291*, 2181-2189.

18   Zhuang, X.; Oyaizu, K.; Niu, Y.; Koshika, K.; Chen, X.; Nishide, H., *Macromol Chem Phys.* **2010**, *211*, 669-679.

19   Whiteoak, C. J.; Kielland, N.; Laserna, V.; Escudero-Adán, E. C.; Martin, E.; Kleij, A. W.; *J. Am. Chem. Soc.* **2013**, *135*, 1228-1231.

20   Lu, X.-B.; Zhang, Y.-J.; Liang, B.; Li, X.; Wang, H.; *J. Mol. Catal. A: Chem.* **2004**, *210*, 31-34.

21   Clegg, W.; Harrington, R. W.; North, M.; Pasquale, R. *Chem. Eur. J.* **2010**, *16*, 6828-6843.

22   Langanke, J.; Greiner, L.; Leitner, W., *Green Chem.* **2013**, *15*, 1173-1182.

23   Whiteoak, C.; Martin, E.; Martínez Belmonte, M.; Benet-Buchholz , J.; Kleij, A. W.; *Adv. Synth. Catal.* **2012**, *354*, 469-476.

24   Darensbourg, D. J.; Lewis, S. J.; Rodgers, J. L.; Yarbrough, J. C., *Inorg. Chem.* **2003**, *42*, 581-589.

25   Aida, T.; Ishikawa, M.; Inoue, S. *Macromolecules* **1986**, *19*, 8-13.

26   (a) Lu, X.-B.; Feng, X.-J.; He, R. *Appl. Catal., A: General* **2002**, *234*, 25-33. (b) Lu, X.-B.; Zhang, Y.-J.; Jin, K.; Luo, L.-M.; Wang, H. *J. Catal.* **2004**, *227*, 537-541.

27   Darensbourg, D. J.; Billodeaux, D. R.; *Inorg. Chem.* **2005**, *44*, 1433-1442.

28   Darensbourg, D.J.; Yarbrough, J.C.; *J. Am. Chem. Soc.* **2002**, *124*, 6335-6342.

29   Buchard, A.; Kember, M.R.; Sandeman, K.G.; Williams, C.K.; *Chem. Commun.*
      2011, *47*, 212-214.

30   Matsumoto, K.; Sato, Y.; Shimojo, M.; Hatanaka, M.; *Tetrahedron: Asymmetry*
      2000, *11*, 1965-1973.

31   Darensbourg, D.J.; Yarbrough, J.C.; Ortiz, C.; Fang, C.C.; *J. Am. Chem. Soc.*
      2003, *125*, 7586-7591.

32   Sugimoto, H.; Ohtsuka, H.; Inoue, S.; *J. Polym. Sci., Part A: Polym. Chem.* **2005**,
      43, 4172-4186.

33   Ropson, N.; Dubois, P.; Jerome, R.; Teyssie, P.; *Macromolecules* **1993**, *26*, 6378-
      6385.

34   Dhammani, A.; Bohra, R.; Mehrotra, R.C.; *Polyhedron* **1998**, *17*, 163-171.

35   Atwood, D.A.; Harvey, M.J.; *Chem. Rev.* **2001**, *101*, 37-52.

36   Haraguchi, H.; Fujiwara, S.; *J. Phys. Chem.* **1969**, *10,* 3467-3473.

37   Tian, D.; Liu, B.; Gan, Q.; Li, H.; Darensbourg, D.J.; *ACS Catal.* **2012**, *2*, 2029-
      2035.

38   Azizi, S. N.; Ehsani-Tilami, S.; *J. Chin. Chem. Soc.* **2009**, *56*, 898-907.

39   Tian, D.; Liu, B.; Zhang, L.; Wang, X.; Zhang, W.; Han, L.; Park, D.-W. *J. Ind..*
      Eng. Chem. **2012**, *18*, 1332-1338.

40   Dengler, J. E.; Lehenmeier, M.W.; Klaus, S.; Anderson, C. E.; Herdtweck, E.;
      Rieger, B.; *Eur. J. Inorg. Chem.* **2011**, 336-343.

41   Supasitmongkol, S.; Styring, Peter *Catal. Sci. Technol.* **2014**, *4*, 1622-1630.

42   Luo, R.; Zhou, X.; Zhang, W.; Liang, Z.; Jiang, J.; Ji, H., *Green Chem.* **2014**, *16*,
      4179-4189.

43   Martín, C., Kleij, A. W.; *Beilstein J. Org. Chem.* **2014,** *10,* 1817-1825.

44   North, M.; Pasquale, R. *Angew. Chem., Int. Ed.* **2009,** *48,*2946-2948.

45   Castro-Osma, J. A.; Lara-Sánchez, A.; North, M.; Otero, A.; Villuendas, P.;
      Catal. Sci. Technol. **2012**, *2*, 1021-1026.

46   Yamaguchi, K.; Ebitani, K.; Yoshida, T.; Yoshida, H.; Kaneda, K., *J. Am. Chem.*
      Soc. **1999**, *121*, 4526-4527.

47   Altomare, A.; Burla, M. C.; Camalli, M.; Cascarano, G. L.; Giacovazzo, C.; Guagliardi, A.; Moliterni, A. G. G.; Polidori, G.; Spagna, R., *J. Appl. Cryst.* **1999**, *32*, 115-119.

48   Sheldrick, G. M., **1997**. SHELXS97 and SHELXL97.University of Göttingen, Germany.

49   Ortep-3 for Windows - A Version of ORTEP-III with a Graphical User Interface (GUI). Farrugia, L. J., *J. Appl. Crystallogr.* **1997**, *30*, 565-566.

50   WinGX Suite for Single Crystal Small Molecule Crystallography. Farrugia, L. J., *J. Appl. Cryst.* **1999**, *32*, 837-838.

Chapter - 4

Halogenated *meso*-phenyl Mn(III) porphyrins as highly efficient catalysts for the synthesis of organic carbonates using CO$_2$ and epoxides

Abstract

The introduction of halogen electron withdrawing atoms (chloro and fluoro) in the ortho position of the aryl groups of meso-tetraphenylporphyrin manganese(III) complexes increased their activity as catalysts in the reaction of carbon dioxide with epoxides, when compared with the meso-tetraphenylporphyrin manganese(III) counterpart, even in the absence of co-catalysts. In the polymerization reaction of carbon dioxide and cyclohexene oxide, almost ten-fold increase of the TOF was observed when 5,10,15,20-tetra(2,6-dichlorophenyl)porphyrinate manganese(III) acetate or 5,10,15,20-tetra(2,6-difluorophenyl)porphyrinate manganese(III) acetate complexes were used as catalysts. Under similar conditions, when terminal epoxides were used as substrates, the selective cycloaddition of CO$_2$ with styrene oxide, epichlorohydrin, propylene oxide, 1,2-epoxyhexane, 1,2-epoxytetradecane yielded exclusively the corresponding cyclic carbonates (conversion 54-98 %).

MnL2a: X = OAc, Y = Cl
MnL2b: X, Y = Cl
MnL3: X = OAc, Y = F
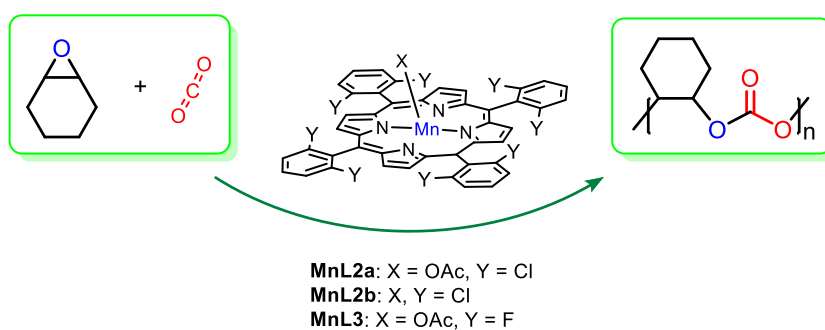
This work has been done in collaboration with Prof. Mariette M. Pereira and co-workers from University of Coimbra, Portugal.

4.1 Introduction

As commented in Chapter 1 and Chapter 3, one of the most promising processes for CO_2 utilization is the alternating copolymerization of CO_2 and epoxides to form polycarbonates, as first reported by Inoue *et al.* in 1969.[1] Subsequent to Inoue's initial discovery, many active catalysts with improved product selectivity have been developed. In the past two decades, some well-defined homogeneous metal complexes have been reported to be highly active and selective catalysts for polymer and/or cyclic carbonate formation, depending on the co-catalyst, substrate and reaction conditions.[2]

It should be mentioned that most of the metal based complexes, of which tetrapyrrolic macrocycles are privileged compounds for many applications,[3,4,5,6,7,8,9,10,11] require the presence of a co-catalyst, acting as nucleophile, whether added to the reaction (binary catalytic systems)[12,13,14,15] or already included in the structure of the complex (bifunctional catalytic systems)[16]. Nevertheless, Inoue *et al.*[17] reported that 5,10,15,20-tetraphenylporphyrinatomanganese(III) acetate ([Mn(TPP)(OAc)] Figure 4.1) in the absence of any additional co-catalyst, was able to promote the copolymerization of CO_2 and cyclohexene oxide (CHO) with a moderate TOF of 16.3 h^{-1} when compared with that reported for Cr(III)-salen based systems (1200 h^{-1})[18]. Darensbourg and Frantz proposed that the low ability of the five-coordinate Mn(III) complexes to bind the epoxide could be a plausible explanation for their low activity.[19] Thus, the introduction of electron-withdrawing groups at the periphery of the porphyrin ligand would strengthen their Lewis acidity, favoring the coordination of the epoxide to the metal center as observed for other catalytic systems.[20]

[Mn(TPP)(OAc)]

MnL2a: X = OAc, Y = Cl
MnL2b X, Y = Cl
MnL3: X = OAc, Y = F
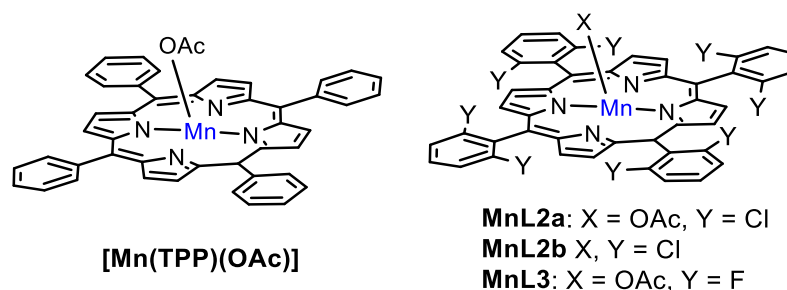
Figure 4.1. Manganese(III) meso-substituted porphyrin based complexes.

Therefore, in the first part of this chapter we present the catalytic study of 5,10,15,20-tetra(2,6-dichlorophenyl)- and 5,10,15,20-tetra(2,6-difluorophenyl)-porphyrinate manganese(III) complexes having acetate or chloride as axial coordination ligands (Figure 4.1) as selective catalysts either for the copolymerization of cyclic epoxides with CO_2 or the cycloaddition of terminal epoxides with CO_2, without the addition of co-catalysts.

Although the high activity and selectivity, the homogeneous catalysts tend to cause difficulties in catalyst recovery and product purification, which is an important issue to develop green reaction processes. Thus, it is vital to apply immobilized catalysts as they can be easily separated from the final mixture.[21] Carbon nanotubes (CNTs), among other nanomaterials, have been the object of extensive research in recent years. They have numerous beneficial properties, such as a substantial surface area and high mechanical and thermal resistance. Indeed, this material found a handful of application in the cyclic carbonate synthesis. For example, 1-hydroxyethyl-3-methylimidazoliumhalides immobilized on CNTs have high catalytic activity, and were recycled five times without any substantial drop in activity. The studies have shown that these catalysts exhibited significantly enhanced catalytic activity in the CO_2 and epoxides reaction in comparison to conventional heterogeneous supports based on silica and polymers.[22] Another example are quaternary ammonium chlorides covalently bound to CNTs which proved to be also an efficient and recyclable heterogeneous catalysts for the cyclic carbonate synthesis at mild conditions.[23]
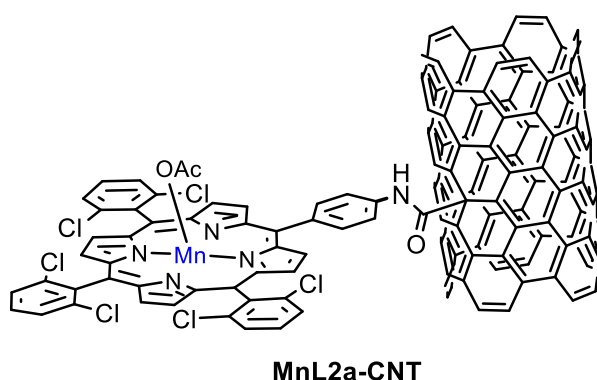
MnL2a-CNT

Figure 4.2. Complex **MnL2a** immobilized in a CNT support.

Thus, in the second part of this chapter we will focus on the evaluation of the recyclability of homogeneous catalyst **MnL2a** by itself and when immobilized in a CNT support (**MnL2a-CNT**, Figure 4.2) for the synthesis of propylene carbonate (PC) with CO_2 and propylene oxide (PO).

4.2 Results and discussion

4.2.1 Catalysts synthesis

The *meso*-substituted porphyrins 5,10,15,20-tetra(2,6-dichlorophenyl)porphyrin (**H₂L2**) and 5,10,15,20-tetra(2,6-difluorophenyl)porphyrin (**H₂L3**) were prepared at the University of Coimbra (Portugal) by the group of *Prof. Mariette M. Pereira*, by mixing equimolar amounts of pyrrol with the desired aldehydes in acetic acid/nitrobenzene using NaY zeolite as solid catalyst,[24,25] while their Mn(III) complexes **MnL2a**, **MnL3** and **MnL2b** were prepared by metal insertion with the appropriate metal salts [Mn(OAc)₂ in the case of **MnL2a** and **MnL3** and MnCl₂ for **MnL2b**], using DMF as solvent by the same group.[26]

4.2.2 Catalytic polymerization studies

The effect of the halogen atoms at the 2,6-positions of the phenyl ring in *meso*-substituted porphyrin manganese(III) complexes was evaluated on the copolymerization of CO_2 and cyclohexene oxide, in the absence of any co-catalyst, and the results are summarized in Table 4.1. First of all, the catalytic activity of **MnL2a** was tested at the same reaction conditions reported by Inoue *et al.* (0.2 mol %, 50 bar of CO_2 and 80 ºC) for direct comparison.[17]

MnL2a complex**,** bearing chlorine atoms in its structure**,** in absence of co-catalyst, afforded poly(cyclohexene carbonate) (PCHC) selectively (no cyclic carbonate was detected by ¹H NMR) with 84 % epoxide conversion and 72 % of polymer isolated yield (entry 1, Table 4.1). Additionally, very high alternate incorporation of CO_2 into the polymer linkages was obtained (98 %), with 4700 g/mol molecular weight.

Then, catalyst loading optimization was performed (from 0.07 mol % to 0.01 mol %; entries 2-4, Table 4.1) leading to a maximum TOF of 154 h⁻¹ at very low catalyst loading (0.01 mol %, entry 4, Table 4.1), which is nearly tenfold higher than the result previously reported using the non-halogenated [Mn(III)(TPP)(OAc)] catalyst.[17] Furthermore, the molecular weight of the copolymer obtained using **MnL2a** catalyst

increased up to 5300-8800 g/mol, together with very narrow polydispersity (M_w/M_n =1.09, 1.20; entries 2-3, Table 4.1). Next, decreasing the temperature to 60 ºC, using **MnL2a** catalyst at 0.07 mol %, only 56 % of epoxide conversion and 48 % isolated yield were obtained, but achieving the highest molecular weight polycarbonate (8800 g/mol; entry 5, Table 4.1).

Table 4.1. Copolymerization of cyclohexene oxide and CO_2 using catalysts **MnL2a**, **MnL3** and [Mn(TPP)(OAc)].[a]
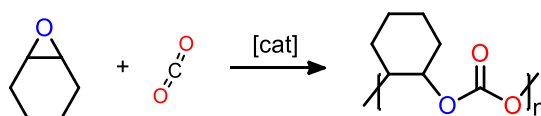
Entry	Cat	Cat (mol %)	P (bar)	T (ºC)	Conv[b] (%) (TOF)	% CO_2[c]	Y[d] (%)	$M_w \cdot 10^3$	M_w/M_n[e]
1	**MnL2a**	0.2	50	80	84 (17)	98	72	4.7	1.50
2	**MnL2a**	0.07	50	80	75 (19)	96	52	8.8[f]	1.20
3	**MnL2a**	0.036	50	80	76 (86)	96	71	5.3	1.09
4	**MnL2a**	0.01	50	80	37 (154)	96	29	3.3	1.09
5	**MnL2a**	0.07	50	60	56 (33)	98	47	8.8[f]	1.22
6[g]	**MnL2a**	0.07	1	80	43 (25)	91	39	1.7	1.12
7[h,i]	**MnL2a**	0.07	50	80	33 (19)	89	23	1.4	1.14
8	**MnL2a**	0.07	120	80	10 (6)	74	10	0.7	1.11
9	**MnL3a**	0.2	50	80	92 (19)	98	77	6.0	1.11
10	[Mn(TPP)(OAc)]	0.01	50	80	3	51	n.d.	-	-

[a]Reaction conditions: t = 24 h, n.d. = not determined; [b]% Based on ^{1}H NMR; [c]Determined by ^{1}H integral ratio of carbonate linkages/(carbonate linkages + ether linkages); [d]Isolated yield; [e]Determined by GPC using polystyrene as standard; [f]bimodal; [g]90 h [h]using DMAP/**MnL2a** = 1/1; [i]78 % selectivity CC: 22 %.

MnL2a catalyst was still active using atmospheric pressure of CO_2, although the reaction proceeded slower than under 50 bar of CO_2, since 43 % conversion of

polycarbonate were obtained only after 90 h (entry 6, Table 4.1). In addition, the use of **MnL2a** catalyst and DMAP as co-catalyst induced a decrease in the epoxide conversion toward the polycarbonate, and a mixture of polymer and cyclic monomeric carbonate was obtained (entry 7, Table 4.1). These results are in good agreement with the ones reported by Inoue and co-workers using [Mn(TPP)(OAc)] catalyst.[17]

An attempt to run the reaction at supercritical conditions (120 bar, 80 ºC) produced only 10 % conversion toward polycarbonate, as well as, low incorporation of carbonate linkages (74 %) and low molecular weight (700 g/mol, entry 8, Table 4.1), which may be attributed to the low solubility of the catalyst in the supercritical media.

Moreover, **MnL3** catalyst (0.2 mol %; PCO_2 = 50 bar; T = 80 ºC), possessing fluorine atoms in its structure, was also evaluated under the same reaction conditions, and 92 % epoxide conversion with 77 % polymer isolated yield was obtained (entry 9, Table 4.1); presenting higher conversion than **MnL2a** (entry 1, Table 4.1). In this case, the average molecular weight of the polycarbonate obtained was 6000 g/mol with a narrow polydispersity (M_w/M_n = 1.11).

To corroborate the relevance of the presence of halogens on the catalyst structure a comparative experiment using [Mn(TPP)(OAc)] as catalyst (0.01 mol %; P_{CO2}=50 bar; T=80ºC) was carried out and only 3 % conversion was obtained (entry 10 *vs* 4, Table 4.1).

To sum up, it can be clearly seen that the presence of halogens at the *meso*-phenyl groups of the Mn(III) porphyrins plays a key role on the efficiency of the catalysts on the reaction of cyclohexene oxide with CO_2 (entries 1, 9 and 10, Table 4.1), being the halogenated ones the best performing catalysts. Moreover, the addition of co-catalyst (DMAP) also caused a significant decrease of the conversion of cyclohexene oxide (entry 7, Table 4.1). Taking into account that DMAP may occupy a coordination site; this demonstrates the considerable effect of the fifth axial ligand, which may favor the ring-closure and formation of the cyclic product.

4.2.3 Catalytic cyclic carbonate synthesis

Using the best reaction conditions previously determined, the **MnL2a** catalyst scope was analyzed in the reaction of CO_2 with different epoxides, at 0.07 mol % catalyst loading, 50 bar of CO_2 pressure and temperature of 80 ºC (Scheme 4.1).
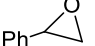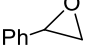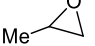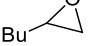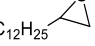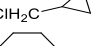
When terminal epoxides such as styrene oxide, propylene oxide, 1,2-epoxyhexane, 1,2-epoxytetradecane, were used as substrates, the corresponding cyclic carbonates were exclusively formed in 56, 54, 74 and 6 % isolated yields, respectively (entry 1-4, Table 4.2). In contrast with CHO, where polycarbonate is more favored, cyclic carbonates are thermodynamically more stable using terminal epoxides.[12] The presence of acetate (AcO⁻) as Mn(III) porphyrin axial ligand enhances the efficiency of the catalyst, when compared with the corresponding Mn(III) porphyrin bearing chloride (Cl⁻) as axial ligand (entries 1 and 2, Table 4.2).
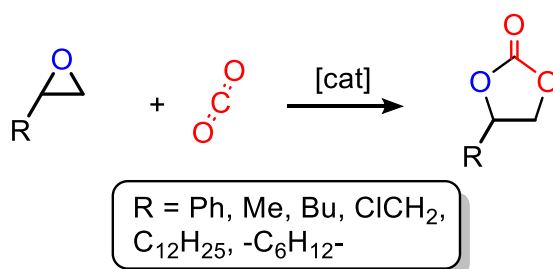
Scheme 4.1. Cycloaddition of CO_2 with different epoxides

In the case of propylene oxide and 1,2-epoxyhexane, a co-solvent (CH_2Cl_2) was required due to the low solubility of the porphyrin complex in the epoxide (entries 3-5, Table 4.2). It is worth mentioning the excellent conversion (> 99 %) and selectivity (> 99 %) obtained in the cycloaddition reaction of epichlorohydrin with CO_2 (entry 6, Table 4.2). Conversely, reaction of cyclic cyclooctene oxide with CO_2 did not occur, neither in the presence of **MnL2a** nor using a combination of **MnL2a** and DMAP as co-catalyst (entries 7-8, Table 4.2).

Table 4. 2. Cycloaddition of CO_2 to different epoxides using **MnL2a** catalyst.[a]

Entry	Epoxide	Cat.	Solvent (ml)	Co-cat (mmol)	Conv. (%)[b]	Select. (%)[b]
1	Ph	**MnL2a**	-	-	56	> 99
2	Ph	**MnL2b**	-	-	6	>99
3	Me	**MnL2a**	CH_2Cl_2 (1.2)	-	54	> 99
4	Bu	**MnL2a**	CH_2Cl_2 (1.8)	-	74	77[c]
5	$C_{12}H_{25}$	**MnL2a**	CH_2Cl_2 (1.8)		6	> 99
6	ClH_2C	**MnL2a**	-	-	> 99	> 99
7		**MnL2a**	CH_2Cl_2 (3)	-	< 1	< 1
8		**MnL2a**	CH_2Cl_2 (3)	DMAP (0.025)	< 1	< 1

[a]Reaction conditions: 35 mmol of epoxide and 0.025 mmol of catalyst (0.07 mol %), P = 50 bar, T = 80 ºC, t = 24 h; [b]determined by ^1H NMR; [c]23 % polycarbonate.

In sum, when terminal epoxides were used, the selectivity for the production of cyclic carbonates was very high, while when cyclohexene oxide was used it was found that the reaction selectivity shifted toward the production of polycarbonates.

4.2.4 Catalyst recycling and immobilization in carbon nanotubes

Addition of water after the reaction of CO_2 with propylene oxide using **MnL2a** catalyst resulted in a precipitation of a brown solid, which was separated by filtration and reused as catalyst using fresh epoxide. The results of the recycling experiments are showed in Figure 4.3. The recovered solid was active although the conversion dropped to 22 % and 9 % in the second and third consecutive runs.
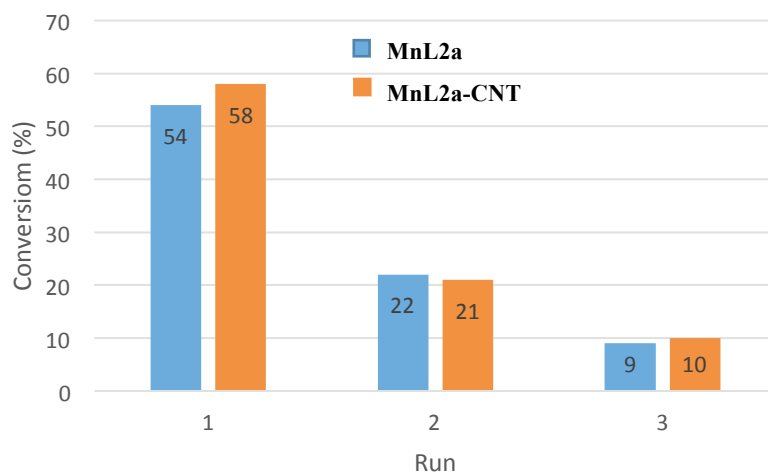
Figure 4.3. Recycling experiments using catalysts **MnL2a** and **MnL2a-CNT**. Reaction conditions: 35 mmol of propylene oxide and 0.025 mmol of catalyst (0.07 mol %), P = 50 bar, T = 80 ºC, t = 24 h, % Conv. = % conversion estimated respect to the epoxide by ^{1}H NMR.

Another reason of catalyst deactivation could be the replacement of the coordinated acetate (OAc$^-$) by water during the work up. So, after the second run, we treated a solution of the used catalyst with a stoichiometric amount of NaOAc to reintroduce the acetate. This later complex was used again as catalyst for the same reaction but, unfortunately, the conversion of propylene oxide was negligible. The UV-visible spectrum of this complex revealed a new absorption band at 434 nm that may be indicative of partial catalyst decomposition (Figure 4.4).
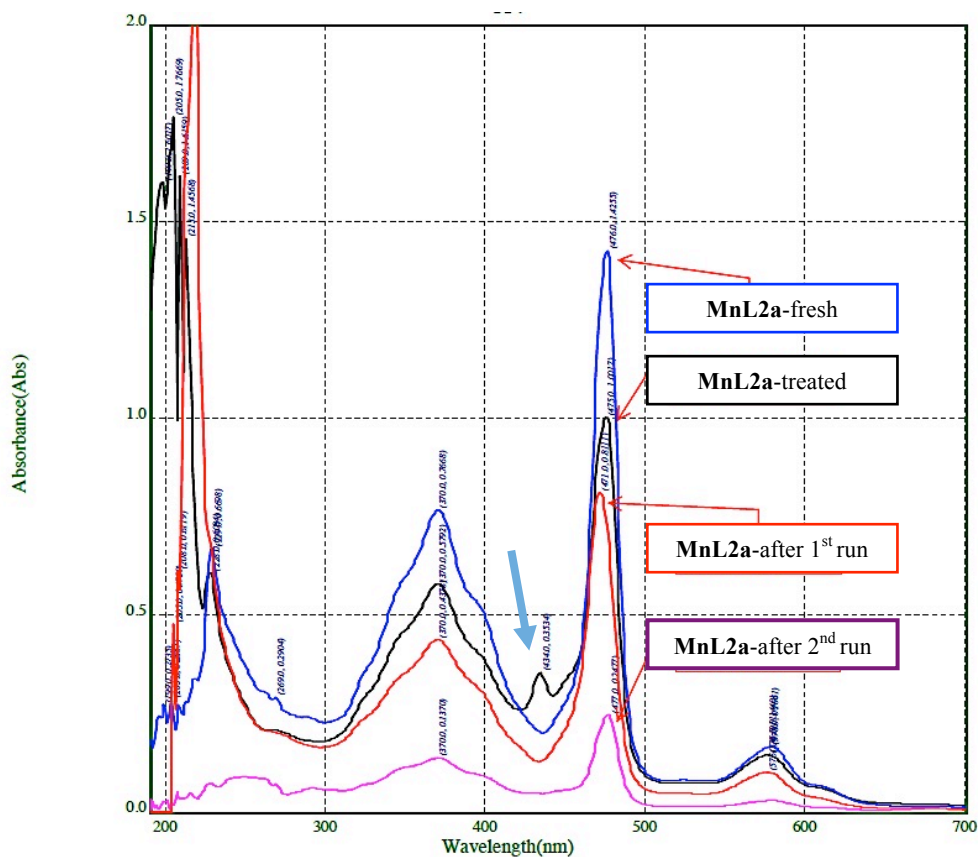
Figure 4. 4. Absorption spectra of fresh **MnL2a**, **MnL2a** recycled in the 1st run with H$_2$O, **MnL2a** recycled in the 2nd run with H$_2$O and treated **MnL2a** in dichloromethane.

MnL2a was immobilized in a CNT support (**MnL2a-CNT**) at the University of Coimbra, (Portugal) by the group of *Prof. Mariette M. Pereira*. This material contained a 1.03 % of manganese (calculated from the nitrogen content obtained by elemental analysis). **MnL2a-CNT** was active in the cycloaddition of CO$_2$ to propylene oxide producing similar conversion than **MnL2a** at the same conditions (Figure 4.3).

MnL2a-CNT was not soluble in the epoxide and after the catalytic reaction was separated by filtration, washed several times with CH$_2$Cl$_2$, dried and reused as catalyst for the same reaction. In the second and third run the conversion followed the same trend observed for catalyst **MnL2a**. This loss of activity may be due to leaching of the manganese porphyrin from the CNT support since the filtrate was brown-colored (Figure 4.3).

4.2.5   MALDI-TOF determination of PCHC chain-end groups

The polycarbonate chain end groups obtained in the experiments described in Table 4.1, entry 5 (using catalyst **MnL2a** at 50 bar, 60ºC), entry 6 (using catalyst **MnL2a** at 1 bar, 80 ºC) and entry 7 (using catalyst **MnL2a**/DMAP), were analyzed by MALDI-TOF mass spectra (Supplementary Information). They all presented repeating peaks at differences of *m/z* 142 corresponding to a cyclohexene carbonate - $C_6H_{10}C(O)O$- repeating unit. A common main peak distribution was observed in all three cases, attributed to fragments at *m/z* 1149.50, that may correspond to a chain with two –OH terminal groups (**a** + K in Figure 4.5, expected for n = 7 $HO(C_7H_{10}O_3)_7C_6H_{10}OH$; *m/z* 1149.52). Using catalyst **MnL2a**/DMAP a different mass spectrum peak distribution was observed, which fitted with the presence of $DMAP^+$ as end group (**b** + H) as well as –OH (observed *m/z* 1215.66; expected for n= 7 $[(DMAP)(C_7H_{10}O_3)_7C_6H_{10}OH]^+$; *m/z* 1215.60).
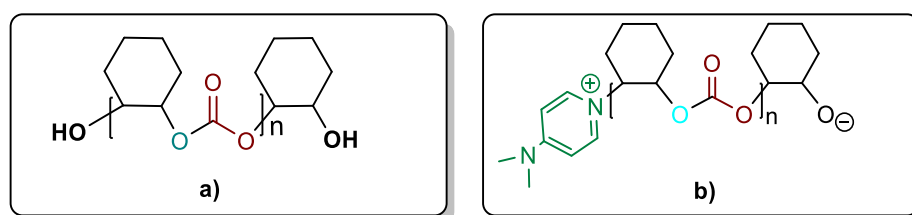
Figure 4. 5. Proposed chain ends on the basis of MALDI TOF analysis.

The formation of poly(cyclohexene carbonate) formed by using catalyst alone (**a**, Figure 4.5) suggests that the initiation step involves the epoxide opening by a nucleophilic attack, with -OH arising from water traces present in the reactor (Scheme 4.2). On the other hand, when DMAP is present, the formation of such a polymer may be explained by an initiation step involving nucleophilic attack of DMAP to the coordinated epoxide and a termination step produced by hydrolysis (Scheme 4.2). The role of DMAP as initiator in the CO_2/propylene oxide polymerization using salen- and salanCr(III)/DMAP catalytic systems was studied by Rao *et al.*[27] He proposed that coordination of DMAP took place before the opening of the epoxide, and simultaneously, the axial ligand anion produced the initiation. Contrary, Darensbourg and co-workers proposed that DMAP coordinates to Mn center and subsequently activate the CO_2 to afford a weak zwitterionic carbamic complex, followed by a reaction with CHO to provide a stabilized zwitterion.[12] We did not find any chain end

containing a carbamate or acetate group; therefore, the role of DMAP should be the ring opening of the epoxide although we do not have evidences whether it coordinates prior to nucleophilic atack (Scheme 4.2).
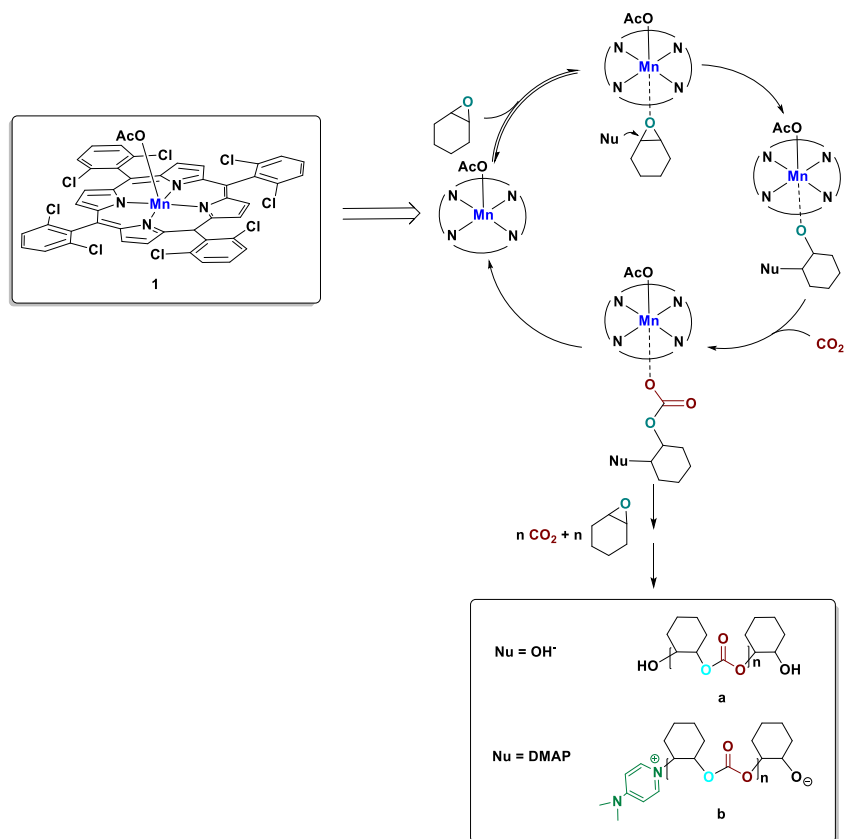
Scheme 4.2. Mechanism proposed for the formation of chains **a** and **b**.

4.3 Conclusions

It was demonstrated the significant beneficial presence of halogen atoms at the *meso*-phenyl groups of the Mn(III) porphyrins, which acted as catalysts for the copolymerisation of cyclohexene oxide with CO_2, without the presence of any co-catalyst, yielding poly(cyclohexene carbonate), with TOF up to 154 h^{-1}. Moreover, we also observed a strong influence of the Mn(III)porphyrin fifth axial ligand, where acetate (AcO$^-$) enhanced the efficiency of the catalyst, while chloride (Cl$^-$) and DMAP axial ligands almost inhibited the reaction.

In addition, a direct correlation between the nature of the epoxide structure and the catalyst used was observed, using the same reaction conditions. Thus, while terminal epoxides exclusively formed cyclic carbonates by cycloaddition with CO_2, cyclohexene

oxide selectively react in the copolymerization with CO_2, forming poly(cyclohexene carbonate).

Unfortunately, the recycling experiments either with homogeneous **MnL2a** or heterogenized **MnL2a-CNT** do not achieved the expected results as, after the second run, the conversion dropped by half in both cases.

4.4 Experimental part

General Comments. Epoxides were dried over CaH_2, distilled and stored under inert atmosphere except 1,2-epoxyhexane and 1,2-epoxydodecane and epichlorohydrin, which were purchased at Sigma-Aldrich and used as received. Solvents were purified by the system Braun MB SPS-800 and stored under nitrogen atmosphere. Carbon dioxide (SCF Grade, 99.999 %, Air Products) was used introducing an oxygen/moisture trap in the line (Agilent). UV-visible spectra were recorded on a UV-3100PC spectrophotometer. NMR spectra were recorded at 400 MHz Varian, with tetramethylsilane (^{1}H NMR and ^{13}C NMR) as internal standards. MALDI-TOF measurements were performed on a Voyager-DE-STR (Applied Biosystems, Franingham, MA) instrument equipped with a 337 nm nitrogen laser. All spectra were acquired in the positive ion reflector mode. Dithranol was used as matrix (solution in MeOH, 10 mg·ml^{-1}). The polymer (5 mg) was dissolved in 1 ml of $CHCl_3$. 1μl of sample, 1μl of matrix and 1μl of potassium trifluoroacetate (KTFA) solution in the case of polymers (1 mg of KTFA in 1ml of THF) were deposited consecutively on the stainless steel sample holder and allowed to dry before introduction into the mass spectrometer. Three independent measurements were made for each sample. For each spectrum 100 laser shots were accumulated. The molecular weights (M_w) of copolymers and the molecular weight distributions (M_w/M_n) were determined by gel permeation chromatography versus polystyrene standards. Measurements were made in THF on a Millipore-Waters 510 HPLC Pump device using three-serial column system (MZ-Gel 100Å, MZ-Gel 1000 Å, MZ-Gel 10000 Å linear columns) with UV-Detector (ERC-7215) and IR- Detector (ERC-7515a). The software used to get the data was NTeqGPC 5.1. Samples were prepared as follow: 10 mg of the copolymer was dissolved with 2 ml of tetrahydrofuran (HPLC grade) stabilized with 2,6-di-*tert*-4-methylphenol. Elemental

analyses were performed at the Serveis Tècnics de Recerca from the Universitat de Girona (Spain). All catalytic experiments were done by duplicate.

General procedure for the catalytic reactions of epoxides with CO_2: The catalytic tests were carried out in a 100 ml Berghof reactor, which was previously kept for 4 hours under vacuum at 100 ºC. After cooling down, a solution under inert atmosphere containing the catalyst dissolved in net distilled substrate or with solvent (when indicated) and the co-catalyst, when indicated, was injected into the reactor. The autoclave was pressurized with CO_2, and then heated to the specific temperature to reach the desired pressure. After the reaction time, the reactor was cooled down with an ice bath and slowly depressurized (using a dichloromethane trap in the case of propylene oxide). The % conversion was determined by ^{1}H NMR of the crude mixture by integral ratio between alkene oxide and cyclic carbonate. The work-up was as follow depending on the substrate.

Work-up for cyclohexene oxide: the final mixture was dissolved in dichloromethane, the solvent was evaporated and the residue dried in vacuum at 100° C for 3 hours to remove excess of cyclohexene oxide. The final residue was washed several times with hexane to purify the poly(cyclohexene carbonate) and was analyzed by ^{1}H NMR spectroscopy. The productivity in polymer was calculated from the mass of the isolated product-weight of the catalyst and co-catalyst.[28]. The % of CO_2 content was calculated from ^{1}H NMR data by the integral ratio between copolymer carbonate linkages ($\delta = 4.65$ ppm) respect to ether linkage signals ($\delta = 3.45$ ppm).

Work-up for styrene oxide, propylene oxide, 1,2-epoxyhexane, 1,2-epoxydodecane, epichlorohydrin and cyclooctene: Purification in the case of the styrene carbonate was performed by extraction with hexane to remove the styrene oxide. The remaining solid was evaporated and diluted in CH_2Cl_2 and passed through a silica pad to remove the catalyst. The purification of propylene carbonate was performed removing the propylene epoxide by vacuum evaporation and the remaining oily residue was diluted in dichloromethane and passed through a silica pad to remove the catalyst. The other epoxides crude mixtures were directly analyzed by ^{1}H NMR with no further purification.

Recycling experiments with MnL2a: The catalytic reaction was carried out using the general catalytic procedure with propylene oxide as substrate. After the reaction time, the reactor was slowly depressurized with a dichloromethane trap and the % conversion was determined by ^{1}H NMR. The remaining propylene oxide in the crude mixture was removed under vacuum. The catalyst was precipitated with water and separated by filtration as a brown solid. The solid was dried under vacuum, weighed and reused as catalyst with the corresponding amount of fresh propylene oxide.

Recycling experiments with MnL2a-CNT: The MnL2a-CNT catalyst was added in a 100 ml Berghof reactor and kept under vacuum during 1h. Then, net propylene oxide was injected into the reactor. The autoclave was pressurized with CO_2, and then heated to the specific temperature to reach the desired pressure. After the reaction time, the reactor was cooled down with an ice bath and slowly depressurized using a dichloromethane trap. The % conversion was determined by ^{1}H NMR. The catalyst was, then separated by filtration, washed several times with dried CH_2Cl_2 and dried under vacuum. The catalyst was weighed and reused again in catalysis with the corresponding amount of fresh propylene oxide.

4.5 Supporting information available

An example of ^{1}H NMR of crude reaction with the different epoxides used, ^{1}H NMR, MALDI-TOF and GPC of the copolymers are available in the supporting information CD.

4.6 References

[1] Inoue, S.; Koinuma, H.; Tsuruta, T. *J. Polym. Sci., Part B: Polym. Lett.* **1969**, *7*, 287-292.

[2] Darensbourg, D. J.; Holtcamp, M. W., *Coord. Chem. Rev.* **1996**, *153*, 155-174.

[3] Calvete, M. J. F.; Silva, M.; Burrows, H. D.; Pereira, M. M., *RSC Advances* **2013**, *3*, 22774-22789.

[4] Calvete, M. J. F., *Int. Rev. Phys. Chem.* **2012**, *31*, 319-366.

5   Henriques, C. A.; Pinto, S. M. A.; Aquino, G. L. B.; Pineiro, M.; Calvete, M. J. F.; Pereira, M. M., *ChemSusChem* **2014**, *7*, 2821-2824.

6   Silva, M.; Calvete, M. J. F.; Gonçalves, N. P. F.; Azenha, M. E.; Burrows, H. D.; Sarakha, M.; Ribeiro, M. F.; Fernandes, A.; Pereira, M. M., *J. Hazard. Mater.* **2012**, *233-234*, 79-88.

7   Calvete, M. J. F.; Simões, A. V. C.; Henriques, C. A.; Pinto, S. M. A.; Pereira, M. M., *Curr. Org. Synth.* **2014**, *11*, 127-140.

8   Marques, A. T.; Pinto, S. M. A.; Monteiro, C. J. P.; Melo, J. S. S.; Burrows, H. D.; Scherf, U.; Calvete, M. J. F.; Pereira, M. M., *J. Polym. Sci. Part A: Polym. Chem.* **2012**, *50*, 1408-1417.

9   Pinto, S. M. A.; Lourenco, M. A. O.; Calvete, M. J. F.; Abreu, A. R.; Rosado, M. T. S.; Burrows, H. D.; Pereira, M. M., *Inorg. Chem.* **2011**, *50*, 7916-7918.

10 Pinto, S. M. A.; Neves, Â. C. B.; Calvete, M. J. F.; Abreu, A. R.; Rosado, M. T. S.; Costa, T.; Burrows, H. D.; Pereira, M. M., *J. Photochem. Photobiol. A: Chem.* **2012**, *242*, 59-66.

11 Roales, J.; Pedrosa, J. M.; Guillén, M. G.; Lopes-Costa, T.; Pinto, S. M. A.; Calvete, M. J. F.; Pereira, M. M., *Sens. Actuator B. Chem.* **2015**, *210*, 28-35.

12 Darensbourg, D. J., *Chem. Rev.* **2007**, *107*, 2388-2410.

13 Klaus, S.; Lehenmeier, M. W.; Anderson, C. E.; Rieger, B.; *Coord. Chem. Rev.* **2011**, *255,* 1460-1479.

14 Babu, H. V.; Muralidharan, K., *Dalton Trans.* **2013**, *42,* 1238-1248.

15 Iksi, S.; Aghmiz, A.; Rivas, R.; González, M. D.; Cuesta-Aluja, L.; Castilla, J.; Orejón, A.; El Guemmout, F.; Masdeu-Bultó, A. M., *J. Mol. Catal. A: Chem.* **2014**, *383-384*, 143-152.

16 a) Nakano, K.; Kamada, T.; Nozaki, K., *Angew. Chem. Int. Ed.* **2006**, *45*, 7274-7277; b) Wu, W.; Sheng, X.F.; Qin, Y.S.; Qiao, L.J.; Miao, Y.Y.; Wang, X.H.; Wang, F.S., *J. Polym. Sci. A: Polym. Chem.* **2014**, *52*, 2346-2355.

17 Sugimoto, H.; Ohshima, H.; Inoue, S., *J. Pol. Sci.: Part A Polym. Chem.* **2003**, *41*, 3549-3555.

18 Darensbourg, D. J.; Mackiewicz, R. M.; Rodgers, J. L., *J. Am. Chem. Soc.* **2005**, *127,* 14026-14038.

19 Darensbourg, D. J.; Frantz, E. B., *Inorg. Chem.* **2007**, *46,* 5967-5978.

20   a) Whiteoak, C. J.; Kielland, N.; Laserna, V.; Castro-Gomez, F.; Martin, E.; Escudero-Adan, E. C.; Bo, C.; Kleij, A. W.; *Chem. Eur. J.* **2014**, *20,* 2264-2275. b) Reiter, M.; Altenbuchner, P. T.; Kissling, S.; Herdtweck, E.; Rieger, B., *Eur. J. Inorg. Chem.* **2015**, 1766-1774. c) Qin, Y.; Guo, H.; Sheng, X.; Wang, X.; Wang, F., *Green Chem.* **2015**, *17*, 2853-2858.

21   Kim, D.-W.; Roshan, R.; Tharun, J.; Cherian, A.; Park, D.-W., *Korean J. Chem. Eng.* **2013**, *30,* 1973-1984.

22   Han, L.; Li, H.; Choi, S.-J.; Park, M.-S.; Lee, S.-M.; Kim, Y.-J.; Park, D.-W., *Appl. Catal. A: Gen.* **2012**, *429–430*, 67-72.

23   Baja, S.; Krawczyka, T.; Jasiaka, K.; Siewniaka, A.; Pawlyta, M, *Appl. Catal. A: General* **2014**, *488*, 96-102.

24   Silva, M.; Fernandes, A.; Bebiano, S. S.; Calvete, M. J. F.; Ribeiro, M. F.; Burrows, H. D.; Pereira, M. M., *Chem. Commun.* **2014**, 6571-6573.

25   Johnstone, R.A.W.; Nunes, M.L.P.J.; Pereira, M.M.; Gonsalves, A.M.A.R.; Serra, A.C., *Heterocycles* **1996**, *43*, 1423-1437.

26   Adler, A. D.; Longo, F. R.; Kallpas, F.; Kim, J., *J. Inorg. Nucl. Chem.* **1970**, *32,* 2443-2445.

27   Rao, D.-Y.; Li, B.; Zhang, R.; Wang, H.; Lu, X.-B., *Inorg. Chem.* **2009**, *48*, 2830-2836.

28   Koning, C.; Wildeson, J.; Parton, R.; Plum, B.; Steeman, P.; Darensbourg, D. J.; *Polymer* **2001**, *42*, 3995-4004.

Novel chromium(III) complexes with N_4-donor ligands as catalysts for the coupling of CO_2 and epoxides in supercritical CO_2

Abstract

New neutral and cationic chromium(III) complexes with N_4 Schiff base ligands have been prepared and characterized. These complexes are active catalysts for the cycloaddition of CO_2 and styrene oxide in CH_2Cl_2, affording epoxide conversions in a 39-92 % range, with encouraging cyclic carbonate yields (up to 63%). It is noteworthy, that the cationic species were significantly more active than their neutral analogs. Addition of TBAX improved the selectivity toward styrene carbonate (87 % yield). Dichloromethane could be avoided using solvent free or supercritical carbon dioxide as a solvent (scCO₂) and, moreover, this improved the catalytic activity of the cationic complexes (TOF up to 652 h^{-1}). Using scCO₂, these chromium catalysts afforded the rapid and selective formation of cyclic carbonates from the coupling of CO_2 to various linear terminal epoxides, such as epichlorohydrin, propylene oxide and long chain terminal oxiranes. Coupling of CHO and carbon dioxide led to mixtures of PCHC and CHC depending on the conditions (pressure and catalyst/co-catalyst ratio). PCHC was isolated with a productivity of 388 g/g Cr. Selective formation of the cyclic cyclohexene carbonate was obtained working under scCO₂ conditions.
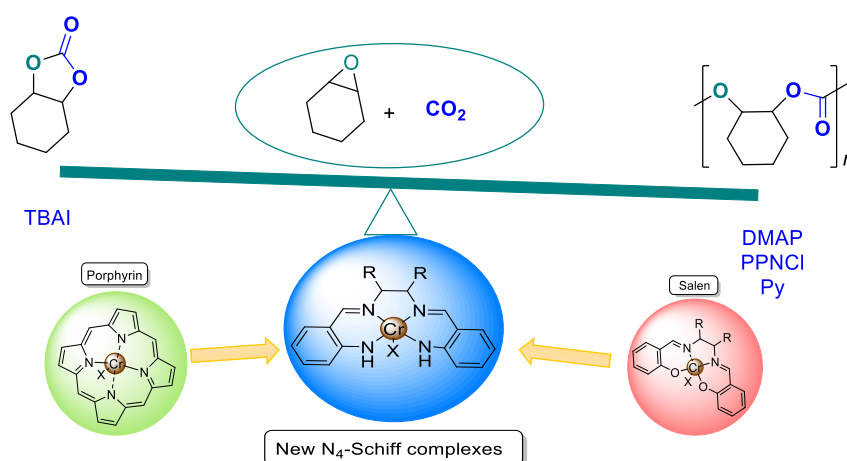
This work has been done in collaboration with the group of Dr. Lorraine Christ from Institut de Recherches sur la Catalyse et l'Environnement de Lyon (IRCELYON), France.

5.1   Introduction

Among the reported homogeneous catalysts for the CO_2 insertion into epoxides, as we have seen in chapter 3 and chapter 4, macrocyclic porphyrins[1,2] and Schiff base salicylimine derivatives (salen-type)[3] have been the most studied and generally used as N_4- and N_2O_2-donor ligands (Figure 5.1).
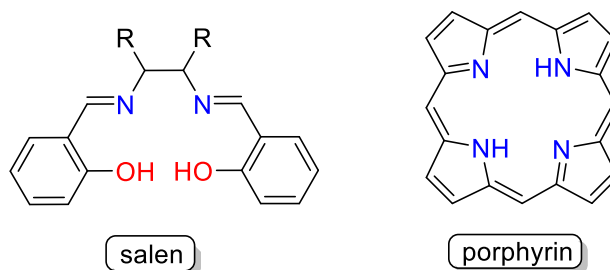
Figure 5.1. Salen and porphyrin ligands.

We are interested in a series of tetraza Schiff base compounds **H₂L4** and **H₂L5** (Figure 5.2) because they can act as porphyrins (N_4-ligands) but having an open and flexible structure as salen ligands.[4] Furthermore, neutral N_4-donor ligands can form cationic complexes, which may show higher Lewis acidity than neutral species; thus favoring the interaction with the epoxide. In contrast with the large number of reports on the use of metal-salen complexes as catalysts for the CO_2/epoxides polymerization or cycloaddition, the catalytic systems containing N_4-donor ligands in the literature are scarce, although some active systems have been reported. For example, aluminum,[1] chromium[2,5,6] or cobalt[7,8] porphyrin complexes in combination with quaternary organic salts or amine co-catalysts transformed epoxides into polycarbonates or cyclic carbonates efficiently.

H₂L4 R,R = -CH₂-CH₂-
H₂L5 R = R = H
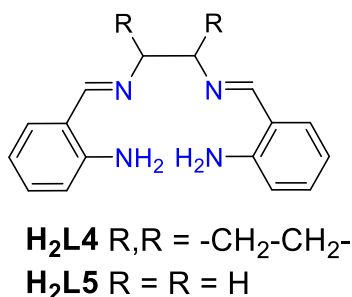
Figure 5.2. N_4 Schiff base ligands.

More recently, an iron(II) complex with a diaminebis(quinoline)-based ligand (**16**, Figure 5.3) has been reported to be active in the cyclization of propylene oxide and carbon dioxide to propylene carbonate providing 80 % conversion in 2 h at 100 ºC and 15 bar CO_2.[9] Moreover, Dinjus and co-workers developed an iron complex bearing a pyridine amide ligand (**18**, Figure 5.3). This complex was also found to be an active catalyst, leading to pure alternating copolymer in the reaction of CO_2 with cyclohexene oxide, and to cyclic carbonate in the reaction of CO_2 with propylene oxide.[10]
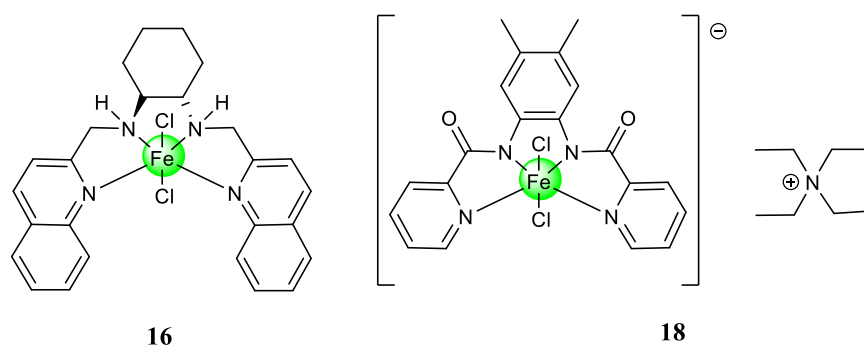
Figure 5.3. Iron complexes bearing N_4-donor ligands active in the coupling of CO_2.and epoxides.

As we have discussed in the introduction, chromium complexes have proved to be among the most effective catalysts for polycarbonate synthesis.[3] They can be easily prepared from available Cr(II) acetate or chloride starting materials and they present high stability.

Concerning catalyst based on Cr(III) with non-porphyrin N_4-donor ligands, Darensbourg and co-workers described a family of Cr-tetraazannulene/PPNX based catalytic systems, which provided TOF of 1500 h^{-1}(X = Cl) in the copolymerization of CO_2 and cyclohexene oxide at mild conditions (1 bar, 80 ºC). These catalytic systems were one order of magnitude more active than their porphyrin analogs and provided polycarbonates with high molecular weight (50,000) and narrow polydispersity (1.07).[11,12,13]

Based on this background, we undertook the preparation of Cr(III) complexes with the tetraza Schiff base ligands **H₂L4** and **H₂L5** (Figure 5.2) in order to use them as catalysts for the cycloaddition of epoxides and CO_2, using solution and supercritical CO_2 conditions. The synthesis of some Cu, Co and Ni complexes with **H₂L4** and **H₂L5**

have been reported, but there is no application of these complexes as catalysts for the reactions involving CO_2.[4,14]

5.2 Results and discussion

5.2.1 Synthesis of Cr(III) complexes with N_4 Schiff ligands H_2L4 and H_2L5

The N_4 Schiff bases (**H₂L4** and **H₂L5**) were prepared according to literature method in collaboration with Dr. Lorraine Christ from Institut de Recherches sur la Catalyse et l'Environnement de Lyon (France).[4] The synthesis is based on the coupling of 2-nitrobenzaldehyde with 1,2-diaminocyclohexane or ethylenediamine (Scheme 5.1). The dinitro compound formed was then carefully hydrogenated to **H₂L4** and **H₂L5** using Pd/C at room temperature.
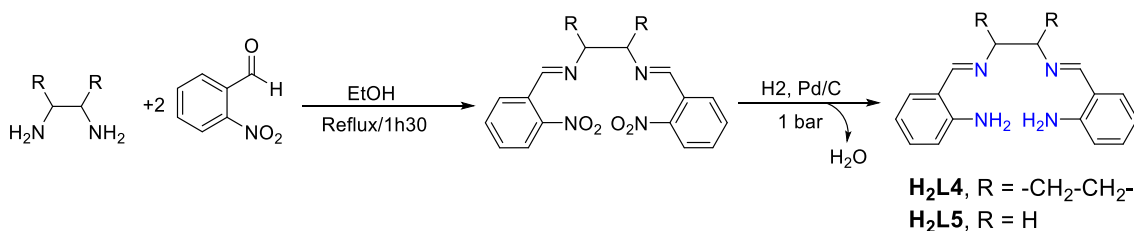
Scheme 5.1. General synthesis of N_4 Schiff bases **H₂L4** and **H₂L5**.

To obtain the neutral complexes, a base (NaH) was used to generate the anionic ligands in anhydrous tetrahydrofuran (THF) under inert atmosphere. Then, this solution was reacted with chromium dichloride ($CrCl_2$) and, subsequently, chromium(II) was oxidized to chromium(III) under air stream (Scheme 5.2).
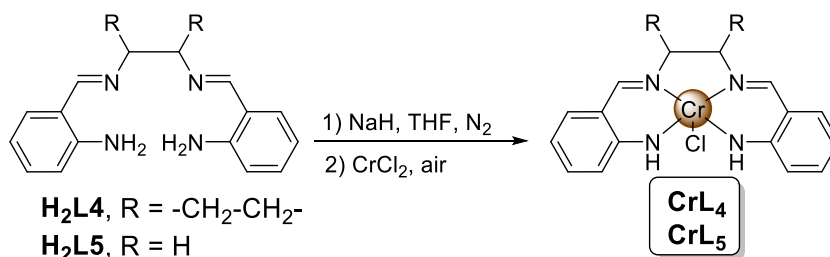
Scheme 5.2. Synthesis of neutral chromium(III) complexes **CrL4** and **CrL5**.

CrL4 and **CrL5** were isolated both as dark brown solids with 48 and 44 % yield, respectively. In the mass spectra the peaks corresponding to the mononuclear fragments of $[Cr(\mathbf{L4\text{-}L5})]^+$ were detected. Deviations found in the elemental analyses

maybe due to their tendency to adopt solvated forms. The infrared and Raman spectral data of the chromium(III) complexes **CrL4** and **CrL5** showed a band at 1611 cm^{-1} attributed to the azomethine ν(C=N) stretching vibration, which was shifted to lower frequencies (1630 cm^{-1} and 1632 cm^{-1} for ligands **H$_2$L4** and **H$_2$L5**, respectively)[15] due to backbonding with the metal.[16] Two new bands in the region 560-680 cm^{-1} observed in the Raman spectrum may be indicative of the presence of two types of Cr-N bonds.[17] The values of molar conductivities for these complexes (39.3 $\Omega^{-1} \cdot$cm$^2 \cdot$mol^{-1} in water for **CrL4** and 50.1 $\Omega^{-1} \cdot$cm$^2 \cdot$mol^{-1} in methanol for **CrL5**) confirmed that they corresponded to neutral species[18] although partial ionization of the chloride ligand may take place in solution.

To obtain the cationic complexes, the neutral N$_4$ Schiff bases were reacted with chromium dichloride (CrCl$_2$) in anhydrous THF and oxidation with air stream in the presence of 1eq. of lithium chloride (LiCl) led to chromium(III) complexes **CrH$_2$L4** and **CrH$_2$L5** (Scheme 5.3).[19]

H$_2$L4, R = -CH$_2$-CH$_2$-
H$_2$L5, R = H

CrH$_2$L4 Y = none; n = 2
CrH$_2$L5 Y = Cl; n = 1
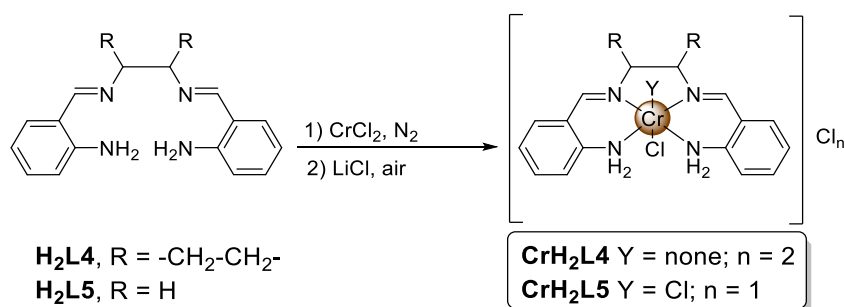
Scheme 5.3. Synthesis of cationic chromium(III) complexes **CrH$_2$L4** and **CrH$_2$L5**.

In the MALDI-TOF mass spectra the fragments corresponding to the [Cr(**L$_4$**-**L$_5$**)]$^{2+}$ species were observed. The coordination of the ligand was confirmed by the presence of the ν(C=N) stretching vibration at 1615 cm^{-1} similar to the neutral complexes.[16] The Raman spectra also showed two new absorptions in the region 570-680 cm^{-1} assigned to Cr-N stretching frequencies.[17] According to microanalysis data they were isolated as hydrated forms. The molar conductivity value of **CrH$_2$L4** corresponded to 1:2 electrolyte (150.6 $\Omega^{-1} \cdot$cm$^2 \cdot$mol^{-1} in CH$_2$Cl$_2$). Instead, the molar conductivity of **CrH$_2$L5** (105.7 $\Omega^{-1} \cdot$cm$^2 \cdot$mol^{-1} in methanol) is indicative of 1:1 electrolyte.[18] Therefore, the formation of the hexacoordinated species [Cr(**L5**)Cl$_2$]Cl is proposed for **CrH$_2$L5**. Magnetic susceptibility measurements of the complexes at room

temperature gave μ_{eff} in the range 3.7-4.1 μ_B corresponding to species with three unpaired electrons.[20]

5.2.2 Catalytic activity

The new complexes **CrL4-CrH₂L4** and **CrL5-CrH₂L5** were initially tested as catalysts in the CO_2/styrene oxide (SO) cycloaddition (Scheme 5.4) using CH_2Cl_2 and scCO_2 as solvents and tetrabutylammonium halides (TBAX) as co-catalysts.
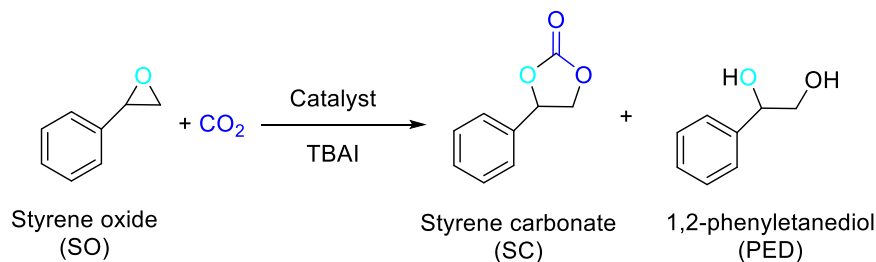
Scheme 5.4. Cycloaddition of CO_2/Styrene oxide.

5.2.2.1 Catalytic reactions in CH₂Cl₂

Chromium(III) complexes **CrL4-CrH₂L4** and **CrL5-CrH₂L5** were tested as catalysts (3 mol %) for CO_2/styrene oxide coupling in CH_2Cl_2. The reactions were conducted with and without addition of TBAI as co-catalyst at 100 ºC and 20 bar of CO_2 during 18 h affording styrene carbonate (SC) as a major product (Table 5.1). The epoxide conversion and the styrene carbonate yield were determined by GC using mesitylene as internal standard. IR and ^{1}H NMR confirmed that poly(styrene carbonate) was not formed.

All the catalytic systems tested were active in the reaction without addition of any co-catalysts and gave good styrene oxide conversions (73-92 %) and yields toward styrene carbonate (39-68 %) (entries 1, 3, 5, 7, Table 5.1). It is noteworthy that Cr-salen complexes have only moderate activity in this reaction.[12,21] 1-phenyl-1,2-etanediol (PED) was also formed (< 18 %) probably due to the presence of residual water or degradation of the cyclic carbonate at 100 ºC, as reported by Babu and Muralidharan.[22] The differences in the epoxide conversion and the products yield, may be attributed to the formation of non-volatile side products from the oligomerization of styrene oxide.

Assuming that the activation of the epoxide takes place by nucleophilic attack of an anion as reported for Cr-salen complexes,[3] we can assume that the Cl⁻ ion present in

the Cr complex maybe responsible of the opening of the epoxide when the reaction is carried out without any co-catalyst. In the case of cationic complexes **CrH₂L4-CrH₂L5**, a combination of a more reactive Cl^- counter anion and higher Lewis acidity than neutral complexes **CrL4-CrH₂L4**, may account for the better conversions observed using cationic complexes.

Table 1.1. Cycloaddition of CO_2/styrene oxide catalyzed by **CrL4-CrH₂L4** and **CrL5-CrH₂L5**/TBAI in CH_2Cl_2.[a]

Entry	Catalyst	Co-cat	Conv. SO (%)[b]	TOF (h^{-1})[c]	Yield SC[b]	Yield PED[b]
1	**CrL4**	-	73	1.4	39	7
2	**CrL4**	TBAI	97	1.8	71	4
3	**CrL5**	-	81	1.5	42	7
4	**CrL5**	TBAI	95	1.7	70	4
5	**CrH₂L4**	-	92	1.7	68	18
6	**CrH₂L4**	TBAI	92	1.7	79	12
7	**CrH₂L5**	-	90	1.6	61	16
8	**CrH₂L5**	TBAI	93	1.7	87	5
9	-	TBAI	55	0.9	55	-

[a]*Reaction conditions:* SO: 0.23ml, 2 mmol; catalyst: 0.06 mmol (3 mol %); TBAI: 0.06 mmol (substrate/co-catalyst/catalyst = 33/1/1), 5ml CH_2Cl_2, T = 100 ºC, time = 18 h, P_{CO2} = 20 bar; [b] calculated by gas phase chromatography (GC).[c]Averaged turn over frequency.

The addition of TBAI as co-catalyst (catalyst/co-catalyst molar ratio = 1/1) resulted in an increase of both, epoxide conversion and cyclic carbonate yield (entries 2, 4, 6, 8, Table 5.1). The best result (93 % SO conversion, 87 % SC yield) was obtained with the catalytic system **CrH₂L5**/TBAI, (entry 8, Table 5.1). Tetrabutylammonium halides have been reported to be able to catalyze this reaction.[23] At the conditions of this study, TBAI showed lower styrene oxide conversion and lower yield toward styrene carbonate than when used in combination with the chromium catalysts (entry 9, Table 5.1). Nevertheless, the selectivity towards cyclic carbonate when using only TBAI as catalyst is very high and no diol was detected. This may confirm that the complex is

also catalyzing the degradation of the cyclic carbonate to PED as reported for other related catalytic systems.[22]

As observed without co-catalyst, cationic **CrH₂L4-CrH₂L5** were found to be more active than neutral ones **CrL4- CrL5**, probably due to their higher Lewis acidity. This suggests that coordination of the substrate by the metallic center is taking place. In the presence of TBAI, no significant differences in catalytic results were found using complexes with **H₂L4** and **H₂L5** ligands.

5.2.2.2   Catalytic reactions in supercritical CO₂

In order to avoid the use of the chlorinated solvent CH_2Cl_2, reactions were run using supercritical carbon dioxide (scCO₂) at different conditions. **CrL4-CrH₂L4** and **CrL5-CrH₂L5b** were also found to be active catalysts for the CO_2/styrene oxide (SO) coupling in scCO₂ at 1.3 mol. % catalyst loading in the presence of TBAX (X = I, Br, Cl). The results obtained are shown in Tables 5.2 and 5.3. The reactions were carried out at 100 ºC and 170 bar of CO_2 during 3 h. At this conditions styrene carbonate was formed as the main-product and no PED or poly(styrene carbonate) were detected by GC or ¹H NMR spectroscopy. However, non-identified oligomerization side products may also be formed.

Using the Cr(III) complexes without co-catalyst in scCO₂ the epoxide conversion and yield in cyclic carbonate were low (19-50 % epoxide conversion and up to 15 % cyclic carbonate yield; entries 1, 3, 5, 7, Table 5.2). The low solubility of these species in scCO₂ media may be the reason for the low activity. The addition of TBAI to the cationic complexes **CrH₂L4** and **CrH₂L5** (molar ratio 1:1), produced an increase of epoxide conversion up to 94-97 % with a yield in the styrene carbonate of ca 70 % (entries 2, 4, 6, 8, Table 5.2).

As observed in CH_2Cl_2 the cationic catalysts led to better conversions and cyclic carbonate selectivity than the neutral ones, and the skeleton of the ligand in the pre-catalyst generally did not affect the results. An average TOF of 25 h⁻¹ was estimated for the catalytic system **CrH₂L4**/TBAI (entry 6, Table 5.2).

Table 2.2. Cycloaddition of CO_2/styrene oxide catalyzed by **CrL4-CrH$_2$L4** and **CrL5-CrH$_2$L5**/TBAX (X = I, Br, Cl) in scCO$_2$.[a]

Entry	Catalyst	Co-cat	Conv. SO (%)[b]	TOF (h^{-1})[c]	Yield SC[b]
1	**CrL4**	-	19	5	0
2	**CrL4**	TBAI	75	19	40
3	**CrL5**	-	21	5	0
4	**CrL5**	TBAI	71	18	31
5	**CrH$_2$L4**	-	50	13	15
6	**CrH$_2$L4**	TBAI	97	25	69
7	**CrH$_2$L5**	-	15	4	0
8	**CrH$_2$L5**	TBAI	94	24	59
9	-	TBAI	47	12	47
10	**CrH$_2$L4**	TBABr	100	26	68
11	-	TBABr	63	16	63
12	**CrH$_2$L4**	TBACl	92	24	63
13	-	TBACl	79	20	79
14	**CrH$_2$L4**	TBAI/TBABr	100	26	100

[a]*Reaction conditions:* SO: 0.23ml, 2 mmol; catalyst: 0.026 mmol (1.3 mol %); TBAI: 0.026 mmol (1.3 mol %) (substrate/co-catalyst/catalyst = 77/1/1), T = 100 ℃, time = 3 h, P_{CO2} = 170 bar; SO = styrene oxide; SC = styrene carbonate. [b]Calculated by gas phase chromatography (GC). [c]Averaged turn over frequency.

A synergistic effect between the chromium complex and the ammonium salt was also observed, since using TBAI alone as catalyst in scCO$_2$ produced only 47 % of epoxide conversion (entry 9, Table 5.2). Little effect on epoxide conversion was observed changing the anion in the ammonium salt: Br$^-$ (100 %) > I$^-$ (94 %) > Cl$^-$ (92 %) (entries 10, 8 and 12, respectively, Table 5.2). Using TBABr or TBACl it was also observed a synergistic effect using the combination of the ammonium salt and **CrH$_2$L4** (entries 11 and 13, Table 5.2). The anion effect of tetrabutylammonium catalysts in the cycloaddition of CO_2 to epoxides reported in the literature is contradictory. Caló and co-workers reported that using a mixture TBAI/TBABr instead of TBAI alone, the yield on cyclic carbonate formation from styrene oxide was increased near six-fold times (83%

yield in 4 h, respect to 80% in 22 h).[23] In our case, using a combination of **CrH₂L4** with an equimolar mixture of TBAI and TBABr, the yield in cyclic carbonate also improved (entry 14, Table 2). On the other hand, in the fixation of CO_2 with propylene oxide and TBAX as catalyst the order of epoxide conversion was X = Cl⁻ (73 %) > Br⁻ (56 %) ≈ I⁻ (54 %), which did not correspond with the relative energy barrier calculated for the rate-determining step (Cl⁻ > Br⁻) found to be the opening of the epoxide by the anion.[24] Leitner *et al.* found Br⁻ to be the best anion in the insertion of CO_2 to methyl epoxyoleate and this fact was attributed to the appropriate combination of nucleophilicity and leaving group ability.[25] In the catalytic systems reported here, the fact that there is no influence of the anion suggests that a mechanism involving both chromium complex and ammonium salt takes place in a synergistic fashion and that the opening of the epoxide is not the rate-determining step.

Table 3.3. Cycloaddition of CO_2/styrene oxide catalyzed by **CrH₂L4**/TBAI catalytic system in scCO₂.[a]

Entry	Subs./cat/co-cat[b]	t(h)	Pressure (bar)	Conv. SO (%)[c]	TOF (h⁻¹)[c]	Yield SC (%)
1	200/1/1	3	170	100	67	74[d]
2	500/1/1	0.5	170	45	450	n.i.
3	500/1/1	0.5	120	65	652	n.i.
4	500/1/1	0.5	20	55	535	n.i.

[a] *Reaction conditions:* **CrH₂L4**: 0.044 mmol; TBAI: 0.044 mmol; T = 100 °C; n.i. = not isolated. [b] Molar ratio. [c] Conversion and averaged turn over frequency measured by ¹H NMR. [d] Isolated product purified by flash chromatography.

To evaluate the initial turn over frequency, the substrate/catalyst ratio was increased using **CrH₂L4**/TBAI catalytic system. For a molar substrate/catalyst ratio of 200/1 (0.5 mol % catalyst loading), the conversion was complete in 3 h (TOF 67 h⁻¹) (entry 1, Table 5.3). At a substrate/catalyst ratio of 500 (0.2 mol.% catalyst loading), in 0.5 h the system achieved approximately 50 % conversion (TOF$_{50\%}$ of 450 h⁻¹, entry 2, Table 5.3). At these conditions, a visual inspection of the inside of the reactor autoclave through the glass window evidenced the presence of colored droplets. These droplets were attributed to the insoluble catalyst in the substrate media indicating that the action

took place at two-phase conditions (Figure 5.4). The catalyst solubility in the supercritical phase can be modified with the CO_2 density. Thus, when decreasing the pressure to 120 bar the less dense phase allowed the highest catalytic activity with a TOF of 652 h^{-1} (65 % epoxide conversion; entry 3, Table 5.3). To evaluate the effect of the CO_2 pressure, we decided to run the reaction under solvent free conditions with the same catalyst loadings, co-catalyst and substrate at 20 bar of CO_2, leading to a decrease of activity with a TOF of 535 h^{-1}, (entry 4, Table 5.3). This confirms that the opening of the epoxide is not the rate-determining step.
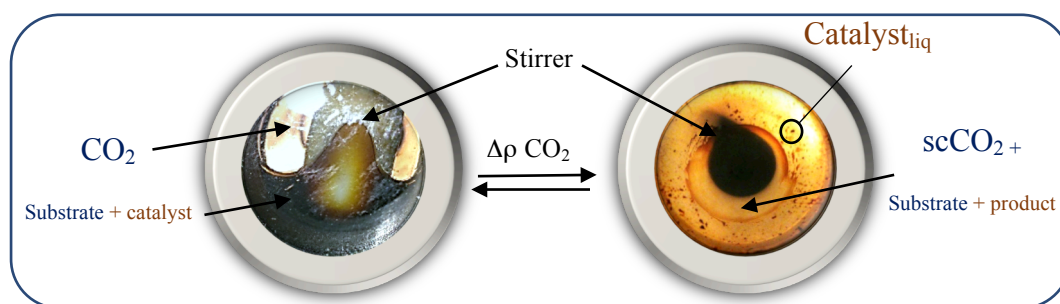
Figure 5.4. Reactor photographs of the reaction system: 20 bar of CO_2 with dissolved catalyst at low CO_2 density (left) and at supercritical CO_2 at 170 bar with precipitated catalyst at high CO_2 density (right).

The reaction of CO_2 with other substrates was evaluated under supercritical conditions (170 bar, 100 ºC, 0.5 mol % catalyst) (Scheme 5.5). High conversions to the cyclic carbonate (58-95 %) were obtained in only 30 min for linear terminal epoxides: propylene oxide, 1,2-epoxyhexane, 1,2-epoxytetradecane and epichlorohydrin (Scheme 5.5). High selectivity was obtained to cyclic carbonates (only the corresponding diol was detected by ^{1}H NMR in the case of propylene oxide and 1,2-epoxytetradecane substrates). Cyclic oxiranes such as cyclohexene and cyclooctene oxides did not react with CO_2 at these conditions (Scheme 5.5) probably due to steric hindrance effect.
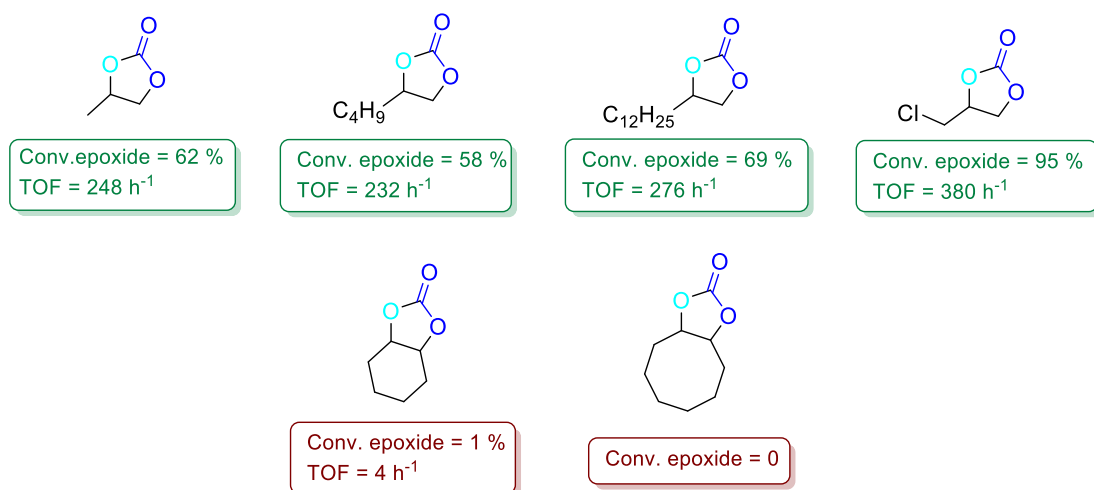
Scheme 5. 5. Cycloaddition of CO_2/epoxides catalyzed by **CrH₂L4**/TBAI in scCO₂. Reaction conditions: 9 mmol; **CrH₂L4**: 0.045 mmol (0.5 mol %); TBAI: 0.045 mmol (substrate/catalyst/co-catalyst = 200/1/1), T = 100 ºC, P = 170 bar, t = 0.5 h. Conversion and turn over frequency were measured by ¹H NMR.

5.2.2.3   Reaction of CO₂/cyclohexene oxide

The reaction of CO_2 and cyclohexene oxide was further investigated using catalyst **CrH₂L4** with other co-catalysts such as DMAP, PPNCl and pyridine (Py) (Table 5.4). The best result was obtained with **CrH₂L4**/DMAP catalytic system (catalyst/co-catalyst = 1/1) at 50 bar of CO_2 and 80 ºC (66 % epoxide conversion, entry 1, Table 5.4). The polymer was isolated by extraction of the cyclic product with hexane obtaining a productivity of 461 g copolymer/g Cr. The isolated polymer showed a high degree of incorporation of carbonate (92 %) measured by ¹H NMR spectroscopy. Similar results were obtained using **CrH₂L4**/PPNCl (entry 2, Table 5.4). With catalytic system **CrH₂L4**/Py the epoxide conversion was low (15 %, entry 3, Table 5.4).

Decreasing the catalyst/co-catalyst ratio to 1/0.5 the conversion decreased to 42 % maintaining the PCHC/CHC ratio (entry 4, Table 5.4). An increase of the catalyst/co-catalyst ratio to 1/5, increased the conversion using both **CrH₂L4**/DMAP and **CrH₂L4**/PPNCl (entries 5 and 6, Table 5.4). Eberhardt *et al.* also found an increase in the cyclic carbonate/polycarbonate ratio increasing the Cr/DMAP ratio in the coupling of CO_2 and propylene oxide.[26] The authors proposed that the excess DMAP suppressed the polymer growing by a backbiting mechanism.

Table 4.4. Reaction of CHO/CO_2 using **CrH$_2$L4**/co-catalyst.[a]

Entry	Co-cat.	cat/co-cat	P (bar)	Conv (%)[b]	TOF (h^{-1})[b]	PCHC /CHC (%)[b]	% CO_2[b]	Prod. gPCHC/gCr (Mw, Mw/Mn)[c]	CHC (%cis/trans)
1	DMAP	1/1	50	66	14	80/20	92	461 (3100, 1.2)	78/22
2	PPNCl	1/1	50	54	11	69/31	90	388 (4400, 1.3)	76/24
3	Py	1/1	50	15	3	73/27	79	45 (1100, 1.1)	55/45
4	DMAP	1/0.5	50	42	9	81/19	90	317	50/50
5	DMAP	1/5	50	75	16	10/90	74	66	78/22
6	PPNCl	1/5	50	72	15	5/95	71	61	92/8
7	PPNCl	1/5	170	80	17	0/100	-	-	90/10

[a]*Reaction conditions:* CHO: 22.5 mmol, 5 ml, catalyst **CrH$_2$L4**: 0.045 mmol (0.2 %) (substrate/catalyst = 500/1); T = 80 ºC, t = 24 h. [b] Measured by ^{1}H NMR. [c] Determined by GPC versus poly(styrene) standards.

When the **CrH$_2$L4**/PPNCl catalytic system was used in scCO_2 media, only cyclic carbonate was obtained and epoxide conversion was higher than the one obtained at 50 bar (entry 7, Table 5.4).

In almost all the examples the stereochemistry of the formed cyclic carbonate was retained to obtain the *cis* isomer as the main product. The predominant retention of the configuration responds to a S$_N$2 mechanism with double inversion. Nevertheless, the formation of the *trans* carbonate indicates that a S$_N$1 pathway also takes place.[25]

To determine the chain end groups of the polycarbonates obtained, the MALDI-TOF mass spectra with KTFA as cationizing agent of the polymers from experiments 3 (**CrH$_2$L4**/Py), 1 (**CrH$_2$L4**/DMAP) and 2 (**CrH$_2$L4**/PPNCl) reported in Table 5.4 were analyzed (Figure 5.5). They all presented repeating units of 142 m/z. The polymer obtained with **CrH$_2$L4**/Py catalyst had low values of m/z in accordance with the low molecular weight observed (1100 Da). The distribution of this polymer showed a unique major series (Figure 5.5a) attributed to fragments with two Cl terminal groups and an ether linkage (a + K in Figure 5.6, expected for n = 12 Cl($C_7H_{10}O_3$)$_{12}C_6H_{10}OC_6H_{10}$ClK, m/z 1993.81; found 1996.38).
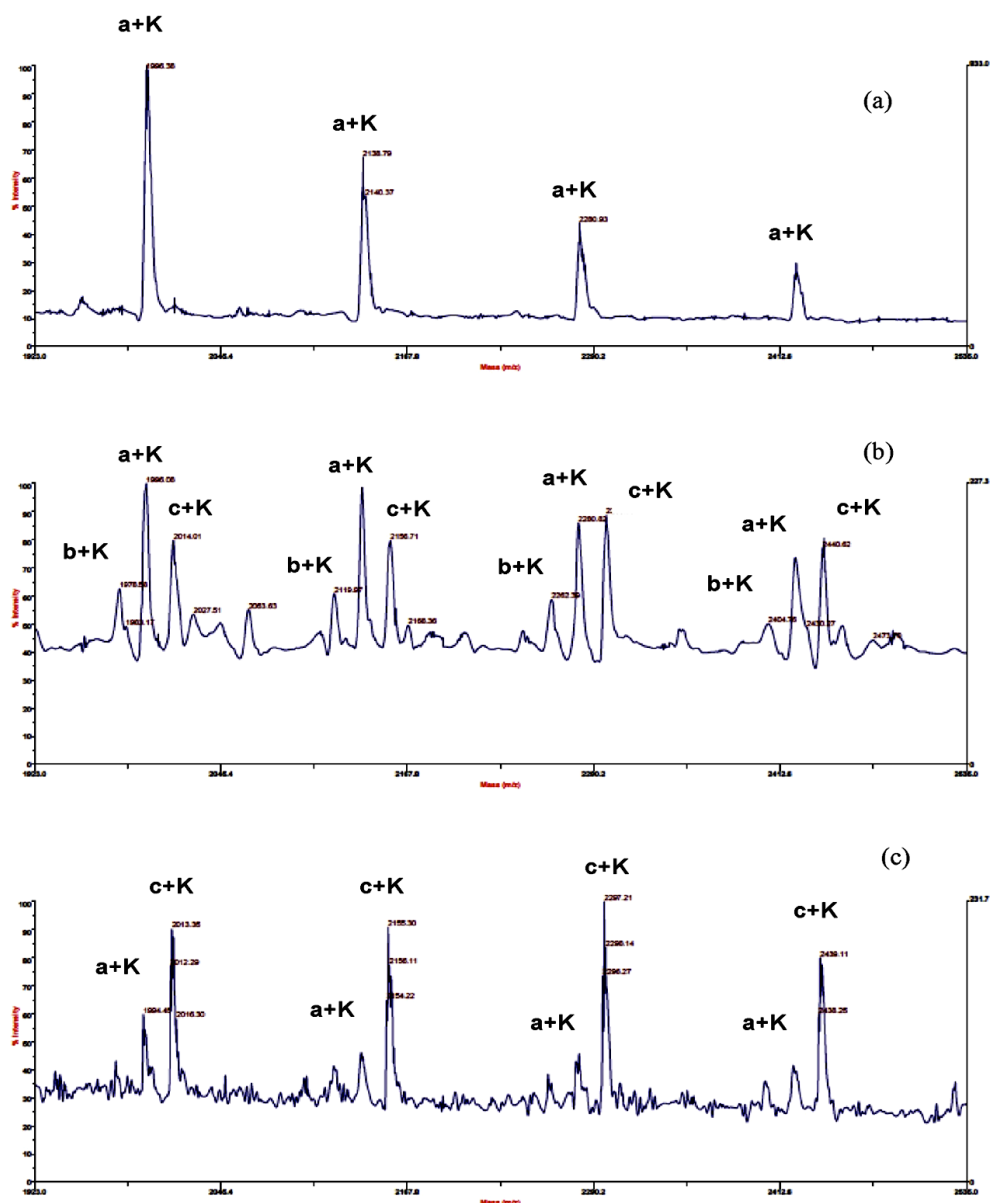
Figure 5. 5. Expanded MALDI-TOF mass spectra (m/z = 1923-2535) of polycarbonates from (a) entry 3, Table 5.4; (b) entry 1, Table 5.4; (c) entry 2, Table 5.4.

According to the literature, the dichloro end groups could be originated from chain transfer between two growing polymer chains resulting from initiating processes involving the chloride ion.[27] The ether linkage may be originated by two epoxide insertions whether in the initiating chain or in the growing steps. This fragment was also present in the polymers obtained with **CrH₂L4**/DMAP and **CrH₂L4**/PPNCl catalytic systems. In the polymer obtained with **CrH₂L4**/DMAP (Figure 5.5b) peaks at m/z 1978.58 suggested the presence of chains with -Cl and -OH terminal groups and an ether linkage (b + K expected for n = 12 $Cl(C_7H_{10}O_3)_{12}C_6H_{10}OC_6H_{10}OHK$, m/z 1975.84, in Figure 5.6). In the polymer formed with **CrH₂L4**/PPNCl (Figure 5.5c) a

peak at at m/z 2013.35 may arise from the polycarbonate with -Cl and -OH terminal groups (c + K, expected for n = 13 $Cl(C_7H_{10}O_3)_{13}C_6H_{10}OHK$, m/z 2019.83). The presence of different chain ends in the polymers obtained with **CrH₂L4**/DMAP and **CrH₂L4**/PPNCl is also reflected in a bimodal distribution of the GPC profile (See supplementary Information).
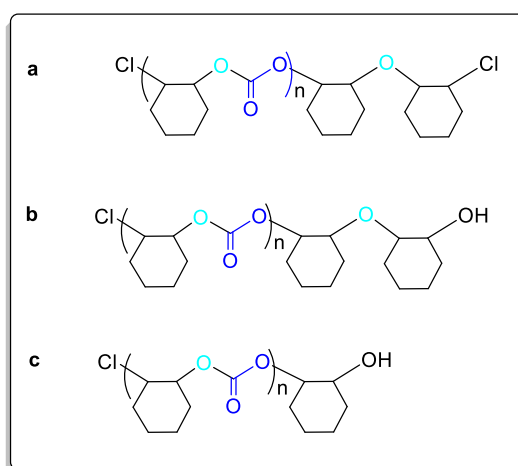
Figure 5.6. Fragments observed in the MALDI-TOF mass spectra.

To sum up, the MALDI-TOF analysis of the poly(cyclohexene carbonate) polymers formed with **CrH₂L4** employing DMAP, Py and PPNCl as co-catalysts, suggests that the initiation step involves the opening of the epoxide by nucleophilic attack of the Cl⁻ anion. Combination of two growing chains and insertion of two consecutive epoxides may take place. The presence of -OH terminal groups indicates the presence of residual water acting as termination group. Consequently, the mechanism proposed involved the coordination of the epoxide though the metal center and the subsequent epoxide opening by the Cl⁻ anion giving the alkoxo species (step a, Scheme 5.6), which may provide the cyclic carbonate by intramolecular attack (step b, Scheme 5.6). Alternate insertions of epoxide and CO_2 led to the polycarbonate growing chain (step c, Scheme 5.6). Termination may occur by the combination of two growing chains or protonolysis of water.
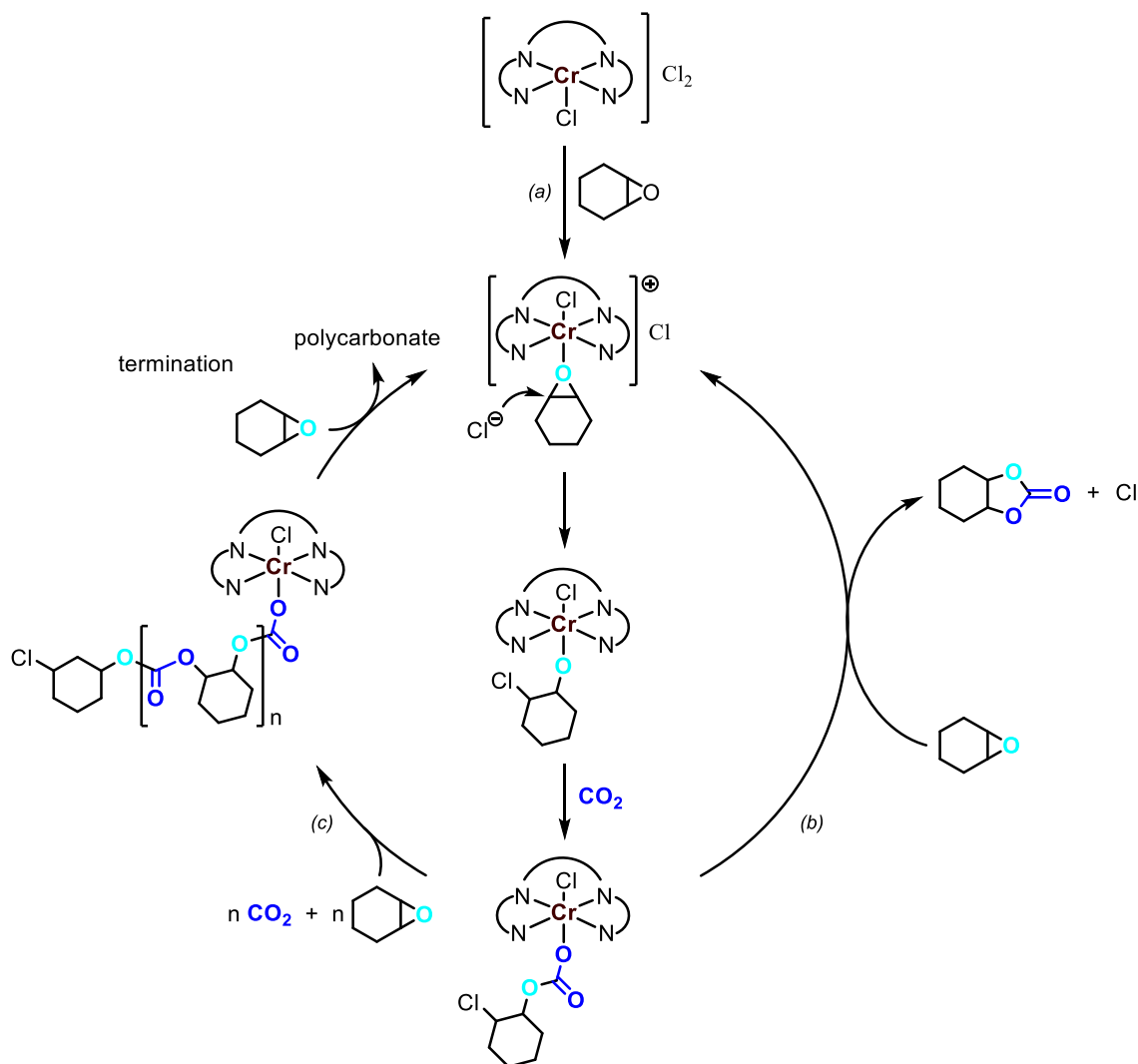
Scheme 5.6. Proposed mechanism for the coupling of CO_2 and CHO catalyzed by **CrH₂L4**/co-catalyst.

5.3 Conclusions

Chromium complexes with N_4-donor Schiff base ligands were found to be active catalysts for the cycloaddition of CO_2 to styrene oxide (conversions up to 92 %) affording cyclic styrene carbonate (up to 68 % yield). Cationic catalysts gave higher conversions than the neutral ones. The addition of tetrabutylammonium halides increased both the conversion and cyclic carbonate selectivity up to 100 % when using dichloromethane as solvent. A beneficial synergistic effect was observed since the ammonium salt provided lower conversion than the combined catalytic system. The chlorinated solvent could be avoided by using solvent free conditions or supercritical

carbon dioxide. Best results were obtained under scCO$_2$ conditions; the catalytic activity increased up to a TOF value of 652 h^{-1}. After work up, pure styrene carbonate was isolated in up to 74 % yield. Other terminal epoxides such as propylene oxide, 1,2-epoxyhexane, 1,2-epoxytetradecane and epichlorohydrin also reacted at high conversions (58-95 %) in only 30 min using a 0.2 mol % catalyst loading and high selectivity in the cyclic carbonate were attained. Using these N$_4$-Schiff base Cr complexes, the reaction of carbon dioxide with cyclohexene oxide produced mixtures of the polycarbonate and cyclic carbonate at different ratios of co-catalyst/catalyst and pressures. Thus at 50 bar CO$_2$ and at catalyst/co-catalyst ratios of 1/0.5-1/1, the polymer was formed as the main product while at 170 bar scCO$_2$ pressure and a catalyst/co-catalyst ratio of 1/5, the cyclic carbonate was the only reaction product. MALDI-TOF analysis of the polycarbonates obtained indicated that the initiating step involved the opening of the epoxide by the Cl$^-$ anion.

5.4 Experimental part

General Comments. Liquid epoxides were distilled over CaH$_2$ and stored under nitrogen. Carbon dioxide (CO$_2$, CP grade 5.3 and SCF Grade, 99.995%) was supplied by Air Products and Air Liquide. Solvents were purified through distillation or purification system Braun MB SPS-800 and stored under nitrogen atmosphere. IR spectra were recorded on a Midac Grams/386 spectrometer in ATR (range 4000-600 cm^{-1}) or KBr (range 4000-400 cm^{-1}). Raman spectrum of **CrL4** was recorded with a LabRam HR Raman spectrometer (Horiba-Jobin Yvon) equipped with BXFM co focal microscope, interference and Notch filters and charge-coupled device detector. The exciting line at 514.5 nm of a 2018 RM Ar$^+$-Kr$^+$ laser with 1 mW (SpectraPhysics) was focused using a ×100 objective and the spectra collected with gratings of 1800 grooves mm^{-1} were accurate within 1 cm^{-1}. All the recorded data were treated using the LABSPEC software (Horiba-Jobin Yvon). Raman spectrum of **CrL5**, **CrH$_2$L4** and **CrH$_2$L5** were recorded with a Raman FT-IR spectrometer (Renishaw) equipped with Leica DM 2500 co focal microscope. The exciting line at 514.5 nm of an Ar$^+$ laser with 4 mW was focused using a ×50 objective and the spectra collected with gratings of 2400 grooves mm^{-1} were accurate within 1 cm^{-1}. All the recorded data were treated using WIRE software. Conductivity was measured with a Crison conductimeter GLP

equipped with a conductivity Pt cell (CH_2Cl_2 or methanol solutions). MALDI-TOF measurements were performed on a Voyager-DE-STR (Applied Biosystems) instrument equipped with a 337 nm nitrogen laser. All spectra were acquired in the positive ion reflector mode. α-Cyano-4-hydroxycinnamic acid or dithranol were used as matrix. The matrix was dissolved in MeOH at a concentration of 10 mg ml^{-1}. The complex (1 mg) was dissolved in 1 ml of THF or CH_2Cl_2 and the polymer (5 mg) was dissolved in1 ml of $CHCl_3$. 1 μl of sample, 1 μl of matrix and 1 μl of potassium trifluoroacetate solution (KTFA) (1 mg of KTFA in 1 ml of THF) were deposited consecutively on the stainless steel sample holder and allowed to dry before introduction into the mass spectrometer. Three independent measurements were made for each sample. For each spectrum 100 laser shots were accumulated. Electrospray ionization mass spectra (ESI-MS) were obtained with an Agilent Technologies mass spectrometer. Typically, a dilute solution of the compound in DMF/methanol (1:99) was delivered directly into the spectrometer source at 0.01 ml min^{-1} with a Hamilton microsyringe controlled by a single-syringe infusion pump. The nebulizer tip operated at 3000-3500 V and 250°C, and nitrogen was both, the drying and the nebulizing gas. The cone voltage was 30 V. Quasi-molecular ion peaks $[M-H]^-$ (negative ion mode) or sodiated $[M + Na]^+$ (positive ion mode) peaks were assigned on the basis of the *m/z* values. Styrene oxide conversions were determined by gas chromatography using Perkin Elmer and Agilent 6850 instruments equipped with a polar column type Supercowax 10 polyethyleneglycol or HP-5 (30 m × 0.25 mm × 0.25 μm) and a FID hydrogen flame detector. A typical program temperature for the GC analysis started at 60°C, then increased in a 40°C/min rate and stopped after 2 min at 240°C. Mesitylene was used as internal standard. The yield was also determined by ^{1}H NMR, using a spectrophotometer Varian 400 MHz with tetramethylsilane as the internal standard. The molecular weights (M_w) of copolymers and the molecular weight distributions (M_w/M_n) were determined by gel permeation chromatography (GPC) versus polystyrene standards. Measurements were made in THF on a Millipore-Waters 510 HPLC Pump device using three-serial column system (MZ-Gel 100 Å, MZ-Gel 1000 Å, MZ-Gel 10,000 Å linear columns) with UV-detector (ERC-7215) and IR-detector (ERC-7515a). The software used to get the data was NTeqGPC 5.1. Samples were prepared as follows: 10 mg of the copolymer was dissolved with 2 ml of tetrahydrofuran (HPLC

grade) stabilized with 2,6-di-tert-4-methylphenol. Magnetic susceptibilities were measured on a Sherwood MSBmk1 magnetic susceptibility balance with KK105 as a calibration standard. All catalytic experiments were done by duplicate.

5.4.1 Synthesis of [Cr(L4)Cl] (CrL4)
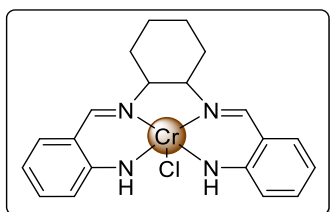
Sodium hydride (31 mg, 1.291 mmol) was washed with hexane and added slowly as a suspension with dry THF (3 ml) to a solution of **H₂L4** (100 mg, 0.312 mmol) in dry THF (2 ml), and the resulting mixture was stirred under nitrogen for 30 min. A gas evolution was observed (H₂). After this time CrCl₂ (43.6 mg, 0.354 mmol) was added to the yellow solution and the brown resulting mixture was stirred under nitrogen at room temperature for 3 h. The mixture was further stirred overnight under air and diluted with *tert*-butyl methyl ether (25 ml). The organic layer was washed with brine (3×25 ml) followed by drying with anhydrous sodium sulfate. After filtration to remove the solid impurities and the drying agent, solvent was removed in vacuum to give a dark brown solid **CrL4**. Yield: 48 %.

Anal. Calcd. (found) for $C_{20}H_{22}ClN_4Cr·2\ OC_4H_8$: C, 61.14 (61.16); H, 6.98 (7.18); N 10.19 (11.94). ESI calculated for $C_{20}H_{18}ClN_4Cr$ *m/z*: 424.0523, found *m/z*: 424.2514 [M-4H+Na]⁺. IR KBr pellet: 1611 cm⁻¹ ($\nu_{C=N}$). Raman (250-800 cm⁻¹): 331, 353, 447, 508, 558, 631, 683 cm⁻¹. Conductivity (distilled H₂O, 0.001 M): 39.3 $\Omega^{-1}·cm^2·mol^{-1}$.

5.4.2 Synthesis of [Cr(L5)Cl] (CrL5)
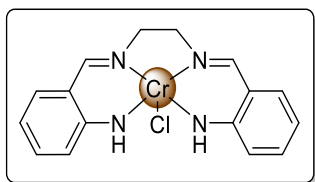
Similar procedure than for **CrL4** was followed to obtain a dark brown solid **CrL5**. Yield: 44 %. Anal. Calcd. (found) for $C_{16}H_{16}ClN_4Cr \cdot 3H_2O$: C, 47.35 (47.51); H, 5.46 (5.36); N 13.81 (10.86). MALDI-TOF (α-Cyano-4-hydroxycinnamic acid) calculated for $C_{16}H_{17}N_4Cr$ *m/z*: 317.0858, found *m/z*: 318.0858 $[M+2H-Cl]^{+*}$. IR KBr pellet: 1611 cm^{-1} ($\nu_{C=N}$). Raman (250-800 cm^{-1}): 335, 384, 422, 454, 486, 502, 562, 594, 615, 639, 739, 785 cm^{-1}. Conductivity (MeOH, 0.001 M): 50.1 $\Omega^{-1} \cdot cm^2 \cdot mol^{-1}$

5.4.3 Synthesis of [Cr(L4)Cl]Cl$_2$ (CrH$_2$L4)
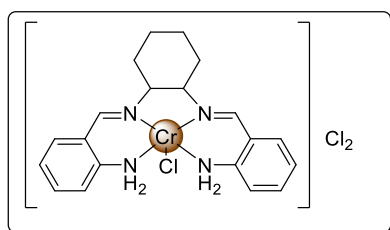
To a stirred solution of **H₂L4** (200 mg, 0.624 mmol) in THF (15 ml) was added CrCl$_2$ (69.7 mg, 0.567 mmol). The resulting mixture was stirred under nitrogen at room temperature for 3 h, and then LiCl (24 mg, 0.566 mmol) was added. The mixture solution was stirred under air for additional 6 h. Cold THF was added to the brown mixture. The suspension was filtered off, the solid was washed with cold THF and vacuum dried to afford a brown solid **CrH₂L4**. Yield: 97 %.

Anal. Calcd. (found) for $C_{20}H_{24}Cl_3N_4Cr \cdot 2H_2O$: C, 46.66 (46.42); H, 5.48 (5.44); N 10.88 (10.52). MASS MALDI-TOF (dithranol) calculated for $C_{20}H_{23}CrN_4$ *m/z*: 371.1328, found *m/z*: 371.3029 $[M-HCl-2Cl]^+$ (100 %).* IR KBr pellet: 1615 cm^{-1} ($\nu_{C=N}$). Raman (250-800 cm^{-1}): 368, 463, 502, 557, 571, 640, 750 cm^{-1}. Conductivity (distilled H$_2$O, 0.001 M): 150.6 $\Omega^{-1} \cdot cm^2 \cdot mol^{-1}$. μ_{eff} (21 ºC) = 3.73 μ_B

---

* Differences between found and calculated mass may be due to calibration of equipment for a different rang of value mass.

5.4.4 Synthesis of [Cr(L5)Cl₂]Cl (CrH₂L5)
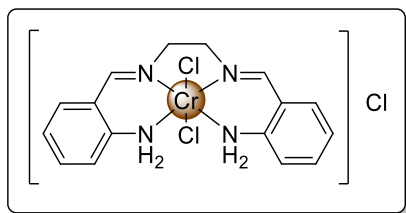
Similar procedure than for **CrH₂L4** was followed to obtain a brown solid **CrH₂L5**. Yield: 88%. Anal. Calcd. (found) for $C_{16}H_{16}Cl_3N_4Cr \cdot 5H_2O$: C, 37.33 (37.20); H, 5.48 (5.07); N 10.88 (10.40). MASS MALDI-TOF (dithranol) calculated for $C_{16}H_{17}CrN_4$ m/z: 317.0858, found m/z: 317.1530 $[M-H-3Cl]^{+}$.[†] IR KBr pellet: 1615 cm⁻¹ ($\nu_{C=N}$). Raman (250–800 cm⁻¹): 364, 449, 588, 676 cm⁻¹. Conductivity (MeOH, 0.001 M): 105.7 $\Omega^{-1} \cdot cm^2 \cdot mol^{-1}$. μ_{eff} (21 °C) = 4.10 μ_B.

Standard catalytic reaction in CH₂Cl₂. In a typical experiment, styrene oxide (0.24 g, 2 mmol), mesitylene (0.23 g, 2 mmol) and 5 ml of CH_2Cl_2 were introduced into a 40 ml autoclave. 0.5 µl of this solution was analyzed by gas chromatography (GC), before adding the catalyst complex (23 mg, 0.06 mmol) and tetrabutylammonium iodide (21 mg, 0.06 mmol). A brown suspension was obtained. The autoclave was closed and purged three times with 5 bar of CO_2 gas, and then pressurized to 15 bar of CO_2 under stirring at room temperature. As a pressure decrease was observed, pressure was then adjusted to 10 bar before heating to 100ºC (pressure raised up to 20 bar). After stirring at 100ºC for 18 h, the mixture was cooled down to room temperature using an ice bath. The unreacted gas was released and the mixture was analyzed by gas chromatography (GC) and IR spectroscopy.

Standard catalytic reaction in scCO₂. In a typical experiment, styrene oxide (0.24 g, 2 mmol) and mesitylene (0.23 g, 2 mmol) were introduced into a 40 ml auto-clave. A 20 µL sample of this reaction was diluted with CH_2Cl_2 up to 100 µL and was analyzed by gas chromatography (GC). The catalyst (10 mg of complex, 0.026 mmol) and tetrabutylammonium iodide (9.6 mg, 0.026 mmol) were introduced. The autoclave was closed and purged three times with 5 bar of CO_2 gas and weighed. Then, liquid CO_2

[†] Differences between found and calculated mass may be due to calibration of equipment for a different rang of value mass.

was rapidly introduced and the autoclave weighed again. The temperature was increased up to 100 ºC (pressure up to 170 bar). After stirring at 100 ºC for 3 h (or the specified time), the mixture was cooled down to room temperature using an ice bath. The autoclave was slowly depressurized, the mixture was analyzed by GC (20 µL of sample diluted with CH_2Cl_2 up to 100 µL) or, without dilution, by NMR (when indicated) and IR spectroscopy. To purify the product the content of the autoclave was dissolved in CH_2Cl_2, the solvent was evaporated and the product was purified by flash chromatography with a silica gel column using a mixture of CH_2Cl_2/EtOAc (1:1) as eluent.

5.5 *Supporting information available*

IR, RAMAN, ESI and MALDI-TOF mass spectra of the complexes, an example of ^{1}H NMR of crude reaction with the different epoxides used, ^{1}H NMR, MALDI-TOF and GPC of the copolymers are available in the supporting information CD.

5.6   *References*

[1]   Aida, T.; Ishikawa, M.; Inoue, S., *Macromolecules* **1986**, *19*, 8-13.

[2]   Kruper, W.J.; Dellar, D.V.; *J. Org. Chem.* **1995**, *60*, 725-727.

[3]   Darensbourg, D.J.; *Chem. Rev.* **2007**, *107*, 2388-2410.

[4]   Karamé, I.; Tommasino, M.L.; Faure, R.; Lemaire, M.; *Eur. J. Org. Chem.* **2003**, *7,* 1271-1276.

[5]   Mang, S.; Cooper, A.I.; Colclough, M.E.; Chauhan, N.; Holmes, A.B.; *Macromolecules* **2000**, *33*, 303-308.

[6]   Chaterjee, C.; Chisholm, M.H., *Inorg. Chem.* **2012**, *51*, 12041-12052.

[7]   Paddock, R.L.; Hiyama, Y.; Mckay, J.M.; Nguyen, S.T., *Tetrahedron Lett.* **2004**, *45*, 2023-2026.

[8]   Anderson, C.E.; Vagin, S.I.; Xia, W.; Jing, H.; Rieger, B., *Macromolecules* **2012**, *45*, 6840-6849.

[9]   Dengler, J.E.; Lehenmeier, M.W.; Klaus, S.; Anderson, C.E.; Herdtweck, E.; Rieger, B., *Eur. J. Inorg. Chem.* **2011**, *3*, 336-343.

10   Adolph, M.; Zevaco, T. A.; Altesleben, C.; Walter, O.; Dinjus, E., *Dalton Trans.* **2014**, *43*, 3285-3296.

11   Darensbourg, D.J.; Fitch, F.J., *Inorg. Chem.* **2007**, *46*, 5474-5476.

12   Darensbourg, D.J.; Fitch, F.J., *Inorg. Chem.* **2008**, *47*, 11868-11878.

13   Darensbourg, D.J.; Fitch, F.J., *Inorg. Chem.* **2009**, *48*, 8668-8677.

14   Karamé, I.; Jahjah, M.; Messaoudi, A.; Tommasino, M.L.; Lemaire, M., *Tetrahedron:Asymmetry* **2004**, *15*, 1569-1581.

15   Cameron, P.A.; Gibson, V.C.; Redshaw, C.; Segal, J.A.; White, A.J.P.; Williams, D.J., *J.Chem. Soc. Dalton Trans.* **2002**, *4*, 415-422.

16   Annigeri, S.M.; Sathisha, M.P.; Revankar, V.K., *Trans. Metal Chem.* **2007**, *32*, 81-87.

17   Kanamori, K.; Kawai, K., *Inorg. Chem.* **1986**, *25*, 3711-3713.

18   Geary, W.J., *Coord. Chem. Rev.* **1971**, *7*, 81-122.

19   Martínez, L.E.; Leighton, J.L.; Carsten, D.H.; Jacobsen, E.N., J. *Am. Chem. Soc.* **1995**, *117*, 5897-5898.

20   Hay, R.W.; Tarafder, M.T.H., *J. Chem. Soc. Dalton Trans.* **1991**, *3*, 823-827.

21   Darensbourg, D.J.; Mackiewicz, R.M.; Rodgers, J.L., *J. Am. Chem. Soc.* **2005**, *127*, 14026-14038.

22   Babu, H.V.; Muralidharan, K., *Dalton Trans.* **2013**, *42*, 1238-1248.

23   Caló, V.; Nacci, A.; Monopoli, A.; Fanizzi, A., *Org. Lett.* **2002**, *4*, 2561-2563.

24   Wang, J.-Q.; Dong, K.; Cheng, W.-G.; Sun, J.; Zhang, S.-J., *Catal. Sci. Technol.* **2012**, *2*, 1480-1484.

25   Langanke, J.; Greiner, L.; Leitner, W., *Green Chem.* **2013**, *15*, 1173-1182.

26   Eberhardt, R.; Allmendinger, M.; Rieger, B., *Macromol. Rapid Commun.* **2003**, *24*, 194-196.

27   Dean, R.K.; Dawe, L.N.; Kozak, C.M., *Inorg. Chem.* **2012**, *51*, 9095-9103.

Chapter - 6

Highly active and selective Zn(II)-NN'O Schiff base catalysts for the cycloaddition of CO_2 and epoxides

Abstract

Mononuclear Zn(II) complexes with tridentate NN'O-donor base Schiff ligands combined with a co-catalyst are active for the cycloaddition of CO_2 and epoxides. They provide cyclic carbonates selectively even with the more hindered substrates such as cyclohexene oxide and methyl epoxyoleate. The best conditions were achieved running the reaction in expanded neat substrate in CO_2 as reaction media. The activity obtained for the cycloaddition of CO_2 to styrene oxide reached an initial TOF of 3733 h^{-1}. The solid state structures of $Zn(NN'O)_2$ was determined by X-ray diffraction methods. Relative stability of the species in solution was analyzed by DFT calculations.
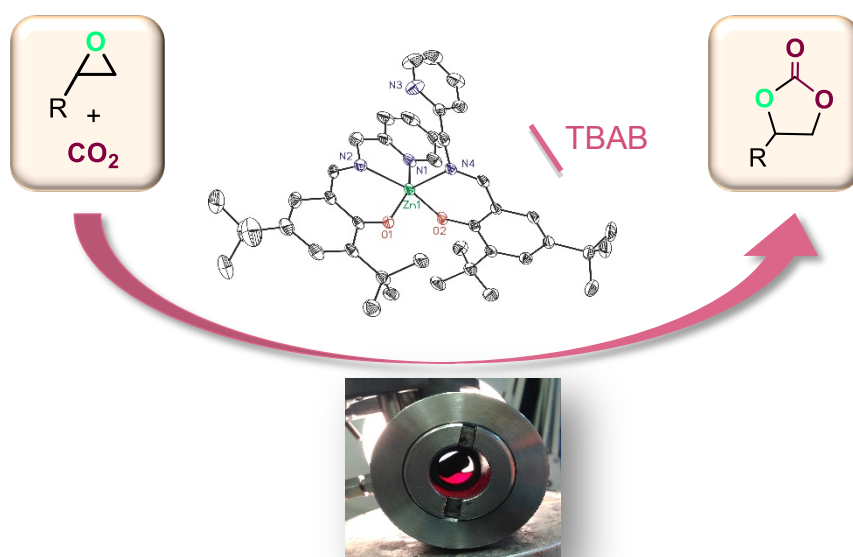
6.1 Introduction

Among the metal complexes used as catalysts for carbonate synthesis from CO_2 and epoxides, Zn-based complexes have extensively been studied as shown in Chapter 1. The key issue in the fixation of CO_2 into carbonates was the discovery of Inoue and Tsuruta that Zn catalysts polymerized CO_2 and epoxides to form polycarbonates.[1] As a matter of fact, one of the enzymes involved in the transformation of CO_2 into organic carbonates is carbonic anhydrase, which contain a zinc cation in its active site.[2] The advantages of Zn-based complexes over other active catalysts such as those based on chromium or cobalt, for example, is their lower toxicity, higher stability towards oxidation and lower price. Moreover, they are active at milder reactions conditions.[3]

Among most efficient Zn(II)-based catalysts are those containing Zn-phenoxides,[4] Zn-pyridine,[5] Zn-β-diiminates,[6] dinuclear anilide-aldimine Zn complexes[7] and Zn- NNONNO complexes.[8] They produce polymerization products, specially starting from CHO and PO. By contrast, catalysts based on Zn tetradentate NNOO-donor salen derived ligands[9,10,11] and tridentate NNN-donor[12,13] produced selectively the cyclic carbonates when combined with tetrabutylammonium bromide as co-catalyst.

Particularly, zinc(II) complexes containing bis(salicylaldimine) ligands were found to display also good catalytic activity for the alternating copolymerization of CO_2 and CHO.[14] Indeed, the introduction of a pendant N, O or P arm attached to the imine nitrogen leads to a new class of ligands (Figure 6.1),[15,16] which have been successfully applied in aluminum(III) catalyzed ethylene polymerization[17] and in calcium(II) and zinc(II) catalyzed ring-opening polymerization of cyclic monomers.[18,19]

Specially, catalytic Zn(II) systems with NN'O-donor ligands have been less extensively studied. The tridentate ligands may offer different possibilities to stabilize the intermediate species. In fact, NN'O-ligands with pyridine/amine-imine-phenolate functionalities have been found to form tetra-, penta- and hexacoordinate species using one or two ligands per metal center.[20] Furthermore the formation of higher coordinative saturated species may benefit the selective formation of the cyclic carbonates by promoting the backbiting mechanism.[21] Cu(II) complexes with dimethylamine-imine-phenolate NN'O-ligands have been reported to be active in the copolymerization of CHO/CO_2.[22]
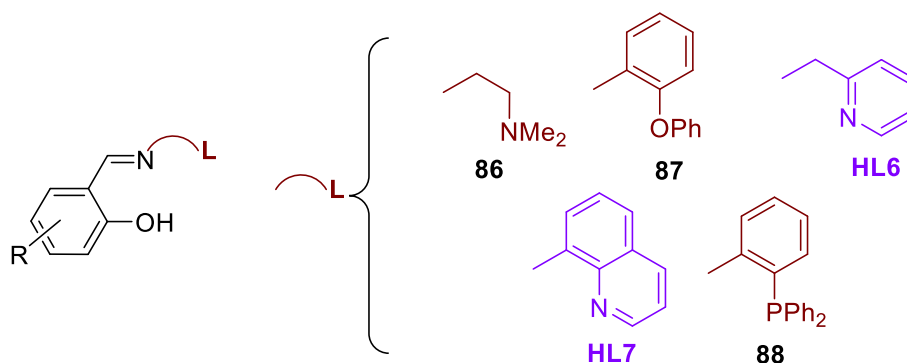
Figure 6. 1. NXO-Schiff base ligands (X = O, N or P).

Recently in our group, we reported that a Cr(III) complex with ligand **HL6** (Figure 6.1) in the presence of a co-catalyst was an active catalytic system for the copolymerization of CHO/CO_2 as well as for the cycloaddition of PO/CO_2 and styrene oxide.[23] The proposed structure for this chromium complex involved one ligand acting as tridentate and another as bidentate, [Cr(**L6**-$\kappa^3 N,N,O$)(**L6**-$\kappa^2 N,O$)Cl]. Using this catalyst and DMAP as co-catalyst, the reaction of CHO with CO_2 produced mixtures of PCHC and CHC. In an attempt to improve the conversion and selectivity obtained with this Cr(III) based catalytic system, we decided to prepare analogous catalysts with Zn(II) for the following reasons: a) they could stabilize mononuclear complexes with different coordination numbers, therefore they would favor the dissociation of the carbonate moieties thus selectively forming the cyclic carbonates; b) Zn(II) catalysts have shown high activity at milder conditions than Cr(III) ones; c) the softer Lewis acid character of the Zn(II) d^{10} complex compared to the Cr(III) one[24] may decrease the strength of M-O bond, leading to the selective formation of the cyclic carbonate;[25] d) the higher lability of Zn(II) compared to Cr(III) complexes towards the substitution reaction may favor the dissociation of the carbonate growing chain; e) the pyridine moieties may act as a pendant groups and could replace the growing chain, favoring the backbiting mechanism, which yield the cyclic product.

In this chapter we report the synthesis and catalytic activity of Zn(II) complexes with ligand **HL6** (Figure 6.2) in the coupling reaction of CO_2 and different epoxides. We focused specially in the coupling of styrene oxide and CO_2 since the reports of high conversions in the cyclic carbonate obtained with Zn(II) catalysts for this substrate are scarce.[26] The catalytic activity of a Zn(II) complex with ligand **HL7** (Figure 6.2) has also been studied for comparative purposes. In addition, a set of calculations based on

density functional theory methods (DFT) were also performed by Dr. Mar Reguero on Zn(II) complexes with **HL6** in order to confirm computationally the hypotheses suggested by the experimental results.
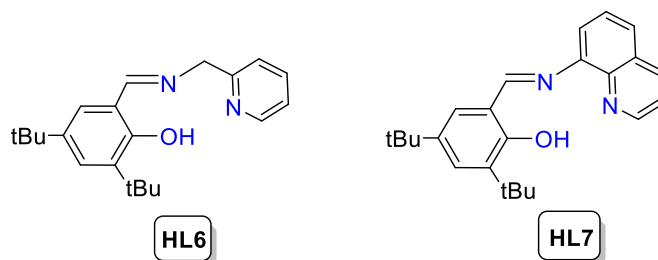
Figure 6. 2. NN'O-Schiff base ligands **HL6** and **HL7**.

6.2 Results and discussion

6.2.1 Zinc Schiff Base complex synthesis

N-(2-Pyridyl)methyl-2-hydroxy-3,5-di-*tert*-butylbenzaldimine (**HL6**) was synthesized following the procedure described by Finney and Mitchell by condensation of 3,5-di-*tert*-butyl salicylaldehyde and 2-methylaminopyridine.[16] In the literature it was reported that reaction of **HL6** with Zn(OAc)$_2$· 2H$_2$O using methanol as solvent in the presence of NEt$_3$ led to the formation of [Zn(**L6**-$\kappa^3 N,N',O$)$_2$].[20e] The authors proposed that this compound adopted a distorted octahedral geometry based on the X-ray structure of the analogous quinoline complex [Zn(**L7**-$\kappa^3 N,N',O$)$_2$] (**ZnL7**) in which the two ligands acted as tridentate and were coordinated in a meridional fashion. In addition, it was previously reported that the reaction of [Zn(N(SiMe$_3$)$_2$)$_2$] with **HL6** in THF (1:2 molar ratio) led to the formation of a brown solid also proposed as [Zn(**L6**-$\kappa^3 N,N',O$)$_2$].[20f] When we reacted **HL6** with ZnI$_2$ in methanol in the presence of a base (NaOH), a yellow solid, **ZnL6**, was formed (Scheme 6.1). Complex **ZnL6** was stable in solid and solution under inert atmosphere. However, it slowly turned red under air and UV-irradiation, especially in solution, maybe due to phenolate oxidation processes (see below).[27]

The absence of a strong absorption band in the IR spectrum of **ZnL6** at ν(O-H) region (*ca* 3600 cm^{-1}) and the shift to low energy of the band assigned to the stretching ν(C=N) (Δν = ν(C=N)free ligand - ν(C=N)complex = 20 cm^{-1}) pointed to the coordination through both phenolate fragment and imine group. Mass spectrum (ESI)

showed a peak at *m/z* = 711.3616 corresponding to the mononuclear species [Zn(**L6**)$_2$] (*calc for* C$_{42}$H$_{54}$N$_4$O$_2$Zn *m/z*: 711.3756 [M+H]$^+$). The electronic spectrum of **ZnL6** in MeOH showed absorptions at 260 and 331 nm associated with the ligand $\pi \rightarrow \pi^*$ and C=N transitions as well as bands at 227 and 390 nm attributed to charge-transfer bands.[28] The ^{1}H NMR spectrum of **ZnL6** in toluene-d$_8$ showed the expected signals assigned to two non-equivalent *tert*-butyl groups (δ 1.40 and 1.67 ppm). The pattern observed in the region δ 6-10 ppm corresponded to equivalent imine, pyridine and phenolate coordinated fragments. All signals were assigned by 2D NMR experiments (COSY, HMQC, HMBC and NOESY, Supplementary Information). The ^{1}H NMR spectrum of **ZnL6** in CDCl$_3$ agrees with the data reported in the literature for the six-coordinate species [Zn(**L6**-κ^3N,N',O)$_2$]^{20f} (see Supplementary Information).
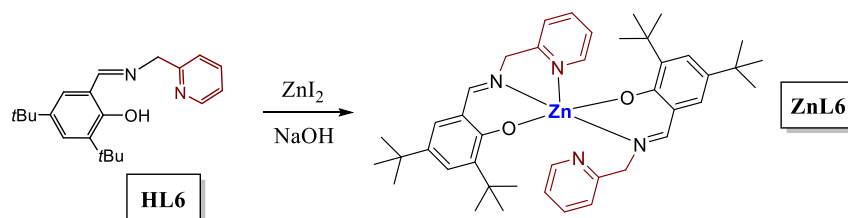
Scheme 6. 1. Synthesis of **ZnL6**.

Nevertheless, the X-ray structure of crystals of **ZnL6**, obtained from a MeOH solution, showed a five-coordinate environment around the Zn(II) center with one ligand acting as tridentate and another one as bidentate, [Zn(**L6**-κ^3N,N',O)(**L6**-κ^2N',O)] (see X-Ray diffraction structure of complex **ZnL6** below). The observation in the ^{1}H NMR spectrum in toluene-d$_8$ of only one set of equivalent signals in the aromatic region can be explained by a fluxional process, which may proceed through six-coordinate species as observed for similar complexes (Scheme 6.2).[12]
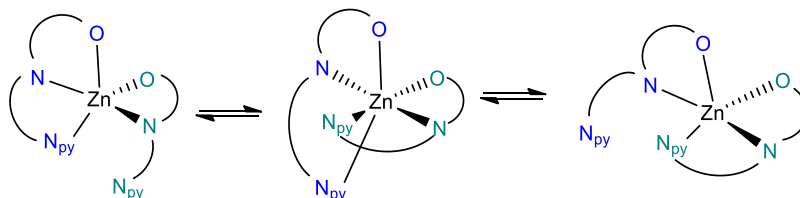
Scheme 6. 2. Fluxional process proposed in solution for **ZnL6**.

Signals corresponding to free ligand (3 %) were also observed in the ^{1}H NMR spectrum. The presence of free ligand may be related with hydrolysis of complex in solution due to traces of water. VT ^{1}H NMR spectra of **ZnL6** in toluene-d$_8$ under nitrogen atmosphere at temperatures from -80 to 80 °C (Figure 6.3) clearly indicated that the equilibrium was fast even at -80 °C. At this range of temperatures the signals of the pyridine protons did not split as expected for a five-coordinate complex with free and coordinated fragments. Increasing the temperature up to 80 °C the signal at δ 7.75 ppm of the aromatic and imine hydrogen atoms shifted up to down field (δ 7.88 ppm). The two doublets of the –CH$_2$- (δ 4.19 ppm) collapsed at 50 °C (δ 4.24 ppm). The relative integration of all signals from the free ligand changed only slightly among the spectra at different temperatures from 2 % (80 °C) to 6 % (-80 ºC).
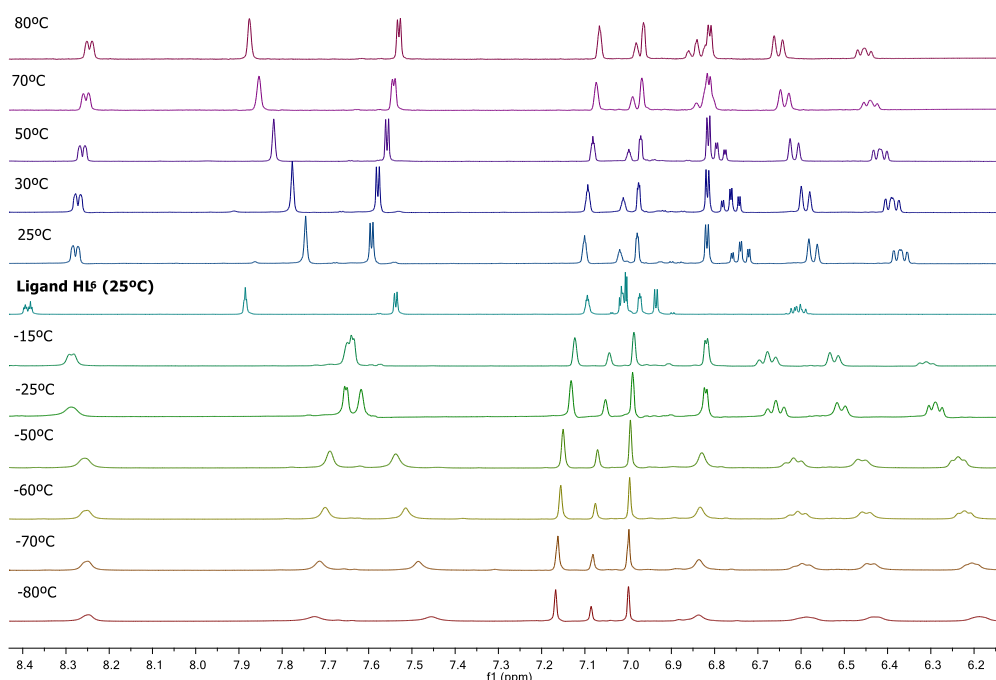
Figure 6. 3. ^{1}H NMR spectra (partial) at different temperatures of **ZnL6** in toluene-d$_8$ and free ligand **HL6** under inert atmosphere.

It was also observed that the yellow complex solution in toluene-d$_8$ or CDCl$_3$ of **ZnL6** standing under air and at room temperature turned red with time. Moreover, the solid **ZnL6** turned slowly into a red solid standing under air at room temperature. A solution of **ZnL6** (10 mg in 10 ml of dry toluene) under air and under irradiation of UV changed to red in 30 minutes (A', Figure 6.4). No change was observed when the

toluene solution of **ZnL6** was irradiated under nitrogen atmosphere during 24 h (B',
Figure 6.4). Neither the solid suffered color changes after this time under air or nitrogen
atmosphere (A and B, Figure 6.4).
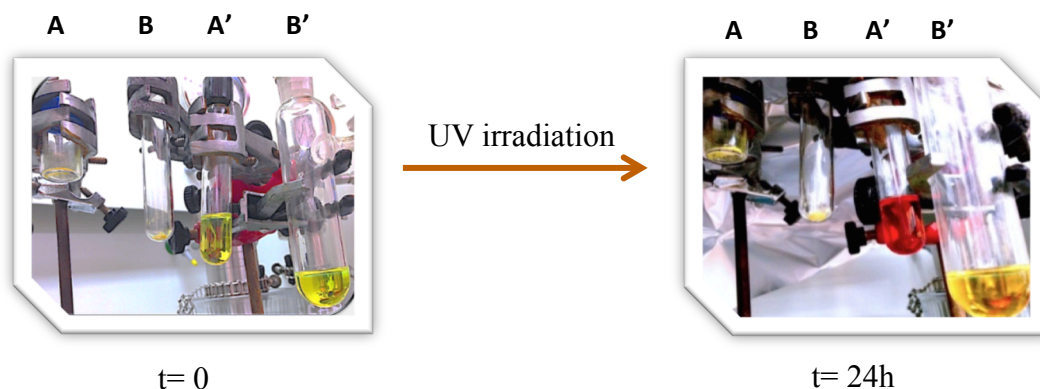
Figure 6. 4. Experiments under UV-irradiation.

The red solid obtained after 1 month standing at room temperature under air
showed a similar pattern of signals in the ^{1}H NMR spectra except that the signals
corresponding to the CH=N and pyridine groups were shifted *ca* 0.025-0.03 ppm
(Figure 6.5). Indeed, the mass spectrometry data, microanalysis and UV-visible of this
red compound were very similar to the ones observed for **ZnL6**. Therefore, we propose
that the change of color is probably due to some phenolate oxidation processes that are
imperceptible in those analytical techniques but sufficient to produce a visible change of
color.[27]
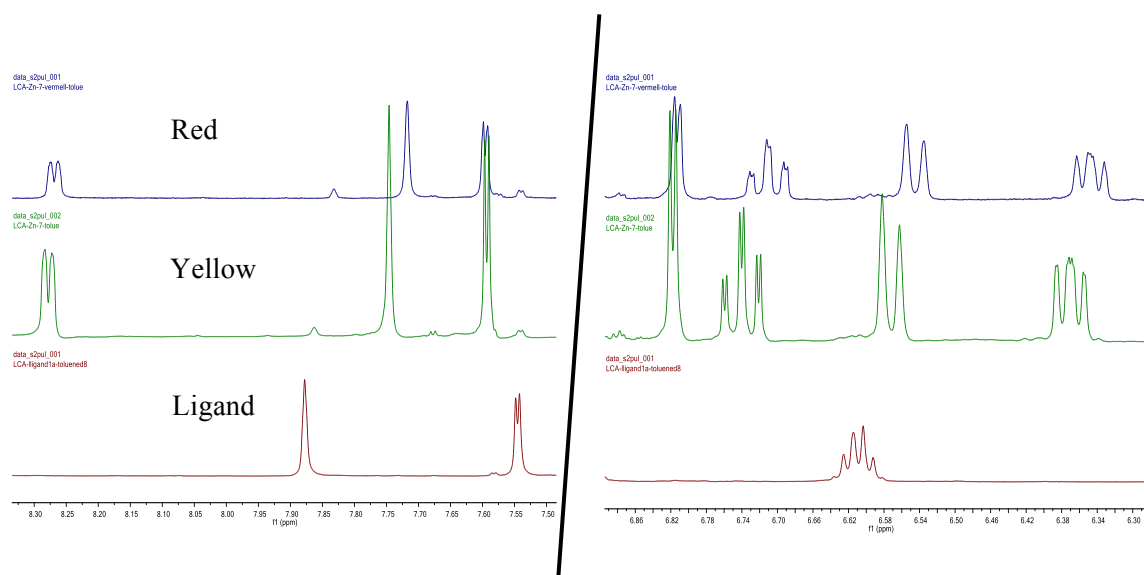
Figure 6. 5. ^{1}H NMR spectra of aromatic region in toluene-d_8.

In order to gain insight into the experimental results, a computational study based on DFT calculations was performed by Dr. M. Reguero (Departament química física i Inorgànica, URV, Tarragona) comparing the different stability of the tetra-, penta- and hexacoordinate species. Calculations modeled the complexes in a toluene solution as environment, where the NMR experiments were recorded. All results are collected in Table 6.1 and the most stable structures for each coordination number are shown in Figure 6.6. Several isomers were found for each coordination number, with *mer* configuration in all cases of hexa- and pentacoordinate species. This is in accord with the reported observation that rigid imine ligands accommodate better in a meridional mode in a Fe(III) octahedral complex.[28]

Table 6.1. Relative energies of the different isomers located computationally for complex **ZnL6** in toluene.

Coordination number	Isomer	ΔE(kcal·mol^{-1})	Population	%
6	**6-mer1**	0.00	1.000	94
5	**5-mer1**	3.74	0.002	0.2
4	**4-iso1**	12.86	0.000	0

6-mer1   5-mer1   4-iso1
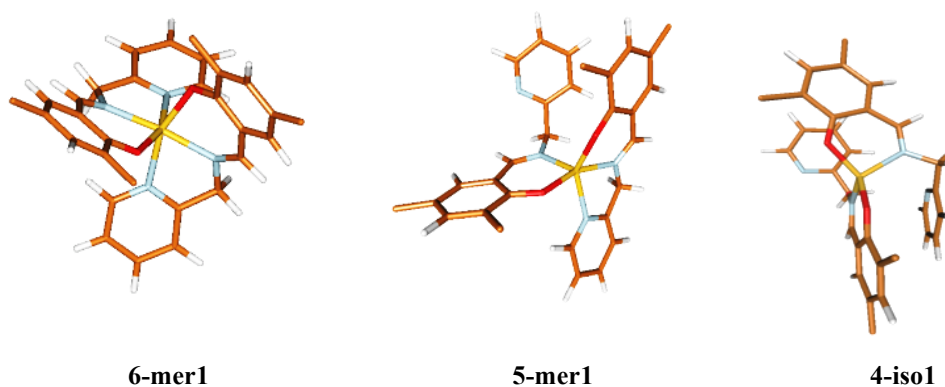
Figure 6. 6. Geometries of the most stable minima located at DFT level, for complex **ZnL6** in toluene for the different coordination numbers. *tert*-butyl groups and H atoms have been omitted for clarity.

The tetracoordinate species (Table 6.1) are significantly less stable than the other geometries, so their presence as long-lived species can be discarded. On the other hand, the small energy differences between hexa- and some of the pentacoordinate species clearly indicate that in solution a coexistence of such species is possible.

It was found that the barrier for the fluxional process (**5-mer1→5-mer1**) was significantly higher (10 kcal/mol) than that of the isomerization **6-mer1→5-mer1** (3 kcal/mol). We can assume, then, that the fluxional process in solution proceeds via the most stable hexa-coordinate species, which is the major species (Scheme 6.2).

6.2.2 X-ray diffraction structure of ZnL6

The structure of **ZnL6** contains one Zn(II) atom in a pseudo square-pyramidal environment bonded to two deprotonated ligands (Figure 6.6). Selected bond lengths and angles are listed in Table 6.2. One of the ligands acts as a tridentate $\kappa^3 NN'O$-donor, coordinating through the O(1) (phenol), N(2) (imine) and N(1) (pyridine) and occupying the square plane. The other ligand coordinates as a bidentate $\kappa^2 N'O$-donor by the O(2) (phenol) and the N(4) (imine) while the pyridine nitrogen N(3) remains non coordinated (distance Zn(1)····N(3) 4.418 A). The N(4) occupies the axial position of the square-pyramid. The phenolate O(2) is *trans* to the coordinated imine group N(2).
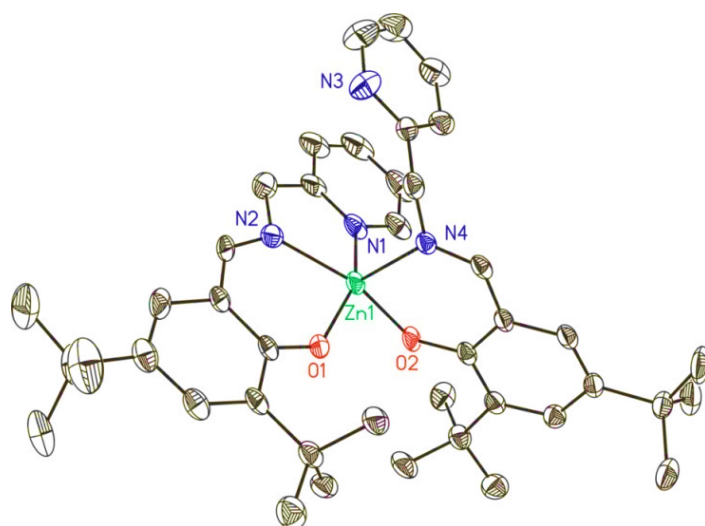
Figure 6. 7. X-ray diffraction structure of **ZnL6**. H atoms are omitted for clarity. Thermal ellipsoids are depicted at 50 % probability.

Table 6.2. Selected bond lengths (Å) and angles (°) for **ZnL6**.

Zn1-O1	1.976(2)	Zn1-N4	2.033(2)
Zn1-O2	1.9785(19)	Zn1-N1	2.152(3)
Zn1-N2	2.086(2)	Zn1·····N3	4.418
N2-C7	1.284(4)	N2-C26	1.457(4)
N4-C28	1.279(4)	N4-C27	1.454(3)
O1-Zn1-O2	95.66(8)	O25-Zn1-O26	98.46(10)
O1-Zn1-N4	103.39(9)	O16-Zn1-O25	91.17(10)
O2-Zn1-N4	92.08(8)	O26-Zn1-N8	121.83(10)
O1-Zn1-N2	86.76(9)	O25-Zn1-N8	137.60(9)
O2-Zn1-N2	153.42(9)	O26-Zn1-N1	101.06(10)
N4-Zn1-N2	113.17(9)	O16-Zn1-N1	149.27(10)
O1-Zn1-N1	155.09(9)	O25-Zn1-N1	85.57(10)
O2-Zn1-N1	90.61(9)	N8-Zn1-N1	74.97(11)
N4-Zn1-N1	100.44(9)		
N2-Zn1-N1	77.23(10)		

Bond distances Zn-O (1.976 (2) and 1.9785 (19) Å), Zn-N (pyridine) (2.152(3) Å) and Zn-N (imine) (2.086(2) and 2.033(2) Å) in complex **ZnL6** lay in the range observed for analogous NN'O-donor ligands (Table 7.2).[20a-c,20e,20g-h] As expected the Zn-N (pyridine) distance is longer than the Zn-N (imine).[20d] The Zn1-N (pyridine) bond distances are 0.021-0.086 A shorter than the Zn1-N(quinoline) distances reported for the hexa-coordinate complex [Zn(**2**-κ^3N,N',O)2],[20e-f] which may be attributed to the higher basicity of the pyridine than the quinoline. The N(imine)-C bond lengths of the imine group C=N (1.454(3) and 1.457(4) Å) are in the range of the ones reported for Zn-N(imine) complexes.[20a, 20c, 20e]

The distortion of the 5-coordinate environment can be described by the τ-factor[29] (Figure 6.8). The low value of τ = 0.03 for **ZnL6** is indicative of a square-pyramidal distortion rather than a distorted trigonal bipyramid geometry (τ = 0 for a perfect square-pyramidal geometry while τ = 1 for a trigonal-bipyramidal one).
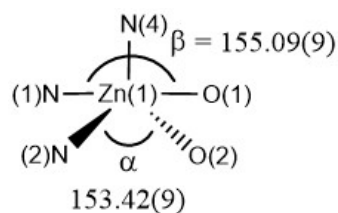
$$\tau \,(\textbf{ZnL6}) = \frac{\beta - \alpha}{60} = 0.03$$

Figure 6. 8. Angles α and β and τ factor for complex **ZnL6**.

6.2.3   Catalysis

6.2.3.1   Cycloaddition of CO$_2$ and styrene oxide

Complex **ZnL6** was tested as catalyst in the cycloaddition of epoxides to CO_2. The effect of co-catalyst, catalyst/co-catalyst ratio, pressure and temperature were optimized in the reaction of CO_2 and styrene oxide. The scope of the catalyst activity was then extended to other substrates.

The cycloaddition of styrene oxide with CO_2 was initially studied using **ZnL6** based catalytic systems. The initial conditions were 50 atm CO_2, 80 °C using 0.2 mol % catalyst in neat substrate as solvent during 24 h. The results are presented in Table 6.3. At these conditions the control experiments using as catalyst **ZnL6** or **HL6** gave very low conversion towards the formation of the corresponding cyclic carbonate (up to 5 %; entries 1 and 2, Table 6.3). This fact suggests that the pendant pyridine group of the coordinated ligand is not able to promote the opening of the cyclic epoxide by itself as reported for monodentate pyridine in [ZnBr$_2$Py$_2$] catalytic systems for the copolymerization of CO_2 and PO.[5b] The effect of adding a co-catalyst was then analyzed. Very high conversion (97 %) was obtained even decreasing the catalyst loading to 0.14 mol % and the molar co-catalyst/catalyst ratio to 1.4 (0.2 mol % co-catalyst, entries 3 and 4, Table 6.3). In this case, the catalytic system was highly selective since only cyclic carbonate was detected by ^{1}H NMR spectroscopy. This result is remarkable since other catalytic systems require high co-catalyst/catalyst ratio in order to displace the bonded carbonate, thus favoring the backbiting mechanism leading to the cyclic product.[25] In the monometallic-based catalytic system **ZnL6**/PPNCl, with a

highly saturated coordination sphere, the formation of the cyclic carbonate is favored. No poly(carbonate) was detected by ^{1}H NMR in any of the experiments.

Table 6.2. Cycloaddition of styrene oxide and CO_2 using **ZnL6** and **ZnL7**.[a]

Entry	Cat	Co-cat	Cat/Co-cat (mol %)[b]	Conv (%)[c]	TOF (h^{-1})[d]	Yield (%)[e]
1	**ZnL6**	-	0.2/-	5	-	n.i.
2	**HL6**	-	0.2/-	2	-	n.i.
3	**ZnL6**	PPNCl	0.2/1.0	85	18	n.i
4	**ZnL6**	PPNCl	0.14/1.0	97	28	68
5	-	PPNCl	-/1.0	32	10	n.i.
6	**ZnL6**	PPNCl	0.14/0.2	97	28	65
7	**ZnL6**	NaI·2H$_2$O	0.14/0.2	40	12	29
8	-	NaI·2H$_2$O	-/0.2	25	7	n.i.
9	**ZnL6**	NaI·2H$_2$O	0.14/1.0	51	15	49
8	**ZnL6**	DMAP	0.14/0.2	83	24	56
9	-	DMAP	-/0.2	30	10	n.i.
10	**ZnL6**	TBAB	0.14/0.2	98	28	63
11[f]	**ZnL6**	TBAB	0.14/0.2	42	48	n.i.
12[f]	-	TBAB	-/0.4	18	8	n.i.
13[g]	**ZnL6**	TBAB	0.05/0.07	12	80	n.i.
14	**ZnL7**	TBAB	0.14/0.2	97	28	78

[a]Reaction conditions: T = 80 ºC, time = 24 h, PCO$_2$ = 50 bar, styrene oxide: 0.0438 mol (5 ml); [b]mol % respect to the substrate; [c]measured by ^{1}H NMR; [d]averaged TOF (mol substrate converted·(mol catalyst)$^{-1}$·h^{-1}; [e]isolated yield; [f]time = 6 h; [g]time = 3 h.

Other co-catalysts were examined. Hydrated simple alkali metal halides such as NaI·2H$_2$O were reported to provide very high conversions.[30] Using **ZnL6**/NaI·2H$_2$O catalytic system the conversion decreased to 40 % (at 0.14 mol % NaI·2H$_2$O, averaged TOF 12 h^{-1}; entry 7, Table 6.3) or 51 % (at 1 mol % NaI·2H$_2$O, averaged TOF 15 h^{-1}; entry 9, Table 6.3). When DMAP was used as co-catalyst high conversion was also

obtained (83 %, entry 8, Table 6.3). With TBAB as co-catalyst the conversion reached a 98 % (isolated yield 63 %; entry 10, Table 6.3). After 6 h of reaction, this catalytic system gave a 42 % of conversion (average TOF 48 h^{-1}; entry 11, Table 6.3). Decreasing catalyst loading to 0.05 mol % after 6 h the conversion was 12 % (average TOF 80 h^{-1}; entry 13, Table 6.3). The average TOF obtained with the chromium related catalyst [Cr(**L6**)$_2$Cl]/PPNCl for this substrate at the same conditions was 52 h^{-1}. Therefore, the catalytic activity improved by replacing the chromium ion for zinc in this complex.

Since we had observed that complex **ZnL6** is pentacoordinate in the solid state and there are evidences of equilibrium with hexacoordinate species in solution, we examined the catalytic activity of the quinoline hexacoordinate complex **ZnL6**.[20e,20f] At the same reaction conditions than **ZnL6**/TBAB, **ZnL7**/TBAB produced similar conversion (98 % versus 97 % respectively; entry 14, Table 6.3). This demonstrates that six-coordinate species may be also active, probably giving place to more reactive systems in solution. The different basicity of the pyridine and quinoline fragments did not produce differences in the catalytic activities of the corresponding catalytic systems.

The effect of pressure and temperature using **ZnL6**/TBAB as catalytic system was then studied at 0.14 mol % catalyst and 0.20 mol % co-catalyst. The results are listed in Table 6.4.

Catalytic system **ZnL6**/TBAB was also active at 10 bar yielding a 79 % of conversion after 24 h (entry 1, Table 6.4). Even at atmospheric pressure, the conversion was still good (42 %, entry 2, Table 6.4). Prolonging the reaction time up to 48 h at these conditions the conversion did not increase very much indicating an inactivation of the catalyst (entry 3, Table 6.4). At 1 bar, increasing the temperature to 100 °C, the conversion reached a 77 % (entry 4, Table 6.4).

The effect of pressure was then analyzed at 100 °C in 3h reaction time (Figure 6.9). Raising the pressure up to 100 bar resulted in an increase of the catalytic activity (TOF up to 520 h^{-1}). Above this pressure a drop in activity was observed. Decreasing the catalyst loading and the reaction time afforded an optimized averaged TOF of 3733 h^{-1} (Reaction done by triplicate, Figure 6.10). It is noteworthy that the catalytic activity obtained with the combination of **ZnL6** and TBAB increases the activity obtained with TBAB alone (Figure 6.10).

Table 6.3. Cycloaddition of styrene oxide and CO_2 with **ZnL6**/TBAB as catalysts at different P and T.[a]

Entry	P (bar)	T (°C)	t (h)	Conv (%)[b]	TOF (h-1)[c]	Yield (%)[d]
1	10	80	24	79	23	
2	1	80	24	42	12	-
3	1	80	48	48	7	42
4	1	100	24	77	22	71

[a]Reaction conditions: styrene oxide: 0.0438 mol (5 ml); catalyst 0.14 mol %; co-catalyst 0.2 mol %; [b]measured by ^{1}H NMR; [c]averaged TOF (mol substrate converted·(mol catalyst)$^{-1}$·h^{-1}; [d]isolated yield.

The behavior of the reaction phase respect to the pressure was analyzed visually with a reactor equipped with sapphire windows. Figure 6.9 a-f shows the reaction mixture *in situ* at different CO_2 pressures.
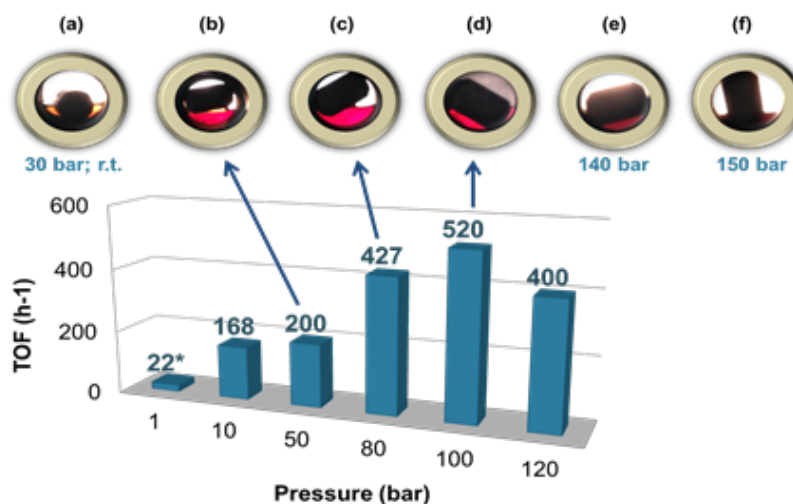
Figure 6. 9. Effect of pressure on the TOF (h^{-1}) using catalytic system **ZnL6**/TBAB. Reaction conditions: styrene oxide: 2.0 ml, 17.5 mmol; catalyst 0.05 mol %, co-catalyst 0.07 mol %, 100 °C, 3h. * styrene oxide: 5.0 ml, 43.8 mmol catalyst 0.14 mol %, co-catalyst 0.2 mol %, 24h, (a-f) Reactor photographs of the reaction systems at different temperatures and pressures.

At low CO_2 pressure and at room temperature (a, Figure 6.9) it was observed that the yellow catalyst was dissolved in the styrene oxide. The solution changed to red by increasing the temperature to 100°C and the pressure to 50 bar (b, Figure 6.9). The change in color observed might be indicative of partial decomposition that did not affect the conversion during 24 h. The volume of the organic phase slightly increased when the pressure increased up to 100 bar due to the formation of the CO_2 expanded substrate phase (c and d, Figure 6.9). Furthermore, at this pressure the gas phase became cloudy indicating partial solubilization of the substrate in the CO_2.
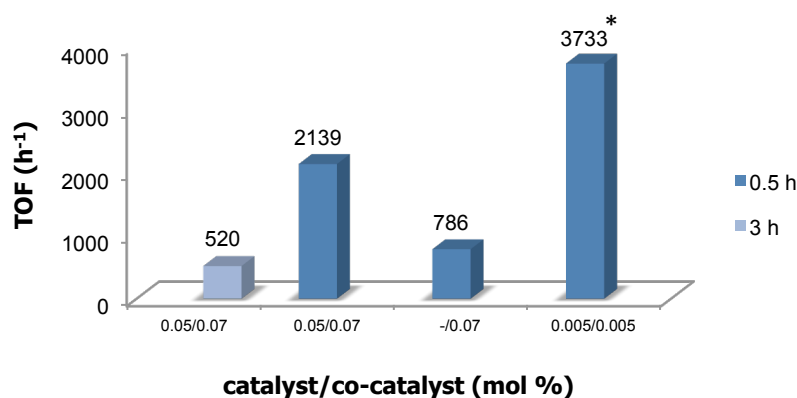
Figure 6.10. Optimization of TOF (h^{-1}) using catalytic system **ZnL6**/TBAB. Reaction conditions: styrene oxide: 2.0 ml, 17.5 mmol; co-catalyst 0.07 mol%, 100 °C, 100 bar. *co-catalyst 0.005 mol %, experiment done by triplicate.

Further increasing of the pressure lead to the dilution of the SO in the CO_2 phase inducing the precipitation of the catalyst (the volume of the liquid phase decreased and became cloudy) with a concomitant decrease in conversion to carbonate (e and f, Figure 6.9). Similar phase behavior was reported by Leiner *et al*. in the reaction of methyl epoxyoleate with CO_2 using TBAB.[31]

The reactivity of **ZnL6**/TBAB with styrene oxide was analyzed by ^{1}H NMR spectroscopy. The ^{1}H NMR spectrum of a mixture of **ZnL6**/SO (1:10) at 60 °C (a, Figure 6.11) showed new low intensity signals (1 %) at δ 3.22 (dd, *J* = 2.4, 4 Hz), 2.85 (dd, *J* = 4, 6 Hz), 2.55 (dd, *J* = 2.4, 6 Hz) and 2.41 ppm (dd, *J* = 4, 6 Hz) that may be attributed to species with coordinated epoxide.[32] These signals disappeared when TBAB (**ZnL$_6$**:TBAB = 1:1) was added to this mixture after being pressurized to 10 bar CO_2

and heated to 60 °C (b, Figure 6.11). At these conditions the formation of the carbonate product was detected by ^{1}H NMR. This suggests that the coordination of the epoxide takes place, although in the high diluted NMR sample the concentration of the M-epoxide species is low.
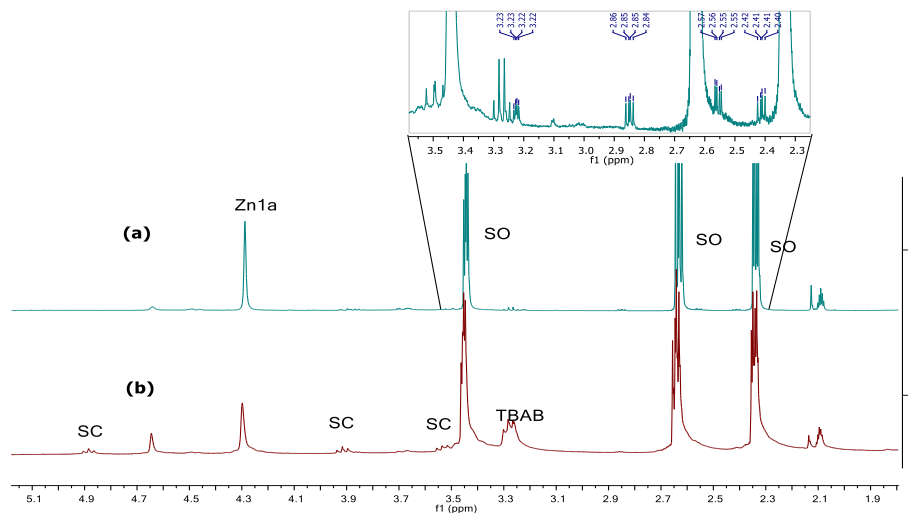
Figure 6. 11. ^{1}H NMR spectrum of **ZnL6**/styrene oxide (1:10) in toluene-d_8 at a) 60 °C and b) added TBAB (1:1 **ZnL6**:TBAB) at 10 bar CO_2 after 1 h.

Reviewing the reported data from the literature concerning the Zn-catalyzed cycloaddition of styrene oxide with CO_2, the most active catalyst is $ZnBr_2$/TBAI at 80 °C, 80 bar CO_2 and a co-catalyst/catalyst ratio of 4 (TOF 966 h^{-1}, entry 1, Table 6.5).[33] At 100 °C and 100 bar, **ZnL6**/TBAB afforded a TOF of 3733 h^{-1} at lower co-catalyst/catalyst ratio (TBAB: **ZnL6** = 1) (entry 2, Table 6.5).
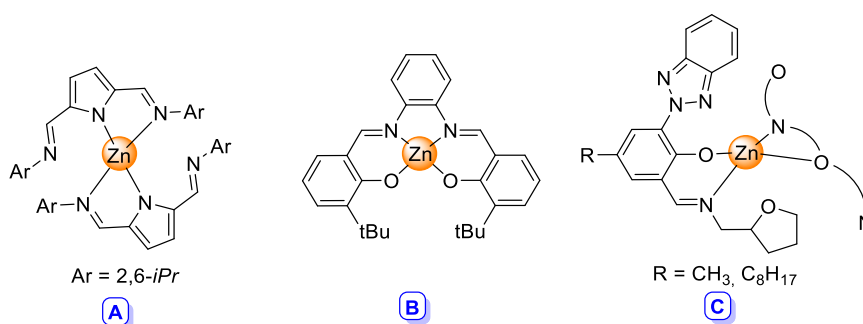
Figure 6.12. Selected Zn(II) catalytic systems from the literature for the cycloaddition of CO_2 to styrene oxide.

Table 6.4. Zn(II) based catalytic systems for the cycloaddition of CO_2 to styrene oxide

Entry	Cat/Co-cat (mol %)	P (bar)	T (°C)	t(h)	Conv./Y (%)	TOF (h^{-1})
1[33]	$ZnBr_2$/TBAI (0.14/0.56)	80	80	0.5	69/-	966
2	**ZnL6**/TBAB (0.005/0.005)	100	100	0.5	55	3733
3[12]	**A**/TBAB (2.5/5)	1	105	2	86/80[a]	17
4[b]	**ZnL6**/TBAB (2.5/5)	1	105	2	93/82	19
5[9c]	**B**/TBAI (2.4/2.4)	10	45	3	-/98	13
6[34]	$ZnCl_2$/TBAI (0.2/0.4)	1-1.2	r.t.	24	27/-	6
7[13]	**C**/TBAB (0.1/0.5)	10[c]	50	24	62/-	3

[a] 9 % diol was formed; [b] Reaction conditions: see Table 6.2; [c] Initial pressure.

Catalysts based on a Zn-pyrrol-imine complex **A** (Figure 6.12)[12] at mild conditions provided a TOF 17 h^{-1} (entry 2, Table 6.5), which is a value close to the one obtained with **ZnL6**/TBAB (entry 3, Table 6.5) but diol formation was reported in the case of catalyst **A**. Similar TOF was reported for the Zn-salphen catalyst **B**/TBAI (Figure 6.12)[9c] although the temperature employed was inferior (entries 4 and 5, Table 6.5). At very mild conditions (r.t. and 1-1.2 bar) $ZnCl_2$/TBAI provided an averaged TOF of 6 h^{-1} (entry 6, Table 6.5).[34] Catalytic system based on Zn-imine-phenol **C** (Figure 6.12)[13] also shows similar results at similar conditions (entry 7, Table 6.5). Although the direct comparison of these data is not possible due to different reactor set ups, the results obtained with **ZnL6**/TBAB are encouraging.

6.2.3.2 Cycloaddition of CO_2 to other epoxides

Catalyst **ZnL6**/TBAB was also active and selective for the cycloaddition of CO_2 to other epoxides at 50 bar and 80 °C (Figure 6.13). Conversions to the cyclic product were high for terminal epoxides (71-92 %, Figure 6.13).
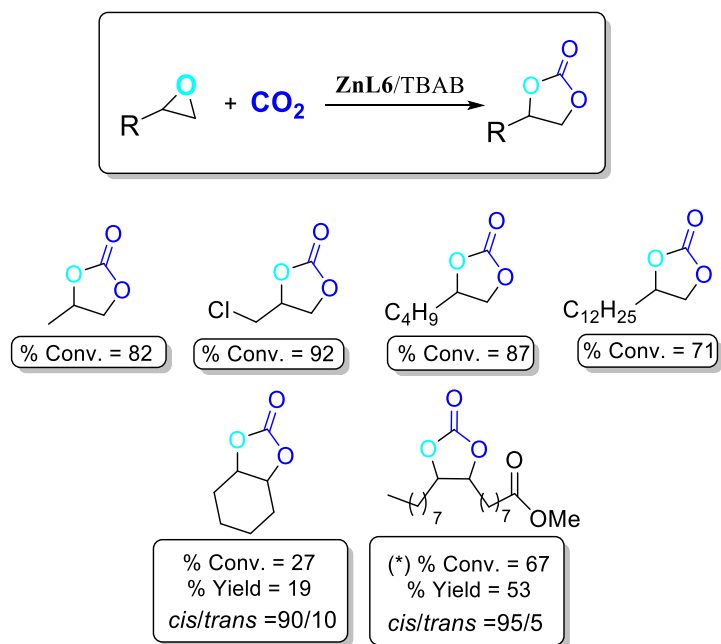
Figure 6. 13. Cycloaddition of different epoxides to CO_2 with catalyst **ZnL6**/TBAB.
Reaction conditions: T = 80 °C, time = 24 h, P_{CO2} = 50 bar, substrate: 0.0438 mol;
catalyst: 0.0633 mmol (0.14 mol %); co-catalyst: 0.4378 mmol (0.2 mol %). (*)
cat/cocat: 2 mol %/2 mol %; T = 100 °C, P_{CO2} = 100 bar.

The polycarbonate was not detected by ^{1}H NMR spectroscopy when neither terminal epoxides nor cyclohexene oxide were used as substrates. It is interesting to remark that although the related chromium catalytic system [Cr(**L6**)$_2$Cl] with PPNCl or DMAP as co-catalysts were more active catalysts than **ZnL6**/TBAB in the reaction of CO_2 and cyclohexene oxide, they produced mixtures of poly(cyclohexene carbonate) and cyclic cyclohexene carbonate.[23] Catalyst **ZnL6**/TBAB was also active for internal hindered substrates, such as the methyl epoxyoleate derived from a natural product, although higher concentration of catalyst was required.[31,35]

6.3   Conclusions

Mononuclear Zn(II) complexes with NN'O-donor base Schiff ligands combined with a co-catalyst are active for the cycloaddition of CO_2 and epoxides. They provide cyclic carbonates selectively with high activity and at low catalyst/co-catalyst ratio. The best conditions were achieved running the reaction in expanded CO_2 in neat substrate as solvent at 100 bar and 100 °C at very low catalyst loading. The activity obtained with

ZnL6/TBAB catalytic system reached an initial TOF of 3733 h^{-1} although it lacks from stability at longer reaction times. The catalytic activity in the cycloaddition of CO_2 to styrene oxide of **ZnL6**/TBAB is higher than the one obtained with analogous Cr(III) complex, [Cr(**L6**)Cl][23] Compared to other Zn(II) reported catalytic systems **ZnL6**/TBAB is highly active in the cycloaddition of CO_2 to styrene oxide at 100 °C and 100 bar although at mild reaction conditions the activity is lower than Zn(II)-salen derived catalysts[9c] High conversions were obtained with catalyst **ZnL6**/TBAB for other terminal aliphatic epoxides. More sterically hindered substrates such as cyclohexene oxide and methyl epoxyoleate, derived from natural products, were also transformed selectively in the cyclic carbonate product but at lower conversion than terminal epoxides.

6.4   Experimental part

General Comments. HL6 was prepared following previously described procedures.[15,16] Epoxides were dried over CaH_2, distilled and stored under inert atmosphere except 1,2-epoxyhexane, 1,2-epoxydodecane and epichlorohydrin, which were purchased at Sigma-Aldrich and used as received. Solvents were purified by the system Braun MB SPS-800 and stored under nitrogen atmosphere. Carbon dioxide (SCF Grade, 99.999 %, Air Products) was used introducing an oxygen/moisture trap in the line (Agilent). IR spectra were recorded on a Midac Grams/386 spectrometer in ATR (range 4000-600) cm^{-1} or KBr range (4000-400 cm^{-1}). UVvisible spectra were recorded on a UV-3100PC spectrophotometer. NMR spectra were recorded at 400 MHz Varian, with tetramethylsilane (^{1}H NMR and ^{13}C NMR) as internal standards. MALDI-TOF measurements of complexes: Voyager-DE-STR (Applied Biosystems) instrument equipped with a 337 nm nitrogen laser. All spectra were acquired in the positive ion reflector mode. α-cyano-4-hydroxycinnamic acid (CHCA) was used as matrix when indicated. The matrix was dissolved in THF at a concentration of 10 mg · ml^{-1}. The complex was dissolved in MeOH (50 mg · l^{-1}). The matrix and the samples were premixed in the ratio 1:1 (matrix:sample) and then the mixture was deposited (1 μl) on the target. For each spectrum 100 laser shots were accumulated. Electrospray ionization mass spectra (ESI-MS) were obtained with an Agilent Technologies mass spectrometer. Typically, a dilute solution of the compound in the indicated solvent (1:99) was

delivered directly to the spectrometer source at 0.01 ml · min^{-1} with a Hamilton microsyringe controlled by a single-syringe infusion pump. The nebulizer tip operated at 3000-3500 V and 250 °C, and nitrogen was both the drying and a nebulizing gas. The cone voltage was 30 V. Quasi-molecular ion peaks [M–H]$^{-}$ (negative ion mode) or sodiated [M + Na]$^{+}$ (positive ion mode) peaks were assigned on the basis of the *m/z* values. Photochemical reactions were performed using a Philips HPL-N 125 W high-pressure mercury lamp, which can be purchased at most commercial lighting stores. Elemental analyses were performed at the *Serveis Tècnics de Recerca* from the *Universitat de Girona* (Spain). High-pressure NMR experiment (HP NMR) was carried out in a 10-mm-diameter sapphire tube with a titanium cap equipped with a Teflon/polycarbonate protection.[36] All catalytic experiments were done by duplicate.

6.4.1 Synthesis of [Zn(L6)$_2$] (ZnL6)
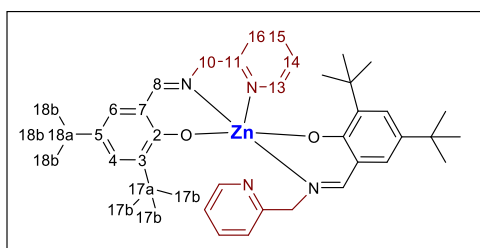
To a solution of ligand **HL6** (400 mg, 1.23 mmol) in MeOH (38 ml), NaOH (49.3 mg, 1.23 mmol) was added. After 10 min stirring, a solution of ZnI$_2$ (196.3 mg, 0.615 mmol) in MeOH (5 ml) was added. The yellow mixture was stirred for 4.5 h at r.t. The resulting solution was dried under vacuum. Cold diethyl ether was added and a white solid appeared and was separated by filtration. The filtrate yellow solution was dried under vacuum, washed with deionized water, filtered off and dried under vacuum to obtain a yellow solid, 357.4 mg (Yield 74 %). The solid was stable kept under nitrogen atmosphere at low temperature. Yellow crystals suitable for X-ray diffraction analyses were obtained by recrystallization of a methanolic solution of the complex.

Anal. Calcd. (found) for C$_{42}$H$_{54}$N$_4$O$_2$Zn: C, 70.82 (69.84); H, 7.64 (7.51); N 7.87 (7.89). ESI (MeOH) calc for C$_{42}$H$_{55}$N$_4$O$_2$Zn m/z: 711.3756 [M+H]$^{+}$, found m/z: 711.3616. UV-vis (MeOH, 4.04·10^{-4} M) λ(nm) (ε, L mol^{-1} cm^{-1}): 338.1 (2228), 394.0 (4824). Selected IR bands (ATR, ν cm^{-1}): 2948 m, 2895 m, 2866 m, 1616 ν(C=N) s, 1527 m, 1432 m, 1411 m, 1329 ν(C-O) m, 1254 m, 1200 m, 1158 s, 1049 m, 834 m,

790 m, 752 m, 636 m. ^{1}HNMR (400MHz, toluene-d$_8$): δ 1.40 (s, 9H, CH$_3$), 1.67 (s, 9H, CH$_3$), 4.15 (d, 1H, CHH, J =16.0 Hz), 4.23(d, 1H, C*H*H, J =16.0 Hz), 6.36 (ddd, 1H, CH$_2$-py, J = 7.4 Hz, J = 5.0 Hz, J = 0.9 Hz), 6.56 (d, 1H, CH 5-py, J = 7.8 Hz), 6.73 (dt, 1H, CH 4-py, J = 7.7 Hz, J = 1.8 Hz), 6.82 (d, 1H, CH 5-phenol, J = 2.7 Hz), 7.59 (d, 1H, CH 3-phenol, J = 2.7 Hz), 7.75 (s, 1H, CH=N), 8.27 (d, 1H, CH 2-py,J = 4.1 Hz); ^{13}CNMR (75.43 MHz, CDCl$_3$): δ 30.1 (CH$_3$, C^{17b}*t*Bu), 31.7 (CH$_3$,C^{18b}*t*Bu), 34.0 (C,C^{17a}*t*Bu), 35.9 (C,C^{18a}*t*Bu), 62.3(C^{10}H$_2$), 118.0(C^2), 121.7 (C^{16}), 122.0 (C^{14}), 129.3 (C^4), 132.9 (C^6), 136.6 (C^3), 141.8 (C^{15}), 148.4 (C^5), 157.0 (C^{11}), 171.1 (C^7), 171.3 (C^8).

General procedure for the synthesis of cyclic carbonates. The catalytic tests were carried out in a 100 ml Berghof or 25 ml Parr reactor, which were previously kept under vacuum 4 h at 100 ºC. After cooling, a solution under inert atmosphere containing the catalyst dissolved in net distilled substrate and the co-catalyst, when indicated, was injected into the reactor. The autoclave was pressurized with CO$_2$ and then heated to the desired temperature to reach the final pressure. After the reaction time, the reactor was cooled down with an ice bath and slowly depressurized through a dichloromethane trap. The % conversion was determined by ^{1}H NMR of the crude mixture by integral ratio between alkene oxide and cyclic carbonate. The work-up was as follow depending on the substrate. All catalytic reactions were carried out in duplicate.

Typical procedure for styrene oxide, propylene oxide, 1,2-epoxyhexane, 1,2-epoxydodecane and epichlorohydrin. Purification in the case of the styrene carbonate was performed by extraction with hexane to remove the styrene oxide. The remaining solid was evaporated and diluted in CH$_2$Cl$_2$ and passed through a silica pad to remove the catalyst. The dichloromethane solution was evaporated to obtain the NMR spectroscopically pure styrene carbonate as a white solid. The purification of propylene carbonate was performed removing the propylene epoxide by vacuum evaporation and the remaining oily residue was diluted in dichloromethane and passed through a silica pad to remove the catalyst.

Typical procedure for cyclohexene oxide. The final crude was dissolved in dichloromethane, the solvent was evaporated and the residue dried in vacuum at 100 ° C for 3 hours to remove excess of cyclohexene oxide and subsequently it was analyzed by ^{1}H NMR spectroscopy. % *cis/trans* cyclic cyclohexylcarbonate ratio was calculated from the integral ratio between the –CH- signals of the *cis*-isomer (δ = 4.63 ppm) and the *trans*- isomer (δ = 3.90 ppm).

HP NMR experiments. The HP NMR tube was filled under N_2 with the mixture of **ZnL6** (0.15 mmol), TBAB (0.15 mmol) and toluene-d$_8$ (1.8 ml). The tube was pressurised to 10 atm of CO_2 and heated to 60 ºC. The ^{1}H NMR spectra were then recorded.

6.4.2 X-ray crystallography

Diffraction data for the structures reported were carried out on a Smart CCD 1000 Bruker diffractometer system with Mo Kα radiation (λ = 0.71073 Å). Cell refinement, indexing and scaling of the data sets were carried out using programs Bruker Smart and Bruker Saint. Crystallographic data is collected in Table 6.5.

The structure was solved by *SIR97*[37] and refined by *Shelxl9*[38] and the molecular graphics with ORTEP-3 *for Windows*.[39] All the calculations were performed using the *WinGX* publication routines.[40]

Table 6.5. Crystallographic data and details of structure refinement for compound **ZnL6**.

	ZnL6
Molecular formula	$C_{42}H_{54}N_4O_2Zn$
Molecular weight	712.26
Crystal system	Triclinic
Space group	$P\bar{1}$
Shape and colour	Plate, orange
Temp. (K)	100(2)
Radiation (λ, Å)	Mo Kα (λ=0.7107 Å)
a (Å)	11.864(2)
b (Å)	13.096(2)
c (Å)	13.124(2)
α (º)	102.491(5)
β (º)	101.466(5)
γ (º)	104.404(5)
Volume (Å3)	1943.0(6)
Z	2
Dx (Mg·m-3)	1.217
F (000)	760
Crystal dimensions (mm)	0.20 x 0.20 x 0.05
μ (Mo Kα) (mm-1)	0.671
θmax (º)	25.35
Reflections collected	18243
Unique reflections	6853
Rint.	0.0429
Observed [$I > 2\sigma(I)$]	5411
Parameters	454
R1 [$I > 2\sigma(I)$]	0.0484
wR2	0.0673
$\Delta\rho$ (e/ Å3)	0.972 -0.642

6.5 *Supporting information available*

An example of ^{1}H NMR of crude reaction with the different epoxides used, ^{1}H NMR, MALDI-TOF and GPC of the copolymers are available in the supporting information CD.

6.6 References

[1] Inoue, S.; Koinuma, H. and Tsuruta, T. *J. Polym.Sci., Polym.Lett.B.* **1969**, *7*, 287-292.

[2] English, N. J.; El-Hendawy, M. M.; Mooney, D. A.; MacElroy, J. M. D., *Coord. Chem. Rev.* **2014**, *269*, 85-95.

[3] Darensbourg, D. J.; Holtcamp, M. W. *Coord. Chem. Rev.* **1996**, *153*, 155-174.

[4] (a) Darensbourg, D. J.; Holtcamp, M. W., *Macromolecules* **1995**, *28*, 7577-7579. b) Darensbourg, D. J.; Holtcamp, M. W.; Struck, G. E.; Zimmer, M. S.; Niezgoda, S. A.; Rainey, P.; Robertson, J. B.; Draper, J. D.; Reibenspies, J. H.; *J. Am. Chem. Soc.* **1999**, *121*, 107-116. c) Darensbourg, D. J.; Wildeson, J. R.; Yarbrough, J. C.; Reibenspies, J. H.; *J. Am. Chem. Soc.* **2000**, *122*, 12487-12496. d) Dinger, M. B.; Scott, M. J., *Inorg. Chem.* **2001**, *40*, 1029-1036.

[5] a) Kim, H. S.; Kim, J. J.; Lee, B. G.; Jung, O. S.; Jang, H. G.; Kang, S. O., *Ang. Chem. Int. Ed.,* **2000**, *39*, 4096-4098. b) Kim, H. S.; Kim, J. J.; Lee, S. D.; Lah, M. S.; Moon, D.; Jang, H. G., *Chem. Eur. J.*, **2003**, *9*, 678-686.

[6] a) Cheng, M.; Lobkovsky, E. B.; Coates, G. W. J. Am. Chem. Soc. **1998**, 120, 11018-11019. b) Cheng, M.; Moore, D. R.; Reczek, J. J.; Chamberlain, B. M.; Lobkovsky, B. W.; Coates, G. W. J. Am. Chem. Soc. **2001**, 123, 8738-8749. c) D. R. Moore, M. Cheng, E. B. Lobkovsky, G. W. Coates, *Angew. Chem. Int. Ed.* **2002**, *41*, 2599-2602.

[7] Lee, B. Y.; Kwon, H. Y.; Lee, S. Y.; Na, S. J.; Han, S. I.; Yun, H. S.; Lee, H.; Park, Y. W., *J. Am. Chem. Soc.* **2005**, *127*, 3031-3037.

[8] Kember, M. R.; Knight, P. D.; Reung, P. T. R.; Williams, C. K., *Angew. Chem., Int. Ed.* **2009**, *48*, 931-933.

[9] a) Decortes, A.; Martínez Belmonte, M.; Benet-Buchholza, J.; Kleij, A. W.; *Chem. Commun.* **2010**, *46*, 4580-4582; b) Decortes, A.; Kleij, A. W., *ChemCatChem* **2011**, *3*, 831-834. c) Taherimehr, M.; Decortes, A.; Al-Amsyar, S. M.; Lueangchaichaweng, W.; Whiteoak, C. J.; Escudero-Adán, E. C.; Kleij, A. W.; Pescarmona, P. P., *Catal. Sci. Technol.* **2012**, *2*, 2231-2237.

10   Fuchs, M. A.; Staudt, S.; Altesleben, C.; Walter, O.; Zevaco, T. A.; Dinjus, E., *Dalton Trans.* **2014**, *43*, 2344-2347.

11   Wang, Z.; Bu, Z.; Cao, T.; Ren, T.; Yang, L.; Li, W., *Polyhedron* **2012**, *32*, 86-89.

12   Babu, H. V.; Muralidharan, K., *Dalton Trans.* **2013**, *42*, 1238-1248.

13   Chen, T.-Y.; Li, C.-Y.; Tsai, C.-Y.; Li, C.-H.; Chang, C.-H.; Ko, B.-T.; Chang, C.-Y.; Lin, C.-H.; Huang, H.-Y., *J. Organomet. Chem.* **2014**, *754*, 16-25.

14   Darensbourg, D.; Rainey, P. and Yarbrough, J. *Inorg. Chem.* **2001**, *40*, 986-993.

15   Mitchell, J.M. and Finney, N. S. *J. Am. Chem. Soc.* **2001**, *123*, 862-869.

16   Cameron, P.A.; Gibson, V.C.; Redshaw, C.; Segal, J.A.; White, A.J.P. and Williams, D.J. *J. Chem. Soc., Dalton Trans.* **2002**, 415-422.

17   Cameron, P.A.; Gibson, V.C.; Redshaw, C.; Segal, J.A.; Bruce, M.D.; White, A.J.P. and Williams, D.J. *Chem. Commun.* **1999**, 1883-1884.

18   Darensbourg, D.J.; Choi, W. and Richers C.P. *Macromolecules* **2007**, *40*, 3521-3523.

19   Darensbourg, D.J.; Choi, W.; Karroonnirun, O. and Bhuvanesh, N. *Macromolecules* **2008**, *41*, 3493-3502.

20   a) Sheng, N., *ActaCryst.* **2009**, *E65*, m1295. b) Trösch, A.; Vahrenkamp, H.; *Z. Anorg. Allg. Chem.* **2004**, *630*, 2031-2034, c) Huang, H.-W., *Acta Cryst.* **2011**, E67, m313   d) You, Z.-L., *Acta Cryst.* **2005**, *C61*, m456-m458, e) Orio, M.; Philouze, C.; Jarjayes, O.; Neese, F.; Thomas, F.; *Inorg. Chem.* **2010**, *49*, 646-658. f) Gallaway, J. B. L.; McRae, J. R. K.; Decken, A.; Shaver, M. P.; *Can. J. Chem.* **2012**, *90*, 419-426. g) Maheswari, P. U.; Barends, S.; Özalp-Yaman, S.; de Hoog, P.; Casellas, H.; Teat, S. J.; Massera, C.; Lutz, M.; Spek, A. L., van Wezel, G. P.; Gamez, P.; Reedijk, J., *Chem. Eur. J.* **2007**, *13*, 5213-5222; h) Zhang, C.; Wang, Z.-X., *J.Organomet. Chem.* **2008**, *693*, 3151-3158.

21   Darensbourg, D. J., *Adv. Polym. Sci.* **2012**, *245*, 1-28.

22   Tsai, C.-Y.; Huang, B.H.; Hsiao, M.-W.; Lin, C.-C.; Ko, B.-T.; *Inorg. Chem.* **2014**, *53*, 5109-5116.

23 Iksi, S.; Aghmiz, A.; Rivas, R.; Gonzalez, M. D.; Cuesta-Aluja, L.; Castilla, J.; Orejon, A.; El Guemmout, F.; Masdeu-Bulto, A. M., *J. Mol. Catal. A: Chem.* **2014**, *383-384*, 143-152.

24 Pearson, R. G., *J. Chem. Ed.* **1965**, *41*, 581-587.

25 Pescarmona, P. P.; Taherimehr, M., *Catal.Sci. Technol.* **2012**, *2*, 2169-2187.

26 a) Sun, J.; Fujita, S.-I.; Zhao, F.; Arai, M., *Appl. Catal. A: General* **2005**, *287*, 221-226; b) Chen, T.-Y.; Li, C.-Y.; Tsai, C.-Y.; Li, C.-H.; Chang, C.- H.; Ko, B.-T.; Chang, C.-Y.; Lin, C.-H.; Huang, H.-Y., *J. Organomet. Chem.* **2014**, *754*, 16-25.

27 Allard, M. M.; Xavier, F. R.; Heeg, M. J.; Schlegel, H. B.; Verani, C. N., *Eur. J. Inorg. Chem.* **2012**, 4622-4631.

28 Imbert, C.; Hratchian, H. P.; Lanznaster, M.; Heeg, M. J.; Hryhorczuk, L. M.; McGarvey, B. R.; Schlegel, H. B.; Verani, C. N.; *Inorg. Chem.* **2005**, *44*, 7414-7422.

29 Addison, A. W.; Rao, T. N.; Reedijk, J.; van Rijn, J.; Verschoor, G. C.; *J. Chem. Soc. Dalton Trans.* **1984**, 1349-1356.

30 Zhou, X.; Zhang, Y.; Yang, X.; Yao, J.; Wang, G., *Chin. J. Chem.* **2010**, *31*, 765-768.

31 Langanke, J.; Greiner, L.; Leitner, W., *Green Chem.* **2013**, *15*, 1173-1182.

32 a) Darensbourg, D. J.; Holtcamp, M. W.; Khandelwal, B.; Klausmeyer, K. K.; Reibenspies, J. H., *J. Am. Chem. Soc.* **1995**, *117*, 538-539; b) Darensbourg, D. J.; Niezgoda, S. A.; Holtcamp, M. W.; Draper, J. D.; Reibenspies, J. H., *Inorg. Chem.* **1997**, *36*, 2426-2432.

33 a) Sun, J.; Fujita, S.-I.; Zhao, F.; Arai, M., *Appl. Catal. A: General* **2005**, *287*, 221-226; b) Chen, T.-Y.; Li, C.-Y.; Tsai, C.-Y.; Li, C.-H.; Chang, C.- H.; Ko, B.-T.; Chang, C.-Y.; Lin, C.-H.; Huang, H.-Y., *J. Organomet. Chem.* **2014**, *754*, 16-25.

34 Kisch, H.; Millini, R.; Wang, I.-J., *Chem. Ber.* **1986**, *119*, 1090-1094.

35 Doll, K. M.; Erhan, S. Z., *J. Agric. Food Chem.* **2005,** *53*, 9608-9614.

36   Cusanelli, A.; Frey, U.; Richens, D. T.; Merbach, A., *J. Am. Chem. Soc.* **1996**, *118*, 5265-5271.

37   Altomare, A.; Burla, M. C.; Camalli, M.; Cascarano, G. L.; Giacovazzo, C.; Guagliardi, A.; Moliterni, A. G. G.; Polidori, G.; Spagna, R., *J. Appl. Cryst.* **1999**, *32*, 115-119.

38   Sheldrick, G. M., **1997**. SHELXS97 and SHELXL97.University of Göttingen, Germany.

39   Ortep-3 for Windows - A Version of ORTEP-III with a Graphical User Interface (GUI). Farrugia, L. J., *J. Appl. Crystallogr.* **1997**, *30*, 565-566.

40   WinGX Suite for Single Crystal Small Molecule Crystallography. Farrugia, L. J., *J. Appl. Cryst.* **1999**, *32*, 837-838.

From alkenes to valuable organic carbonates using low-toxic and easy-to-handle Fe(III)-NN'O Schiff-based catalysts

Abstract

*Environmental friendly Fe(III) complexes with tridentate NN'O-donor base Schiff ligands combined with TBAB are active for selective formation of cyclic carbonates with terminal epoxides as well as with most hindered cyclohexene oxide and methyl epoxyoletate substrates. Using PPNCl as co-catalyst, mixtures of cyclohexene carbonate and poly(cyclohexene carbonate) were achieved in the CHO/CO$_2$ coupling. These Fe(III) catalysts were found also to be active for the epoxidation of alkenes obtaining the best results when TBHP (5.5 M in decane) was used as oxidant. The preliminary study of the direct oxidative carboxylation of styrene towards styrene carbonate using **FeL8**/TBAB catalytic system and scCO$_2$ is promising although low yields of styrene carbonate were obtained.*
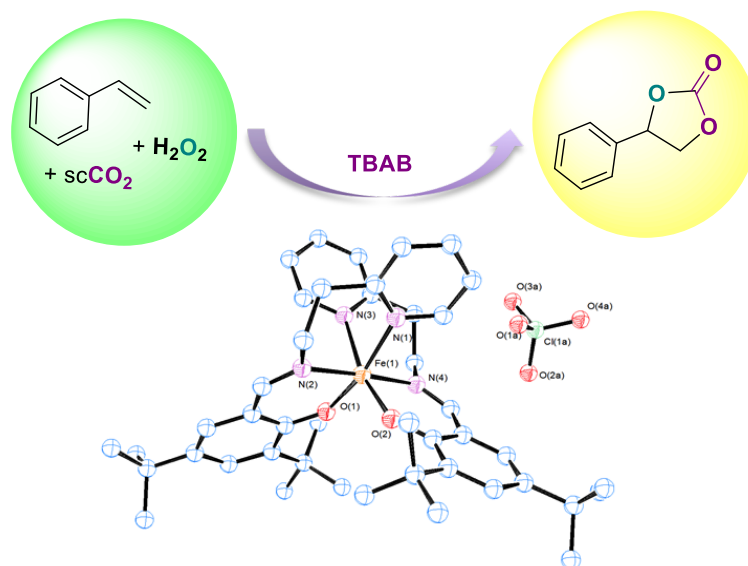
7.1   Introduction

As we have seen during the course of this Thesis, we have developed quite efficient catalytic systems for the preparation of organic carbonates. However, such reaction requires the initial synthesis of an epoxide; an additional step that sometimes involves expensive or toxic reagents and requires chemical separations.[1] A safe, energy efficient and even cheaper approach would be the direct synthesis of cyclic carbonates starting from olefins by reaction with an oxidant and CO_2. This three-component coupling, also called oxidative-carboxylation of olefins, has no received so much attention since it was introduced in 1962,[2] and only a few reports are available in the literature.[3,4,5,6] However, low selectivity towards the carbonates, formation of numerous oxidation by-products and long reaction times were often the major problems of this reaction.[7] Additionally, stability of the catalysts under the oxidizing environment and high temperature and pressure conditions are very important factors when choosing a catalyst. The ideal metal complexes for this reaction are on the first row transition elements, such manganese and iron being the best options. But particularly, iron possesses the advantage of being non-toxic, widely available and cost effective. Therefore, due to these characteristics and the variable redox chemistry, iron-based complexes may be good options since they seem to be active both in olefin oxidation and also in carbonate formation with CO_2, separately.

Although iron based catalysts have been extensively used in epoxidation reactions, few examples for the CO_2 and epoxide coupling to provide either cyclic carbonate or polycarbonate have been reported to date (See Chapter 1).[8] Kleij and co-workers developed a new iron(III) catalyst based in amine triphenolate ligand (**13a**, Figure 1.7, Chapter 1),[9,10,11,12] which were active catalysts, with a suitable co-catalyst, to obtain cyclic carbonate products for a wide scope of substrates even when internal epoxides such as cyclohexene oxide and oxetanes were used. Most recently, the same group reported an analogous iron(III) catalyst bearing a pyridylamine-bis(phenolate) ligand (**14**, Figure 1.7, Chapter 1), which was also highly versatile in the conversion of a broad scope of substrates. Particularly, with terminal epoxides the cyclic carbonate was the main product, whereas with cyclohexene oxide and vinylcyclohexene oxide as substrates, it was also possible to selectively obtain polycarbonates with high percentage incorporation of carbonate linkages.[13]

In this chapter, we present an investigation about iron(III) complexes bearing tridentate NN'O-donor base Schiff ligands, **HL6** and **HL8** (Figure 7.1) as novel homogeneous catalysts for the epoxidation of olefins and the subsequent coupling reaction with CO_2 for carbonate formation. Iron(III) complexes with **HL6** may lead to more stable catalytic systems than **ZnL6**, since they stabilize higher coordination number complexes. Ligand **HL8** differed from **HL6** as it has an ethylene fragment between the pyridine and the imine functionalities instead than a methylene. This may confer more flexibility to the active center. Analogous chromium(III) complexes were previously investigated by our group in the coupling of CO_2 and epoxides.[14] Manganese(III) complexes with **HL6** were active catalysts in the epoxidation of alkenes,[15] but these were not active for the coupling of CO_2 and epoxides.[16] Moreover, we also present a preliminary study involving the direct oxidative-carboxylation of styrene towards styrene carbonate using iron(III) complex/TBAB catalytic system based in the reported methodology used results obtained by Arai and co-workers.[4]

The best advantage of these iron(III) complexes is that they could be obtained in quantitative yields in an only two-step procedure, the synthesis of the ligand and the complexation of the iron(III) precursor. They have also the added value, with respect to Zn(II) complexes, to be very robust in the presence of air and moisture as they did not require any inert conditions for handling and storage.

7.2 Results and discussion

7.2.1 Synthesis of Iron(III) complexes

The tridentate Schiff base ligands **HL6** and **HL8** shown in Figure 7.1, were synthetized following the described procedures by Williams and co-workers involving the condensation of 2-(aminomethyl)pyridine or 2-(aminoethyl)pyridine with 3,5-di-*tert*-butylsalicylaldehyde.[17] Iron(III) complexes iron were synthetized to assess the influence of the length in the pyridine arm in the ligand rigidity. It was reported that treatment of **HL6** ligand with hydrated ferric perchlorate lead to complex [Fe(**L6**)$_2$][ClO$_4$] (**FeL6** in which one iron(III) is surrounded by two tridentate ligands.[18]
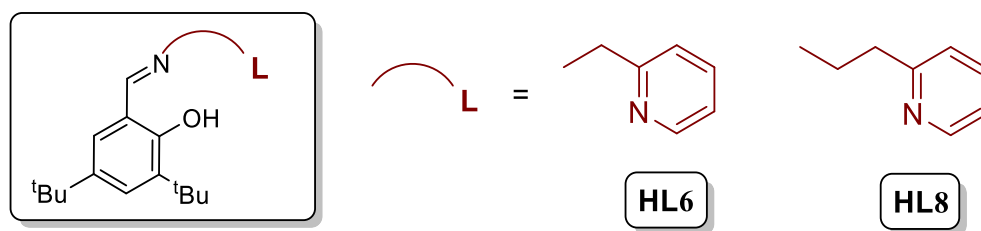
Figure 7.1. Ligands **HL6** and **HL8**.

HL8 and **FeL8** were, then, synthetized and characterized as reported in the literature (Scheme 7.1). It should be noted that the synthesis and characterization of a similar complex to **FeL8**, without *tert*-butyl substituents in the phenyl group, was also reported in the literature. Nevertheless, these iron(III) complexes were never used as catalysts in carbonate synthesis nor epoxidation reaction.[19]
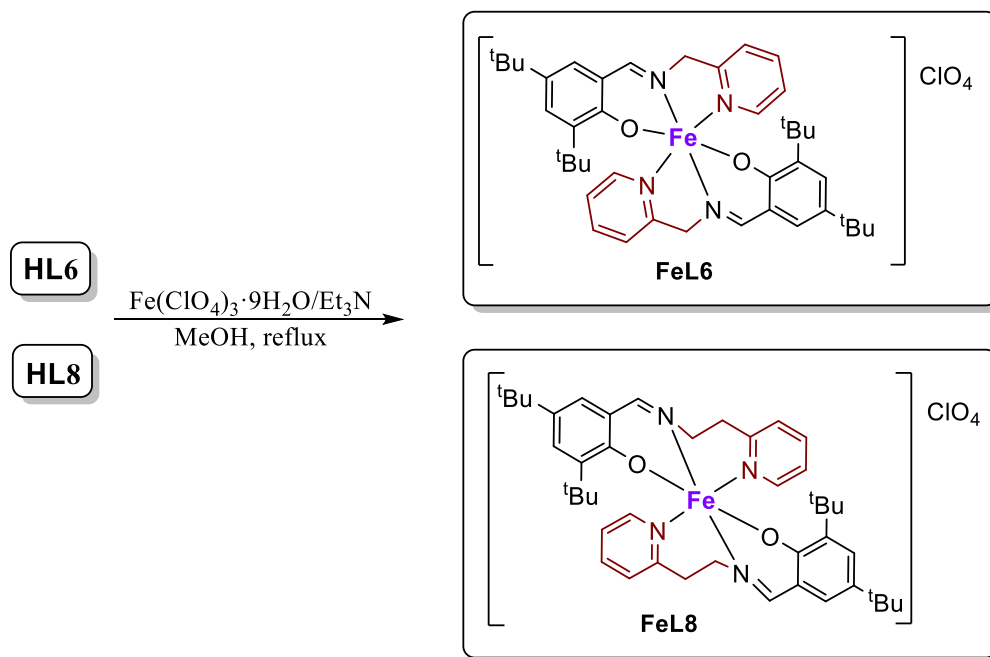
Scheme 7.1. Preparation of monometallic iron(III) complexes with **HL6** and **HL8** tridentate ligands.

Good elemental analysis was obtained for **FeL8**, which agrees with [Fe(**L8**)$_2$][ClO$_4$]. ESI mass spectrometry in the positive mode in methanol gave a well-defined peak corresponding to mononuclear fragment [Fe(**L8**)$_2$]$^+$. The infrared spectral data of **FeL8** complex showed weak bands at 2870-2950 cm^{-1}, which were attributed to ν(C-H) stretching vibration from *tert*butyl groups. The **HL8** ligand showed a strong

peak at 1631 cm^{-1} attributed to azomethine stretching vibration ν(C=N) that shifted to lower frequencies, 1601 cm^{-1} upon coordination. In addition, the absence of a strong absorption at the ν(O-H) region (*ca* 3600 cm^{-1}) pointed to the coordination by both phenolate fragments. The ring skeletal vibration of ν(C=C) appears in the range 1552-1413 cm^{-1} and the phenolate ν(C-O) stretching vibrations appeared around 1250 cm^{-1} all of them at lower vibration frequency with respect of free ligand.[19] A single band assigned to the perchlorate counterion, ν(ClO$_4$), was found at 1085 cm^{-1} confirming its non-coordinating behaviour.[20] The molar conductivity value of **FeL8** (164.9 Ω^{-1}·cm^2·mol^{-1} in acetonitrile) is indicative of 1:1 electrolyte.[21] Magnetic susceptibility measurement was recorded at room temperature and gave μ_{eff} of 6.03 μ_B that was in good agreement with magnetic susceptibility values of paramagnetic iron(III) complexes (5.7-6.0 μ_B).[8]

The electronic spectra of **HL8** and **FeL8** were measured in acetonitrile to compare differences between the reported **HL6** and **FeL6** (Table 7.1). Both **HL6** and **HL8** presented intraligand $\pi \rightarrow \pi^*$ bands at *ca* 260 nm, attributed to pyridine and phenolate moieties.[22] Another band attributed to the imine group is observed at *ca* 330 nm . The electronic spectra of iron(III) complexes show in both cases two different absorptions at 344, 582 nm and 343, 573nm for **FeL6** and **FeL8**, respectively. Transitions p$\pi_{\text{phenolate}} \rightarrow$ d$\pi^*_{\text{iron(III)}}$ are associated to the band at 573 and 582 nm, whereas the higher-energy absorption band at 343 and 344 nm are attributed to a p$\pi_{\text{phenolate}} \rightarrow$ d$\sigma^*_{\text{iron(III)}}$ ligand-to-metal charge transfer (LMCT).[23]

Table 7.1. UV-Visible Data for tridentate ligands and iron(III) complexes

	λ (nm)/ ε (L mol^{-1}cm^{-1})	Reference
[a]**HL6**	264 (17000); 332 (4500)	18
HL8	262 (26185); 326 (21105)	This work
[b]**FeL6**	278 (39700); 344 (12500); 582 (4400)	18
[b]**FeL8**	241.0 (24484); 343 (4060); 573 (944)	This work

[a]1.0 10^{-4} M in dichloromethane; [b]2.5 10^{-5} M in acetonitrile.

Single crystals of **FeL8** suitable for a structure determination were obtained by slow evaporation of a hexane/diethylether solution standing at room temperature. The

ORTEP diagram is shown in Figure 7.2 and selected bond lengths and angles are listed in Table 7.2. X-ray analysis showed that **FeL8** consisted in a monometallic molecule composed of an iron(III) ion surrounded by two deprotonated ligands in a 6-coordinated environment (Figure 7.2). As in the structure of complex **FeL6** reported by Verani *et al*.,[18] both tridentate ligands were meridionally coordinated through the iron(III) center forming a pseudo-octahedral geometry. As well as, bond distances and angles are in agreement with **FeL6** and similar Fe(III) complexes.[18,24] The Fe-N(imine) (2.121(2) and 2.110(2) Å), Fe-N(pyridine) (2.255(2) and 2.249(2) Å) and Fe-O(phenolate) (1.9083(18) and 1.9044(17) Å) bond distances are in agreement with high-spin iron(III) ion (See **FeL1** example in Chapter 3).[25,26,27] The meridional coordination of each ligand leads to a *cis* orientation of the two pyridines with an N3-Fe1-N1 angle of 81.61(8)°. Similarly, the two phenolate rings are *cis* to each other with an O2-Fe1-O1 angle of 102.73(8)°. The trans imine nitrogen atoms had an N4-Fe1-N2 angle of 176.59(8)°. The non-coordinated perchlorate ion is also present.
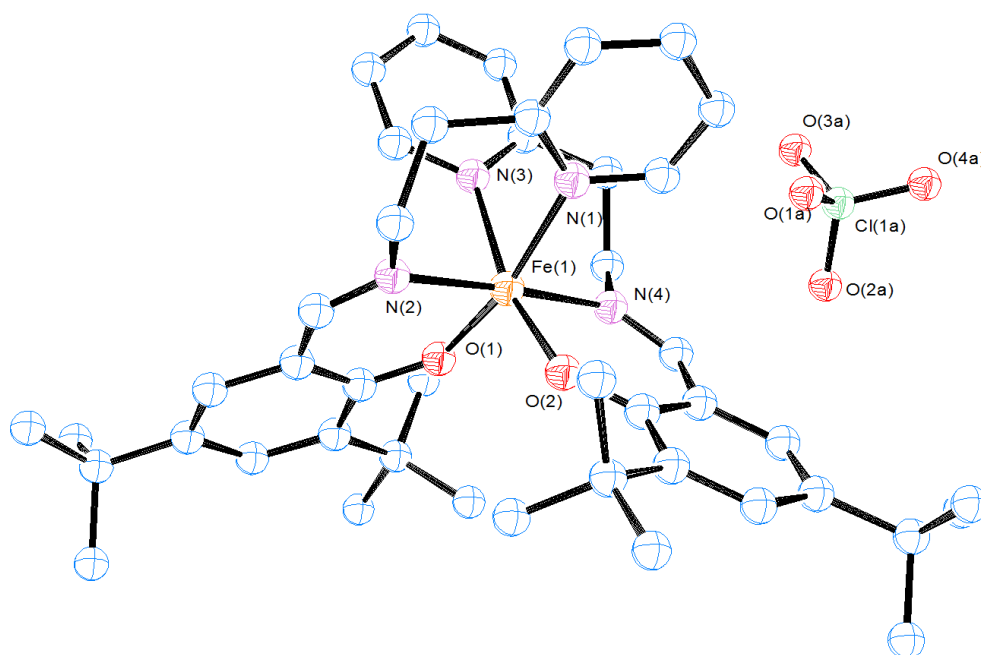
Figure 7.2. ORTEP drawing of complex of **FeL8**. All hydrogen atoms and solvent molecules are omitted for clarity. Thermal ellipsoids drawn at the 50 % probability level.

Table 7.2. Selected bond lengths (Å) and angles (°) for **FeL8**.

Fe1-O2	1.9044(17)	Fe1-N2	2.121(2)
Fe1-O1	1.9083(18)	Fe1-N3	2.249(2)
Fe1-N4	2.110(2)	Fe1-N1	2.255(2)
O2-Fe1-O1	102.73(8)	O2-Fe1-N4	86.37(8)
O1-Fe1-N4	90.29(8)	O2-Fe1-N2	93.02(8)
O1-Fe1-N2	86.57(8)	N4-Fe1-N2	176.59(8)
O2-Fe1-N3	166.01(8)	O1-Fe1-N3	89.83(8)
N4-Fe1-N3	87.43(8)	N2-Fe1-N3	93.89(8)
O2-Fe1-N1	86.56(8)	O1-Fe1-N1	169.17(8)
N4-Fe1-N1	95.90(8)	N2-Fe1-N1	87.41(8)
N3-Fe1-N1	81.61(8)		

7.2.2 Catalytic results

7.2.2.1 *Coupling of epoxides to CO_2*

Initially, we studied the catalytic activity of **FeL6** in the cycloaddition of CO_2 to organic epoxides using styrene oxide as a model substrate under initial conditions (50 bar, 80 ºC, 24 h) shown in Scheme 7.2. The effect of the catalyst, co-catalyst, co-catalyst/catalyst ratio and reaction time were studied and then optimized. The scope with different epoxides using **FeL8**/TBAB catalytic system was then studied. Since both iron(III) complexes and TBAB are soluble in the selected neat epoxides, the catalytic coupling required no organic co-solvent.
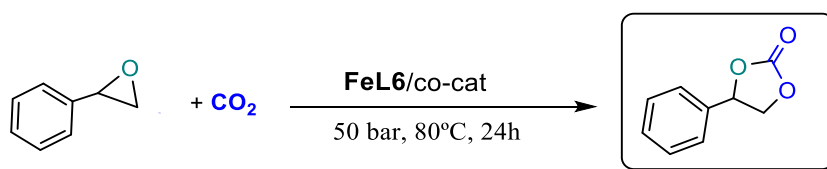
Scheme 7.2. Cycloaddition of styrene oxide and CO_2 using **FeL6** as catalyst.

Firstly, the effect of adding a co-catalyst in the catalytic system was studied using 0.2 mol % of **FeL6** and 0.4 mol % of co-catalyst in neat styrene oxide. These results are graphically represented in Figure 7.3. Catalyst **FeL6** alone showed no

activity towards the CO_2 cycloaddition to epoxides at these conditions confirming that the absence of a nucleophile precludes the ring opening of the epoxide. This was confirmed by using the binary **FeL6**/PPNCl catalytic system in the same reaction. At these conditions a high conversion of styrene oxide (74 %) with total selectivity towards the cyclic carbonate was achieved. Changing the co-catalyst to tetrabutylammonium bromide an enhancement on the catalytic activity was observed obtaining complete conversion of the epoxide with a TOF of 21 h^{-1}. The synergistic effect of combining the Lewis acid iron(III) catalyst with TBAB onium salt co-catalyst was confirmed with the blank experiment using TBAB as catalyst at the same conditions, where only a 18 % of styrene oxide conversion was achieved. It's not surprising that TBAB showed a moderate conversion as it is known that onium salts were active towards this reaction.[28,29]
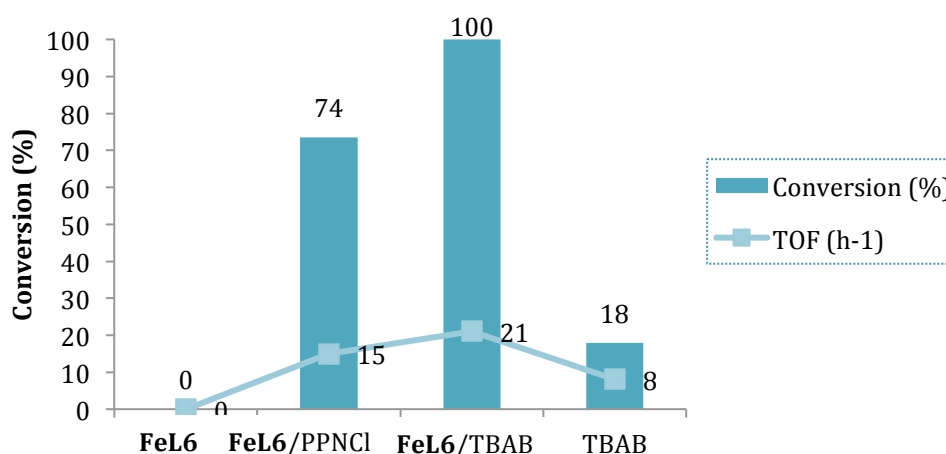
Figure 7.3. Co-catalyst effect on the coupling of styrene oxide and CO_2 using **FeL6** as catalyst. Reaction conditions: catalyst 0.2 mol %, co-catalyst 0.4 mol %, temp. = 80 °C. P_{CO2} = 50 bar, time = 24 h.

With the optimized **FeL6**/TBAB binary catalytic system the conversion of styrene oxide was monitored along reaction time to assess when the reaction was completed. To perform this experiment four batch catalytic runs using always the same reactor set ups were used. The catalytic results are represented in Figure 7.4. The reaction needed at least 3 h to reach > 80 % styrene oxide conversion (averaged TOF 129 h^{-1}) and at 6 h, 97 % of styrene carbonate as a single product according to ^{1}H NMR was already achieved.
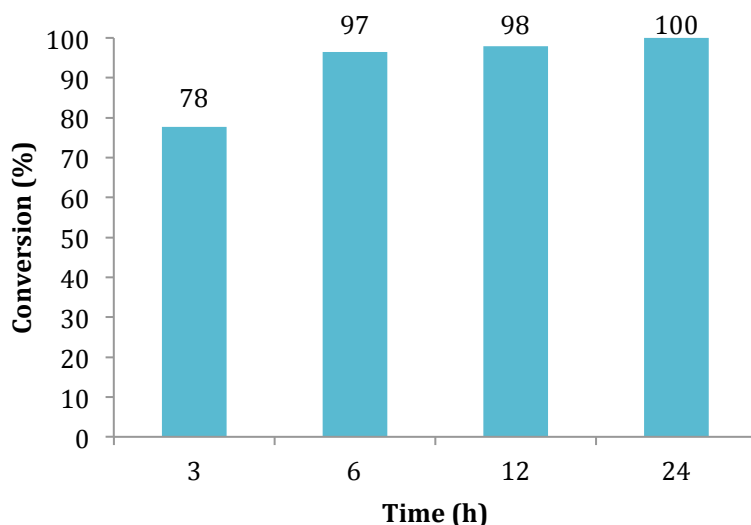
Figure 7.4. Coupling of styrene oxide and CO_2 along over time using **FeL6**/TBAB catalytic system. Reaction conditions: catalyst 0.2 mol %, co-catalyst 0.4 mol %, temp. = 80 ºC. P_{CO2} = 50 bar

At the optimized time of 3 h (entry 1, Table 7.3), increasing the co-catalyst loading up to 1.0 mol % (co-catalyst/catalyst molar ratio = 5) an enhancement in the catalytic activity was observed (97 % conversion, entry 2, Table 7.3). At the optimized co-catalyst/catalyst ratio of 5 we further optimized reaction time and catalyst loading to evaluate the initial maximum TOF. Decreasing the reaction time to 1 h the TOF was 190 h^{-1} (entry 3, Table 7.3). Lowering the catalyst/co-catalyst concentration to 0.1/0.5 mol % the TOF was 270 h^{-1} (entry 4, Table 7.3). A further decrease of the catalyst/co-catalyst concentration to 0.05/0.25 mol % the initial TOF of 401 h^{-1} at 29 % conversion (entry 5, Table 7.3).

With the reaction conditions optimized, we studied the catalytic activity of **FeL8**. As expected, **FeL8** showed very low catalytic activity without the addition of a co-catalyst (entry 6, Table 7.3). Adding TBAB, the conversion to styrene carbonate reached a 29 % (TOF 580 h^{-1}, entry 7, Table 7.3). The higher activity of **FeL8**/TBAB with respect to **FeL6**/TBAB and even **ZnL6**/TBAB may be related with the more flexible structure of the first, which may favor the dissociation of the pyridine fragment to allow the epoxide coordination. In all those complexes, the ability of the pyridine group to act as a pendant arm could replace the growing chain and consecutively favor the backbiting mechanism yielding the cyclic carbonate. With this catalytic system a

maximum TOF of 900 h^{-1} was obtained at a catalyst/co-catalyst loading of 0.025/0.125 mol % in 0.5 h of reaction time. (entry 4, Table 7.3).

Table 7.3. Cycloaddition of styrene oxide and CO_2 catalyzed by iron(III)-systems.[a]

Entry	Cat	Co-cat	Time (h)	Cat/Co-cat (mol %)[b]	Conv (%)[c,d]	TOF (h^{-1})[e]	Y (%)[f]
1	**FeL6**	TBAB	3	0.2/0.4	78	129	n.d.
2	**FeL6**	TBAB	3	0.2/1.0	97	162	n.d.
3	**FeL6**	TBAB	1	0.2/1.0	38	190	21
4	**FeL6**	TBAB	1	0.1/0.5	27	270	16
5	**FeL6**	TBAB	1	0.05/0.25	20	401	15
6	**FeL8**	-	24	0.2/-	6	1	n.d.
7	**FeL8**	TBAB	1	0.05/0.25	29	580	21
8	**FeL8**	TBAB	0.5	0.025/0.125	12	900	11

[a]Reaction conditions: T = 80 ºC, P_{CO2} = 50 bar, styrene oxide: 43.8 mmol (5 ml); [b]mol % respect to the substrate; [c]measured by ^{1}H NMR; [d]Selectivity for the cyclic carbonate product >99 % [e]averaged TOF (mol substrate converted·(mol catalyst)$^{-1}$·h^{-1}; [f]Isolated product by flash chromatography.

Iron(III) catalyst based in amine triphenolate ligand developed by Kleij *et al.* was found to be also active for styrene carbonate formation in conjunction of TBAB co-catalyst.[9] They were able to obtain high conversion (91 %) and high SC yield (87 %) at milder conditions (room temperature and 20 bar of CO_2). Nevertheless, higher amount of TBAB (5 mol %) was added with a catalyst/co-catalyst molar ratio of 1/10.

To find out the applicability of **FeL8** catalyst we performed a screening using a range of commercially available epoxides. The cycloaddition reactions with CO_2 were carried out under the optimized conditions of 80 ºC, 50 bar of CO_2, catalyst/co-catalyst concentration of 0.025/0.125 mol % and during 0.5 h (Scheme 7.3). The results are listed in Table 7.4. Yields were estimated by ^{1}H NMR using mesitylene as an internal standard.
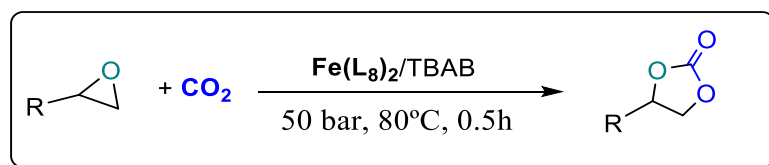
Scheme 7.3. General scheme of the cycloaddition reaction with epoxides and CO_2.

Table 7.4. Cycloaddition of CO_2 with different epoxides using catalytic system **FeL8**/TBAB.[a]

Entry	Epoxide	Product	Conv (%)[b]	Selectivity (%)[c]	TOF (h^{-1})[d]	Yield (%)[e]
1			21	>99	1639	12
2			4	>99	299	3
3			2	>99	160	1
4			18	>99	1404	11
5			46	>99	3640	44
6[f]			95	>99 (cis/trans: 33/67)	2	85

[a]Reaction conditions: T = 80 °C; P_{CO_2} = 50 bar; time = 0.5 h epoxide: 3 ml; catalyst: 0.025 mol%; TBAB: 0.125 mol% [b]measured by ^{1}H NMR; [c]Selectivity for the cyclic carbonate product >99 % [d]averaged TOF (mol substrate converted·(mol catalyst)$^{-1}$·h^{-1}; [e]Yield of carbonate product determined by ^{1}H NMR using mesitylene as the internal standard; [f]cat/co-cat: 2 mol %/2 mol %; T = 100 °C; P_{CO2} = 100 bar, 24h.

All of these different substrates were efficiently converted into the corresponding cyclic carbonate, with a selectivity of > 99 %. Under the selected conditions propylene oxide was found to be more active than styrene oxide with a conversion up to 21 % with an initial TOF of 1639 h^{-1} (entry 1, Table 7.4). Almost no conversion was observed using largest linear epoxides such as 1,2-epoxyhexane and 1,2-epoxytetradecane (entries 2 and 3, Table 7.4). This suggests probably an unfavorable competition between coordination of the epoxide and decoordination of the pyridine ligand moiety at the iron(III) center.

The other monosubstituted epoxides like epichlorohydrine and glycidol produced also the desired cyclic carbonates and showed quantitative conversions (TOF of 1404 and 3640 h^{-1}) (entries 4 and 5, Table 7.4). These results indicated the good versatility of the catalytic system with functionalized epoxides such as glycidol and also styrene oxide with which presented the highest catalytic activities.

Concerning the copolymerization reaction of CO_2 with cyclohexene oxide using **FeL8** as catalyst, the reactions were conducted in neat CHO, at conditions of 80 ºC, 50 bar of carbon dioxide during 24 h.[30] The results are listed in Table 7.5. As expected, **FeL8** alone showed no catalytic activity neither to cyclic carbonate nor polycarbonate (entry 1, Table 7.5). The addition of a bromide ammonium salt as a co-catalyst was evaluated with the optimized co-catalyst/catalyst ratio of 5. This reaction conducted to good conversion of the cyclohexene oxide (74 %) obtaining cyclic carbonate as a single product (entry 2, Table 7.5). The selectivity of the reaction was strongly influenced by the use of other co-catalysts,[15] as well as by the co-catalyts/catalyst ratio.[31] Consequently, PPNCl was evaluated as co-catalyst. Iron(III) complexes/PPNCl catalytic system was frequently used in the literature producing poly(cyclohexene carbonate) in better selectivities than TBAB.[10] **FeL8**/PPNCl was evaluated at standard conditions with a co-catalyst/catalyst ratio of 1 and afforded lower conversion (37 %), producing mixtures of copolymer and cyclic carbonate product (entry 3, Table 7.5). Although not negligible 21 % of selectivity was obtained over the copolymer, the incorporation of carbonate linkages into the polymer was only 58 %.

Table 7.5. Cyclohexene oxide (CHO) and CO_2 coupling reaction using **FeL8** as catalyst.[a]

Entry	Cat	Co-cat	cat/co-cat (mol %)[b]	Conv (%)[c]	PCHC/ CHC (%)[c]	% CO_2 Content[c]	TOF (h^{-1})[d]
1	**FeL8**	-	0.2	0	-	-	-
2	**FeL8**	TBAB	0.2/1.0	74	0/100	-	0/15
3	**FeL8**	PPNCl	0.2/0.2	37	21/79	58	2/6

[a]Reaction conditions: Cyclohexene oxide: 29.70 mmol (3 ml), P_{CO2} = 50 bar, T = 80 ºC, time = 24 h ; [b]mol % respect to the substrate; time = 24h [c]measured by ^{1}H NMR; [d]averaged TOF (mol substrate converted into carbonate/polycarbonate·(mol catalyst)$^{-1}$·h^{-1}).

FeL8/PPNCl catalytic system is not as efficient as the other homogeneous iron-based copolymerization catalysts documented by Williams[17] and Kleij.[10] Then, it would need further study of the catalytic conditions to yield valuable copolymer with higher conversions and selectivity.

7.2.2.2 *Epoxidation of alkenes*

Viewing the good potential of these iron(III) complexes with N,N'O-donor ligands for the formation of valuable cyclic carbonates with CO_2 and epoxides it was interesting to evaluate them also in the previous step of epoxidation of alkenes.

The first epoxidation studies focused on the use of **FeL6** as catalyst to convert *cis*- and *trans*-stilbenes. These olefins were chosen as model substrates because of their non-volatility and the stability of the epoxide. *Tert*-butyl hydroperoxide (TBHP) was chosen as the oxygen atom source in acetonitrile solution taking literature conditions.[32] The catalytic reactions were performed at 60 ºC by slow dropwise addition of 2 equiv. of TBHP (70 % in water) over 5 min, in order to minimize peroxide disproportionation. The epoxidation results are summarized in Table 7.6. The control experiment revealed that the presence of catalyst is essential for the oxidation reaction (entry 1, Table 7.6). When **FeL6** was added the *trans*-stilbene conversion increased from 10 % to nearly 60 % and provided excellent epoxide selectivity (entry 2, Table 7.6). The epoxidation of *cis*-stilbene was observed to be low yielding with a conversion

of only 13 % giving *trans*-stilbene oxide with total selectivity (entry 3, Table 7.6). This low conversion could be due of steric constraints caused by *cis*-oriented phenyl groups and the highly hindered metal center, although more mechanistic studies should be necessary. It has been observed that *cis*-stilbene reacts with iron-porphyrin complexes to give high yields of *cis*-stilbene epoxide containing a minor amount of the corresponding *trans*-isomer.[33,34,35,36] Therefore, it is interesting that epoxidation of *cis*-stilbene gave total selectivity of *trans*-stilbene epoxide. Mn(salen) and iron(III) salicylaldimine derivatives also showed the same behavior favoring essentially the production of *trans*-epoxide products.[37,38,39,40] There is no clear mechanism for the selective formation of *trans*-epoxides from *cis*-olefins but it could be explained by the mechanism of Mn(salen)-catalized *cis*-stilbene epoxidation which suggests a radical mechanism in which the C-C rotation in the expected Mn-O-C-C intermediate competes with the ring closure to form the final epoxide.[37]

Table 7.6. Catalytic oxidation of *cis*- and *trans*-stilbene using **FeL6** and **FeL8** as catalysts.[a]

Entry	Subs.	Cat (mol %)[b]	Solvent	subs/oxidant (mmol)	Conv (%)[c]	Select. (%)[c]	TOF (h^{-1})[d]
1	*trans*	-	MeCN	1.5/3.0	10	>99 (trans)	0.6
2	*trans-*	**FeL6** (0.22)	MeCN	1.0/2.0	60	>99 (trans)	11
3	*cis-*	**FeL6** (0.22)	MeCN	1.0/2.0	13	>99 (trans)	2
4	*trans-*	**FeL6** (0.67)	MeCN	1.5/3.0	64	>99 (trans)	4
5	*trans-*	**FeL6** (0.67)	Acetone	1.5/3.0	39	>99 (diol)	-
6	*trans-*	**FeL8** (0.67)	MeCN	1.5/3.0	66	>99 (trans)	5

[a]Reaction conditions: solvent: 5 ml; TBHP (70 % in water) (added dropwise during the reaction); time = 24 h. [b]mol % respect to the substrate; mesitylene as internal standard [c]measured by ^{1}H NMR; [d]averaged TOF (mol substrate converted into epoxide·(mol catalyst)$^{-1}$·h^{-1}).

In order to enhance the olefin conversion the iron(III) catalyst loading was increased up to 0.67 mol % with respect to *trans*-stilbene. At these conditions the conversion obtained was moderately higher with a 64 % (entry 4, Table 7.6). The election of the adequate solvent is known to be an important feature for this reaction. For example, Kozak and coworkers studies showed that only *tert*-amyl alcohol, acetonitrile and acetone gave significant conversions with excellent selectivity, combining $FeCl_3 \cdot 6H_2O$ and 1-methylimidazole using H_2O_2 as oxidant.[41] In our case, the use of acetone in the reaction proceeded uniquely towards the diol 1,2-diphenyl-2-hydroxypropanol by-product formation with a 39 % of conversion (entry 5, Table 7.6). The highest activity in acetonitrile was probably related to the highest solubility of the catalyst in that solvent.

At these conditions, **FeL8** catalyst was then evaluated achieving a slight improvement in the conversion (66 %) towards *trans*-stilbene epoxide as the only product (entry 6, Table 7.6).

7.2.2.2.1 *Effect of the oxidant*

In view of these results, the influence of the oxidant was also studied for the epoxidation of *cis*- and *trans*-stilbene using **FeL8** as catalyst. The screening of the different selected oxidants was carried out also at 60 °C, 24 h and using acetonitrile as solvent. The catalyst loading was increased to 3.3 mol % and the amount of oxidant was, in some cases, slightly modified in concordance with the best results obtained from the literature. The oxygen sources were chosen according to their reported efficiency in epoxidation reactions. The selected oxidants were PhIO,[33,37,42,43,44] H_2O_2,[41,45,46,47,48] H_2O_2/AcOH,[49,50,51] MCPBA,[52] and NaOCl,[53,54,55] commonly used in the literature. Table 7.7 shows the conversion and selectivity (%) for *cis*- and *trans*-stilbene using the selected oxidants. The epoxidation reaction, in the presence of iodosylbenzene, was done at the optimized amount of substrate and PhIO by Kochi and co-workers (0.3 and 0.15 mol %, respectively).[37] Conversions of 13 % and 23 % for *trans*- and *cis*-stilbene, respectively, were obtained at these conditions (entries 1 and 2, Table 7.7). In the case of *trans*-stilbene a selectivity of > 99 % was obtained towards the *trans*-stilbene oxide, whereas, with *cis*-stilbene a 90 % of *cis*-stilbene epoxide was obtained. Interestingly, the *cis*-epoxide selectivity suggests that when PhIO was used as a terminal oxidant the

epoxidation proceeds by a different mechanism compared to TBHP. The use of hydrogen peroxide as an oxidant has a great interest in catalysis since it is easy to handle, very cheap and forms water as a byproduct.[56] It is known that the mode of H_2O_2 addition is crucial, as this reagent decomposes rapidly in the presence of iron.[57] However, no conversion was observed, neither for *trans*-stilbene nor *cis*-stilbene, using H_2O_2 (30 % aqueous) by dropwise addition during 10 min (entries 3 and 4, Table 7.7).
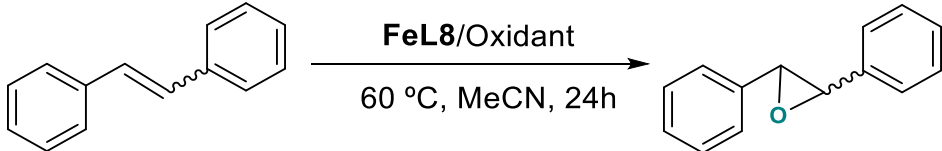
Peracetic acid (AcOOH) is also a desirable oxidant because the non-toxic acetic acid byproduct. Unlike H_2O_2, AcOOH is not prone to metal-based decomposition. AcOOH is readily prepared by the reaction of concentrated aqueous H_2O_2 and AcOH with a strong acid catalyst, typically sulfuric acid.[58] Que and co-workers determined that non-heme iron(II) complexes bearing N-donor ligands catalyze the *in situ* formation of AcOOH from H_2O_2 and AcOH and then utilize the incipient AcOOH for epoxidation.[49] Notably, the introduction of 0.33 mmol of AcOH into our reaction mixture enhanced the epoxide formation obtaining a 16 % and 14 % of *trans*- and *cis*-stilbene conversion, respectively. Total selectivity towards *trans*-epoxide was obtained for *trans*-stilbene, whereas, mixtures of *cis*- and *trans*- epoxide and also an 11 % of phenylacetophenone by-product were obtained for *cis*-stilbene (entries 5 and 6, Table 7.7).

Olefin epoxidation by heme iron catalysts in the presence of *m*-chloroperbenzoic acid (MCPBA) is well established and involves a $Fe^{IV}=O$ porphyrin cation radical intermediate.[59] However, there are a few mononuclear non-heme iron complexes that are active in combination with MCPBA.[52,60] The combination of the iron(III) catalyst with MCPBA oxidant afforded moderate conversions of 41 and 35 %, for *trans*- and *cis*-stilbene, respectively (entries 7 and 8, Table 7.7). Being the conversion of *cis*-stilbene the highest obtained so far using **FeL8** as catalyst. Nevertheless, mixtures of *cis*- and *trans*- epoxide were obtained.

Sodium hypochlorite (NaOCl) acts a poorer terminal oxidant than PhIO in epoxidation of *trans*-stilbene with Mn(III)(salen)X complexes.[42] It was established that with NaOCl the epoxidation proceeds with the formation of active intermediate [Cl-O-Mn(III)(salen)X], which is too unstable to generate epoxide in appreciate amount, whereas with PhIO, the reaction proceeds by the formation of more active intermediate [O=Mn(V)(salen)X] yielding high amount of epoxide. However, in the case of analogous Fe(III)(salen)X complexes, only catalyzed reactions by the formation of the

sterically crowded intermediate similar to [Cl-O-Mn(III)(salen)X] both with PhIO and NaOCl.[53] With our catalytic system, very low conversions where achieved using NaOCl as a terminal oxidant, either with *trans*- or *cis*-stilbene, indicating that the reaction may proceeded with formation of a non-stable active intermediate (entries 9 and 10, Table 7.7).

Table 7.7. Catalytic oxidation of *cis*- and *trans*-stilbene using **FeL8** as catalyst.[a]

Entry	Subs.	Oxidant	subs/oxidant (mmol)	Conv (%)[b]	Select. (%)
1	*trans*	PhIO	0.3/0.15	13	>99 (trans)
2	*cis-*	PhIO	0.3/0.15	23	90/10 (cis/trans)
3	*trans-*	H$_2$O$_2$	0.3/0.6	0	-
4	*cis-*	H$_2$O$_2$	0.3/0.6	0	-
5	*trans-*	H$_2$O$_2$/AcOH	0.3/0.6/0.33	16	>99 (trans)
6	*cis-*	H$_2$O$_2$/AcOH	0.3/0.6/0.33	14	56/31[c] (cis/trans)
7	*trans-*	MCPBA	0.3/0.3	41	>99 (trans)
8	*cis-*	MCPBA	0.3/0.3	35	43/57 (cis/trans)
9	*trans-*	NaOCl	0.3/0.3	3	>99 (trans)
10	*cis-*	NaOCl	0.3/0.3	5	>99 (trans)
11	*trans-*	TBHP	0.3/0.6	88 (80)[d]	>99 (trans)
12	*cis-*	TBHP	0.3/0.6	23	>99 (trans)

[a]Reaction conditions: solvent: 5 ml; catalyst: 3.3 mol % respect to the substrate; TBHP(5.5 M in decane), H$_2$O$_2$ and H$_2$O$_2$/AcOH were added dropwise during the reaction; time = 24 h. [b]measured by ^{1}H NMR using mesitylene as an internal standard; [c]11 % of phenylacetophenone by-product; [d]% conversion at 16 h.

Finally, TBHP (5.5 M in decane) was used as oxidant at the same reaction conditions. At this point, the highest conversion was obtained in the case of *trans*-

stilbene substrate (88 %) with a total selectivity towards the *trans*-stilbene oxide. Even at 16 h of reaction time the conversion was up to 80 % (entry 11, Table 7.7). With *cis*-stilbene a conversion of only 23 % was achieved. Although the conversion was not the highest, the selectivity was total towards *trans*-stilbene oxide (entry 12, Table 7.7).

7.2.2.2.2   *Effect of reaction time*

The progress of epoxidation reaction of *trans*-stilbene was monitored for the optimized **FeL8**/TBHP catalytic system. A plot of conversion *versus* time is given in Figure 7.5. From this observation, it was found that the rate of epoxide formation is higher in the first 6 h of reaction obtaining almost 50 % of the olefin conversion. Then, the reaction rate decreases over time; nevertheless, the epoxidation continues to proceed over the duration of the experiment. In conclusion, long reaction time is required, at these conditions, in order to achieve highest olefin conversions.
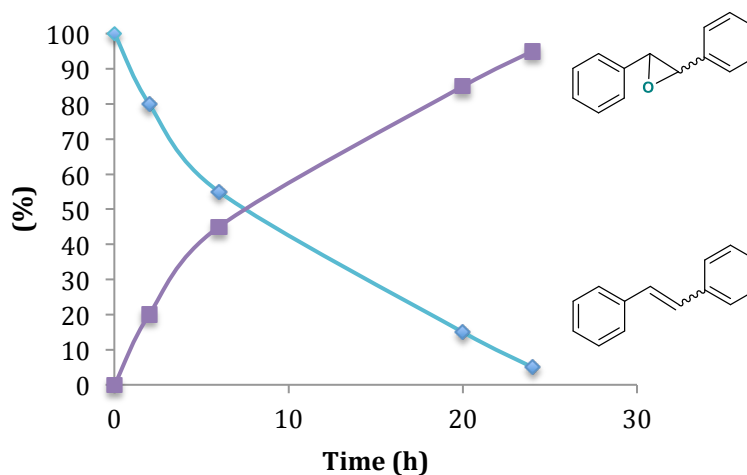
Figure 7.5. Monitoring the progress of epoxidation of *trans*-stilbene. Reaction conditions: substrate: 270.4 mg, 1.5 mmol; MeCN: 5 ml; TBHP (5.5 M in decane): 0.55 ml, 3 mmol (added dropwise during the reaction); **FeL8**: 8.3 mg, 0.01 mmol, temperature: 60 ºC.

7.2.2.2.3   *Catalyst recycling*

The possibility of recycling the catalyst **FeL8** in the epoxidation reaction of *trans*-stilbene with both TBHP (70 % H_2O) and TBHP (5.5 M decane) was studied in two consecutive runs (Figure 5.6). After the first run in acetonitrile, the complex was precipitated with hexane and filtered off. In both cases, the conversion of *trans*-stilbene

decreased drastically in the second run, although the catalyst was washed several times with hexane and dried under vacuum before reuse. An explanation of this behavior could be the decomposition of the iron(III) species after the first run since some decomposed ligand could be observed by ^{1}H NMR spectroscopy.
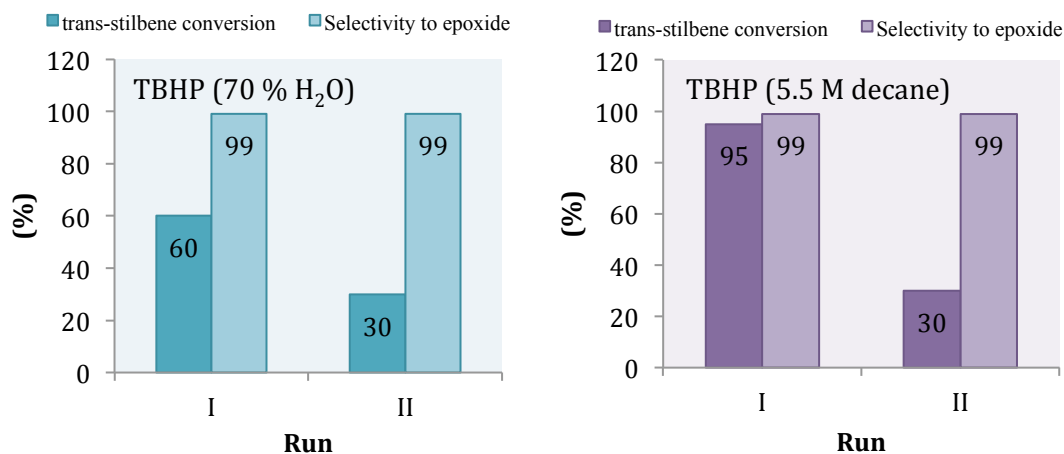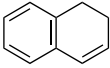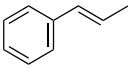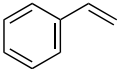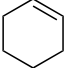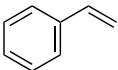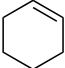
Figure 5.6. Reuse of **FeL8** catalyst in epoxidation of *trans*-stilbene to *trans*-stilbene oxide using TBHP, either in water or decane, as oxidant source. Reaction conditions: substrate: 270.4 mg, 1.5 mmol; MeCN: 5 ml; TBHP (70 % H_2O): 3 mmol TBHP (5.5 M in decane): 0.55 ml, 3 mmol (added dropwise during the reaction); **FeL8**: 8.3 mg, 0.01 mmol, temperature: 60 ºC.

7.2.2.2.4 *Epoxidation of other alkenes*

Finally, in order to explore the catalytic potential of **FeL8**, the oxidation of various olefins was performed under the optimized reaction conditions with TBHP (5.5 M in decane) as terminal oxidant. We have studied cyclic and phenyl substituted olefins as substrates. A yield up to 85 % of naphthalene, identified by ^{1}H NMR, was obtained in the oxidation of 1,2-dihydronaphtalene (entry 1, Table 7.8), whereas high selectivity with a 100 % yield towards *trans*-epoxide was obtained with *trans*-β-methylstyrene (entry 2, Table 7.8). Naphthalene sub-product that resulted from oxidative dehydrogenation of 1,2-dihydronaphtalene was also reported to be formed using Kegin-type metal substituted polyoxotungstates catalysts with H_2O_2.[61] Unfortunately, styrene and cyclohexene substrates were no epoxidized at these conditions (entries 3 and 4, Table 7.8). It is well established that the presence of a nitrogenous base like imidazole

as a co-catalyst increased the conversion of some olefins using iron catalysts.[53] With this in mind we added imidazole as neutral donor co-catalyst. Styrene gave a moderate yield towards the epoxide product of 24 % (entry 5, Table 7.8). Moreover, with cyclohexene only a yield of 3 % towards cyclohexene oxide was achieved (entry 6, Table 7.8).

Table 7.8. Catalytic oxidation of *cis*- and *trans*-stilbene using **FeL8** as catalyst.[a]

Entry	Subs.	subs/oxidant (mmol)	Select. (%)[b]	Yield (%)[b]
1		0.3/0.6	>99 (naphtalene)	85
2		0.3/0.6	>99 (trans)	100
3[c]		0.3/0.6	-	-
4[c]		0.3/0.6	-	-
5[c]		1.5/3.0	-	24[d]
6[c]		1.5/3.0	-	3[d]

[a]Reaction conditions: solvent: 5 ml; catalyst: 3.3 mol % respect to the substrate; TBHP (5.5 M in decane) was added dropwise during the reaction; time = 24 h. [b]measured by ^{1}H NMR using mesitylene as internal standard; [c]0.33 mmol of imidazole; [d]Yields were determined by GC using mesitylene as internal standard.

7.2.2.2.5   *Mechanistic proposal*

We previously observed that, unlike other olefins, such as cyclohexene and styrene, the epoxidation of *cis*-stilbene provides two epoxidation products, *cis*-stilbene oxide and *trans*-stilbene oxide. Thus, the study of *cis*-stilbene can provide additional

mechanistic information through the simple act of determining the ratio of the *cis* and *trans* isomers of the stilbene oxide produced.

As shown in Table 7.7 the epoxidation of *cis*-stilbene with TBHP and NaOCl provides *trans*-stilbene oxide as a single product, which is consistent with the radical pathway in which t-BuOO$^{\cdot}$ or ClO$^{\cdot}$ are the reactive intermediates (Scheme 7.4).[62]
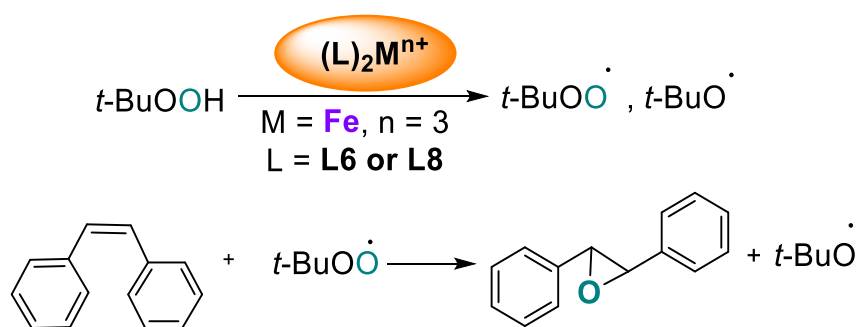
Scheme 7.4. Proposed radical mechanism for olefin epoxidation with *tert*-butylhydroperoxide.

One of the most viable mechanistic model for epoxidation of *cis*-stilbene with PhIO as terminal oxidant is the Lewis acid pathway, in which an oxygen atom is transferred directly from an oxoiron(V) intermediate complex to the olefinic double bond (Scheme 7.6(a), pathway A). Nevertheless, the selectivity of this reaction should be exclusively towards *cis*-stilbene oxide as a sole product since there was only one reactive intermediate (oxoiron(V)) involved. An alternative explanation of the 10 % selectivity towards *trans*-stilbene oxide observed (entry 2, Table 7.7) could be a radical mechanism where the selectivity of the different epoxides obtained may be due to a ligand effect which favor the C-C bond rotation (Scheme 7.5(b), pathway C) than the epoxide ring closure (Scheme 7.5(b), pathway B). This behavior was also confirmed by Nam and coworkers using manganese(III) porphyrines/iodosylarenes.[63] They observed an axial ligand effect on the reactivity of the oxomanganese(V) active intermediate.

In the hexacoordinate iron systems of this work we assume that a dissociation of one pyridine arm should take place to allow the formation of the oxo- active intermediate (Scheme 7.5). Then, a radical pathway would explain the lack of retention of the configuration in the epoxide. The low catalytic activity of these complexes may be related to the high coordinative saturated environment of iron center.
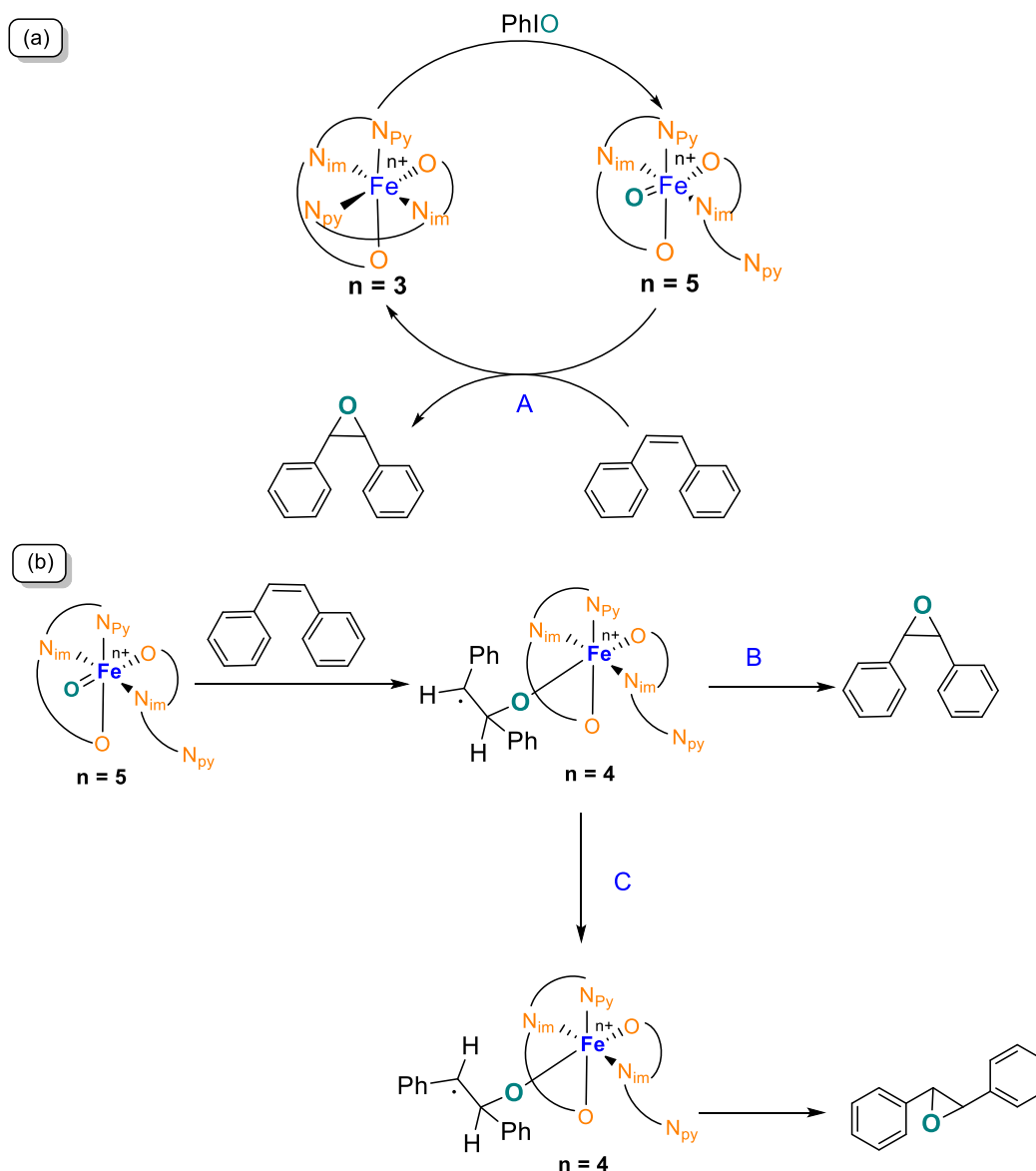
Scheme 7.5. Proposed reaction pathways for the ligand effect on the diastereoselectivity in *cis*-stilbene epoxidation by **FeL8** and PhIO.

7.2.2.3 *One-pot oxidative carboxylation of olefins*

In order to achieve an even more efficient, economic and environmentally friendly process for production of cyclic carbonates, we did a preliminary study to develop a one-pot procedure for the direct synthesis of cyclic carbonate without the isolation of the intermediate epoxide. The direct oxidative carboxylation of olefins utilizing CO_2 as a building block, couples two processes, epoxidation of olefins and CO_2 cycloaddition to epoxides (Scheme 7.6).
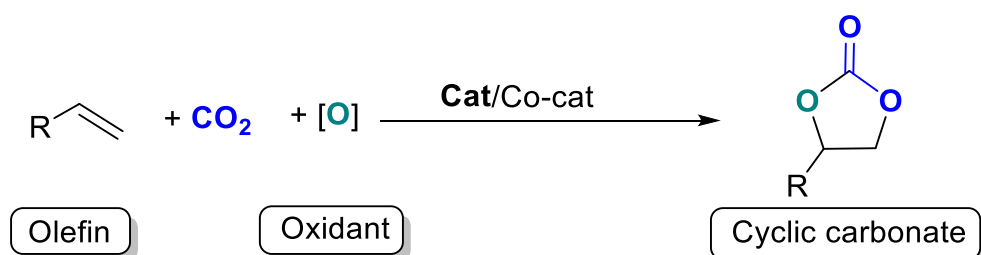
Scheme 7.6. Schematic representation of synthesis of cyclic carbonates from olefins and CO_2.

Taken into account the good results obtained by Arai and co-workers for the one-pot synthesis of styrene carbonate from styrene, TBAB, compressed CO_2 and TBHP as oxidant, we tried to analyze the potential of adding the iron(III) complex in this reaction media. At optimized conditions they obtained a moderate yield of styrene carbonate of 38 %.[4] Using more ecologically friendly H_2O_2 as oxidant good styrene conversion of 62 % but lower styrene carbonate yield of 4 % was obtained.

Table 7.9. One-pot synthesis of styrene carbonate using **FeL6**/TBAB as catalyst system.[a]

Entry	Catalyst	Conv (%)[b]	Yield (%)[c] SC	Yield (%)[c] SO	Ref
1[d]	TBAB	62	4	2	4
2[e]	**FeL6**/TBAB	19	17	-	This work

[a]Reaction conditions: temperature: 80 °C; P_{CO2}: 150 bar; [b]Conversion was determined by GC based on starting substrate; [c]Yield was determined by GC based on undecane internal standard; [d]TBAB: 2 mmol; styrene: 17.3 mmol; H_2O_2: 25.4 mmol; times : 6 h; [e]catalyst: 0.2 mmol; TBAB: 0.2 mmol; styrene: 1.75 mmol; H_2O_2 (30 % in water): 25.4 mmol; time : 6 h.

Using **FeL6**/TBAB catalytic system to convert styrene to styrene carbonate using H_2O_2 as terminal oxidant at 150 bar of CO_2, 80 °C and during 16 h we obtained 19 % of styrene conversion. The styrene carbonate product was determined by gas chromatography comparing the retention time with a standard styrene carbonate sample. As shown in Table 7.9, the styrene conversion appeared to be lower compared with

TBAB alone with only 19 % (entry 2, Table 7.9). Nevertheless, a higher yield towards styrene carbonate was achieved without the observation of styrene oxide intermediate product (See supporting information). It should be noted that the direct comparison of both results is overrated as reactor set ups are different; however, it should be a good starting point. On a positive note, supercritical CO_2 was used both as reactive and solvent in this reaction, with no co-solvent addition, providing an enormous benefit from an ecological point of view.

The low activity of this catalytic system may be due to a decomposition of the complex since we already observed it in the recycling experiments of the epoxidation.

7.3 Influence of the metal in the CO_2/epoxides coupling by NN'O-Schiff metal complexes and mechanism proposal

In the last two chapters (Chapter 6 and Chapter 7) we described catalytic activity of Zn(II) and Fe(III) complexes bearing tridentate NN'O-donor Schiff base ligands for the coupling of CO_2 and epoxides as well as for epoxidation reactions. At this point, it is fundamental to do a comparison between those lower toxic metal complexes and also with earlier studies of analogous Cr(III) complexes developed by our group. It was shown that using Zn(II) and Fe(III) complexes a complete selectivity and high activities were achieved for the coupling of CO_2 and terminal epoxides. Although, the catalytic conditions were not comparable, the optimized TOF using **ZnL6**/TBAB for the cycloaddition of SO was higher (3733 h^{-1}, 100 ºC) than the one for **FeL6**/TBAB (400 h^{-1}, 80 ºC). However, the stability of the iron complex was higher. **FeL8**/TBAB produced a TOF of 900 h^{-1}. Analogous **CrL6**/PPNCl provided also high conversions although the initial TOF was not evaluated.

Using most hindered substrates as methyl epoxyoleate, the highest reactivity was obtained with **FeL8**/TBAB with a 95 % of conversion and 85 % of carbonate yield. Isomer selectivities are different in both systems as in the case of Zn(II) the *cis*-methyloleate carbonate was the major species with a selectivity of a 95 % and a 67 % of *trans*-methyloleate carbonate was obtained in the case of Fe(III) (Scheme 7.8).
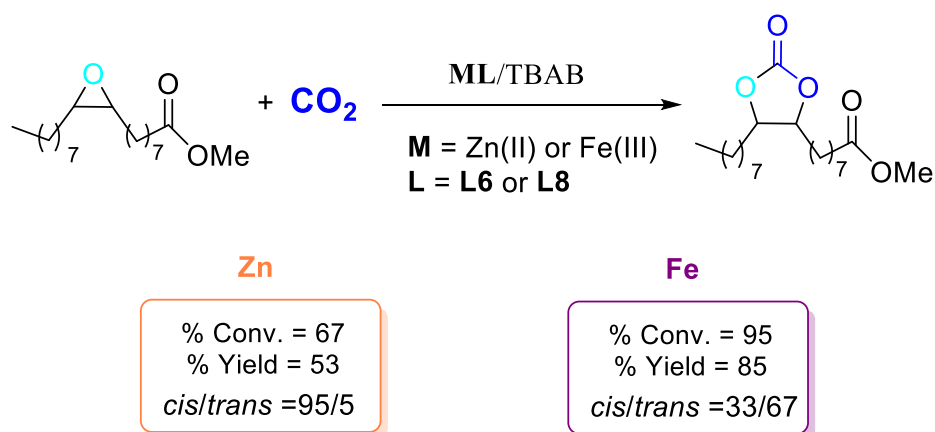
Scheme 7.8. Cycloaddition of methyl epoxyoleate to CO_2 with catalyst **ZnL6**/TBAB and **FeL8**/TBAB catalytic systems. Reaction conditions: catalyst/co-catalyst: 2 mol %/2 mol %; T = 100 °C, P_{CO2} = 100 bar, 24h.

In the reaction of cyclohexene oxide and CO_2 different behaviors were observed from the different metal catalytic systems. Using TBAB as co-catalyst, the catalytic activity of **FeL8** is higher than the one obtained with **ZnL6**, (entry 1 vs 2, Table 7.10), although, the direct comparison is overrated since less amount of TBAB was used (0.2 vs 1.0 mol %). However, these results reveal that switching the central atom from zinc to iron had an improvement in the synthesis of cyclohexene carbonate as a main product and the complete selectivity towards cyclic carbonate was maintained.

Table 7.10. Cyclohexene oxide (CHO) and CO_2 coupling reaction using catalysts **FeL8**, **ZnL6** and **CrL6**.[a]

Entry	Cat	Co-cat	cat/co-cat (mol %)[b]	Conv (%)[c]	PC/CC (%)[c]	% CO_2 content[c]	TOF (h^{-1})[d]	Ref
1	**FeL8**	TBAB	0.2/1.0	74	0/100	-	0/15	This work
2	**ZnL6**	TBAB	0.14/0.2	27	0/100	-	0/8	Chap. 6
3	**FeL8**	PPNCl	0.2/0.2	37	21/79	58	2/6	This work
4[e]	**CrL6**	PPNCl	0.12/1.0	95	32/68	81	21/45	14

[a]Reaction conditions: Cyclohexene oxide: 29.70 mmol (3 ml) P_{CO2} = 50 bar, T = 80 °C, time = 24h; [b]mol % respect to the substrate; [c]measured by ^{1}H NMR; [d]averaged TOF (mol substrate converted into carbonate/polycarbonate·(mol catalyst)$^{-1}$·h^{-1}); [e]12 h.

Changing the co-catalyst to PPNCl, mixtures of cyclohexene carbonate and poly(cyclohexene carbonate) were obtained, similar to those obtained with analogous **CrL6**. Nevertheless, lower conversion was achieved switching the central atom from chromium to iron (entries 3 vs 4, Table 7.10). Despite the low reactivity, **FeL8** may be promising in terms on switching the metal from toxic chromium(III) or not selectivity tunable and less stable zinc(II) to more greener metal such iron(III).

According to the evidences obtained from these catalysts, it could be proposed a plausible general mechanism for the coupling of CO_2 and epoxides involving those metal-NN'O Schiff complexes (Scheme 7.9).
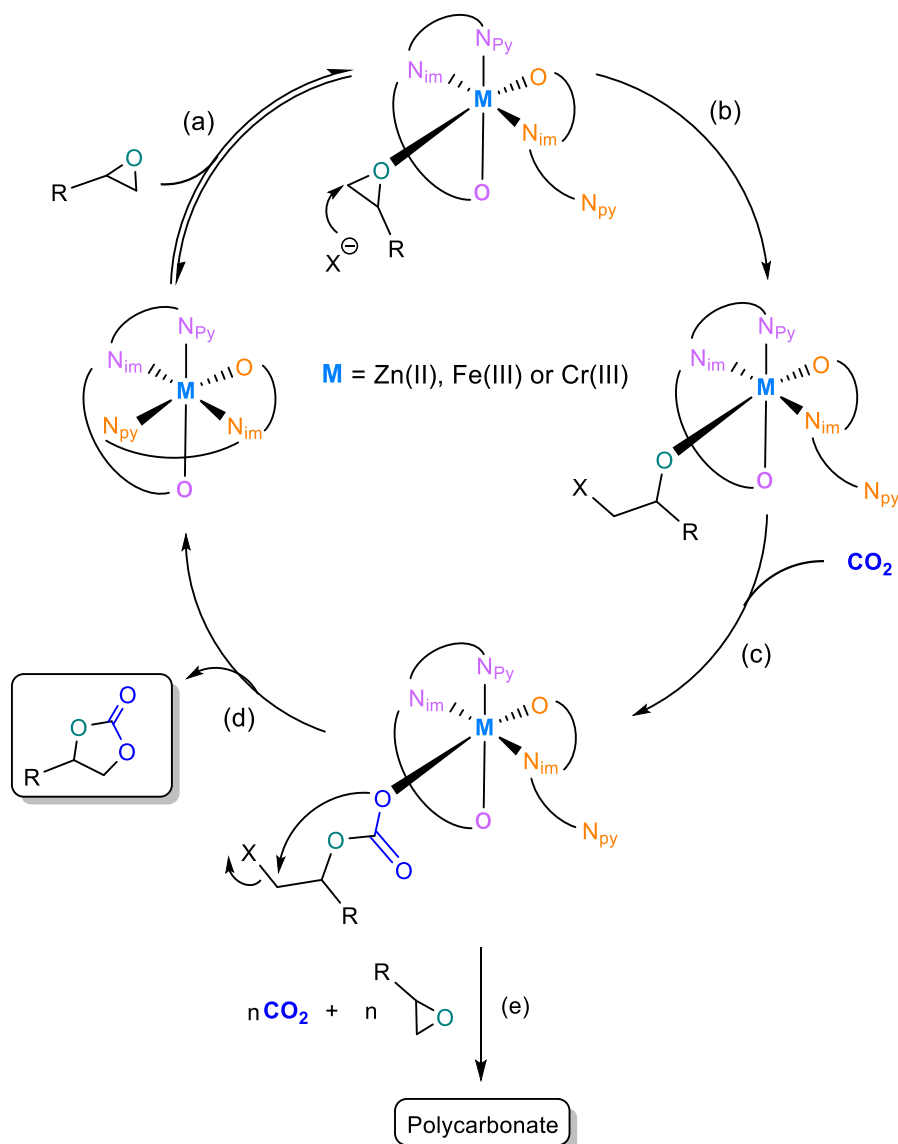
Scheme 7.9. Proposed reaction mechanism for the conversion of epoxides into the corresponding carbonates with catalyst system **ML6-8**/co-catalyst.

The initial step in the catalytic cycle involves the activation of the epoxide by coordination to the metallic center and formation of a metal-alkoxide active species. To do this, a substitution of a pyridine moiety must take place (step a, Scheme 7.9). Once the epoxide is activated, a nucleophilic attack with the Br⁻ or Cl⁻ from co-catalyst (TBABr and PPNCl) takes place (step b, Scheme 7.9). Evidences for this substitution were obtained by ^{1}H NR spectroscopy of the reaction of **ZnL6** with SO. The next step is the insertion of a carbon dioxide molecule into the metal-alkoxide bond leading to a carbonate linkage (step c, Scheme 7.9). This intermediate can either form a cyclic monomer through intramolecular rearrangement by a "back-biting" mechanism or polycarbonate through further alternating insertions of epoxide and carbon dioxide molecules. The stability of the hexacoordinate species may favor the ring closing step (step d, Scheme 7.9) against the formation of the poly(carbonate) (step e, Scheme 7.9).

7.4   Conclusions

In summary, we have presented low toxic and easy to handle iron(III) complexes bearing tridentate NN'O Schiff ligands that proved to be efficient catalysts for the formation of organic carbonates using terminal epoxides and carbon dioxide, as well as in the previous olefin epoxidation step. Using harsher conditions, the catalyst also shows to be active for the more sterically congested methyl epoxyoleate substrate. The catalyst seems to show a high potential for the direct oxidative carboxylation of styrene towards styrene carbonate using supercritical carbon dioxide as both reactive and solvent. Further work is needed to access a more refined catalysis approach in order to increase the carbonate yield and to improve the catalyst recycling.

7.5   Experimental section

General Comments. HL6 ligand and **FeL6** complex were prepared following described procedures in the literature.[17,18,19] Epoxides were dried over CaH_2, distilled and stored under inert atmosphere except 1,2-epoxyhexane, 1,2-epoxydodecane and epichlorohydrin, which were purchased at Sigma-Aldrich and used as received. Solvents were purified by the system Braun MB SPS-800 and stored under nitrogen atmosphere. Carbon dioxide (SCF Grade, 99.999 %, Air Products) was used introducing

an oxygen/moisture trap in the line (Agilent). IR spectra were recorded on a Midac Grams/386 spectrometer in ATR (range 4000-600) cm^{-1} or KBr range (4000- 400 cm-1). UV-visible spectra were recorded on a UV-3100PC spectrophotometer. NMR spectra were recorded at 400 MHz Varian, with tetramethylsilane (^{1}H NMR) as internal standards. Electrospray ionization mass spectra (ESI-MS) were obtained with an Agilent Technologies mass spectrometer. Typically, a dilute solution of the compound in the indicated solvent (1:99) was delivered directly to the spectrometer source at 0.01 ml·min^{-1} with a Hamilton microsyringe controlled by a single-syringe infusion pump. The nebulizer tip operated at 3000-3500 V and 250 °C, and nitrogen was both the drying and a nebulizing gas. The cone voltage was 30 V. Quasi-molecular ion peaks [M–H]$^-$ (negative ion mode) or sodiated [M + Na]+ (positive ion mode) peaks were assigned on the basis of the m/z values. Elemental analyses were performed at the Serveis Tècnics de Recerca from the Universitat de Girona (Spain). Conductivity was measured with a Crison conductimeter GLP equipped with a conductivity Pt cell (CH$_2$Cl$_2$ or methanol solutions). Magnetic susceptibilities were measured on a Sherwood MSBmk1 magnetic susceptibility balance with KK105 as a calibration standard. A typical program temperature for the GC analysis started at 60°C, then increased in a 40°C/min rate and stopped after 2 min at 240°C. Mesitylene was used as internal standard. All catalytic experiments were done by duplicate.

7.5.1 Synthesis of HL8
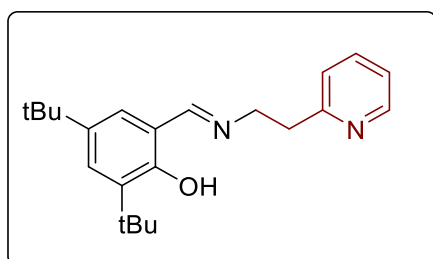
A solution of 2-(2-pyridyl)ethylamine (1.28 ml, 10 mmol) in MeOH (15 ml) was added to a warm solution of 3,5-di-*tert*-butyl-2-hydroxybenzaldehyde (2.41 g, 10 mmol) in MeOH (25 ml) and the mixture was refluxed for 4h. The solvent was removed and the product was washed with diethyl ether, affording the desired compound as a bright yellow syrup (3.45 g, 100%).

ESI (MeOH) Calcd for $C_{23}H_{30}N_2O$ *m/z* [M-H]$^+$: 339.2431, found: 339.2851.FT-IR (neat) in v cm^{-1}: 1631 (C=N), 1590 (C=C), 1570 (C=C). ^{1}H NMR (400 MHz, CDCl$_3$) δ in ppm: 13.73 (s, 1H, OH); 8.53 (ddd, 1H, $J_{6,3}$= 0.9 Hz, $J_{6,4}$= 1.8 Hz, $J_{6,5}$= 5.0 Hz, py-H6); 8.27 (s, 1H, H-CN); 7.56 (ptd, 1H, $J_{4,3}$= 7.7 Hz, $J_{4,5}$= 7.6 Hz, $J_{4,6}$= 1.8 Hz, py-H4); 7.33 (d, 1H, $J_{6',4'}$= 2.4 Hz, ph-H6'); 7.14 (bd, 1H, $J_{3,4}$= 7.7 Hz, py-H3); 7.10 (ddd, 1H, $J_{5,3}$= 1.0 Hz, $J_{5,4}$= 7.6 Hz, $J_{5,6}$= 5.0 Hz, py-H5); 7.00 (d, 1H, $J_{4',6'}$= 2.4 Hz, ph-H4'); 3.97 (t, 2H, *J*= 7.2 Hz, CH$_2$N); 3.16 (t, 2H, *J*= 7.2 Hz, CH$_2$); 1.41, 1.26 (s, 9H, ^{t}Bu). ^{13}C NMR (100.6 MHz, CDCl$_3$) δ in ppm: 166.2 (H-CN); 159.4 (py-C2); 158.2 (ph-C2'); 149.6 (py-C6); 140.0 (py, C4); 136.7 (ph-C6'); 136.5 (ph-C4'); 126.9 (py-C3); 126.0 (py-C5); 123.8 (ph-C5'); 121.6 (ph-C5'); 121.6 (ph-C3'); 117.9 (ph-C1'); 59.2 (CH$_2$N); 39.8, 35.2 (C, ^{t}Bu); 34.2 (CH$_2$); 31.6, 29.6 (3x CH$_3$, ^{t}Bu).

7.5.2 Synthesis of FeL8
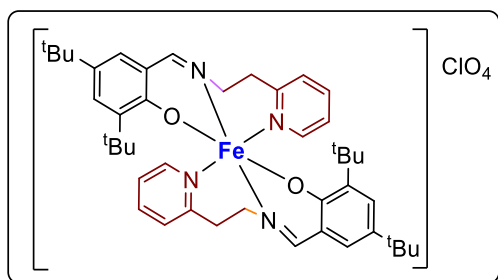
A solution of Fe(ClO$_4$)$_3$·9H$_2$O (283.7 mg, 0.55 mmol) in 5 ml MeOH was added dropwise to solution containing (354.0 mg, 1.05 mmol) of **HL8** and Et$_3$N (0.15 ml, 1.05 mmol) in 15 ml MeOH. The resulting solution change color (dark blue) and was gently refluxed for 1 h, when finished was filtered while warm and concentrated to one-third of the original volume to render a dark purple oil. This oil was further washed with hexane and dried in vacuum. Dark blue solid, 388.4 mg, (Yield 89 %).

Anal. Calcd. (found) for $C_{44}H_{58}ClFeN_4O_6$: C, 63.65 (62.77); H, 7.04 (6.62); N 6.75 (6.63). HR ESI (MeOH) calculated for $(C_{44}H_{58}FeN_4O_2)^+$ m/z: 730.3909, found m/z: 730.3916 [M-ClO$_4$]. Selected IR bands (ATR, ν, cm^{-1}): 2952-2869 ν(C-H from *tert*butyl groups) m, 1601 ν(C=N) s, 1552 m, 1537 s, 1441 m, 1413 m, 1360 m, 1317 m, 1275 m, 1250 ν(C-O) s, 1085 ν(ClO$_4$) br, 840 m, 780 m, 762 m. Conductivity (Λ_M, MeCN, 4.04·10^{-4} M): 164.9 Ω^{-1}·cm^2·mol^{-1}. UV-vis (CH$_3$CN, 2.5·10^{-5} M): λ(nm) (ε, l mol^{-1} cm^{-1}): 214.0 (65904), 241.0 (24484), 343.0 (4060), 573.0 (944). μ_{eff} (21 ºC) = 6.03 μ_B.

CAUTION! *Although no difficulties were experienced, complexes **FeL6** and **FeL8** were isolated, as their perchlorate salts, and therefore they should be handled as potentially explosive compounds.*

Standard procedure for the synthesis of cyclic carbonates. The catalytic tests were carried out in a 100 ml Berghof or 25 mL Parr reactor, which were previously kept for 4 hours under vacuum at 100 ºC. After cooling, a solution under inert atmosphere containing the catalyst dissolved in neat distilled substrate and the co-catalyst, when indicated, was injected into the reactor. The autoclave was pressurized with CO_2, and then heated to the specific temperature to reach the desired pressure. After the reaction time, the reactor was cooled with an ice bath and slowly depressurized (With propylene oxide a dichloromethane trap was used). The % conversion was determined by ^{1}H NMR of the crude mixture by integral ratio between epoxide and cyclic carbonate. The % yield was determined by ^{1}H NMR using mesitylene as internal standard.

Standard procedure for copolymerization with cyclohexene oxide: Using the same procedure for the synthesis of cyclic carbonates the % conversion was also determined by ^{1}H NMR of the crude mixture by integral ratio between alkene oxide with copolymer and cyclic carbonate. The % yield was determined by ^{1}H NMR using mesitylene as internal standard. The final mixture was dissolved in dichloromethane, the solvent was evaporated and the residue dried in vacuum at 100 ° C for 3 hours to remove excess of cyclohexene oxide. The final residue was washed several times with hexane to purify the poly(carbonate) and was analysed by ^{1}H NMR spectroscopy. % of CO_2 content was calculated from ^{1}H NMR data by the integral ratio between copolymer carbonate linkages (δ = 4.65 ppm) respect to ether linkage signals (δ = 3.45 ppm).

Standard epoxidation reaction: Oxidation reactions were performed in a stirred Schlenk tube fitted with a water-cooled condenser. The reactions were carried out under atmospheric pressure in air in an oil bath at 60±1 ◦C with acetonitrile as a solvent and the corresponding oxidant. In a typical experiment a mixture the catalyst, 5.0 ml solvent, the olefin and mesitylene as internal standard were added on a Schlenk tube. After the mixture was heated to 60 ◦C, the oxidant was added (dropwise during the period of 5 min in the case of TBHP and H_2O_2). At appropriate intervals, aliquots were

removed and analyzed immediately by GC (styrene and cyclohexene) or dried under vacuum and analyzed by ^{1}H NMR. Oxidation products yields based on the starting substrate were quantified by comparison with mesitylene internal standard.

Recycling epoxidation experiments with FeL8: The catalytic reaction was carried out using the general epoxidation procedure. After the reaction time, the % conversion and yield was determined by ^{1}H NMR. The acetonitrile solvent was removed under vacuum. The catalyst was precipitated with hexane and separated by filtration as a dark blue solid. The solid was dried under vacuum, weighed and reused as catalyst.

Standard oxidative carboxylation reaction: In a typical reaction procedure, **FeL$_6$** and TBAB were added to the mixture of styrene and H_2O_2 in a 25 ml Parr reactor. Then, CO_2 was injected to the reactor. The reactor was stirred continuously at the desired temperature. After the completion of reaction, the reactor was cooled to 0 °C by ice water and slowly depressurized. Products were dissolved in acetonitrile and analysed by gas chromatograph using undecane as internal standard.

7.5.3 X-ray crystallography

Dark blue crystals of **FeL8** suitable for X-ray diffraction analyses were obtained by slow evaporation of a hexane/diethyl ether solution. Diffraction data for the structures reported were carried out on a Smart CCD 1000 Bruker diffractometer system with Mo Kα radiation ($\lambda = 0.71073$ Å). Cell refinement, indexing and scaling of the data sets were carried out using programs Bruker Smart and Bruker Saint. All the structures were solved by *SIR97*[64] and refined by *Shelxl9*[65] and the molecular graphics with ORTEP-3 *for Windows*.[66] All the calculations were performed using the *WinGX* publication routines.[67] Crystallographic data is collected in Table 7.11.

Table 7.11. Crystallographic data and details of structure refinement for compound **FeL8.**

	FeL8
Molecular formula	$C_{45}H_{62}ClFeN_4O_7$
Molecular weight	862.28
Crystal system	Triclinic
Space group	$P\bar{1}$
Temp. (K)	100(2)
Radiation (λ, Å)	Mo Kα (λ=0.71073 Å)
a (Å)	11.5299(3)
b (Å)	11.5621(3)
c (Å)	17.9493(5)
α (º)	74.2077(10)
β (º)	78.1792(10)
γ (º)	76.8703(11)
Volume (Å^3)	2216.04(10)
Z	2
Dx (Mg·m^{-3})	1.292
F (000)	918
Crystal dimensions (mm)	0.10 x 0.01 x 0.01
μ (Mo Kα) (mm-1)	0.454
θmax (º)	27.384
Reflections collected	35739
Unique reflections	9382
Rint.	0.0501
Observed [I >2σ(I)]	9382
Parameters	537
R1 [I >2σ(I)]	0.0530
wR2	0.1350
$\Delta\rho$ (e/ Å3)	0.870, -0.933

7.6   *Supporting information*

NMR spectra, FTIR, ESI mass spectra of **HL8** and **FeL8**, the NMR and GC spectra of the catalytic products and the pdf file containing CIF files giving crystallographic data for **FeL8**, are available in the supporting information CD.

7.7   *References*

[1]   Eghbali, N.; Li, C.-J., *Green Chem.* **2007**, *9*, 213-215

[2]   Verdol, J. A., U.S. Pat. 3 205 305, **1962**.

[3]   Aresta, M.; Quaranta, E.; Ciccarese, A., *J. Mol. Catal.* **1987**, *41*, 355-359.

[4]   Sun, J.; Fujita, S.-I.; Bhanage, B. M.; Arai, M., *Catal. Today* **2004**, *93-95*, 383-388.

[5]   Ramidi, P.; Felton, C. M.; Subedi, B. P.; Zhou, H.; Tian, Z. R.; Gartia, Y.; Pierce, B. S.; Ghosh, A., *J. CO$_2$ Util.* **2015**, *9*, 48-57.

[6]   Bai, D.; Jing, H., *Green Chem.* **2010**, *12*, 39-41.

[7]   Jacobsen, S. E., U.S. Pat. 4 325 874, **1982**.

[8]   Buonerba, A.; De Nisi, A.; Grassi, A.; Milione, S.; Capacchione, C.; Vagin, S.; Rieger, B., *Catal. Sci. Technol.* **2015**, *5*, 118-123.

[9]   Whiteoak, C.; Martin, E.; Martínez Belmonte, M.; Benet-Buchholz , J.; Kleij, A. W.; *Adv. Synth. Catal.* **2012**, *354*, 469-476.

[10]   Taherimehr, M.; Al-Amsyar, S. M.; Whiteoak, C. J.; Kleij, A. W.; Pescarmona, P. P., *Green Chem.* **2013**, *15*, 3083-3090.

[11]   Whiteoak, C. J.; Gjoka, B.; Martin, E.; Belmonte, M. M.; Escudero-Adan, E. C.; Zonta, C.; Licini, G.; Kleij, A. W., *Inorg. Chem.* **2012**, *51*, 10639-10649.

[12]   Whiteoak, C. J.; Martin, E.; Escudero-Adán, E.; Kleij, A. W., *Adv. Synth. Catal.* **2013**, *355*, 2233-2239.

[13]   Taherimehr, M.; Cardoso Costa Sertã, J. P.; Kleij, A. W.; Whiteoak, C. J.; Pescarmona, P. P., *ChemSusChem* **2015**, *8*, 1034-1042.

[14]   Iksi, S.; Aghmiz, A.; Rivas, R.; González, M. D.; Cuesta-Aluja, L.; Castilla, J.; Orejón, A.; El Guemmout, F.; Masdeu-Bultó, A. M., *J. Mol. Catal. A: Chem.* **2014**, *383-384*, 143-152.

15   Aghmiz, A.; Mostfa, N.; Iksi, S.; Rivas, R.; González, M. D.; Díaz, Y.; El Guemmout, F.; El Laghdach, A.; Echarri, R.; Masdeu-Bultó, A. M., *J. Coord. Chem.* **2013**, *66*, 2567-2577.

16   Iksi, S.; Aghmiz, A.; Masdeu-Bultó, A. M., *private communication*, **2013**.

17   Cameron, P. A.; Gibson, V. C.; Redshaw, C.; Segal, J. A.; White, A. J. P.; Williams, D. J., *J. Chem. Soc., Dalton Trans.* **2002**, 415-422.

18   Imbert, C.; Hratchian, H. P.; Lanznaster, M.; Heeg, M. J.; Hryhorczuk, L. M.; McGarvey, B. R.; Schlegel, H. B.; Verani, C. N., *Inorg. Chem.* **2005**, *44*, 7414-7422.

19   Asadi, M.; Hemmateenejad, B.; Mohammadikish, M., *J. Coord. Chem.* **2010**, *63*, 124-135.

20   Nakamoto, K., Infrared and Raman spectra of inorganic and coordination compounds, Wiley & Sons, New York, **1998**.

21   Geary, W.J., *Coord. Chem. Rev.***1971**, *7*, 81-122.

22   Neves, A.; Verani, C. N.; Brito, M. A.; Vencato, I.; Mangrich, A.; Oliva, G.; Dulce D. H.; Souza. F.; Batista, A. A. *Inorg. Chim. Acta* **1999**, *290*, 207-212.

23   (a) Glaser, T. Z. *Anorg. Allg. Chem.* **2003**, *629*, 2274-2281. (b) Karpishin, T. B.; Gebhard, M. S.; Solomon, E. I.; Raymond, K. N., *J. Am. Chem. Soc.* **1991**, *113*, 2977-2984.

24   O'Reilly, R. K.; Gibson, V. C.; White, A. J. P.; Williams, D. J.; *J. Am. Chem. Soc.* **2003**, *125*, 8450-8451.

25   Hwang, J. W.; Govindaswamy, K.; Koch, S. A. *Chem. Commun.* **1998**, 1667-1668.

26   Shyu, H.L.; Wei, H.H.; Lee, G.H.; Wang, Y.; *J. Chem. Soc., Dalton Trans.* **2000**, 915-918.

27   Martinho, P. N.; Vicente, A. I.; Realista, S.; Saraiva, M. S.; Melato, A. I.; Brandão, P.; Ferreira, V.; Carvalho, M. D., *J. Organomet. Chem.* **2014**, *760*, 48-54.

28   Caló, V.; Nacci, A.; Monopoli, A.; Fanizzi, A., *Org. Lett.* **2002**, *4*, 2561-2563.

29   (a) Shim, J.-J.; Kim, D.; Sup Ra, C., *Bull. Korean. Chem. Soc.* 2006, 27, 744-746. (b) Ju, H.-Y.; Manju, M.-D.; Kim, K.-H.; Park, S.-W.; Park, D.-W.; *J. Ind. Eng.*

Chem. **2008**, *14*, 157-160. (c) Wang, J.-Q.; Dong, K.; Cheng, W.-G.; Sun, J.; Zhang, S.-J., *Catal. Sci. Technol.* **2012**, *2*, 1480-1484.

30 Darensbourg, D. J.; Yarbrough, J. C.; *J. Am. Chem. Soc.* **2002**, *124*, 6335-6342.

31 Cuesta-Aluja, L.; Djoufak, M.; Aghmiz, A.; Rivas, R.; Christ, L.; Masdeu-Bultó, A. M., *J. Mol. Catal. A: Chem.* **2014**, *381*, 161-170.

32 Monfareda, H. H.; Sadighiana, S.; Kamyabia, M.-A.; Mayer, P., *J. Mol. Catal. A: Chem.* **2009**, *304*, 139-146.

33 Groves, J. T.; Nemo, T. E.; Myers, R. S., *J. Am. Chem. Soc.* **1979**, *101*, 1032-1033.

34 Groves, J. T.; Nemo, T. E., *J. Am. Chem. Soc.* **1983**, *105*, 5786-5791.

35 Groves, J. T.; Watanabe, Y., *J. Am. Chem. Soc.* **1988**, *110*, 8443-8452.

36 Groves, J. T.; Viski, P., *J. Org. Chem.* **1990**, *55*, 3628-3634.

37 Srinivasan, K.; Michaud, P.; Kochi, J. K., *J. Am. Chem. Soc.* **1986**, *108*, 2309-2320.

38 Chang, S.; Galvin, J. M.; Jacobsen, E. N., *J. Am. Chem. Soc.* **1994**, *116*, 6937-6938.

39 Finney, N. S.; Pospisil, P. J.; Chang, S.; Palucki, M.; Konsler, R. G.; Hansen, K. B.; Jacobsen, E. N., *Angew. Chem. Int. Ed.* **1997**, *36*, 1720-1723.

40 Shyu, H.-L.; Wei, H.-H.; Lee, G.-H.; Wang, Y., *J. Chem. Soc. Dalton Trans.* **2000**, 915-918.

41 Hasan, K.; Brown, N.; Kozak, C. M., *Green Chem.* **2011**, *13*, 1230-1237.

42 Chattopadhyay, T.; Islam, S.; Nethaji, M.; Majee, A.; Das, D., *J. Mol. Catal. A: Chem.* **2007**, *267*, 255-264.

43 Yang, L.; Wei, R.-N.; Li, R.; Zhou, X.-G.; Zuo, J.-L., *J. Mol. Catal. A: Chem.* **2007**, *266*, 284-289.

44 Suh, Y.; Seo, M. S.; Kim, K. M.; Kim, Y. S.; Jang, H. G.; Tosha, T.; Kitagawa, T.; Kim, J.; Nam, W., *J. Inorg. Biochem.* **2006**, *100*, 627-633.

45 Chisiro, T.; Kon, Y.; Nakashima, T.; Goto, M.; Sato, K., *Adv. Synth. Catal.* **2014**, *356*, 623-627.

46   Bruijnincx, P. C. A.; Buurmans, I. L. C.; Gosiewska, S.; Moelands, M. A. H.; Lutz, M.; Spek, A. L.; van Koten, G.; Gebbink, R. J. M. K., *Chem. Eur. J.* **2008**, *14*, 1228-1237.

47   Perandones, B. F.; del Río Nieto, E.; Godard, C.; Castillón, S.; De Frutos, P.; Claver, C., *ChemCatChem* **2013**, *5*, 1092-1095.

48   Mairata-Payeras, A.; Ho, R. Y. N.; Fugita, M.; Que, L. Jr., *Chem. Eur. J.* **2004**, *10*, 4944-4953.

49   Fugita, M.; Que, L. Jr., *Adv. Synth. Catal.* **2004**, *346*, 190-194.

50   Mas-Ballesté, R.; Fugita, M.; Hemmila, C.; Que, L. Jr., *J. Mol. Catal. A: Chem.* **2006**, *251*, 49-53.

51   Mas-Ballesté, R.; Que, L. Jr., *J. Am. Chem. Soc.* **2007**, *129*, 15964-15972.

52   Lee, S. H.; Han, J. H.; Kwak, H.; Lee, S. J.; Lee, E. Y.; Kim, H. J.; Lee, J. H.; Bae, C.; Lee, S. N.; Kim, Y.; Kim, C., *Chem. Eur. J.* **2007**, *13*, 9393-9398.

53   Chattopadhyay, T.; Das, D., *J. Coord. Chem.* **2009**, *5*, 845-853.

54   Pietikäinen, P.; Haikarainen, A., *J. Mol. Catal. A: Chem.,* **2002**, *180*, 59-65.

55   Zhang, W.; Jacobsen, E. N.; *J. Org. Chem.,* **1991**, *56*, 2296-2298.

56   Grigoropoulou, G.; Clark, J. H.; Elings, J. A., *Green. Chem.* **2003**, *5*, 1-7.

57   Nam, W.; Ho, R.; Valentine, J. S., *J. Am. Chem. Soc.* **1991**, *113*, 7052-7054.

58   Swern, D.; *Organic Peroxides*, John Wiley & Sons*, New York,* **1970**, Vol. 1.

59   Oh, N. Y.; Suh, Y.; Park, M. J.; Seo, M. K.; Kim, J.; Nam, W., *Angew. Chem.* **2005**, *117*, 4307-4311; *Angew. Chem. Int. Ed.* **2005**, *44*, 4235-4239.

60   Martinho, M.; Banse, F.; Bartoli, J.-F.; Mattioli, T. A.; Battioni, P.; Horner, O.; Bourcier, S.; Girerd, J.-J., *Inorg. Chem.* **2005**, *44*, 9592-9596.

61   Estrada, A.C.; Simões, M.M.Q.; Santos, I.C.M.S.; Neves, M.G.P.M.S.; Silva, A.M.S.; Cavaleiro, J.A.S.; Cavaleiro. A.M.V., *Catal. Lett.* **2009**, *128*, 281-289.

62   Yin, G.; Danby, A. M.; Kitko, D.; Carter, J. D.; Scheper, W. M.; Busch, D. H., *Inorg. Chem.* **2007**, *46*, 2173-2180.

63   Park, S.-E. Song, W. J.; Ryu, Y. O.; Lim, M. H.; Song, R.; Kim, K. M.; Nam, W., *J. Inorg. Biochem.* **2005**, *99*, 424-431.

64   Altomare, A.; Burla, M. C.; Camalli, M.; Cascarano, G. L.; Giacovazzo, C.; Guagliardi, A.; Moliterni, A. G. G.; Polidori, G.; Spagna, R., *J. Appl. Cryst.* **1999**, *32*, 115-119.

65   Sheldrick, G. M., **1997**. SHELXS97 and SHELXL97.University of Göttingen, Germany.

66   Ortep-3 for Windows - A Version of ORTEP-III with a Graphical User Interface (GUI). Farrugia, L. J., *J. Appl. Crystallogr.* **1997**, *30*, 565-566.

67   WinGX Suite for Single Crystal Small Molecule Crystallography. Farrugia, L. J., *J. Appl. Cryst.* **1999**, *32*, 837-838.

Chapter - 8

Conclusions

8.1 *Conclusions*

The aim of this doctoral Thesis was to develop new catalytic metallic systems to produce organic carbonates using renewable carbon dioxide, lowering the environmental impact as much as possible and trying to elucidate the mechanistic behavior of each component.

The concluding remarks extracted from this work are summarized as follow.

✓ We were capable to find the high potential of a low toxic Al(III) and Fe(III) complexes bearing a tetradentate N_2O_2-donor salabza ligand (**H₂L1**). In particular, the combination of a complex with an earth-abundant metal, **AlL1**, with low amounts of TBAB co-catalyst formed an active binary catalytic system for production of cyclic carbonates selectively, with excellent conversions at low pressures of CO_2 (up to 94 % at 10 bar).

✓ Kinetic experiments and ^{27}Al NMR analyses revealed a first order dependence on **AlL1** catalyst, TBAB and CO_2 concentration and the role of each component. We could, then, propose a plausible catalytic cycle for styrene carbonate formation based on monometallic aluminum species.

✓ On the other hand, the catalytic system **AlL1**/PPNCl produced poly(cyclohexene carbonate) (M_w up to 2900, $M_w/M_n = 1.3$) at room temperature with 84 % of selectivity using CHO as substrate. MALDI-TOF analyses indicate that the initial step involve the opening of the epoxide with Cl⁻ and OH⁻ (from water traces) anions.

✓ We demonstrated the beneficial effect of introducing halogen atoms in the Mn(III)-porphyrin skeleton for either copolymerization of CO_2 and CHO (a ten fold increase of TOF) and cyclic carbonate synthesis with aliphatic epoxides. We want to emphasize the non-necessity of introducing a co-catalyst in the reaction system.

✓ An attempt to recycle the Mn-porphyrin catalyst for PC synthesis was, unfortunately, not successful neither with homogeneous **MnL2a** nor heterogenized **MnL2a-CNT** since after the second run, the conversion dropped by half in both cases.

✓ Cr(III) catalysts with N_4-donor Schiff base ligands, in conjunction with TBAI co-catalyst, were found to be active for the cycloaddition of CO_2 and SO (conversions up to 92 %) using dichloromethane as solvent. Particularly, cationic **CrH₂L4** and **CrH₂L5** complexes gave higher conversions than neutral ones.

✓ The high toxic chlorinated solvent could be avoided by using solvent free conditions or supercritical carbon dioxide as reaction media. The best catalytic activity for styrene carbonate production was obtained under $scCO_2$ with **CrH₂L4**/TBAI catalytic system (TOF of 652 h^{-1}).

✓ Terminal epoxides were easily converted with high conversions (58-95 %) and selectivities to cyclic carbonates at best conditions under $scCO_2$ in only 30 min with a catalyst loading of 0.2 mol %.

✓ **CrH₂L4** catalyst in conjunction of PPNCl, DMAP or Py was discovered to be also an active catalytic system using high sterically hindered CHO with tunable selectivity. At 170 bar $scCO_2$ pressure and at co-catalyst/catalyst ratio of 5/1 the CHC was the only product, whereas at 50 bar and at catalyst/co-catalyst ratios of 1/0.5-1/1, the polymer was formed as the main product. We proposed that Cl^- anion initiates the opening of the epoxide as indicated MALDI-TOF analyses of the polycarbonates.

✓ We were able to synthetize low toxic and highly active Zn(II) and Fe(III) complexes analogous to our previously reported Cr(III) bearing N,N'O-donor ligands. The solid-state structures of **ZnL6** and **FeL8** were determined by X-ray diffraction methods showing a penta- and hexa-coordinate structure, respectively. Relative stability of the species in solution was analyzed for **ZnL6** by DFT calculations. We can assume, then, that a fluxional process could happen in solution proceeding via the most stable hexacoordinate species, which is the major species.

✓ Those complexes in the presence of TBAB as co-catalyst are proved to be efficient catalysts for the formation of cyclic carbonates with terminal epoxides, being the **ZnL6**/TBAB catalytic system the most efficient achieving an initial TOF of 3733 h^{-1} in the formation of styrene carbonate. This catalytic activity in the cycloaddition of CO_2

to styrene oxide of **ZnL6**/TBAB is higher than the one obtained with analogous Cr(III) complex, **CrL6**/PPNCl, although **ZnL6** decomposes at long reaction time.

✓ The catalytic results obtained using most sterically hindered CHO as substrate show different behaviors when using Fe(III) or Zn(II) complexes. **ZnL6** catalyst achieves low conversions but total selectivity towards CHC. On the other hand, **FeL8** in conjunction with PPNCl affords mixtures of CHC and PCHC (PCHC/CHC = 21/79), similarly to those Cr(III) analogous but al lower conversions (37 % vs 95 %).

✓ An important and greener goal of this thesis was to obtain methyl oleate carbonate, which was derived from epoxidized natural oils, those economical, low-toxic and metal earth abundant Zn and Fe complexes. The best result was obtained with **FeL8** in conjunction with TBAB as co-catalyst, we successfully obtained good conversions (95 %) and yields at catalyst/co-catalyst loading of 2 mol %/2 mol %, 100 ºC, 100 bar of CO_2 pressure during 24 h.

✓ Complexes **FeL6** and **FeL8** are also active as catalysts for the olefin epoxidation. The best catalytic result was obtained for the epoxidation of *trans*-stilbene using TBHP (5.5 M in decane) as oxidant source, 0.67 mol % of **FeL8**, without the addition of any co-catalyst with a conversion of 95 % and >99 % of selectivity towards *trans*-stilbene oxide.

✓ Moreover, the preliminary study of direct oxidative carboxylation of styrene towards styrene carbonate using $scCO_2$ as both reactive and solvent using Fe(III) complexes with NN'O-donor Schiff ligands results promising (Conversion and selectivity). Nevertheless, a more refined catalysis approach is needed in order to increase the carbonate yield for this reaction.

Chapter - 9

Summary

9.1. Summary

In the recent years sustainable chemistry has completely changed the scientific concept of chemical and engineering research. That philosophy of green chemistry encourages the design of chemicals products and processes utilizing more efficient, effective, safe and more environmentally benign chemical substances whereas minimizing or eliminating the use and generation of hazardous substances.

One of the major goals of green chemistry is to produce new chemical feedstock derived from natural and renewable resources instead of fossil fuels. This lead to explore an important way to use a renewable source of carbon for C-C bond formation with an environmentally friendly CO_2 reagent in catalysis because of its low cost, its natural abundance and relatively low toxicity.

In **Chapter one**, a general introduction and literature background about the use of carbon dioxide as both C_1 building block for the synthesis of useful industrial chemical compounds and its uses as a plausible alternative solvent is given. Specially, there were empathized the studies about the addition of carbon dioxide to epoxides to produce valuable products such as cyclic carbonates and polycarbonates. A large number of catalytic systems have been investigated to promote this reaction selectively in the recent years, being the homogenous metal-based complexes the most widely employed catalysts. So, in this chapter, we highlight the most recent developments in the field of catalytic synthesis of cyclic carbonates and polycarbonates focusing on the catalytic potential of the different metal-catalyzed systems. More attention is therefore given to the catalytic processes that have disclosed new reactivity patterns, improved activity and high selectivity, that uses milder reaction conditions and environmentally friendly metal catalysts and also that elucidates the possible reaction mechanism giving a plausible catalytic role of each component.

In **Chapter two**, the general and also the specific objectives of this Thesis are detailed.

Chapter 3, is dedicated on the synthesis and characterization of a low toxic and earth-abundant Al(III) and Fe(III) as well as analogous Cr(III) and Co(III) complexes bearing a tetradentate N_2O_2-donor salabza **H$_2$L1** ligand. The molecular structures of **CrL1**, **FeL1** and **CoL1** were determined by X-ray diffraction method. Those complexes

were tested for the production of cyclic carbonates in conjunction with low amounts of TBAB as co-catalyst. The binary **AlL1**/TBAB catalytic system was found to be the most active, producing excellent conversions and selectivity al low pressures of CO_2. ^{27}Al NMR spectroscopy revealed the coordination of the substrate towards the Lewis acid aluminum center and kinetic experiments showed a first order dependence on catalyst, co-catalyst and CO_2 concentration obtaining a plausible catalytic cycle proposal for styrene carbonate formation. On the other hand, **AlL1**/PPNCl catalytic system was capable to produce poly(cyclohexene carbonate) selectively (M_w up to 2900, M_n/M_w up to 1.3) at mild reaction conditions. MALDI-TOF analysis of the initiation and end group from the polycarbonates was studied, being observed the initiation and termination by Cl^- and OH^- (from water traces) anions.

The beneficial effect of introducing halogen atoms in the Mn(III)-porphyrin skeleton for the copolymerization of CO_2 and CHO and the cyclic carbonate synthesis with aliphatic epoxides was evaluated on **Chapter 4**. With the non-necessity of introducing a co-catalyst in the reaction system a maximum TOF of 154 h^{-1} was obtained with homogeneous **MnL2a** catalyst for the copolymerization of CHO and CO_2. Catalyst recycling experiments were done both with the homogeneous and the heterogenenized **MnL2a-CNT** catalysts. Unfortunately, in both cases a deactivation or catalyst leaching afford a conversion drop by a half in a second catalytic run in both cases.

Chapter 5 deals with the synthesis of a novel Cr(III) catalysts bearing a N_4-donor Schiff base ligands (**H₂L4** and **H₂L5**). Neutral salen-analogs **CrL4** and **CrL5** and cationic **CrH₂L4** and **CrH₂L5** complexes were obtained following different procedures and well-characterized with FT-IR, Raman, MALDI-TOF analyses, ionic conductivity, elemental analysis and magnetic susceptibility. All complexes were found to be active for the cycloaddition of CO_2 and styrene oxide (conversions up to 92 %) using TBAI as co-catalyst and CH_2Cl_2 as solvent. Particularly, cationic complex **CrH₂L4** achieve the best conversions. Using $scCO_2$ as both reactant and solvent, the use of the highly toxic CH_2Cl_2 solvent could be avoided obtaining best catalytic activities and selectivities towards cyclic SC. (TOF up to 652 h^{-1}). At those conditions terminal epoxides were also easily converted to cyclic carbonates with high conversions (58-95 %) and total

selectivity. Using PPNCl, DMAP or Py as co-catalysts with CHO as substrates the selectivity can be tuned easily changing the CO_2 pressure and the co-catalyst/catalyst ratio. MALDI-TOF analyses of the polymers obtained showed that the Cl^- anion initiates the opening of the epoxide.

In **Chapter 6** a highly active Zn(II) catalyst bearing a tridentate N,N'O-donor Schiff ligand was discovered for the selective synthesis of cyclic carbonates with CO_2 and epoxides. X-ray structure of **ZnL6** showed a pentacoordinate structure with one pyridine moiety acting as a pendant group. Nevertheless, NMR spectroscopy revealed that, in solution, a hexacoordinate structure with the two ligands acting as a tridentate towards the zinc center, even at high and low temperatures. DFT calculations of the relative stability of **ZnL6** indicate that a fluxional process could happen in solution via the most stable hexacoordinate species. This complex was tested as a catalyst, with TBAB as co-catalyst, for the selective formation of cyclic carbonates with terminal and sterical hindered epoxides. At 100 ºC and 100 bar of CO_2 an initial TOF of 3733 h^{-1} was obtained for the formation of styrene carbonate. That catalytic activity is higher that the one obtained with analogous Cr(III) complex, **CrL6** developed previously in our group.

Chapter 7 described the use of environmental friendly and earth abundant Fe metal for the synthesis of Fe(III) complexes bearing tridentate **HL6** and **HL8** N,N'O-donor Schiff ligands. The X-ray structure of **FeL8** revealed a hexacoordinate structure with both ligands acting as tridentate. These Fe(III) complexes were quite active and stable for the selective formation of cyclic carbonates with terminal epoxides at moderate mild conditions with TBAB as co-catalyst. On the other hand **FeL8**/PPNCl catalytic system, for the CHO/CO_2 coupling reaction, afforded mixtures of CHC and PCHC, similarly to those Cr(III) analogous but at lower conversions. Moreover, **FeL6** and **FeL8** complexes were found to be also active for epoxidation of stilbenes. An screening of the reaction conditions and oxidation source leaded to the best catalytic result of 95 % of conversion of *trans*-stilbene with a *trans*-stilbene oxide selectivity of > 99 % using **FeL8**, TBHP (5.5M in decane) without the addition of any co-catalyst. The preliminary results in the direct oxidative carboxylation of styrene towards styrene

carbonate using **FeL8**/TBAB catalytic system, and scCO$_2$ as both reactive and solvent are promising, although low yields of styrene were obtained.

In this thesis methyl oleate carbonate, derived from natural resources, was obtained using those economical, low toxic and earth abundant **AlL1**, **ZnL6** and **FeL8** complexes, with TBAB as co-catalyst, revealing high conversions and yields although harsher conditions (100 ºC and 100 bar of CO$_2$) were required.

Chapter - 10

Appendix

10.1 *List of publications*

- L. Cuesta-Aluja, M. Djoufak, A. Aghmiz, R. Rivas, L. Christ, A. M. Masdeu-Bultó, *Novel chromium (III) complexes with N4-donor ligands as catalysts for the coupling of CO_2 and epoxides in supercritical CO2*. J. Mol. Catal. A Chem., 381, (2014), 161.

- S. Iksi, A. Aghmiz, R. Rivas, M. D. González, L. Cuesta-Aluja, J. Castilla, A. Orejón, F. El Guemmout, A. M. Masdeu-Bultó, *Chromium complexes with tridentate NN'O Schiff base ligands as catalysts for the coupling of CO_2 and epoxides.* J. Mol. Catal. A Chem., 383-384, (2014), 143.

- L. Cuesta-Aluja, A. Campos-Carrasco, J. Castilla, M. Reguero, A. M. Masdeu-Bultó, A. Aghmiz, *Highly active and selective Zn(II)-NN'O Schiff base catalysts for the cycloaddition of CO_2 to epoxides.* Dalton Trans., in evaluation.

- L. Cuesta-Aluja, J. Castilla, A. M. Masdeu-Bultó, C. A Henriques, M. J. F. Calvete, M. M. Pereira, *Halogenated meso-phenyl Mn(III) porphyrins as highly efficient catalysts for the synthesis of organic carbonates using carbon dioxide and epoxides.* Appl. Catal. A: Gen., submitted.

10.2 *Conferences and scientific meetings*

- *"Organic carbonate synthesis from CO_2/epoxides coupling using metal complexes as catalysts in scCO2"*. **Oral comunication**. Flucomp VII, Reunión de Expertos en Fluidos Comprimidos, Barcelona, Spain, 2014.

- *"Síntesi de carbonats a partir de CO_2 i epòxids emprant complexos de Crom"*. **Oral comunication**.VIII Trobada de joves investigadors dels països catalans, Andorra la Vella, Andorra, 2013

- *"Polycarbonates and cyclic carbonates by Mn(III) haloporphyrines-catalysed coupling of CO_2/epoxides"* **Poster**. XXXII Congreso Grupo especializado en química organometalica (GEQO), Tarragona, Spain, 2014.

- *"Highly selective synthesis of cyclic carbonates from CO_2/epoxides catalysed by Zn(II) and Fe(III) Schiff base complexes at mild conditions"* **Poster**. XXXII Congreso Grupo especializado en química organometalica (GEQO), Tarragona, Spain, 2014.

- "Carbonate synthesis from CO_2 and epoxides catalyzed with chromium(III) complexes" **Poster**. ISHC XVIII, 18th International Symposium on Homogeneous Catalysis, Toulouse, France, 2012.

10.3 Research stays abroad

- **(May-July 2015, 3 months)** Dipartimento di Scienze chimiche, Università degli studi di Napoli Federico II (Italy).

Advisors: Prof. Vincenzo Busico and Dr. Angela D'Amora.

Project: Use of high throughput platforms for catalyst synthesis and catalysis.

- (**March-June 2012, 3 months**) Institut de recherches sur la catalyse et l'environnement de Lyon (IRCELYON), University of Lyon 1 (France).

Advisor: Dr. Lorraine Christ.

Project: Polycarbonate synthesis from CO_2 and epoxides.

10.4 List of acronyms

A

Å:	Angstrom
AcOH	Acetic acid
Ar:	Aromatic
ATR:	Attenuated total reflectance (IR)

B

BArF:	tetrakis(3,5-bis(trifluoromethyl)phenyl)borate)
BDI:	β-diiminate

C

Cat:	Catalyst
CC:	Cyclic carbonate
CDCl$_3$:	Deuterated chloroform
CHC:	Cyclohexene carbonate
CHO:	Cyclohexene oxide
CNTs:	Carbon nanotubes
CO$_2$	Carbon dioxide
Co-cat:	Co-catalyst

D

DMF	Dimethylformamide
DFT:	Density functional theory
DMAP:	Dimethylaminopyridine
DMSO	Dimethylsulfoxide
d:	Doublet (NMR)
dd:	Double doublet (NMR)

E

EC:	Ethylene carbonate
ESI-MS:	Electrospray ionization-Mass spectrometry
EtOH:	Ethanol

EO:	Ethylene oxide
F	
FTIR:	Fourier-Transformation infrared spectroscopy
G	
GC:	Gas chromatography
GPC:	Gel permeation chromatography
H	
h:	Hour
HMPA	Hexamethylphosphoramine
HPLC:	High-performance liquid chromatography
I	
IR:	Infrared spectroscopy
K	
KBr:	Potassium bromide
KTFA:	Potassium trifluoroacetate
k:	Rate constant
k_{obs}:	Observed rate constant
L	
L:	Ligand
ln:	Natural logarithm
M	
M:	Metal
m:	multiplet (NMR)
MALDI-TOF:	Matrix-assisted laser desorption/ionization time of flight
m-CPBA:	Meta-chloroperbenzoic acid
MeOH:	Methanol
MeCN:	Acetonitrile
mmol:	Milimol

min:	Minute
ml:	Milliliter
MHz:	Megahertz
MPa:	Mega Pascal
M_w:	Molecular weight
M_w/M_n:	Molecular weight distribution

N

NaOCl:	Sodium hypochlorite
NIP:	Non-isocyanate polyurethanes
NMIM:	N-methylimidazol
NMP:	N-methylpyrrolidone
n.d:	Non-determined
nm:	Nanometer

P

P_c:	Critical pressure
P:	Pressure
PC:	Propylene carbonate
PDI:	Polydispersity
PPC:	Poly(propylene carbonate)
PCHC:	Poly(cyclohexene carbonate)
PhIO:	Iodosylbenzene
PO:	Propylene oxide
POMs:	Polyoxometalates
PPNCl:	Bis(triphenylphosphinine)iminium chloride
PTAT	Phenyltrimethylammonium tribromide
Py:	Pyridine

R

ROOH:	Alkyl peroxides
r.t.:	Room temperature

S

Salen:	*N,N*- bis(salicylidene)ethylenediamine
scCO$_2$:	Supercritical carbon dioxide
SC	Styrene carbonate
SCF:	Supercritical fluid
SO:	Styrene oxide
ST:	Styrene
Subs.:	Substrate
s:	Singulet (NMR)

T

t:	Time
T:	Temperature
T$_c$:	Critical temperature
TBAB	Tetrabutylammonium bromide
TBAI	Tetrabutylammonium iodide
TBACl	Tetrabutylammonium chloride
TBHP:	*tert*-butylhydroperoxide
TPP:	Tetraphenylporphyrin
TDCPP:	Tetra(2,6-dichlorophenyl)-porphyrine
TOF:	Turn-over frequency
THF:	Tetrahydrofuran

U

UV-Vis:	Ultraviolet-Visible

Y

Y:	Yield
^{1}H NMR:	Proton nuclear magnetic resonance
^{13}C NMR:	Carbon nuclear magnetic resonance
^{27}Al NMR:	Aluminum nuclear magnetic resonance
δ_c:	Critical density

Λ_M:	Molar conductivity
v:	Vibration frequency (IR)
δ:	Chemical shift (NMR)
μl:	Microliter
e:	Extinction coefficient
m:	Magnetic susceptibility
l:	Wavelength

Λ_M: Molar conductivity